LOANA HENRÍQUEZ SÁNCHEZ

ANÁLISE DA PROBABILIDADE DE FALHA EM PAVIMENTOS FLEXÍVEIS ATRAVÉS DO CONCEITO DE CONFIABILIDADE

Programa de Pós-graduação em
Engenharia de Transportes da EESC-USP

Exemplar definitivo (corrigido). O exemplar original está disponível na CPG da EESC-USP

São Carlos, **16/08/2021**

RESOLUÇÃO CoPGr N º 6018, DE 13 DE OUTUBRO DE 2011, artigo 5º

Tese apresentada ao Departamento de Engenharia de Transportes da Escola de Engenharia de São Carlos, da Universidade de São Paulo, como parte dos requisitos para obtenção do título de Doutor em Ciências.

Área de concentração: Infraestrutura de Transportes.

Orientador: Prof. Titular Dr. José Leomar Fernandes Júnior

SÃO CARLOS
2021

AUTORIZO A REPRODUÇÃO TOTAL OU PARCIAL DESTE TRABALHO, POR QUALQUER MEIO CONVENCIONAL OU ELETRÔNICO, PARA FINS DE ESTUDO E PESQUISA, DESDE QUE CITADA A FONTE.

Ficha catalográfica elaborada pela Biblioteca Prof. Dr. Sérgio Rodrigues Fontes da EESC/USP com os dados inseridos pelo (a) autor (a).

Sánchez, Loana Henríquez
S518p Análise da probabilidade de falha em pavimentos flexíveis através do conceito de confiabilidade / Loana Henríquez Sánchez; orientador José Leomar Fernandes Júnior. São Carlos, 2021.

Tese (Doutorado) - Programa de Pós-Graduação em Engenharia de Transportes e Área de Concentração em Infraestrutura de Transportes -- Escola de Engenharia de São Carlos da Universidade de São Paulo, 2021.

1. Probabilidade de falha. 2. Confiabilidade. 3. Pavimentos flexíveis. 4. Tipo de eixo. 5. Pressão de enchimento. 6. Sobrecarga I. Título.

Eduardo Graziosi Silva - CRB - 8/8907

LOANA HENRIQUEZ SANCHEZ

PROBABILITY OF FAILURE ANALYSIS IN FLEXIBLE PAVEMENTS THROUGH THE RELIABILITY CONCEPT

Programa de Pós-graduação em
Engenharia de Transportes da EESC-USP

Exemplar definitivo (corrigido). O exemplar original está disponível na CPG da EESC-USP

São Carlos, **16/08/2021**

RESOLUÇÃO CoPGr N º 6018, DE 13 DE OUTUBRO DE 2011, artigo 5º

Dissertation submitted to the Department of Transportation Engineering of the Sao Carlos School of Engineering – University of Sao Paulo in partial fulfillment of the requirements for the degree of Doctor of Philosophy.

Subject Area: Transport Infrastructure.

Advisor: Prof. Jose Leomar Fernandes Junior (Full Professor)

SAO CARLOS
2021

I AUTHORIZE THE TOTAL OR PARTIAL REPRODUCTION OF THIS WORK, FOR ANY CONVENTIONAL OR ELECTRONIC MEANS, FOR STUDY AND RESEARCH PURPOSES, SINCE THE SOURCE IS CITED.

Index card adapted from the official format of the Library Prof. Dr. Sergio Rodrigues Fontes of the EESC/USP with data entered by the author.

Sanchez, Loana Henriquez
S518p Probability of failure analysis in flexible pavements through the reliability concept / Loana Henriquez Sanchez; Advisor Jose Leomar Fernandes Junior. Sao Carlos, 2021.

PhD. Dissertation (Doctor of Philosophy) – Graduate Program in Transportation Engineering, Subject area Transportation Infrastructure -- Sao Carlos School of Engineering, University of Sao Paulo, 2021.

1. Probability of failure. 2. Reliability. 3. Flexible pavements. 4. Axle type. 5. Tire pressure. 6. Axle Overload I. Title.

Eduardo Graziosi Silva - CRB - 8/8907

LOANA HENRÍQUEZ SÁNCHEZ

ANÁLISIS DE LA PROBABILIDAD DE FALLA EN PAVIMENTOS FLEXIBLES A TRAVÉS DEL CONCEPTO DE CONFIABILIDAD

Programa de Pós-graduação em
Engenharia de Transportes da EESC-USP

Exemplar definitivo (corrigido). O exemplar original está disponível na CPG da EESC-USP

São Carlos, **16/08/2021**

RESOLUÇÃO CoPGr N º 6018, DE 13 DE OUTUBRO DE 2011, artigo 5º

Tesis presentada al Departamento de Ingeniería de Transportes de la Escuela de Ingeniería de São Carlos de la Universidad de São Paulo en cumplimiento parcial a los requisitos para obtener el grado de Doctor Ciencias.

Área de especialidad: Infraestructura de Transportes.

Asesor: Prof. Titular Dr. José Leomar Fernandes Júnior

SÃO CARLOS
2021

AUTORIZO LA REPRODUCCIÓN TOTAL O PARCIAL DE ESTE TRABAJO, A TRAVÉS DE CUALQUIER MEDIO CONVENCIONAL O ELECTRÓNICO, PARA FINES DE ESTUDIO E INVESTIGACIÓN, SIEMPRE QUE SEA CITADA LA FUENTE.

Ficha catalográfica adaptada del modelo oficial de la Biblioteca Prof. Dr. Sérgio Rodrigues Fontes de la EESC/USP con los datos proporcionados por el autor (a).

Sánchez, Loana Henríquez
S518p Análisis de la probabilidad de falla en pavimentos flexibles a través del concepto de confiabilidad / Loana Henríquez Sánchez; asesor José Leomar Fernandes Júnior. São Carlos, 2021.

Tesis (Doctorado) - Programa de Posgrado en Ingeniería de Transportes, Área de Especialidad Infraestructura de Transportes -- Escuela de Ingeniería de São Carlos de la Universidad de São Paulo, 2021.

1. Probabilidad de falla. 2. Confiabilidad. 3. Pavimentos flexibles. 4. Tipo de eje. 5. Presión de neumático. 6. Sobrecarga de eje I. Título.

Eduardo Graziosi Silva - CRB - 8/8907

FOLHA DE JULGAMENTO

Candidata: Engenheira **LOANA HENRIQUEZ SANCHEZ.**

Título da tese: "Análise da probabilidade de falha em pavimentos flexíveis através do conceito de confiabilidade".

Data da defesa: 18/02/2021.

Comissão Julgadora	**Resultado**
Prof. Titular **Jose Leomar Fernandes Junior (Orientador)** (Escola de Engenharia de São Carlos – EESC/USP)	**APROVADA**
Dr. **Luis Miguel Gutierrez Klinsky** (Banco de Desenvolvimento de Américas Latina/CAF)	**APROVADA**
Profa. Dra. **Heliana Barbosa Fontenele** (Universidade Estadual de Londrina/UEL)	**APROVADA**
Profa. Dra. **Ana Paula Furlan** (Escola de Engenharia de São Carlos – EESC/USP)	**APROVADA**
Prof. Dr. **Francisco Heber Lacerda de Oliveira** (Universidade Federal do Ceará/UFC)	**APROVADA**

Coordenador do Programa de Pós-Graduação em Engenharia de Transportes:
Prof. Associado **Adalberto Leandro Faxina**
Presidente da Comissão de Pós-Graduação:
Prof. Titular **Murilo Araujo Romero**

I dedicate this dissertation to my grandfather ***Jose Ignacio Henriquez Carcamo*** in loving memory, who didn't have the opportunity to study, but always said "The beautiful thing about learning is nobody can take it away from you".

ACKNOWLEDGMENTS

First, I want to thank God for the wisdom, strength, peace of mind and good health in order to finish this dissertation.

Will like to express my sincere thanks and appreciation to my advisor Professor Jose Leomar Fernandes Junior for the continuous support, thoughtful guidance and encouragement. His guidance helped me become a researcher with critical thinking and a better human being.

Besides my advisor, I would like to thanks the rest of my PhD Qualifying Exam committee: Prof. Ana Paula Furlan and Prof. Glauco Tulio Pessa Fabbri, for their constructive suggestions and thoughtful advices in the completion of this dissertation.

Words cannot adequately express my gratitude to my parents Victor and Maria Elena and my siblings, Mariusa and Luis Roberto, for their support, and encouragement, throughout this period. Also, I will like to thank with love my husband Jorge Braulio Cossio Duran, my best friend and great companion, who loved, supported, encouraged, entertained, and helped me through this agonizing period in the most positive way. Likewise, to Andiara Isabella and Lucas Gabriel, my kids, for their love, endless support, patience and being my constant source of inspiration to finish.

Special thanks to the Creche EESC USP, Margarete Silva, Keila Targas, Sineide Polveiro, Dilma Sao Marcos, Andrea Cremonezi, Beatriz Boriollo, Liliane Araujo, Ivannia Aparecida, Ismalia Silvatti, Margarete Marchetti, Magali Lima for all the education, care and love given to our son Lucas Gabriel, thanks for all the incredible works you do with every child in this amazing place, this preschool is crucial for pos graduate student and mom.

I want to thanks my friends and colleagues Jenny Ventura, Gustavo Sabillon, Maria Jose Zagatto, Danilo Bisconsini, Rosuel Krum, Ricardo Freire, and Anthony Gomes from the Department of Transportation Engineering for their friendly and continuous support during this journey of my PhD Studies.

This research was financed in part by the Coordenação de Aperfeiçoamento de Pessoal de Nivel Superior-Brazil (CAPES) – Finance Code 001.

“Nothing in life is to be feared, it is only to be understood. Now is the time to understand more, so that we may fear less”

Marie Curie

RESUMO

SANCHEZ, L. H. (2021). **Análise da Probabilidade de Falha em Pavimentos Flexíveis através do Conceito de Confiabilidade.** Tese (Doutorado em Ciências) – Departamento de Engenharia de Transportes, Escola de Engenharia de São Carlos, Universidade de São Paulo, São Carlos, Brasil.

Projetar pavimentos envolve o risco da vida útil do pavimento ser menor ou até maior do que a vida útil de projeto, o que pode resultar em configurações de estrutura sub ou superdimensionadas e, consequentemente, gerar um impacto econômico adverso para qualquer agência rodoviária. No entanto, embora a teoria da probabilidade de falha, bem como o conceito de confiabilidade, tenha sido incorporada em muitos procedimentos de projeto de pavimentos, há necessidade de uma maneira acessível de entender esses conceitos e também de um procedimento fácil de aplicá-los. Esta pesquisa visa desenvolver uma abordagem alternativa para a análise da probabilidade de falha em pavimentos flexíveis com base no conceito de confiabilidade, a fim de capturar aspectos importantes que muitas vezes são ignorados na análise de confiabilidade tradicional, como o sub ou superdimensionamento de muitas configurações estruturais. Assim, 4 estruturas de pavimento, representativas no Brasil, foram estudadas a partir de 4 respostas estruturais que calcularam-se levando em consideração o efeito de 6 diferentes tipos de eixos submetidos a 5 condições de sobrecarga e a 3 níveis de pressão de enchimento dos pneus. O software mePADS foi usado para calcular as respostas estruturais e a partir delas obtiveram-se as previsões empíricas da vida útil do pavimento pelo criterio do Instituto do Asfalto dos Estados Unidos, em termos do número de ciclos até a falha para os defeitos trincas por fadiga (Nf) e deformação permanente (Nr). Os menores valores entre Nf e Nr foram adotados como Resistências Críticas, enquanto as Solicitações foram determinadas a partir da variação de Fatores de Segurança (SF). Na sequência, curvas margem (M) envolvendo valores médios e desvios-padrão foram geradas a fim de identificar as áreas onde a probabilidade de falha poderia ocorrer e, finalmente, foram obtidos os índices de confiabilidade (β) e as probabilidades de falha (Pf). Os principais resultados mostraram que os eixos tandem-espaçado e tandem estão relacionados a baixos valores de β e Pf principalmente em comparação com os eixos simples e de rodagem dupla. Além disso, três dos quatro modelos de regressão linear multivariada indicaram correlações fortes e positivas e níveis adequados de significância. Em geral, observou-se que uma análise baseada em confiabilidade pode ser facilmente realizada a partir de valores de resistências precisos e dados de solicitações que podem ser obtidos a partir de qualquer critério que forneça os ciclos de falha de uma certa configuração estrutural do pavimento. A abordagem desenvolvida nesta pesquisa é fácil de ser adotada na prática da engenharia e, portanto, tem o potencial de se tornar uma ferramenta prática no projeto de pavimentos empírico-mecanicista baseado em confiabilidade.

Palavras-chave: Probabilidade de Falha, Confiabilidade, Pavimentos Flexíveis, Tipo de Eixo, Pressão de Enchimento, Sobrecarga.

ABSTRACT

SANCHEZ, L. H. (2021). **Probability of Failure Analysis in Flexible Pavements through the Reliability Concept.** PhD. Dissertation (Doctor of Philosophy) – Department of Transportation Engineering, São Carlos School of Engineering, University of São Paulo, São Carlos, Brazil.

Pavement design involves the risk of the pavement life be shorter or even larger than the design life, which can result in undersized or oversized structure configurations and, as a consequence, generate an adverse economic impact for any highway agency. However, even though the probability-of-failure theory, as well as the reliability concept, have been incorporated in many pavement design procedures, there is a need for an accessible way to understand these concepts and also an easy procedure to apply them. This research aims to develop an alternative approach for a probability-of-failure analysis in flexible pavements based on the reliability concept, in order to capture important aspects that are often ignored in traditional reliability analysis of pavement structures, such as the undersizing or oversizing of structural configurations. Accordingly, four representative Brazilian pavement structures were studied from four structural responses that were calculated taking into account the effect of six different axle types subjected to five overload conditions and to three levels of tire pressure. The mePADS software was used to calculate the structural responses and empirical Asphalt Institute's pavement life predictions in terms of the number of cycles to failure for fatigue cracking (Nf) and rutting (Nr) pavement distresses were carried out. The smaller values between Nf and Nr were adopted as Critical Resistances while Solicitations were determined from the variation of Safety Factors (SF). In sequence, margin curves (M) involving average values and standard deviations were generated in order to identify the areas where the probability of failure might occur and finally the reliability indices (β) and the probabilities of failure (Pf) were obtained. Principal results showed that tandem-spaced and tandem axles are related to low β and Pf values mainly compared to single and dual axles. Furthermore, three of four multivariate linear regression models indicate strong and positive correlations and adequate levels of significance. In general, it was observed that a reliability-based analysis can be easily performed from accurate resistances and solicitations data that can be obtained from any criteria that provide the cycles to failure of the pavement structure configuration. The approach developed in this research is easy to be adopted in the engineering practice and thus has the potential to become a practice tool in the reliability-based mechanistic-empirical pavement design.

Keywords: Probability of Failure, Reliability, Flexible Pavements, Axle Type, Tire Pressure, Axle Overload.

RESUMEN

SANCHEZ, L. H. (2021). **Análisis de la Probabilidad de Falla en Pavimentos Flexibles a través del Concepto de Confiabilidad.** Tesis (Doctorado en Ciencias) – Departamento de Ingeniería de Transportes, Escuela de Ingeniería de São Carlos, Universidad de São Paulo, São Carlos, Brasil.

Diseñar pavimentos implica el riesgo de que la vida útil del pavimento sea más corta o incluso mayor que la vida de diseño, lo que puede resultar en configuraciones estructurales sub o súper dimensionadas que, consecuentemente, pueden generar un impacto económico adverso para cualquier agencia vial. Sin embargo, aunque la teoría de la probabilidad de falla, así como el concepto de confiabilidad, se han incorporado en muchos procedimientos de diseño de pavimentos, existe la necesidad de una forma accesible para comprender estos conceptos y también de un procedimiento sencillo para aplicarlos. Esta investigación tiene como objetivo desarrollar un enfoque alternativo para un análisis de probabilidad de falla en pavimentos flexibles basado en el concepto de confiabilidad, con el fin de capturar aspectos importantes que a menudo se ignoran en el análisis de confiabilidad tradicional de estructuras de pavimentos, como el sub o súper dimensionamiento de diversas configuraciones estructurales. De este modo, se estudiaron 4 estructuras de pavimento, representativas en Brasil, a partir de 4 respuestas estructurales que se calcularon teniendo en cuenta el efecto de 6 tipos de ejes diferentes sometidos a 5 condiciones de sobrecarga y a 3 niveles de presión de neumáticos. Se utilizó el software mePADS para calcular las respuestas estructurales y se obtuvieron predicciones empíricas de la vida útil del pavimento a través del criterio del Instituto del Asfalto de los Estados Unidos, en términos del número de ciclos hasta la falla para los defectos de grietas por fatiga (Nf) y deformación permanente (Nr). Los valores más pequeños entre Nf y Nr se adoptaron como Resistencias Críticas mientras que las Solicitaciones se determinaron a partir de la variación de Factores de Seguridad (SF). En secuencia, se generaron curvas de margen (M) que involucran valores promedio y desviaciones estándar para identificar las áreas donde podría ocurrir la probabilidad de falla y finalmente se obtuvieron los índices de confiabilidad (β) y las probabilidades de falla (Pf). Los principales resultados mostraron que los ejes tándem-espaciados y tándem están relacionados con valores bajos de β y Pf principalmente en comparación con los ejes simples y dobles. Además, tres de los cuatro modelos de regresión lineal multivariada indicaron correlaciones fuertes y positivas, así como niveles adecuados de significancia. En general, se observó que un análisis basado en confiabilidad se puede realizar fácilmente a partir de valores de resistencias precisos y de solicitaciones que se pueden obtener con cualquier criterio que proporcione los ciclos de falla de una determinada configuración estructural del pavimento. El enfoque desarrollado en esta investigación es fácil de adoptar en la práctica de la ingeniería y, por lo tanto, tiene el potencial de convertirse en una herramienta de práctica en el diseño de pavimentos mecánico-empírico basado en confiabilidad.

Palabras clave: Probabilidad de Falla, Confiabilidad, Pavimentos Flexibles, Tipo de Eje, Presión de neumáticos, Sobrecarga de Eje.

ABBREVIATIONS & SYMBOLS

AASHTO - American Association of State Highway and Transportation Officials

CDF - Cumulative Distribution Function

CONTRAN - National Traffic Council (Brazil)

DER/SP - Highway Department of the State of Sao Paulo (Brazil)

DNIT - National Department of Transport Infrastructure (Brazil)

FEM - Finite Element Method

FHWA - Federal Highway Administration

FORM - First Order Reliability Method

GEIPOT - Brazilian Transportation Planning Company (old)

IBM-SPSS - Statistical Package for the Social Sciences of the International Business Machines Corporation

IRI - International Roughness Index

LEF - Load Equivalency Factors

M - Margin Curve

MePADS - Pavement Analysis and Design software package based on the South African Mechanistic Pavement Design procedure

MEPDG - Mechanistic-Empirical Pavement Design Guide

NCHRP - National Cooperative Highway Research Program

Nf - Number of load repetitions to rutting failure

Nr - Number of load repetitions to fatigue cracking failure

PDF - Probability Density Function

Pf - Probability of Failure

PMF - Probability Mass Function

PSI - Present Serviceability Index

RMS - Root Mean Square

S_0 - Overall Standard Deviation

SF - Safety Factor

SN - Structural Number

USACE - United States Army Corps of Engineers

Z_R - Design Reliability Level

β - Reliability Index

δ_1 - Pavement surface displacements or deflections

εht_1 - Horizontal tensile strain at the bottom of the asphalt layer

εvc_1 - Vertical compressive strain at the bottom of the asphalt layer

εvc_m - Vertical compressive strain at the top of the subgrade layer

μM - Margin Mean

μs - Solicitations Mean

μs - Resistances Mean

σM - Margin Standard Deviation

σr - Resistances Standard Deviation

σs - Solicitations Standard Deviation

LIST OF FIGURES

FIGURE 1: MEPDG DESIGN PROCESS FOR FLEXIBLE PAVEMENTS NCHRP (2004A) 37
FIGURE 2 FATIGUE FAILURE IN A PAVEMENT, PRIEST & TIMM (2006) 39
FIGURE 3: SENSITIVITY OF ONE EXAMPLE OF FLEXIBLE PAVEMENT DESIGN (FHWA 2006) .. 42
FIGURE 4: RELIABILITY CONCEPT IN THE MEPDG ARA (2004). 46
FIGURE 5 TYPES OF AXLES OF TRUCK FLEET PRESENT IN HIGHWAY ROADS IN BRAZIL, DNIT (2007) 53
FIGURE 6: MAKES A RELATION THAT AS AXLE OVERLOAD INCREASES PAVEMENT LIFE DECREASES, PINTO & PREUSSLER (2002) 57
FIGURE 7: FLEET REPRESENTATIVE VEHICLE FACTORS OVER THE YEARS OF THE RESEARCH VALE *ET AL.* (2018) 58
FIGURE 8: SIMPLIFIED DIAGRAM OF FORCES ACTING ON A ROTATING WHEEL (NCHRP, 2009) 59
FIGURE 9 MEASURED TIRE IMPRINT FOR ONE TIRE OF DUAL ASSEMBLY AL-QADI ET AL. (2005) 59
FIGURE 10 BOUSSINESQ'S EQUATION IN POLAR COORDINATES, ULLIDTA (1987) 65
FIGURE 11: VALUES OF I_B FOR USE IN THE BOUSSINESQ FORMULA 65
FIGURE 12: TWO-LAYER SYSTEM, BURMISTER (1943) 67
FIGURE 13: INFINITESIMAL VOLUME ELEMENT IN CYLINDRICAL COORDINATES, OLIVEIRA (2013) 68
FIGURE 14 : DIAGRAM OF SHEAR STRESSES ACTING IN A LAYER SYSTEM HUANG (2004) ... 69
FIGURE 15: UNCERTAINTY IN PAVEMENT LIFE-CYCLE, XIAO (2012) 71
FIGURE 16: PROBABILITY DISTRIBUTION OF C AND D, KENIS & WANG (2004) 75
FIGURE 17 FUNDAMENTALS OF RISK EVALUATIONS, HALDAR & MAHADEVAN (2000). 76
FIGURE 18: PROBABILITY DENSITY FUNCTION, ADAPTED FROM BORGES ET AL. (1985). 79
FIGURE 19: HASOFER-LIND RELIABILITY INDEX FOR LINEAR LIMIT STATE FUNCTION, HALDAR & MAHADEVAN, 2000 79
FIGURE 20 MEPADS SOFTWARE INTERFACE WHERE PAVEMENT STRUCTURE CHARACTERISTICS ARE STABLISHED 91
FIGURE 21 MEPADS LOADS AND EVALUATION POINTS INTERFACE 91
FIGURE 22 RESPONSE POINTS IN PAVEMENT STRUCTURES ACCORDING TO THE AXLE TYPE 92
FIGURE 23 STRESSES AND STRAIN OBTAINED BY THE MEPADS SOFTWARE 93
FIGURE 24: CONTOUR PLOT OF THE VERTICAL PLANE OF STRUCTURE A, TANDEM AXLE ... 94
FIGURE 25 RELIABILITY INDEX CONCEPT 96
FIGURE 26 SURFACE DISPLACEMENTS IN STRUCTURE A 100
FIGURE 27 SURFACE DISPLACEMENTS IN STRUCTURE B 100
FIGURE 28 SURFACE DISPLACEMENTS IN STRUCTURE C 101
FIGURE 29 SURFACE DISPLACEMENTS IN STRUCTURE D 101

FIGURE 30 MINIMUM SURFACE DISPLACEMENTS BY AXLE TYPE 102
FIGURE 31 MAXIMUM SURFACE DISPLACEMENTS BY AXLE TYPE 102
FIGURE 32 AVERAGE RATE OF INCREASE FOR SURFACE DISPLACEMENTS 103
FIGURE 33 HORIZONTAL STRAIN AT THE BOTTOM OF THE ASPHALT LAYER IN STRUCTURE A 103
FIGURE 34 HORIZONTAL STRAIN AT THE BOTTOM OF THE ASPHALT LAYER IN STRUCTURE B 104
FIGURE 35 HORIZONTAL STRAIN AT THE BOTTOM OF THE ASPHALT LAYER IN STRUCTURE C 104
FIGURE 36 HORIZONTAL STRAIN AT THE BOTTOM OF THE ASPHALT LAYER IN STRUCTURE D 105
FIGURE 37 MINIMUM HORIZONTAL STRAIN AT THE BOTTOM OF THE ASPHALT LAYER BY AXLE TYPE 106
FIGURE 38 MAXIMUM HORIZONTAL STRAIN AT THE BOTTOM OF THE ASPHALT LAYER BY AXLE TYPE 106
FIGURE 39 AVERAGE RATE OF INCREASE FOR HORIZONTAL STRAIN AT THE BOTTOM OF THE ASPHALT LAYER 107
FIGURE 40 VERTICAL STRAIN AT THE BOTTOM OF THE ASPHALT LAYER IN STRUCTURE A107
FIGURE 41 VERTICAL STRAIN AT THE BOTTOM OF THE ASPHALT LAYER IN STRUCTURE B108
FIGURE 42 VERTICAL STRAIN AT THE BOTTOM OF THE ASPHALT LAYER IN STRUCTURE C 108
FIGURE 43 VERTICAL STRAIN AT THE BOTTOM OF THE ASPHALT LAYER IN STRUCTURE D 109
FIGURE 44 MINIMUM VERTICAL STRAIN AT THE BOTTOM OF THE ASPHALT LAYER BY AXLE TYPE 109
FIGURE 45 MINIMUM VERTICAL STRAIN AT THE BOTTOM OF THE ASPHALT LAYER BY AXLE TYPE 110
FIGURE 46 AVERAGE RATE OF INCREASE FOR HORIZONTAL STRAIN AT THE BOTTOM OF THE ASPHALT LAYER 110
FIGURE 47 VERTICAL STRAIN AT THE TOP OF THE SUBGRADE IN STRUCTURE A 111
FIGURE 48 VERTICAL STRAIN AT THE TOP OF THE SUBGRADE IN STRUCTURE B 112
FIGURE 49 VERTICAL STRAIN AT THE TOP OF THE SUBGRADE IN STRUCTURE C 112
FIGURE 50 VERTICAL STRAIN AT THE TOP OF THE SUBGRADE IN STRUCTURE D 113
FIGURE 51 MINIMUM VERTICAL STRAIN AT THE TOP OF THE SUBGRADE BY AXLE TYPE ... 113
FIGURE 52 MAXIMUM VERTICAL STRAIN AT THE TOP OF THE SUBGRADE BY AXLE TYPE .. 113
FIGURE 53 AVERAGE RATE OF INCREASE FOR HORIZONTAL STRAIN AT THE BOTTOM OF THE ASPHALT LAYER 114
FIGURE 54 SURFACE DISPLACEMENTS VS ASPHALT LAYER THICKNESSES 115
FIGURE 55 HORIZONTAL STRAIN AT THE BOTTOM OF THE ASPHALT LAYER VS THICKNESSES 115

FIGURE 56 VERTICAL STRAIN AT THE BOTTOM OF THE ASPHALT LAYER VS THICKNESSES 116
FIGURE 57 VERTICAL STRAIN AT THE BOTTOM OF THE ASPHALT LAYER VS THICKNESSES 116
FIGURE 58 PAVEMENT LIFE REDUCTION IN TERMS OF DECREASE PERCENTAGES OF CRITICAL N NUMBERS 119
FIGURE 59 HISTOGRAMS FOR RESISTANCE, SOLICITATION, RELIABILITY INDEX, AND PROBABILITY OF FAILURE DATA 120
FIGURE 60 HISTOGRAMS FOR RESISTANCE, SOLICITATION, RELIABILITY INDEX, AND PROBABILITY OF FAILURE DATA (TRANSFORMED) 121
FIGURE 61 RELIABILITY INDEX (B) VS PROBABILITY OF FAILURE (PF) 122
FIGURE 62 RELIABILITY INDICES VS SAFETY FACTORS FOR THE STRUCTURE A 124
FIGURE 63 PROBABILITIES OF FAILURE VS SAFETY FACTORS FOR THE STRUCTURE A 125
FIGURE 64 RELIABILITY INDICES VS SAFETY FACTORS FOR THE STRUCTURE B 125
FIGURE 65 PROBABILITIES OF FAILURE VS SAFETY FACTORS FOR THE STRUCTURE B 126
FIGURE 66 RELIABILITY INDICES VS SAFETY FACTORS FOR THE STRUCTURE C 126
FIGURE 67 PROBABILITIES OF FAILURE VS SAFETY FACTORS FOR THE STRUCTURE C 127
FIGURE 68 RELIABILITY INDICES VS SAFETY FACTORS FOR THE STRUCTURE D 127
FIGURE 69 PROBABILITIES OF FAILURE VS SAFETY FACTORS FOR THE STRUCTURE D 128
FIGURE 70 EHT1 STRAIN BY ASPHALT & BASE LAYER THICKNESSES 133
FIGURE 71 EVC_M STRAIN BY ASPHALT & BASE LAYER THICKNESSES 134
FIGURE 72 CRITICAL RESISTANCES BY ASPHALT & BASE LAYER THICKNESSES 134
FIGURE 73 SAMPLE SPREADSHEET TO CALCULATE THE PF OF A CERTAIN PAVEMENT STRUCTURE CONFIGURATION 135
FIGURE 74 DOWNGRADE-COLORED-SCALE MATRIX FOR PF VALUES WITH SF BETWEEN 0.20 AND 0.80 137
FIGURE 75 DOWNGRADE-COLORED-SCALE MATRIX FOR PF VALUES WITH SF BETWEEN 2.0 AND 5.0 138

TABLE LIST

TABLE 1 SUGGESTED LEVEL OF RELIABILITY FOR VARIOUS ROAD CLASSIFICATIONS (AASHTO 1986) 42
TABLE 2: SUGGESTED LEVEL OF RELIABILITY FOR FUNCTIONAL CLASSIFICATIONS (AASHTO 1993) 43
TABLE 3: STANDARD NORMAL DEVIATE FOR DIFFERENT LEVELS OF RELIABILITY (AASHTO 1993) 43
TABLE 4: LIMITATIONS ABOUT RELIABILITY IN THE AASHTO (1993) 44
TABLE 5: MAXIMUM PERMITTED WEIGHTS AND DIMENSIONS OF MAJOR VEHICLE CONFIGURATIONS USED IN BRAZIL 48
TABLE 6: DESCRIPTION OF THE TYPES OF AXLES OF TRUCK FLEET PRESENT IN HIGHWAYS/ROADS IN BRAZIL (DNIT 2007). 54
TABLE 7: COMPARISON OF THE MAXIMUM LOAD LIMITS IN BRAZIL, USA AND EUROPA MODIFIED FROM ALBANO (2005) 55
TABLE 8: CONTRAN LOAD TOLERANCE RESOLUTIONS (DNIT, 2007) 56
TABLE 9: LOAD EQUIVALENT FACTORS AASHTO AND USACE, DNIT (2006A) 62
TABLE 10: MULTI-LAYER COMPUTER PROGRAM FOR PAVEMENT ANALYSIS AND DESIGN ... 69
TABLE 11 TARGET RELIABILITY INDICES, USACE (1997) 78
TABLE 12: THICKNESS AND MATERIAL PROPERTIES OF THE FOUR ASPHALT PAVEMENT STRUCTURES 87
TABLE 13: AXLE CONFIGURATION 88
TABLE 14: AXLE CONFIGURATION USED IN THE ANALYSIS 89
TABLE 15 MULTIVARIATE LINEAR REGRESSION MODELS 97
TABLE 16 AVERAGE CYCLES TO FAILURE (N NUMBERS) FOR FATIGUE CRACKING AND RUTTING BY AXLE TYPE 117
TABLE 17 MINIMUM, MAXIMUM, AND AVERAGE CRITICAL N NUMBERS BY STRUCTURE 117
TABLE 18 RMS CRITICAL RESISTANCES (N) VS OVERLOAD (%) BY AXLE TYPE AND STRUCTURE 118
TABLE 19 DESCRIPTIVE STATISTICS FOR SOLICITATIONS, RELIABILITY INDICES, AND PROBABILITIES OF FAILURE 119
TABLE 20 TESTS OF NORMALITY FOR TRANSFORMED VARIABLES 120
TABLE 21 PEARSON CORRELATIONS BETWEEN TRANSFORMED RESISTANCES, SOLICITATIONS, RELIABILITY INDICES (B), AND PROBABILITIES OF FAILURE (PF) 121
TABLE 22 REGRESSION MODELS SUMMARY 122
TABLE 23 REGRESSION COEFFICIENTS 123
TABLE 24 RESIDUAL STATISTICS 123
TABLE 25 THICKNESS AND MATERIAL PROPERTIES OF THE ASPHALT PAVEMENT STRUCTURE 129

TABLE 26 CRITICAL RESISTANCE STATISTICS 135

TABLE OF CONTENTS

1 INTRODUCTION 31

1.1 Motivation 31

1.2 Research Objectives 32

1.3 Dissertation Structure 32

2 LITERATURE REVIEW 35

2.1 Incorporation of Geotechnical Factors in Pavement Design 35

2.1.1 Pavement Design Methodologies 35

2.1.1.1 Empirical Design 35

2.1.1.2 Mechanistic Design 36

2.1.1.3 Mechanistic-Empirical Design 36

2.1.2 Pavement Distress Models 38

2.2 Evolution of Reliability on Pavement Design Methodologies 40

2.2.1 AASHTO 1986 40

2.2.2 AASHTO 1993 42

2.2.3 MEPDG 2004 44

2.2.4 DNIT 2006 46

2.3 Risk and Uncertainties in Pavement Design 47

2.3.1 Traffic Loads 47

2.3.1.1 Vehicle Fleet 48

2.3.1.2 Axle Load Distribution 53

2.3.1.3 Brazilian Maximum Legal Load 55

2.3.1.4 Tire-pavement Interaction 58

2.3.1.5 Load Equivalency Factors 61

2.3.2 Environmental Conditions 63

2.3.3 Structures and Materials 63

2.3.4 Structural Response Models 64

2.3.4.1 Boussinesq's Equation for Point Loads 64

2.3.4.2 Two-layer Theory 66

2.3.4.3 Multi-Layer Theory 67

2.3.4.4 Multi-Layer Computer Program 69

2.3.4.5 Finite Element Method 70

2.3.5 Uncertainties in Reliability Assessment 71

2.4 Reliability **72**
2.4.1 Basic Concepts 73
2.4.2 Measurements 74
2.4.3 Reliability Analysis Methods 78
2.4.3.1 Monte Carlos Simulation Technique 80
2.4.3.2 First Order Reliability Method (FORM) 81
2.4.3.3 First Order Second Moment Method (FOSM) 84
2.4.3.4 Point Estimate Method (PEM) 85

3 METHODOLOGY AND DATA **87**

3.1 Pavement Structures **87**

3.2 Axle Configurations **87**

3.3 Structural Responses **90**

3.4 Cycles to Failure ("N" numbers) **93**

3.5 Reliability Analysis **94**

3.6 Critical Resistance vs Overload **97**

3.7 Statistics **97**

4 RESULTS AND DATA ANALYSIS **99**

4.1 Structural Responses **99**
4.1.1 Surface Displacements or Deflections (δ1) 99
4.1.2 Horizontal Tensile Strain at the Bottom of the Asphalt Layer (εht_1) 103
4.1.3 Vertical Compressive Strain at the Bottom of the Asphalt Layer (εvc_1) 107
4.1.4 Vertical Compressive Strain at the Top of the Subgrade (εvc_m) 111
4.1.5 Structural Responses vs Thickness 114

4.2 Pavement Life Predictions **116**
4.2.1 Asphalt Institute's Cycles to Failure ("N" numbers) 116
4.2.2 Critical Resistance 117
4.2.2.1 Resistances vs Overloads 118

4.3 Reliability Index and Probability of Failure **119**
4.3.1 Descriptive Statistics 119
4.3.2 Pearson Correlations 121
4.3.3 Regression Analysis 122

4.3.4 Reliability Indices (β) and Probabilities of Failure (Pf) by Safety Factors (SF) and Axle Types 124
4.3.4.1 Structure A 124
4.3.4.2 Structure B 125
4.3.4.3 Structure C 126
4.3.4.4 Structure D 127

5 METHOD APPLICATION EXAMPLE 129

5.1 Axle Type and Tire Pressure 129

5.2 Structural Responses 129

5.3 Cycles to Failure 130

5.4 Example Results 132
5.4.1 mePADS Output Data & N numbers 132
5.4.2 Reliability Analysis 135

5.5 Example Conclusions 139

6 CONCLUSIONS 141

6.1 Structural Responses 141

6.2 Pavement Life Predictions 144

6.3 Reliability Index and Probability of Failure 145

6.4 Reliability Indices and Probabilities of Failure by Safety Factors and Axle Types 146

6.5 Final Remarks 147

7 REFERENCES 149

APPENDIX A – SURFACE DISPLACEMENTS 159

APPENDIX B – HORIZONTAL TENSILE STRAIN AT THE BOTTOM OF THE ASPHALT LAYER 165

APPENDIX C – VERTICAL TENSILE STRAIN AT THE BOTTOM OF THE ASPHALT LAYER..... 171

APPENDIX D – VERTICAL COMPRESSIVE STRAIN AT THE TOP OF THE SUBGRADE 177

APPENDIX E – CRITICAL N NUMBERS..... 183

APPENDIX F – CRITICAL RESISTANCE VS OVERLOAD..... 187

APPENDIX G – PAVEMENT LIFE REDUCTION..... 193

APPENDIX H – RESIDUALS STATISTICS 197

1 INTRODUCTION

Achieving durability of pavement structures is crucial not only for Highway Agencies in Brazil but for any other highway authority in the world. Asphalt pavements which are designed for 15-year usage are often highly damaged in the early period. It is difficult to accurate design and predict the life and form of distress of pavement structure because of all the complex variables involved such as traffic prediction, material properties and layer thickness are random, uncertain and deterministic. These variables vary in space and time resulting in a variability in the pavement performance.

From a reliability point of view, most pavement design are designed without taking into consideration reliability as important factor, where in most cases is about 50% higher or lower. On average about one half of all pavement design will fail before the design service life.

1.1 MOTIVATION

The design of civil structures is a very complex process where many factors have to be considered for a given design.

The conventional pavement design is based in deterministic approaches and none of the design input variables are actually deterministic, because of the considerable amount of heterogeneity in the materials, environment and structural properties.

The method preconized by DNIT (2006a) is based on “Design of Flexible Pavements Considering Mixed Loads and Traffic Volume” by Turnbull et al. (1962) where the main purpose is to protect the subgrade layer against shear failure stress. Suzuki et al. (2001, 2004) strongly highlighted the need to incorporate the concept of reliability in pure deterministic Brazilian methods, where most of the pavement are over or under designed even in cases of 99.9% of reliability there is a need to increase the thickness of the granular material between 10 to 20%, this is very important not only the cost of materials, but also to the cost associated with the overall construction, rehabilitation, and maintenance of pavement structures that as rise considerable. Therefore, it is a great responsibility for designer to provide the most accurate predictions so that the

pavement structures being designed perform as they are expected through their design lives.

1.2 RESEARCH OBJECTIVES

The main objective of this research is to develop an alternative approach for a probability-of-failure analysis in flexible pavements based on the reliability concept, in order to capture important aspects that are often ignored in traditional reliability analysis of pavement structures, such as the undersizing or oversizing of structural configurations. Toward this purpose, four representative Brazilian pavement structures were studied in terms of four structural responses that were calculated under the effect of six different axle types, subjected to five overload conditions and to three levels of tire pressure.

In order to achieve this objective, the following tasks must be accomplished:

1. Evaluate surface displacements (δ_1); horizontal tensile strain at the bottom of the asphalt layer (εht_1); vertical compressive strain at the bottom of the asphalt layer (εvc_1); and vertical compressive strain at the top of the subgrade (εvc_m) by single, dual, tandem, tandem-spaced, tridem, and tridem-spaced axles subjected to 0; 7.5; 10; 20; and 30% of overload and to 550, 690, and 830 KPa of tire pressure for each pavement structure proposed;
2. Analyze the effect of axle type, overload percentage, and tire pressure on pavement life predictions in terms of Asphalt Institute's cycles to failure ("N" numbers);
3. Calculate and analyze Reliability Indices (β) and Probabilities of Failure (Pf) from critical resistances and solicitations as a function of a variety of Safety Factors (SF); and,
4. Exemplify a simple application of the reliability-based analysis in pavement design, based on resistances and solicitations, and show its potential as a practical tool in the engineering practice.

1.3 DISSERTATION STRUCTURE

This dissertation is organized as follows:

- Chapter 1 explains the motivations that led to develop this research; describes the research objectives; and presents the structure of the dissertation;
- Chapter 2 summarizes the literature review on the incorporation of geotechnical factors in pavement design; the evolution of reliability on pavement design methodologies, the risk and uncertainties in pavement design; and the reliability concepts;
- Chapter 3 describes the methodology and data used in this research. The pavement structures studied; axle configurations; structural responses; cycles to failure; reliability analysis process; critical resistances vs overload percentages; and data statistics process;
- Chapter 4 discusses the data analysis and findings of the study. This chapter comprises the following sections: structural responses; pavement life predictions; and reliability index and probability of failure. Also, this chapter include statistical comparisons in the form of Pearson´s correlations and regression analyses;
- Chapter 5 presents a practical example of the reliability-based method developed in this thesis to determine the Pf of a flexible pavement, results are shown in the form of a red-yellow-green downgrade-colored-scale matrix that improves data visualization and facilitates the decision-making process in pavement design.
- Chapter 6 presents the conclusions of the research and some recommendations for further studies.
- Chapter 7 lists the references used in this dissertation as well as appendices section starts by presenting charts and tables that complement the visualization of the data presented in chapter 4.

2 LITERATURE REVIEW

2.1 INCORPORATION OF GEOTECHNICAL FACTORS IN PAVEMENT DESIGN

2.1.1 Pavement Design Methodologies

The design of flexible pavement structure is a complex task, by the number of variables include; it is very common to consider variables as fixed or deterministic. Traffic loading is heterogeneous mix of vehicles, axles types, and axle loads with climate distribution that may vary with time through the day and over the pavement.

The empirical, mechanistic and mechanistic-empirical design are frequently used to identify general methods of pavement design.

2.1.1.1 Empirical Design

Many pavement design procedures adopted an empirical design approach. Where parameters input such as traffic loads, materials properties, layer configuration, climatic variations were obtained through engineering experience, experimental observation or a combination of both. To overcome this limitation, designer shifted toward mechanistic design model relating pavement structural behavior and performance to traffic loading and environmental influences based on theories of mechanics.

Pavement materials have complex characteristics such as nonlinearities, time, temperature, dependency and anisotropy. The simple behavior to be assumed is isotropic linear elastic which in most cases does not characterize adequately the pavement condition.

The principal advantages of empirical design approach are that they are simple to apply and are based on actual-real world date. The mayor disadvantage is that the empirical relationships are limited to the conditions in the underlying data from which they were concluded. New materials, construction procedures and the traffic characteristics cannot be incorporated into empirical design procedures.

2.1.1.2 Mechanistic Design

This method basically consists of a two-step process. The first step consists of a mechanistic determination of the pavement response by simplification of mathematical formulations such as a multi-layer linear elastic analysis, or finite element analysis. The second step is estimating the pavement performance as a function of the previously estimated pavement responses by means of field and laboratory data. The mechanistic approach for flexible pavements has its roots in Burmister development during the 1940s with the multilayer theory to compute stress, strain and deflections in pavement structures.

The key element of this design method is the accurate prediction of the response of the pavement materials. The elasticity-based solutions by Boussinesq, Burmister and Westergaard were an important first step. Nonetheless the linear elastic material behavior assumption underlying these solutions means that they will unable to predict the nonlinear and inelastic cracking, permanent deformation and other distresses of interest in pavement system.

2.1.1.3 Mechanistic-Empirical Design

This method combines both mechanistic and empirical approaches. The mechanistic element is a mechanics-based determination of pavement responses such as stress, strain and deflections due to loading and environmental influences. These responses are related to the performance of the pavement via empirical distress models. A clear example a linearly elastic mechanics model that can be used to calculate the tensile strain at the bottom of the asphalt layer due to an applied load; this strain is them related to empirically to the accumulation of fatigue cracking distress. The empirical relationship links the mechanistic response of the pavement to its expected performance.

The Mechanistic-Empirical Design Guide for New and Rehabilitated Pavement Structures, NCHRP (2004a), or simply as MEPDG was released under the NCHRP Project 1-37A. MEPDG provides significant benefits over the AASHTO (1993) Guide. A much more realistic characterization of in-service pavement and provides guidelines for designing the common features of flexible, rigid and composite pavement, Li *et al.* (2011). It also has the option for evaluation existing pavements and gives

recommendations for rehabilitation treatments, drainage and foundation improvements.

The MEPDG Software is used to predict the various pavement distresses. To perform pavement analysis using the MEPDG, detailed data on climate, material properties, traffic and the pavement structure is required.

The main steps involved in the procedure for the design of flexible pavement are briefly described as follows:

1. The guide requires as input the details of pavement structure such as traffic, climate and pavement structure, it implements an integrated analysis approach for predicting pavement condition over time (fatigue, rutting and thermal cracking);
2. Allows considerations of special loadings with multiple tires or axles;
3. Provides a means for evaluating design variability and reliability.
4. If the design does not meet the criteria, another pavement configuration shall be analyzed until a criterion is met, predicted distress values and reliability are to be observed to avoid over designed pavement structures.

Figure 1 is an illustration of the design process for flexible pavements.

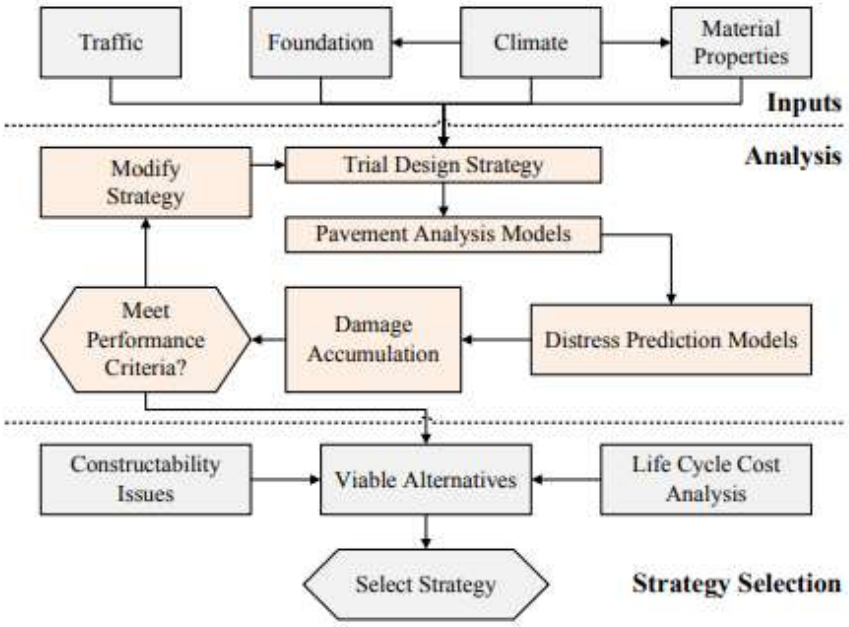

Figure 1: MEPDG Design Process for Flexible Pavements NCHRP (2004a)

An important advancement in the MEPDG is the characterization of design inputs. Due to the complexity of inputs such as traffic loadings, environmental conditions and material characterization in detailed form, the guide introduces a hierarchal approach for design inputs according to the availability and quality of the inputs as mentioned above:

Level 1: Data is required such as traffic data, material properties and environmental information. This level provides the highest level of accuracy and the lowest level of uncertainty or error, according to the NCHRP 1-37A Report this level is typically used for designing heavily trafficked roads where premature failure is economically undesirable.

Level 2: Intermediate level of accuracy, would be selected possibly from an agency database. This level can be used to justify when there is no equipment and resources that would be required at level 1, in this way regressions analyzes are used. Prozzi & Hong (2005) point out that in this level it is important the axle load spectral with specific vehicle classification and category. Inputs are obtained through empirical correlations.

Level 3: Lowest level of accuracy, values of the region analyze are used average. Traffic data are obtained from weighing, manual counts or automatic vehicle or even from local experience. According to Mehta *et al.* (2008) this level has standard values national and regional; an uneconomical design can be generated, since the values provided by the State Road Agencies are not always standard values. This level would be selected where there are minimal consequences of early failure, such as low volume roads, Li *et at.* (2011).

2.1.2 Pavement Distress Models

The MEPDG incorporates the main models to evaluate stress and strain in pavement (horizontal and vertical). The two main distresses are fatigue cracking and permanent deformation. The horizontal tensile strain $(\varepsilon ht_1)_{at}$ the bottom of the asphalt layer and the vertical compression strain at the top of the subgrade (εvc_m) are critical parameters for fatigue and rutting failure.

a) Fatigue Failure

As observed in Figure 2, Fatigue is the most common type of flexible pavement distress, in fact the major one. In this distress series of interconnected cracks appears due to the fatigue failure of the hot asphalt mix surface when it experiences repeated traffic, another factor that can contribute to this type of distress is aging, temperature changes or inadequate drainage. Most of the cracks start at the bottom and propagate upwards to the top, which is also termed as “bottom up” fatigue cracking. Recent studies demonstrated that in most cases, cracks start at the pavement surface on the wheel path and propagate downward, Myers *et al.* (2001).

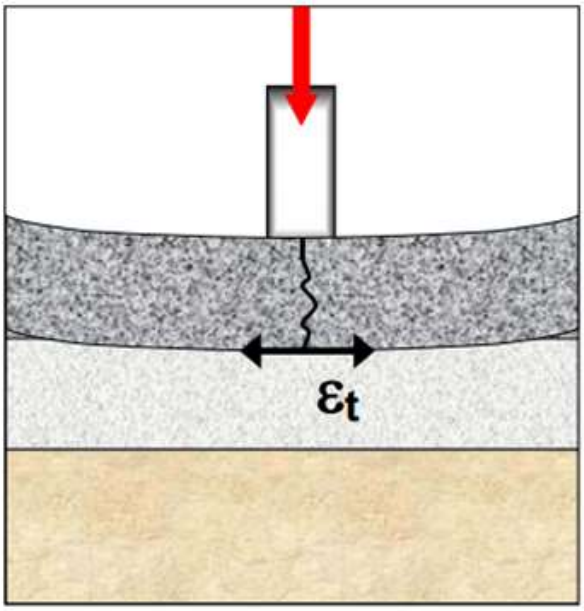

Figure 2 Fatigue failure in a pavement, Priest & Timm (2006)

At first stage is reached when the asphalt layer fails completely due to failure. This type of cracks is identified by its alligator skip shape.

The empirical equation for fatigue failure (N_F) suggested by the Asphalt Institute (Asphalt Institute, 1999) and used for hot mix asphalt is presented in Equation 1:

(1)

$$N_F = 0.0796 * \left(\frac{1}{\varepsilon ht_1}\right)^{3.291} * \left(\frac{1}{E_1}\right)^{0.854}$$

In which, ɛht₁ is the horizontal tensile strain developed at the bottom of the asphalt layer due to traffic load and E_1 is the modulus of elasticity of the asphalt layer.

b) Rutting Failure

Rutting is the permanent deformation of the pavement due to load application of traffic along its wheel path. The vertical compression strain at the top of the sub-base is assumed as the index of rutting to occur in a pavement.

The numbers of standard axle load repetitions sustained by the pavement before reaching the failure (N_R) is known as rutting life.

The empirical model suggested by the Asphalt Institute (1999) is described in Equation 2:

$$N_R = (1.365 * 10^{-9}) * \left(\frac{1}{\varepsilon vc_m}\right)^{4.477} \quad (2)$$

In which εvc_m is the vertical compression strain at the top of the subgrade.

In general, stress and strain values calculated using several approaches such as elastic solution; finite element method; and response of surface method, among others.

2.2 Evolution of Reliability on Pavement Design Methodologies

2.2.1 AASHTO 1986

Southgate (1991) cited that in AASHTO (1986) Guide identify fourteen major new considerations relating to the structural design of pavements. These considerations are: (1) Reliability, (2) Resilient Modulus, (3) Resilient modulus of flexible pavement, (4) Drainage, (5) Improved environmental considerations, (6) Tie concrete shoulders and/or widened lanes, (7) sub-base erosion for rigid pavements, (8) Life cycle cost analyses, (9) Pavement Rehabilitation, (10) Pavement Management, (11) Extension of load equivalency data, (12) Improved traffic data, (13) Design of pavement for low volume roads, (14) State of knowledge on mechanistic empirical design concepts.

Xiao (2012) stated that the AASHTO (1986) Guide include the reliability factor into the design, expanded treatment of rehabilitation (both with and without overlays) and life cycle cost analysis.

The enhancements to the flexible pavement design procedures in the AASHTO (1986) Guide Included the following:

- The use of the resilient modulus for determining the structural layer coefficients for both stabilized and unstabilized unbound materials in flexible pavements. The structural layer coefficients a_2 for base and a_3 and subbase materials are estimated via correlations with the resilient modulus. It is important to remember that this relations for the structural layer coefficient are mainly empirical and are based primarily on engineering judgment with limited amount of data.
- Guidance for the design of subsurface drainage systems and modifications to the flexible pavement design equations to take advantage of the improvements performance due to a good drainage. The main benefits of drainage are incorporated into the structural number via empirical drainage coefficients as observed in Equation 3:

$$SN = a_1 D_1 + a_2 D_2 m_2 + a_3 D_3 m_3 \quad (3)$$

Where SN is the structural number, a_1, a_2, a_3 are the layer coefficients, D_1, D_2 and D_3 thicknesses of asphalt layer and m_2 and m_3 are the drainage coefficients for the base and sub base layers.

The modified version of Equation 1 for flexible pavements employed in the AASHTO (1986) Guide follows Equation 4:

$$\log_{10}(W_{18}) = Z_R S_0 + 9.36 \log_{10}(SN+1) - 0.20 + \frac{\log_{10}\left(\frac{\Delta PSI}{4.2-1.5}\right)}{0.40 + \frac{1094}{(SN+1)^{5.19}}} + 2.32 \log_{10}(MR) - 8.07 \quad (4)$$

In which W_{18} is the predicted number of 18-kip equivalent single axle load application; Z_R is a standard normal deviate; S_o is a measure of the overall uncertainty or variability of the design inputs and performance predictions; M_R is the subgrade resilient modulus; SN is the structural number; and ΔPSI is the difference between the initial serviceability index and the terminal serviceability index.

Guide incorporates the normal deviate as a function of the design reliability level (Z_R) and the overall standard deviation (S_0) is a measure of the overall uncertainty or variability of the prediction.

In the AASHTO (1986) there is the recommendation for design reliability for different road categories as presented in Table 1:

Table 1 Suggested level of reliability for various road classifications (AASHTO 1986)

Functional Classification	Recommended Level of Reliability (%)	
	Urban	Rural
Interstate and other freeways	85-99.90	80-99.9
Principal arterials	80-99	75-95
Collectors	80-95	75-95
Local	50-80	50-80

In 3 can be seen an example of sensitivity analysis of flexible pavement design (FHWA, 2006), where it can be clearly appreciated that for higher reliability levels increasing from 50% to 99.9% increase the Structural Number and the cost for the pavement by approximately 50%.

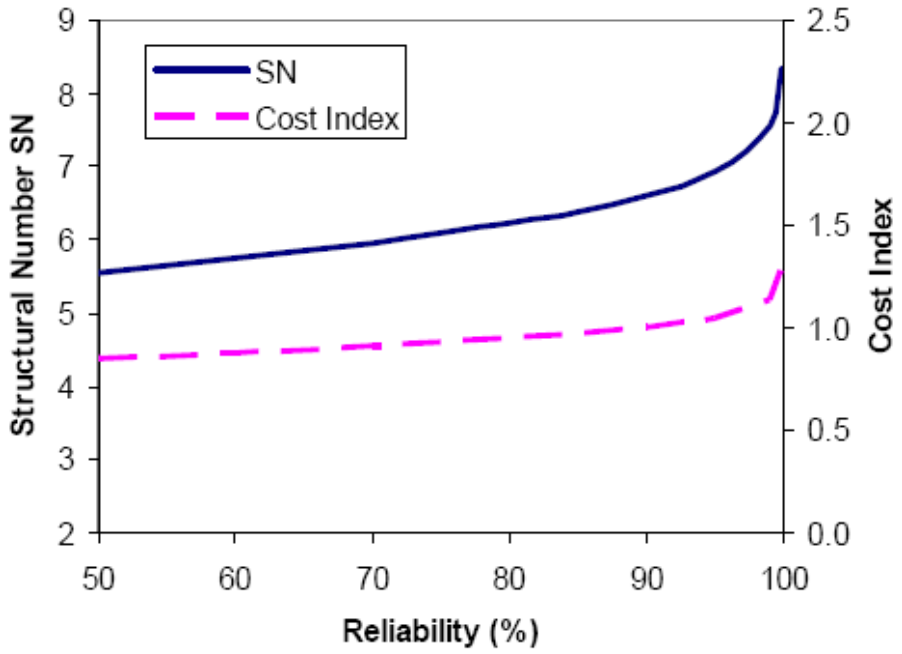

Figure 3: Sensitivity of one example of flexible pavement design (FHWA 2006)

2.2.2 AASHTO 1993

Modifications incorporated into the AASHTO (1993) guide included major revisions of the overlay design procedures. Xiao (2012) mentioned that in this guide traffic was simplified with equivalent single axle load (ESAL) and the design output is the structural number (SN) for flexible pavement. AASHTO (1993) also cites the standard normal deviate Z_R correlated to the level of reliability determined by designer according to Tables 2 and 3, the combined standard error of the traffic and the normal variation in pavement performance prediction S_o (standard deviation). The suggested range of S_o values in AASHTO (1993) are 0.40 to 0.50 for flexible pavement, and 0.30 to 0.40 for rigid pavement.

Table 2: Suggested Level of Reliability for Functional Classifications (AASHTO 1993)

Functional Classification	Recommended Level of Reliability	
	Urban	Rural
Interstate and other freeways	85-99.90	80-99.90
Principal arterials	80-99	75-95
Collectors	80-95	75-95
Local	50-80	50-80

Table 3: Standard Normal Deviate for different levels of reliability (AASHTO 1993)

Reliability (%)	Standard Normal Deviate ($\boldsymbol{Z_R}$)	Reliability (%)	Standard Normal Deviate ($\boldsymbol{Z_R}$)
50	0	93	-1.476
60	-0.253	94	-1.555
70	-0.524	95	-1.645
75	-0.674	96	-1.751
80	-0.841	97	-1.881
85	-1.037	98	-2.054
90	-1.282	99	-2.327
91	-1.340	99.90	-3.090
92	-1.405	99.99	-3.750

The higher reliability should be considered, depending on the traffic volume as it increases, reliability should be increased, allowing to set the level of certainty in the design.

Mentioned by Bekele (2011), the design procedure has a probabilistic approach that assumes that all the parameters to be corresponding mean values. The uncertainties in the local traffic prediction makes it important that the overall Standard Deviation (S_0) to be included in the design. As well as the standard deviation in the Standard Normal Deviate (Z_R).

For a reliability level (R), the reliability factor (FR) according with AASHTO (1993) is defined as follows in Equation 5

$$FR + 10^{Z_R * S_0} \tag{5}$$

Where $\mathbf{Z_R}$ is the standard is normal deviate and $\mathbf{S_0}$ is the overall standard deviation and should be selected to represent the local conditions.

Xiao (2012) mentioned that in AASHTO (1993) the only effective way to achieve the reliability requirement was making a pavement thicker, not considering other techniques as reducing the possibility of pavement rutting by subgrade reinforcement.

The AASHTO (1993) approach has certain limitations encountered by the following authors (Table 4):

Table 4: Limitations about reliability in the AASHTO (1993)

Author	Limitation
Prozzi *et al*. (2005)	By analyzing the reliability of AASHTO method design by means of simulations, the researchers consider the thickness of each different pavement layer and weekly traffic as random variables, they found that the AASHTO reliability level usually differs significantly from the actual reliability of the pavement structure, in some cases by as much as 40%
Rogness (1988)	The AASHTO Guide does not allow considering reliability in the stage of the construction process, which make reliability set to be a fixed level for the entire pavement structure, but it is impossible to assign different variability to each pavement layer individually.
NCHRP (2000)	Suggested a different procedure of estimating the reliability that consisted of two steps Load (performance of pavement structure is determined) and Resistance Factor Design (LRFD) (reliability is estimated by means of analytical estimates) approach, similar to the ones applied in the design of bridge and others concrete or metal structures.
Kulkarni (1994)	Advised replacing the $Z_R S_0$ term in the AASHTO design equations by a safety margin that is a function of previously assumed distributions of the Wt (supplied capacity) and wt (load applied to the pavement structure). Z_R and S_0 were used design factors, FR with the predicted total traffic, represented by ESAL's, and this multiplication could produce a large number of traffic loads that were beyond the range applied at the AASHO Road Test (Guide was based)
Xiao (2012)	Sensitivity analysis equation are not sensitive at S_0 and Z_R when reliability is lower than 95% Higher level of reliability requires a larger SN or D, these limitations consider that the only way to fulfill the reliability requirement is to make pavement thicker.
Moreno et al. (2017)	Method is deterministic and don't take into consideration the uncertainties in the design, construction and operation, where expected performance of the solution cannot be guaranteed.

2.2.3 MEPDG 2004

Mechanistic Empirical Pavement Design Guide (MEPDG), reliability is defined as the probability that the pavement distress will be less than the critical level of distress over the design period (Equation 6).

$$\mathrm{R} = \mathrm{P}[Predicted\ distress\ < critical\ distress\ level] \quad (6)$$

In the MEPDG the following steps must be followed.

- Before creating a pavement structure, the MEPDG uses an initial assumption of a trial pavement structure where it considers site conditions: structures, properties of materials, traffic levels and climate. As well as some basic details to identify the project level design, acceptable limits of the key distresses and the reliability targets for each of these distresses over the pavement life.
- Them the software computes pavement responses to load (stress and strain) induced by traffic loads, which are used to compute damage (distresses and loss of rideability) and the reliability targets are incorporate.
- If the trial design fails to meet the performance and reliability requirements, the designer has to check the initial trial input and perform the analysis again, until it meets the designer specified performance criteria.

As cited by Xiao (2012), a flexible pavement design may pass the fatigue cracking, thermal cracking and smoothness (International Roughness Index - IRI) criteria but fail the rutting at the desired level of reliability, them it is possible to revise the design to satisfy the rutting requirements by increasing surface or base thickness or changing the asphalt mixture design.

Luo *et al*. (2014) commented that the MEPDG is not a single closed form solution. Recent approaches for estimating reliability in the MEPDG are still deficient. Hall et al. (2012). Many researchers have made significant contributions to develop the reliability base framework for MEPDG, Hall et al. (2014); Banerjee et al. (2009); Retherford & McDonald (2010); Tarefder et. al (2010); Thyagarajan et al. (2011); McInvale et al. (2012); Luo et al. (2013).

Xiao (2012) mentioned that from the user's perspective, reliability in MEPDG was the same as in the AASHTO (1993) (see Figure 4) with the only difference that in the MEPDG the reliability overall performance (Present Serviceability Index – PSI) was broken down into several distresses.

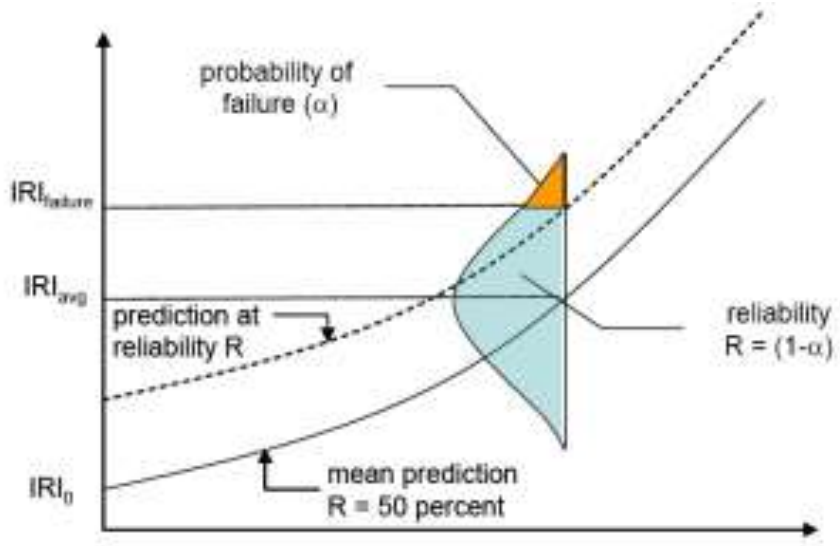

Figure 4: Reliability Concept in the MEPDG Ara (2004).

A terminal level for a IRI of 2.5 m/km may be associated with a chosen reliability level of 90% but cracking for rehabilitation of say 100% may be only accompanied by a 50% of reliability level indicating that there is a 50% possibility that the predicted distress in this case IRI will be higher or lower than this value. As mentioned by Dalla (2015) for practically all projects, the designer will need a reliability higher than 50% only this way will be possible to meet the performance criteria over the design life. On the design process is an iterative process that start with a trial design and finish with predicted distress levels that meet the acceptable limits and desired level of reliability for a specific design.

2.2.4 DNIT 2006

The DNER (DNIT, 2006a) proposed by the Brazilian Engineer Murillo Lopes de Souza in the 1960s. This method is based on Turnbull et al. (1962) from the USACE and adopts the deterministic approach and conclusions from AASHTO Road Test that since its first version uses probabilistic concepts.

Suzuki *et al*. (2001, 2004) cited the necessity to incorporate the concept of reliability in the purely deterministic Brazilian pavement design. For a reliability of 99.9% (determined by the DNIT method) there is a mandatory to increase the thickness in terms of granular material between 10% and 20%.

Santos et al. (2016) cited that the essentially deterministic results in structures with the success probability of the order of 50% and in some situations, this may not be sufficient.

Probabilistic method explored in the pavement analysis programs in Brazil are:

- Rosenblueth Method used by Motta (1991);
- Monte Carlos simulations in the Ayra Program by Ayres (1997);
- Reliability analyzes of the result of the FEPAVE & Pave programs used by Franco (2000);
- Determining reliability on the design of asphalt pavement is directly linked to the variability of parameters of the design traffic and the admissible traffic used by Santos (2011).

Deterministic design is used asphalt pavement methods in Brazil. The Brazilian design method mostly used is DNIT *(Departamento Nacional de Infraestructura de Transportes)*, and the DER/SP *(Departamento de Estradas de Rodagem do Estado de Sao Paulo)* this two methods are based in a deterministic approach.

The design method of the USACE is purely deterministic (USACE, 1996), and requires only a value, typically the mean value for each input parameter and ignores its variation during the design process. The most important task from this method is to protect the subgrade layer against shear failure stress.

2.3 RISK AND UNCERTAINTIES IN PAVEMENT DESIGN

2.3.1 Traffic Loads

Pavement are designed to resist the action of traffic over a certain period of time, a combination of various types of vehicles will pass on the design road and numerous factors will influence pavement damage. Traffic loading on road pavements is characterized by different types of vehicles with variations in load, magnitude, number of axles, axles configuration (single, tandem, tridem), wheel configurations (single, dual) and inflation pressures. These loads are distributed through the pavement structure to the subgrade soil. This combination contributes and is responsible for pavement fatigue cracking and rutting, which shortens the pavement service life and increases agency cost to maintain pavement condition at an acceptable level.

According to Yoder & Witczak (1991) and Huang (1993), traffic is the main factor when designing a pavement structure. The main factors to evaluate the structure of a pavement design are traffic volume and the type of vehicle. Road traffic load is quite diverse in types of vehicles and load being transported. One of the main difficulties to design the pavement is to anticipate the evolution of traffic over time and the destructive power, relatively, of the various axles loads, Medina & Motta (2005).

2.3.1.1 Vehicle Fleet

The Brazilian classification of vehicles is presented. According to DNIT (2005) there are five basic types of vehicles for pavement design (see Table 5):

• *Passenger Car (PC):* light vehicles, similar in geometric and operational terms with the automobile, including vans, utilities, pick-ups and the like;

• *Rigid commercial vehicle (CO):* these are non-articulated vehicles composed of a simple tractor unit; encompass conventional trucks and buses of two axles and six wheels.

• *Long-distance buses (O):* this group represents the commercial vehicles with rigid structures. Include tour buses and long trucks, generally of three axles and dimensions superior to the vehicle type CO;

• *Semi-trailers (ST):* Articulated load vehicles, single traction unit compounds and a semi-trailer without a front axle;

• *Trailers (T):* road haulage vehicles with trailers; It is composed of a simple tractor unit, a semi-trailer and a trailer and is known as *bitrem*.

Table 5: Maximum permitted weights and dimensions of major vehicle configurations used in Brazil

Type	***No. axles***	***PBT/CMT Max(t)***	***Characteristics***	***Class***
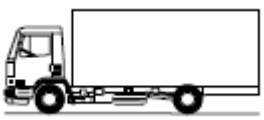	2	16 (17,6)	single front axle with tire tread simple maximum load (ML)= 6t, back axle with single axle and double tire tread and ML= 10t, spacing between axles is d12 ≤ 3.5m	2C

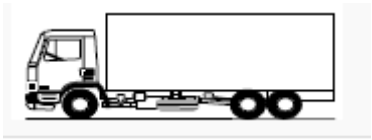	3	23 (25,30)	single front axle with tire tread simple maximum load (ML)= 6t, back with group of axles in double tandem and ML= 17t, spacing between axles is d12>2.40m 1.20<d23≤ 2.40m	3C
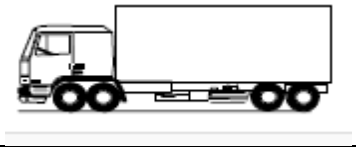	4	29 (31,90)	Set of directional axles maximum load (ML)= 12t, back double tandem and ML= 17t, spacing between axles is 1.20<d34≤ 2.40m	4CD
	4	36 (39,6)	single front axle maximum load (ML)= 6t, second axle third and fourth axle is a double axle with ML=10t each spacing between axles is d12, d23, d34 >2.40 m	2C2
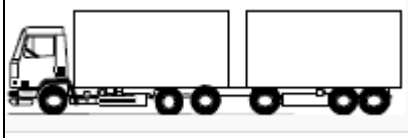	6	50(55)	single front axle maximum load (ML)= 6t, second and third axle double tandem ML=17t, fourth double axle with double tire tread ML=10t fifth and sixth axle is double tandem with ML=17t each spacing between axles is d12, d23, d45 >2,40m 1.20m<d23; d56≤2.40m	3D3
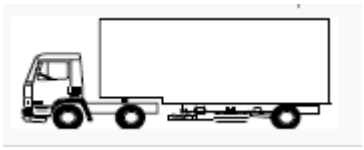	3	26 (28.6)	single front axle with tire tread simple maximum load (ML)= 6t, second axle with double axle and double tire tread and ML= 10t and third axle with double axle and double tire tread and ML= 10t spacing between axles d12, d23 >2.40m	2S1
	4	33 (36.30)	single front axle with single tire tread maximum load (ML)= 6t, second axle with double axle and double tire tread and ML= 10t and third and fourth axle is double tandem and ML= 17t spacing between axles d12, d23 >2.40m 1.20m<d34≤2.40m	2S2

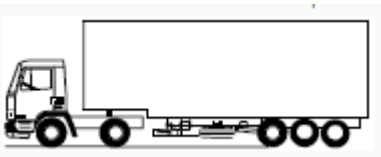	5	41.50 (45.65)	single front axle with single tire tread maximum load (ML)= 6t, second axle with double axle and double tire tread and ML= 10t and third, fourth and fifth axle is triple tandem and ML= 25.5t spacing between axles d12, d23 >2.40m 1.20<d34, d45≤2.40m	2S3
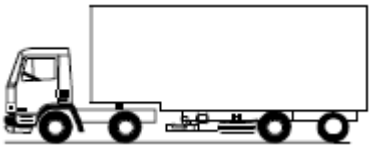	4	36(39. 6)	single front axle with single tire tread maximum load (ML)= 6t, second, third and fourth axles with double axle and double tire tread and ML= 10t spacing between axles d12, d23 >2,40m	2I2
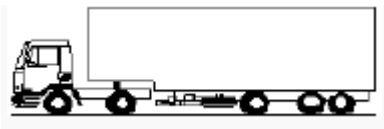	5	43(47. 30)	single front axle with single tire tread maximum load (ML)= 6t, second and third axles with double axle and double tire tread and ML= 10t and fourth and fifth axle is double tandem and ML= 17t spacing between axles d12, d23 >2,40m 1.20<d45≤2.40m	2J3
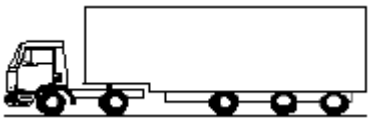	5	46 (57,2)	single front axle with single tire tread maximum load (ML)= 6t, second, third, fourth and fifth axles with double axle and double tire tread and ML= 10t each one spacing between axles d12, d23 d34, d45>2,40m 1.20<d34, d45≤2.40m	2I3
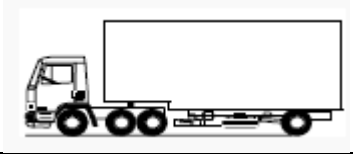	4	33 (36,30)	single front axle with single tire tread maximum load (ML)= 6t, second and third axles with double tandem ML= 17t and fourth axle is double axle and ML= 10t spacing between axles d12, d34 >2,40m 1.20<d23≤2.40m	3S1
	4	40(44)	single front axle with single tire tread maximum load (ML)= 6t, second and third axles with double tandem ML= 17t and fourth and fifth axle is double axle and ML= 17t spacing between axles d12, d34 >2.40m 1.20<d23, d45≤2.40m	3S2

	6	48.5(53,13)	single front axle with single tire tread maximum load (ML)= 6t, second and third axles with double tandem ML= 17t and fourth, fifth and sixth axles are triple tandem ML= 25,5t spacing between axles d12, d34 >2.40m 1.20<d23, d45, d56≤2.40m	3S3
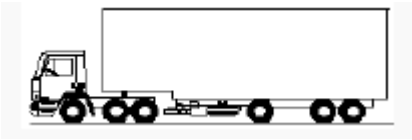	6	50(55)	single front axle with single tire tread maximum load (ML)= 6t, second and third axles with double tandem ML= 17t and fourth axle is double axle with double tire tread ML=10t, fifth and sixth axles are double tandem ML= 17t spacing between axles d12, d34, d45 >2,40m 1.20<d23, d56≤2.40m	3J3
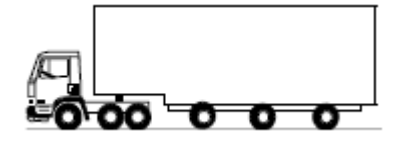	6	53 (58.30)	single front axle with single tire tread maximum load (ML)= 6t, second and third axles with double tandem ML= 17t and fourth, fifth and sixth axles are double tandem with double tire tread ML= 10t spacing between axles d12, d34d45, d56 >2,40m 1.20<d23≤2.40m	3I3
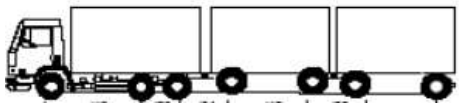	7	63(69,30)	single front axle with single tire tread maximum load (ML)= 6t, second and third axles with double tandem ML= 17t and fourth, fifth, sixth and seventh axles are double axle with ML= 10t spacing between axles d12, d34, d56, d67 >2.40m 1.20<d23≤2.40	3Q4
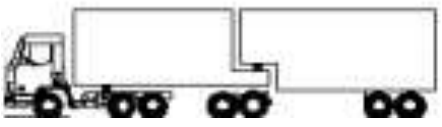	7	57 (62.70)	single front axle with single tire tread maximum load (ML)= 6t, second, third, fourth, fifth and sixth axles with double tandem ML= 17t each, spacing between axles d12, d34, d56, >2.40m 1.20<d23, d45, d67≤2.40	3D4
	9	74(81.40)	single front axle with single tire tread maximum load (ML)= 6t, second, third, fourth, fifth and sixth, seventh, eighth, ninth axles with double tandem ML= 17t	3T6

			each, spacing between axles d12, d34, d56, d78 >2.40m 1.20<d23, d45, d67, d89≤2.40	
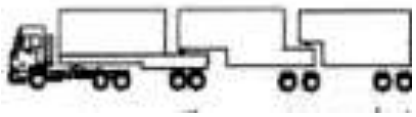	9	74(81,40)	single front axle with single tire tread maximum load (ML)= 6t, second and third axles with double tandem ML= 17t and fourth axle is double axle with double tire tread ML=10t, fifth and sixth axles are double tandem ML= 17t spacing between axles d12, d34, d45 >2,40m 1.20<d23, d45, d67, d89≤2.40m	3T6
	2	16(17, 60)	single front axle with single tire tread maximum load (ML)= 6t, second axle with double axle, double tire tread and ML=10t spacing between d12≤3.50	2CB
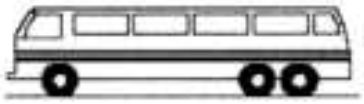	3	19.50(21.45)	single front axle with single tire tread maximum load (ML)= 6t, second and third axles with double axle, with 6 tires and ML=13.5t spacing between d12>2.40 1.20<d23≤2.40	3CB
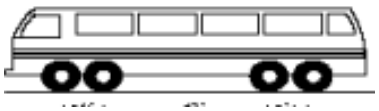	4	25.5(2 8.05)	single and second axles with directional axle (ML)= 12t, third and fourth axles with double tandem, with 6 tires and ML=13.5t spacing between 1.20<d34≤2.40	4CB
	3	26 (28.60)	single front axle with single tire tread maximum load (ML)= 6t, second and third axles with double axle, ML=10 spacing between d12d23>2.40	2SB1
	4	36 (39.60)	single front axle with single tire tread maximum load (ML)= 6t, second, third and fourth axles with double axle, with double tire tread and ML=10t spacing between d12, d23, d34>2.40	2IB2

2.3.1.2 Axle Load Distribution

Based on axle configuration and spacing, truck axles used in Brazilian can be of two types:

- Isolated (single axle) its configuration can be one with single wheels or two wheels; and,
- Tandem group of two or more axles placed in closed arrangement.

It is important to notice that there are single axles with single or double wheels. DNIT (2007) draw attention to the double and triple tandem where the distances between each axle are greater than 2.40 m, in some cases they are considering isolated or single axle. Figure 5 shows the four types of axle normally circulating in Brazilian highways.

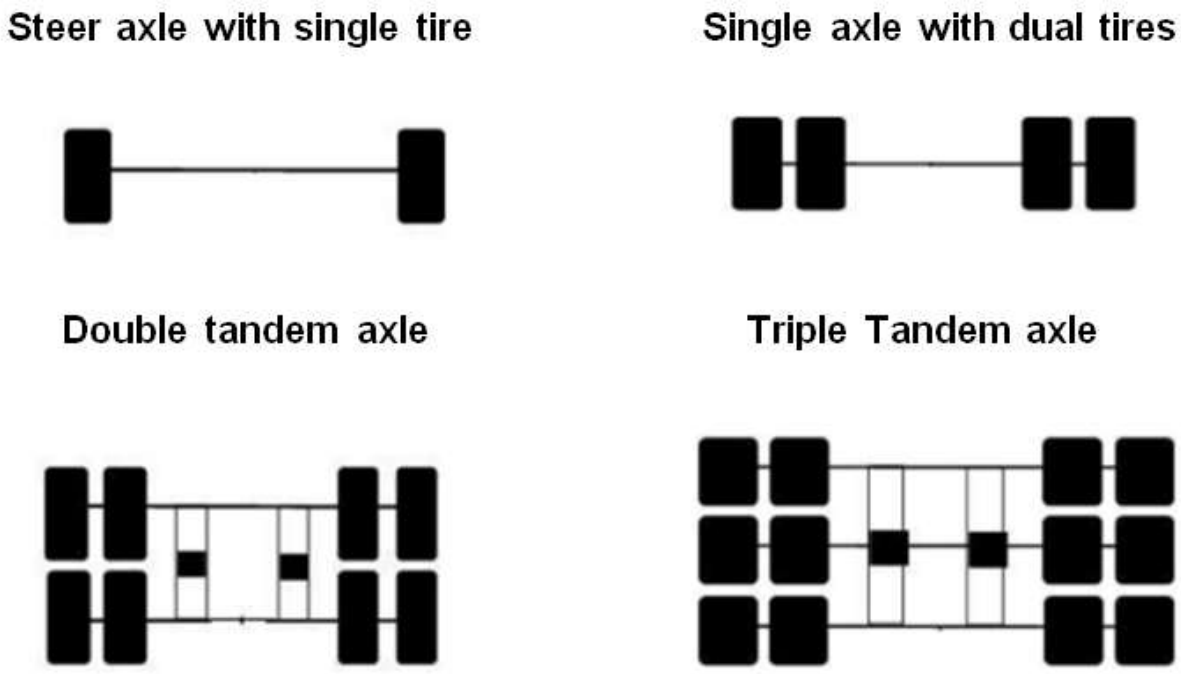

Figure 5 Types of axles of truck fleet present in highway roads in Brazil, DNIT (2007)

According to Fernandes Jr. (1994), in many countries the tandem axle is limited to the double tandem, however, in Brazil, the triple tandem has been increasingly used and it's a critical to pavement performance life with higher axle load (see Table 6).

The single axle with single tire may be responsible for pavement deterioration Fernandes Jr. et. al (2007).

Table 6: Description of the types of axles of truck fleet present in highways/roads in Brazil (DNIT 2007).

Configuration	Distance between axles	No. of axles	No. of tires	Suspension	Maximum authorize load
	------	1	2	------	6t
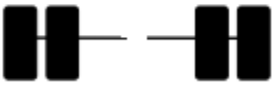	------	1	4	------	10t
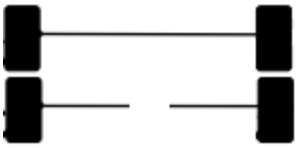	------	2	4	------	12t
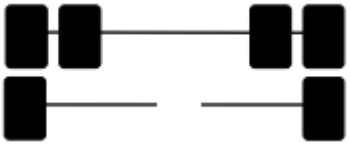	<1.20m	2	6	Special	9t
	1.20 ≤2.40m	2	6	Special	13.5t
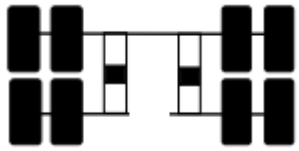	>1.20≤2.40m	2	8	Tandem	17t
				Not Tandem	15t
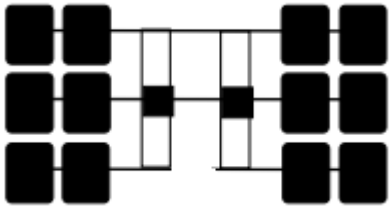	>1.20≤2.40m	3	12	Tandem	25.5t
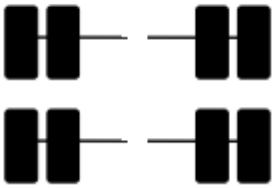	>2.40m	2	8	------	20
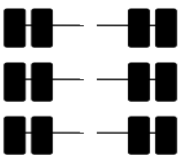	>2.40m	3	12	------	30

Weight control of the vehicles and truck fleet are not very well inspected in Brazil, mainly due to the lack of initiative of DNIT and the lack of understanding of the importance of the pavement preservation by the DERs, this is changing through actions such as weighing plans in implementation nationwide.

In many countries of Europe, United States, Canada and Australia this load limitations parameters are taken very seriously Albano (2005). Table 7 shows a comparison between the maximum load limits authorized that exists in USA, Europe and Brazil.

Table 7: Comparison of the maximum load limits in Brazil, USA and Europa modified from Albano (2005)

Axle type	Brazil (t)	USA (t)	Europa(t)
Single front axle	6	--	10
Single axle dual wheel	10	8.90	10
Double tandem	17	15.13	16
PBT	45	35.60	44

2.3.1.3 Brazilian Maximum Legal Load

Vale *et. al* (2018) studies indicate that excess loads in Brazilian highways are recurrent and are increasing due to higher axle load tolerance. It is well known that small increases in load result in an exponential impact of the fourth power on pavement provoking pavement damage that will be decreasing the pavement performance.

With the evolution of the production of cargo trucks, in Brazil and in other countries around the world that may support more load with tires inflation greater, for these reasons there has been a constant pressure of the truck operator to increase this load limit, Albano (2005).

According to Fernandes Jr. *et. al* (2006), there are, immediate financial advantages bringing economic benefits for those who travel overloaded and consequently the premature pavement deterioration becomes accentuated and the operating cost increase. DNIT (2006a, 2006b) trucks are the largest consumer of the pavement structure with higher load apply on this surface, among the heavy trucks not all cause the same damage it depends from it axles location and type, suspension, number of wheels and pressure.

The Brazilian Nation Traffic Council (CONTRAN) establishes the followings regulations (see Table 8):

- The roads, the vehicle must obey the limits defined, regarding weigh and dimensions. Overweight should be measured by weighing equipment, additionally a percentage will charge over the limit of the total overweigh transmitted by the vehicle to the road.
- Passenger or cargo vehicles will not travel with capacity or load above the limited defined by the manufacturer or neither exceed the limit capacity.

Table 8: CONTRAN load tolerance resolutions (DNIT, 2007)

Date	Law	Percentage
November 25, 1995	Law No. 7408, Article 1	5%
August 31,1999	CONTRAN Resolution No.102, Article 1	7.5%
December 21, 1999	CONTRAN Resolution No. 104, Article 6	5%
November 30, 2007	CONTRAN Resolution No. 258 Revoked No. 102/99 and 104/99 to CONTRAN Resolution no. 114/00	5%
December 18, 2008	CONTRAN Resolution No. 301,328, 337,353, 365, Deliberation 117, 403, 430, 467	7,5%
June 05, 2014	CONTRAN Resolution No. 489	10%
March 2, 2015	Revoked Law 7408 Article 1	10%

One of the first surveys to register data about commercial fleet weighing was conducted by Brazilian Ministry of Transport Policies Group (GEIPOT) between 1976 and 1981 and indicated than on the Brazilian roads trucks travel with an overload of 10 to 30% beyond their limits Fernandes Jr. (1994).

Pinto & Preussler (2002) argues that the variations of axle overload have corresponding destructive effects over the pavement, take place exponentially, indicating the importance of avoiding using overloaded vehicle (Figure 6).

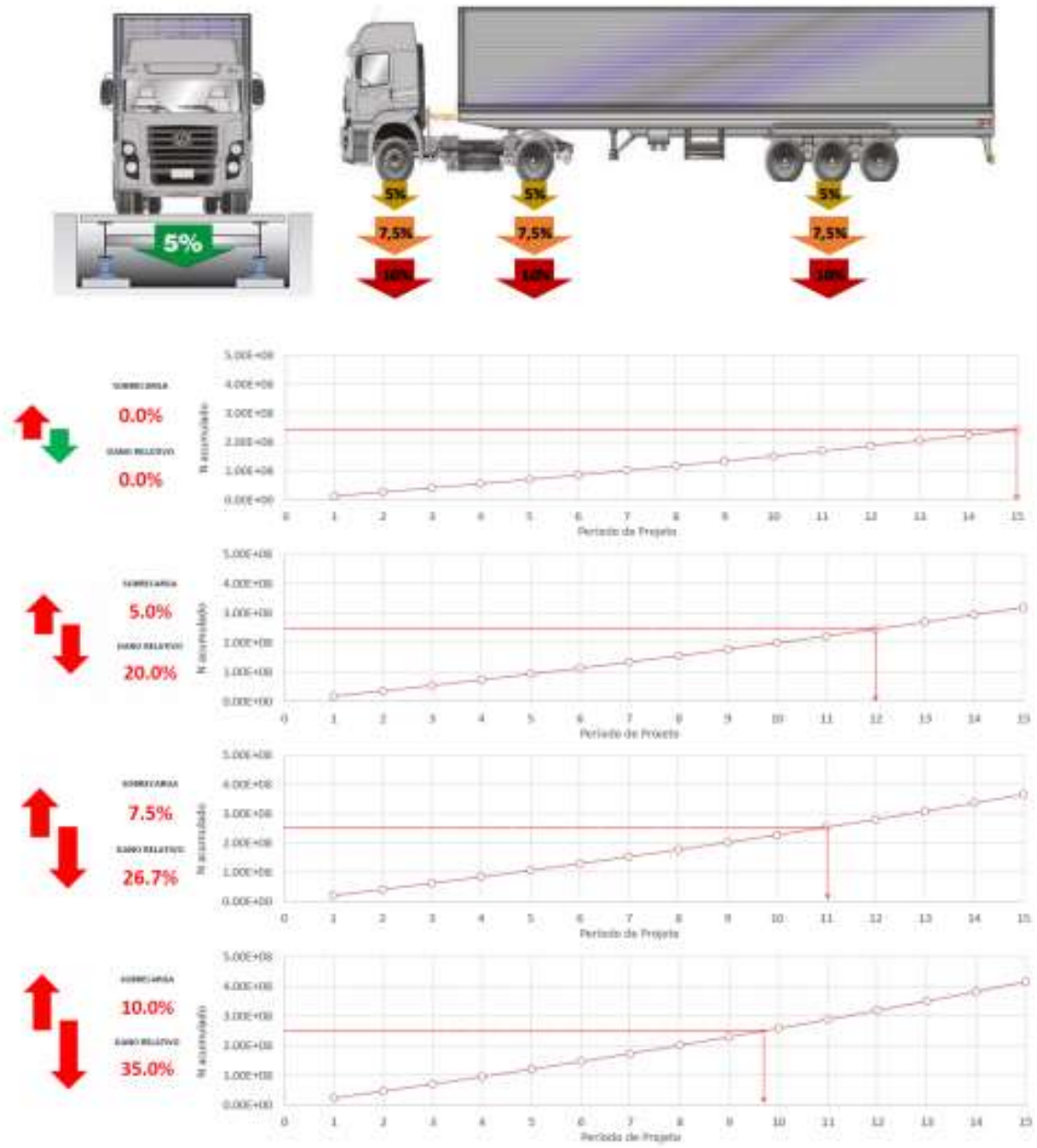

Figure 6: Makes a relation that as axle overload increases pavement life decreases, Pinto & Preussler (2002)

Vale *et al.* (2018) realized a research in a weighting station on a main highway in Sao Paulo, from the month May 2013-May 2014 and from August 2014-May 2016. In Figure 6, it can be observed the fleet representative vehicle factor for each month and it tolerance scenarios considered. According to the researchers mentioned above, the increase in the legal load limited vehicle factors also demonstrate the incorporation of the tolerance on the total gross weight. On Figure 7, it can be clearly observed that in the vehicle factors real, limited at 12.5%,10%, 7.5% and 5% and tolerance are roughly at their 30%, 20%, 18%, and 15% higher than the limited without any tolerance clearly,

contributing to the pavement deterioration rate involving increases on pavement maintenance costs.

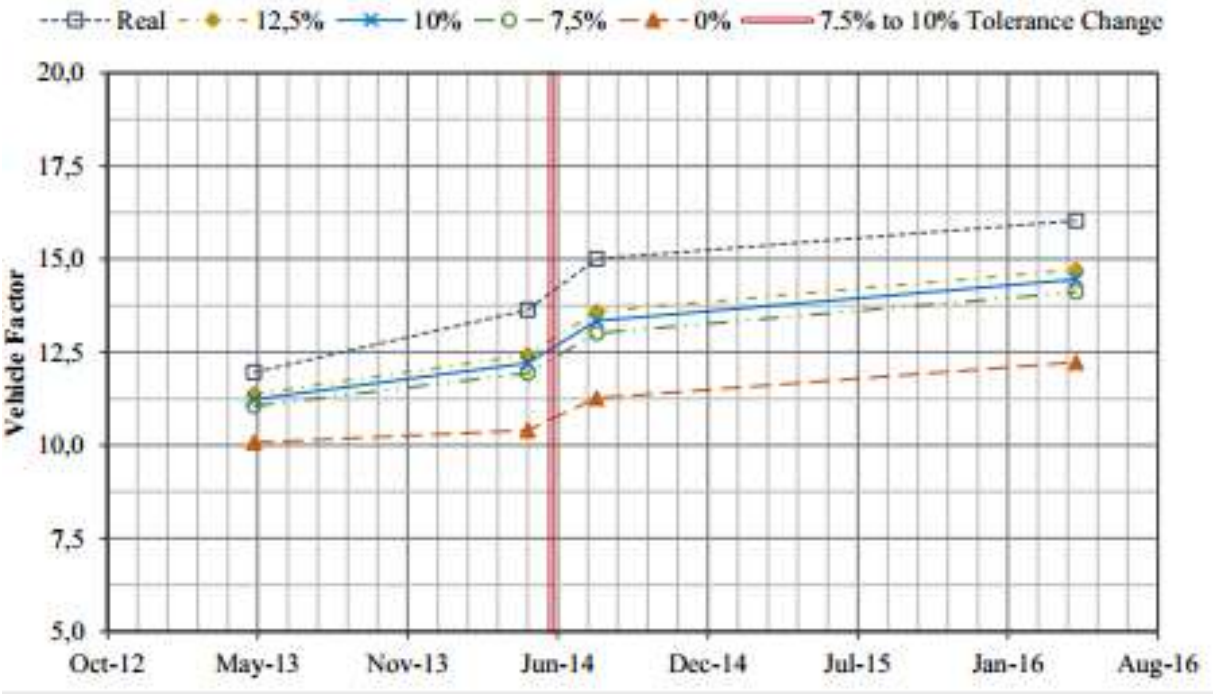

Figure 7: Fleet representative vehicle factors over the years of the research Vale *et al.* (2018)

2.3.1.4 Tire-pavement Interaction

Tires serve for many purposes during in a traveling vehicle cushioning the vehicle against pavement roughness, controlling stability, maneuvering direction and providing safety riding conditions among others (NCHRP, 1993).

The characteristic of a tire pavement interaction are the followings:

- Vertical displacement of pavement interfaces;
- Vertical strain in pavement layers;
- Horizontal strain at the base of the bound layer;
- Vertical and shear strain at the shallow depth:
- Support loads acting on the axles;
- Distribute the vertical loads of vehicles on a contact surface relatively small reducing friction and minimizing bearing capacity: and,
- Vehicle's suspension system, helping to increase comfort reduction of pavement deterioration.

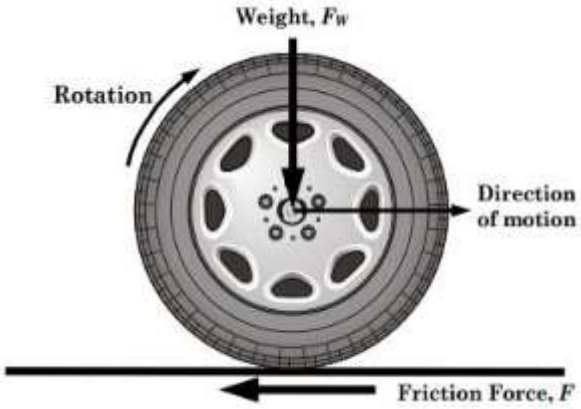

Figure 8: Simplified diagram of forces acting on a rotating wheel (NCHRP, 2009)

Feng (2005) the tire pressure has increased in recent decades. An increase in tire pressure would contribute to the reduction of the tire pavement contact area causing damaging effect on the structure (see Figure 8).

There are two important factors in pavement interaction mechanism according to Wang (2011): the contact area and the contract stresses. Many researches around the world have used circular or equivalent rectangular contact area in pavement loading analysis Huang (1993). According to Al-Qadi *et al* (2005) the contact area of a truck tire is actually closer to a rectangular than circular shape as can be observed in Figure 9.

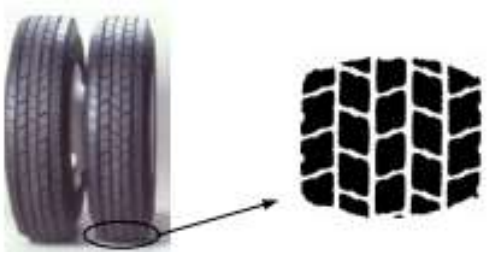

Figure 9 Measured tire imprint for one tire of dual assembly Al-Qadi et al. (2005).

Weissman (1999) claimed that the length of the contact area depends primarily on the applied load, while the contact width will remain nearly constant as load increases, due to the rigidity present on the tire wall. Douglas *et al.* (2000) developed a steel bed traducer device to measure vertical and tangential contact stresses and found that the vertical contact stresses under the tire is extremely non-uniform under heavy loads with low inflation pressure, and that longitudinal contact stresses at the trailing edge of the tire contact patch are significantly greater when the inflation pressure was low. Machemehl et al. (2005) the authors found out that the conventional uniform load assumption underestimated pavement responses at low tire inflation pressures and overestimated pavement response at high tire pressure

Fernandes Jr. et al. (2006; 2007) analyzed the effects of the traffic on the pavement performance of Brazilian and Portuguese flexible pavements and confirmed that this countries pavement design method should consider a specific Load Equivalent Factor for single axle with single tire instead of using the same Load Equivalent Factor developed for a single axle with dual tire. The single tire presents Load Equivalent Factors three to five times higher than conventional dual tires carrying the same load. Mainly in Brazil based in collected data from urban areas Fernandes Jr. (1994) indicated that the steering axle is responsible for most of pavement deterioration and legal limits had increased from 5% to 10% actually.

Al-Qadi & Yoo (2007) developed a validated 3D finite element pavement model and incorporated the measured 3D contact stresses and moving load. The surface tangential contact stresses increased potential and cause the development of top-down cracking, primary rutting and fatigue damage.

Wang (2011) reported that the tire pavement contact stresses induce greater or smaller pavement responses, compared to conventional uniform contact stress distribution, and these variations depends mainly on the tire load, pressure, material stiffness, pavement thickness, and that this difference can only be accurately accounted by utilizing a modeling approach that simulate a realistic contact stress distribution at the tire pavement interface.

Peng *et al.* (2016) developed a 3D finite element model of a tire to investigate the interaction between pavement and tire and found out that the model was validated with the static tire pressure test, vertical and shear contact pressure act non-uniform on pavement surface, and this non-uniformity decreased as the load increased. Jiang *et al.* (2017) analyzed the flexible base of a specific asphalt pavement structure under non uniform tire contact pressure in a 3D Finite element model, comparisons were made between the distribution of non-uniformity and uniformity on pavement surface layer and vertical compressive strain at the top of the subgrade and they found out that compared with the uniform distribution on convex non uniform distribution produces larger deflection on the pavement surface and maximum tensile strain at the bottom of the asphalt concrete surface layer, while the concave creates larger shear strain on the pavement structure.

2.3.1.5 Load Equivalency Factors

Represents the relative damage caused by any axle load (single, tandem, tridem) configuration related to the damage cause by the Standard Axle (18-kips single axle). Due to the great variability of traffic load factors the cumulative effect is expressed by the Load Equivalence.

The pavement design method of the AASHTO (1993) is based in the standard 18-kips (80-kN) single axle, based on empirical results, the definition and quantification of these effects was the main objective of the AASHO Road Test, where it was established as standard equivalent axle the single axle of dual tires of 8.2 t (80.1 kN) spaced at 300 mm (each set of dual tires).

In the AASHO test, according HRB (1962) the damage due to the passage of each individual single axle load can be estimated by the Law of the Fourth Power, and according to this law any damage caused to the pavement increases proportionally as the axle load increases.

The load equivalence factor can be expressed as following:

$$LEF_i = \frac{N_0}{N_i} \tag{7}$$

Where N_0 is the number of applications of the standard axle to the deterioration level Dand N_i is the number of applications of the loading condition i to the same deterioration level D. According to Fernandes Jr. (1994) in Brazil the Load Equivalency Factors (LEF) used for new and rehabilitated pavement is the standardized by the DNIT (empirical).

Vale et al. (2018) stated that to convert the vehicle fleet into an equivalent traffic it is necessary to applied the load equivalent factors, where it allows converting a selected axis by a given load into a determined number of applications of a standard axle that should produce an equivalent effect.

Some models of obtaining the LEF have been taken traditionally over time, for example AASHTO and USACE (DNIT, 2006b) are shown in Table 9:

Table 9: Load Equivalent Factors AASHTO and USACE, DNIT (2006a)

Axle Type	AASHTO	Load(t)	USACE
Single Front	$\left(\frac{P}{7.77}\right)^{4.32}$	0-8	$2.0782 \text{ x } 10^{-4} \text{ x } p^{4.0175}$
Single Back	$\left(\frac{P}{8.17}\right)^{4.32}$	≥8	$1.8320\text{x } 10^{-6} \text{ x } p^{6.2542}$
Dual Tandem	$\left(\frac{P}{15.08}\right)^{4.14}$	0-11 ≥11	$1.592 \text{ x } 10^{-4} \text{ x } p^{3.472}$ $1.528 \text{ x } 10^{-6} \text{ x } p^{5.484}$
Triple Tandem	$\left(\frac{P}{22.95}\right)^{4.22}$	0-18 ≥18	$8.0359 \text{ x } 10^{-5} \text{ x } p^{3.3549}$ $1.3229 \text{ x } 10^{-7} \text{ x } p^{5.5789}$

According to Fontenele (2011) the LEF commonly used in pavement design are based in the empirical design method that does not allow extrapolations for different conditions from those in which they were created. As a result, Fernandes Jr. (1994); Fernandes Jr. & Soria (1996) emphasized that for the development of LEF for the mechanistic empirical we have to know, in addition the Miner Law and the equation or model to predict the pavement performance.

This relates a certain level of deterioration with the number of repetitions of a given structural response. Typically, the level of deterioration adopted is that corresponding to the end of the service life (number of repetitions, permissible, N) resulting from pavement structural analysis and the consideration of predictive pavement performance models are the most indicated to reflect the situation in field. The LEF of the mechanistic empirical method will adopt the following equation:

(8)

$$\boldsymbol{LEF_i = \left(\frac{\rho_i}{\rho_0}\right)^b}$$

Where:

ρ_i is the structural response corresponding to the request under analyze;

ρ_0 is the structural response corresponding to the predetermine or standard request;

b= exponent associated with the form of pavement deterioration, the structural response considered, the type of the structure analyzed.

As stated by Fernandes Jr. (1994), Mechanistic-Empirical load equivalent factors are based in programs for calculating the structural pavement response to individual traffic. Mechanistic empirical models aim to predict the structural pavement performance

represented by the equation related to service (number of allowable applications N) to the magnitude of the response.

2.3.2 Environmental Conditions

Environmental conditions have a significant effect on the performance of flexible pavement, the major influencers are the moisture and temperature NCHRP (2004a), and some of the effects are:

- Chance in the modulus of layers containing asphalt binder due to the visco-elastic nature of the material;
- Have a direct effect on the stresses and strain of the upper layer;
- As the moisture increases the modulus of unbound materials decreases and in the same time increases the stress in the pavement due to the hydrostatic pressure and suction that can affect the properties of bound materials.

Solar radiation causes a hardening effect on the asphalt pavement surface that causes the volatilization of the lighter components of the asphalt binder Read & Whiteoak (2003).

2.3.3 Structures and Materials

The most important selection in a pavement to be design is the materials used in the different layers that are the responsible for the performance of the pavement structures. It is extremely important to identify material properties that precisely characterize the materials in demand NCHRP (2004b).

In the hot mix it is important to have material properties such as dynamic modulus (E^*), master curves (cover all temperature and loading frequency) and Poisson's ratio. Viscosity and volumetric properties of the asphalt mix have effect on the pavement performance.

Unbound base and subbase materials it is important to know the resilient modulus (M_R) adjusted for seasonal variations, Poisson ratio, unit weight and coefficient of lateral pressure.

According to Aguiar-Moya & Prozzi (2011) the pavement structure in the bedrock it is important to take into consideration the elastic modulus (E), Poisson's ratio and the unit weight and depth of the location.

Huang (2003) mentioned the important to take into consideration the design variables that are not independent from one another. Critical conditions can occur when increase in traffic loading under very warm temperature can lead to considerable rutting and shoving or a decrease in the volatile component of the asphalt binder due to several factors (aging) can facilitate the cracking on the pavement surface due to the increase in stiffness.

2.3.4 Structural Response Models

For the proper pavement design, it is necessary to take into consideration the structural responses of materials, that were developed to investigate the response (deflection, strain, stress) of the pavement under diverse traffic loads. Responses at some critical points are used to analysis the horizontal tensile strain at the bottom of the asphalt layer may be used to predict the fatigue failure in the asphalt. The vertical compressive strain at the top of subgrade used to predict the rutting failure.

2.3.4.1 Boussinesq's Equation for Point Loads

The first pavement response model developed by the French mathematician Boussinesq (1885), these equations main function is to determine stresses, strain and deflections subjected to a concentrated load in a soil mass at any depth. This model assumed the pavement layer as elastic, isotropic, homogeneous and semi-infinite, the soil is weightless; the load is a point load acting on the surface, Murphy (2002).

A semi-infinite soil is the one bounded in one side by horizontal surface and infinite in all the other directions. The soil is isotropic when the properties are identical elastic throughout the mass and in every direction. Homogeneous when there share identical elastic properties at every point of the mass in identical directions, Murphy (2002).

Figure 10 presents the coordinates for Boussinesq's equation, where *z* is the depth and *r* is the horizontal distance between the load P and the point where the response desired.

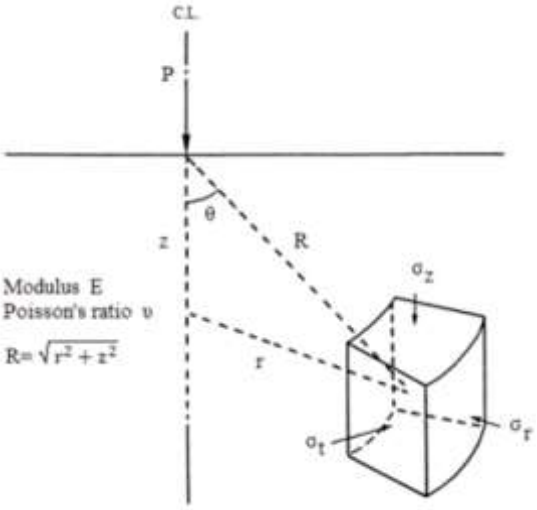

Figure 10 Boussinesq's equation in polar coordinates, Ullidta (1987)

The expression obtained by Boussinesq for computing vertical stress σ_z at a point P (Figure 10) due to the load P is:

$$\sigma_z = \frac{3Q}{2\pi z^2}\frac{1}{\left(1+\left(\frac{r}{z}\right)^2\right)^{5/2}} = \frac{Q}{z^2} \quad I_B \tag{9}$$

Where:

r= horizontal distance between arbitrary point P below the surface and the vertical axis through the point load Q.

z= vertical depth of the point P from the surface.

I_B= Boussinesq stress coefficient:

$$= \frac{3}{2\pi}\frac{1}{\left(1+\left(\frac{r}{z}\right)^2\right)^{5/2}} \tag{10}$$

I_B

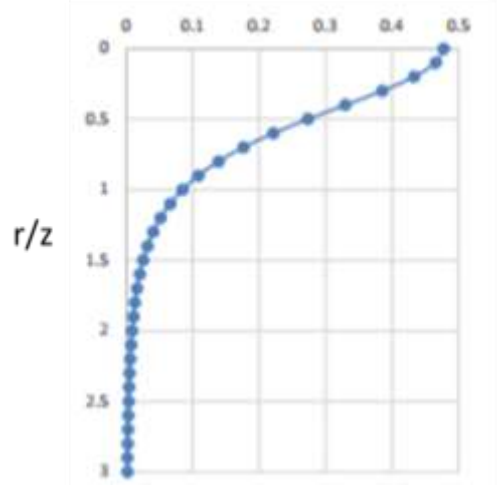

Figure 11: Values of I_B for use in the Boussinesq formula

The variation of the Boussinesq coefficient I_B can be determined for a number of values of r/z. It can be seen from Figure 11 that the I_B has a maximum value of 0.48 at r/z=0 indicating through that the stress is a maximum below the point load.

There are other theories for calculating stresses produces by a point load, in where there is no necessary to take into account some of the assumptions of Boussinesq (1885) as that the soil is neither is elastic, isotropic and homogeneous. However, this assumption is not the reality that can be found in nature where soil is neither isotropic nor homogeneous. A British Scientist Westergaard proposed in 1938 a formula for the computational of vertical stress σ_z by a point load Q at the surface.

However, is preferable to use the solution given by Boussinesq because is more conservative results are obtained. The Boussinesq's formula is applicable only where the difference between the modulus of the layers that constitute the pavement structure is close to 0. The theory is applicable for a single layer, according to Murphy (2002). The main advantage of this model is its simplicity and covers the basic for several pavement structural models which are currently being used Qin (2010).

2.3.4.2 Two-layer Theory

A typical pavement structure is composed of several layers. Consequently, Boussinesq's equation point load model cannot accurately simulate the structure and so a better model is needed. Burmister (1943) developed a closed form solution for two layered. In his model, certain assumptions were taken into consideration in order to compute the stress, strain and deflection. The basic assumptions made by Burmister in two-layer elastic models that must be fulfill are the following, according to Huang (2004):

- Each layer material is homogeneous, isotropic, and linearly elastic with an elastic modulus E ans Poisson's ration υ;
- The material must by weightless and infinite in areal extent;
- The lateral direction of the surface layer is infinite in extent even though the vertical direction does have a finite depth. Both the horizontal and vertical directions of the bottom layer are infinite in size and thickness;
- A uniform pressure q is applied on the surface over a circular are of radius a;

- Continuity conditions are satisfied at the layer interfaces, as indicated by the same vertical stress, shear stress, vertical displacement, and radial displacement;
- The shearing forces are not present in the surface. The continuity of shear stress and radial displacement is replaced by zero shear stress at each side of the interface; this because the load applied on the pavement is represented by the uniformly distributed pressure; and,
- Dynamic and thermal effects are not taken into consideration.

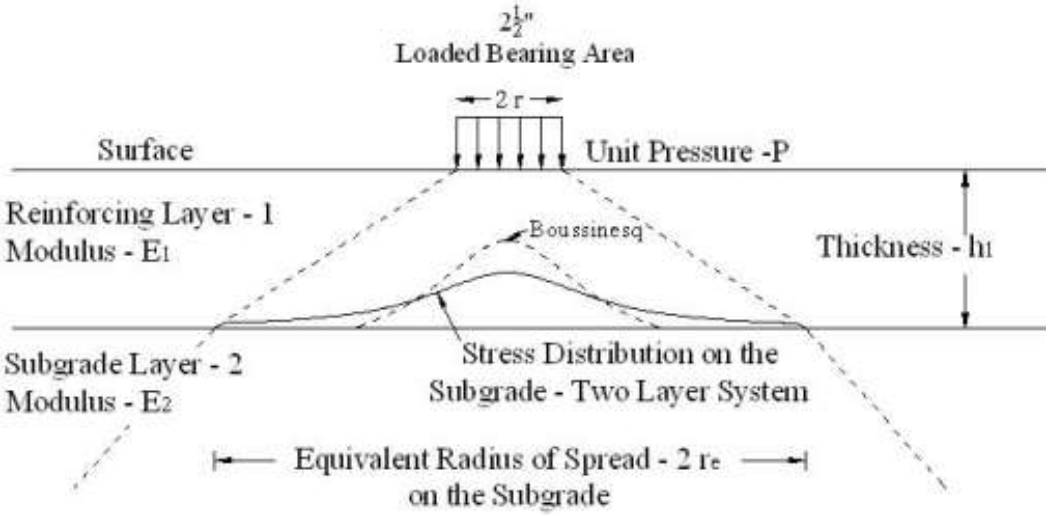

Figure 12: Two-layer system, Burmister (1943)

From the pavement analyses point of view the Burmister model (Figure 12) can be used to determine the stress, strain and deflections in the subgrade if the relationship between the modulus E of the pavement and the subgrade is close to the unit, if not the modeling is more complex.

Analytically, it is a more complex procedure than those based on the first model with could be solved with simple equations: the model of Burmister introduces the Fourier transforms requiring Bessel functions for the solution and without the help of a computer program it is impossible to model structures of more than two layers.

2.3.4.3 Multi-Layer Theory

Based on the mechanics of a continuous medium, this model state is created by an overlap of homogeneous and isotropic layers characterized by a modulus of elasticity E and Poisson's ration υ.

Even though it is considered as limitation of this model, the consideration of an infinite layers in the plane, with allows simplification in the calculation process. Considering circulate load acting in the pavement can be treated as revolution solid that deforms symmetrically with respect to the axis, which allows to treat the problem in cylindrical coordinates.

Figure 13 illustrates the advantage of the revolution solid that deforms symmetrically (Oliveira, 2013). For balance considerations it can be stated that $(\tau_{rz} = \tau_{zr}, \tau_{z\theta} = \tau_{\theta z}, \tau_{\theta r=}\tau_{r\theta})$ which allows reducing the number of nine variables to 6 variables, the revolution that deform symmetrically this because all the derivate in order to θ are null, which allows to conclude that $\tau_{z\theta} = \tau_{\theta z} = \tau_{\theta r} = \tau_{r\theta} = 0$ and consequently reduce the number to four variables.

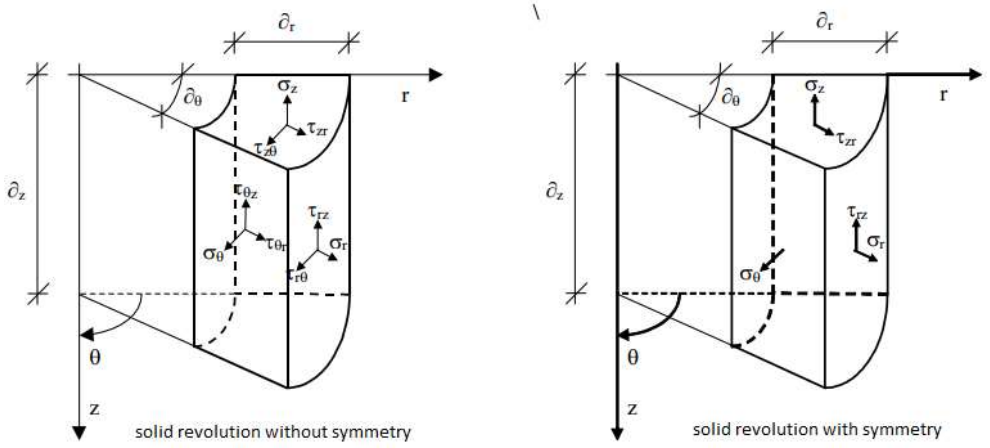

Figure 13: Infinitesimal volume element in cylindrical coordinates, Oliveira (2013)

Burmister's theory states that stress at any point in a pavement layer are characterized by nine types of stresses cited as follows:

- Three normal stresses $(\sigma_z, \sigma_r, \sigma_t)$ acting on the faces of the element.
- Six shear stresses $(\tau_{rt}, \tau_{tr}, \tau_{rz}, \tau_{zr}, \tau_{tz}, \tau_{zt})$ that act parallel to the face of the element.

Under conditions of static equilibrium, the tangential stresses act on the intersecting faces are equal to $(\tau_{rz} = \tau_{zr}, \tau_{rt} = \tau_{tr}, \tau_{tz} = \tau_{zt})$. Exists always an orientation at each point where the tangential stresses are zero and the normal are the principal stresses defined as (see Figure 14):

- Major principal stress σ_1
- Intermediate principal stress σ_2
- Minor principal stress σ_3

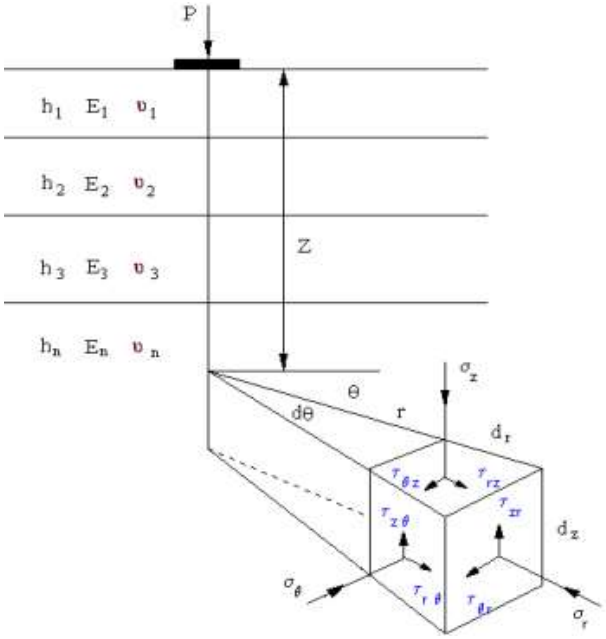

Figure 14 : Diagram of Shear stresses acting in a layer system Huang (2004)

2.3.4.4 Multi-Layer Computer Program

With the advancement on the computer technology, many programs were developed for pavement analysis based in a multi-layer elastic theory (Table 10).

Table 10: Multi-layer computer program for pavement analysis and design

Program	Description	Inventor
CHEVRON	The software is capable to analyze a multi-layer elastic pavement structure under single and dual wheel loads, capable to analyze 5 layers	Chevron Research Company
BISAR	Based on a linear elastic theory, can be used to calculate stress and strain profiles deflections, and slip on pavement layer via shear spring compliance at the interface. One advantage is that uses different elastic modulo, Poisson's ratios, layer thickness and interface bonding conditions specified for each layer.	Shell Oil Co.
CIRCLY	Capable of accounting for the anisotropy of unbound granular materials, the tire pressure is modeled as uniformly distributed on a circular contact surface for analyze.	L. Wardle
KENLAYER	Software cannot model anisotropy but is capable of modeling nonlinearity through iterative calculations.	Huang
ELSYM5	Program is able to analyze a pavement structure up to 5 linear elastic layers and 20 multiple wheel loads. The principal stress, strain, and displacement can be calculated at specified locations.	Federal Highway Administration (FHWA)
WESLEA	Capable of analyzing more than 10 layers with more than 10 loads.	U.S. Army Corps of Engineers
EVERSTRESS	Program that can be used to determine stresses, strain and deflection in a layered elastic system (semi-infinite) under circular surface loads. The program can analyze up to five layers, 20 loads and 50 evaluation points.	Washington State Department of Transportation

Usually, this software is able to compute the stresses, strain, and deflections under a circular surface load. The main inputs are layer thickness, material properties (modulus and Poisson ratio), load conditions (magnitude of load, contact pressure and radius).

2.3.4.5 Finite Element Method

The finite element method is a numerical method used for analysis of stresses, strain and deformations in a pavement structure. Many researchers and engineers are trying their best to learn how to utilize the numerical models, arranging from Finite Element Method (FEM) to finite layer approach which is used to compute primary responses in the asphalt pavement structure as emphasized by Jiang et al. (2017).

Two-dimensional FEM models where the first successful examples of the applications of the FEM in pavement analysis. ILLI_PAVE is one of the most common axisymmetric FEM models, where the modulus can be stress-dependent and the Mohr-Coulomb failure criterion is used for granular and fine-grained soils materials according to Elliott & Thompson (1985).

As cited by Zaghloul & White (1993) the advance of the computer technology and algorithmic improvements the use of the 3-D FEM analysis has become widespread in pavement structural analysis. If comparing the simple layer elastic theory or 2-D axisymmetric model to a 3-D model can consider many analysis scenarios cited by Wang (2011):

- Non-uniform tire pavement contact stress;
- Discontinuities in pavement (cracks or joints);
- Viscoelastic and nonlinear materials properties;
- Infinite foundation:
- Quasi static or dynamic analysis;
- Crack propagation;
- Temperature effect;
- Bonded or unbounded interface.

Liu et al. (2016) emphasized that software of FEM such as ABAQUS and ANSYS, are powerful tools that can simulate asphalt pavement responses to a certain magnitude. On the other hand, the complexity, time consuming process, license cost often turns it impossible to be used by road engineers.

2.3.5 Uncertainties in Reliability Assessment

As cited by Hu et al. (2014) is important to consider variation and uncertainties so that pavement can be designed to the desired level of reliability, some sources of variations and uncertainty are:

- Errors in estimating traffic loading, axles, tire pressures;
- Fluctuations in climate over the years;
- Variations in layer thickness, material properties, subgrade characteristic along the pavement project;
- Predictions model limitations and errors.

According to AASHTO (1993); Sánchez-Silva et al. (2005), and Moreno et al. (2017), reliability is always involved in a way to take into consideration of the uncertainty variables such as:

- Traffic growth;
- Traffic loads;
- Environmental conditions;
- Damage progression;
- Mechanical properties;
- Structural performance of the materials;
- Quality of the construction process.

Xiao (2012) agrees that uncertainties in reliability in pavement life cycles are related to design, construction and maintenance and performance as observed in Figure 15.

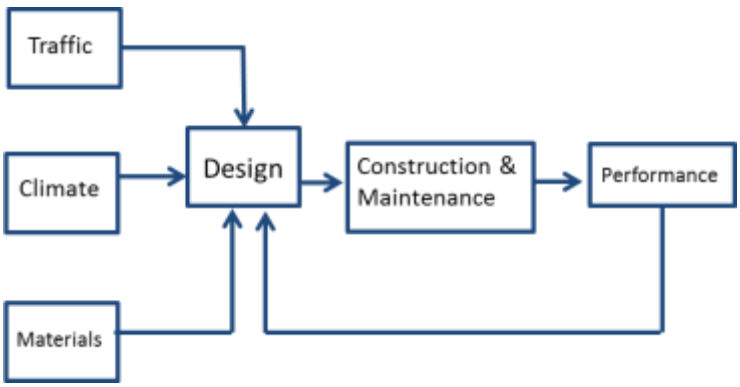

Figure 15: Uncertainty in pavement life-cycle, Xiao (2012)

Uncertainty should be wisely investigated and quantified to developed better pavement design procedure.

Huang (2004) cited three major sources of uncertainty that contribute to variability in pavement design process:

- Variance from traffic load (empirical data used) or design factors (errors in improper measurements etc.)
- Statistical uncertainty as a result of the uncertainty in the constants derived and used in the design equation.
- Model uncertainty that arises from inadequacy of the design procedure or lack of fit of a design equation.

Alhasan et al. (2018) claim that the sources of uncertainty related to pavement design and performance modeling can be classified as:

a) *Constitutive and performance modeling errors*: due to the lack of knowledge in the true mechanical nature of the materials and their long-term behavior;
b) *Forecasting uncertainties*: Include traffic loads, environmental loads and any other sources of loading, will induce uncertainties in the predictive performance models;
c) *Systematic measurement errors:* take in consideration two components. a) bias-consistent and uniform shift in the measured values. b.) variance-fluctuation in the measurements around the mean value. These two errors can be due to the lack of knowledge in testing device behavior, lack of repeatability and limited number of tests conducted in the sampling domain;
d) *Errors due to indirect testing techniques*: many of the field test measures, do not measure fundamental mechanical nature of the materials; and,
e) *Inherent spatial variability of material properties*: variations in soil formation, historical loading conditions, paving material and properties, compaction and practices.

2.4 RELIABILITY

Many terms are used to describe the reliability of an engineering system; some of the terms are self-explanatory, whereas others are not. The commonly used term *probability of failure* is always associated with a particular performance criterion.

Reliability is the probability of successful performance; thus, is the converse of the term *probability of failure.* It is common to express reliability in terms of decimals such as

0.999 or 0.9999 (the corresponding probability of failure will be 0.001 or 0.0001 respectively).

2.4.1 Basic Concepts

Every engineering project consist of planning, design, constructing and maintenance (buildings, bridge, dams and levees, foundations, power plants, offshore structures, tunnels, aqueducts, highways, airports, harbors, ports etc.) utilizes the concept that the capacity, resistance should satisfy the demand, to ensure satisfactory performance.

In transportation Engineering a highway or airport is designed considering the future traffic needs; the capacity must meet the traffic demand. Although there are subject to varying degrees of randomness as structural deficiencies, material defects, human errors, consequently the satisfactory performance cannot be absolutely warrant. As cited by Harr (1987) the measure of success is called “reliability”, which can be defined, quantified, tested and confirmed. In engineering terms, reliability can be defined as the probability of an object (item or system) performing its required function adequately for a specific period of time under stated conditions.

Four essential elements are expressed in the above-mentioned definition that are:

- Reliability is expressed as a probability;
- A quality of performance is expected;
- Over certain period of time;
- Expected to perform satisfactory under specified conditions.

According to Haldar & Mahadevan (2000), risk and reliability are complementary terms, risk is not just the probability of failure but the consequence of failure, so risk can be defined as the product of the probability of failure. Reliability can be defined as the probability of a successful performance and can be quantified by using the methods of probability (statistic to compute likelihood of specific event) and statistics (mean; standard deviation, etc.). A measurement of reliability is indicated from 0-1, where 1 indicates that the structure will perform satisfactorily and 0 indicates that the structure will fail.

According to Haldar & Mahadevan (2000), reliability analysis requires information about uncertainties in the system to be analyzed.

These uncertainties can be classified as:

1) Quantitative sources and this one can be classified in three types:
   a) Inherent randomness in all physical observation;
   b) Statistical uncertainty;
   c) Modeling uncertainty.
2) Qualitative sources that can be classified as:
   a) Certain parameters such as; structural performance, quality deterioration, skills and experience construction workers, engineers, environmental Project, condition of existing structure;
   b) Human factors;
   c) Interrelationship among the parameters.

2.4.2 Measurements

The main measurements of reliability are:

a) Factors of Safety

According to Harr (1987); Kenis & Wang (2004); Xiao (2012); and Dalla (2015), any structure must be designed with appropriate capacity or resistance (C) that will be the load apply on a structure and must satisfy a demand or solicitation (D) of the structure with a factor of safety:

$$F_s = \frac{C}{D} \tag{11}$$

The capacity depends on the variabilities of the layer materials and construction process, although de demand depends primarily of the uncertainties associated with vehicle type, loadings and environmental effects cited by Kenis & Wang (2004). A schematic representation of the capacity and demand function as probability distributions is show in Figure 16.

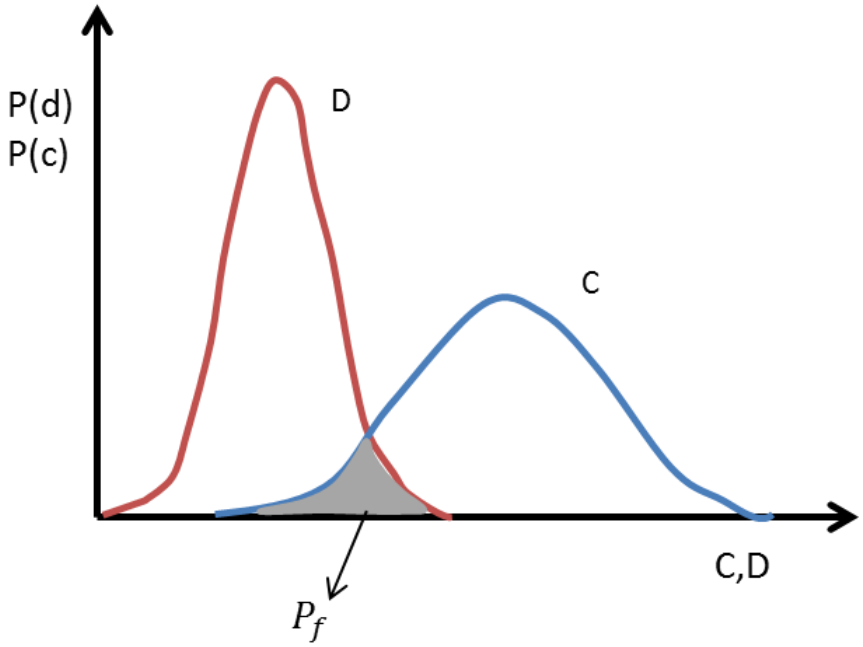

Figure 16: Probability Distribution of C and D, Kenis & Wang (2004)

In a specific case system with randomly distributed C is subjected to an independent distributed D, the probability of D exceeds C at a given value is a real, causing an overlap between the two distributions causing a probability of failure P_f of the system.

According to Haldar & Mahadevan (2000), where $f_s(S)$ stands for loads in the system and $f_r(R)$ for strength the overlap of the two curves (shaded region) which provides a qualitative measure of the probability of failure, this area of overlap depends mainly of:

- The position: as the distance between the two curves reduces the overlapped area, decreasing the probability of failures. The position of the curve can be represented by the means μ_R , μ_S of the two variables, as shown in Figure 17.
- Dispersion of the curves: If the curves are narrow, the overlap and the probability of failure are smaller, dispersion can be characterized by the standard deviations ($\sigma_R$and σ_S).
- Shape: the curves are represented by the probability of density factors $f_r(R)$ and $f_s(S)$.

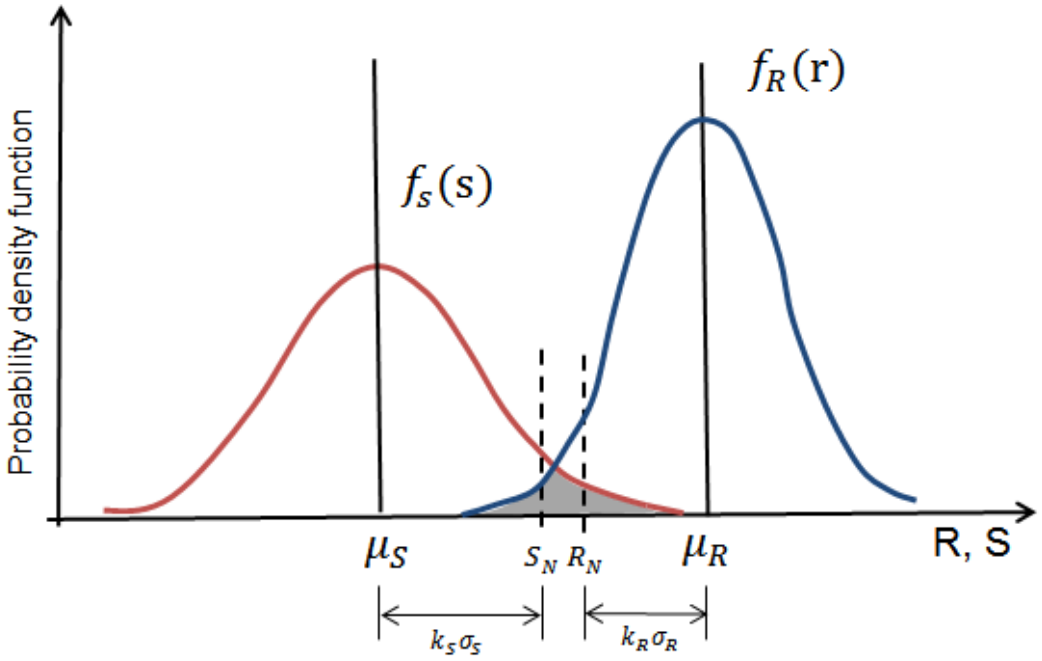

Figure 17 Fundamentals of risk evaluations, Haldar & Mahadevan (2000).

Kenis & Wang (2004), considered that the reliability of a system can be defined as:

$$R = P[(C - D) > 0] \tag{12}$$

As commented by Xiao (2012), the capacity can be defined as the traffic that the designed pavement could support or tolerate; the demand will be the real traffic traveling in the pavement after its construction period.

$$FS = \frac{ESAL\ Capacity}{ESAL\ Demand} \tag{13}$$

The reliability of the design can be defined as:

$$R = P\ (ESAL\ Capacity\ > ESAL\ Demand) \tag{14}$$

b) Central Factor of Safety

As mentioned by Harr (1987) the probabilistic version of the safety factor can be expressed as:

$$CFS = \frac{E[C]}{E[D]} = \frac{\mu_R}{\mu_s} \tag{15}$$

Where E [ ] is the expected value.

c) Safety Margin

The safety margin(S) can be defined as:

$$S = C - D \tag{16}$$

The shaded area denoted as the probability of failure of the system can be expressed according to Harr (1987) as:

$$p(f) = P[(C - D) \leq 0] = P[S \leq 0] \tag{17}$$

d) Reliability Index

A good measure of the reliability of a system is by obtaining the Reliability Index β which is defined as S is the mean value of the safety margin and $\sigma[S]$ standard deviation:

$$\beta = \frac{\bar{S}}{\delta[S]} = \frac{\bar{C} - \overline{D}}{\delta[S]} = \frac{\mu_r - \mu_s}{\sqrt{\sigma^2[C] + \sigma^2[D] - 2\rho\sigma[C]\sigma[D]}} \tag{18}$$

C and D are normally distributed and correlated ρ is the coefficient of correlation between C and D. When C and D are not correlated $\rho = 0$ and the equation can be reduced Harr (1987) to:

$$\beta = \frac{\mu_r - \mu_s}{\sqrt{\sigma^2[C] + \sigma^2[D]}} \tag{19}$$

For a limit state of interest $g(C, D)$ will be:

$$g(C, D) = S = 0 \tag{20}$$

- $S > 0$; Safe state
- $S < 0$; Failure state
- $S = 0$; Limit state

The greater the reliability index the safer the structure:

$$p(f) = 1 - \Phi\left(\frac{\mu_r - \mu_s}{\sigma[S]}\right) = 1 - \Phi(\beta) \tag{21}$$

Where Φ represent the standard normal cumulative distribution density function of and β (distance between two curves).

According to the USACE (1997) reliability indices are a relative measure of the current conditions and provide a qualitative estimate of the expected performance of a system that lies between 1.0 and 5.0 corresponding to probabilities of failure ranging from about 0.16 to $3x10^{-7}$, as shown in the following Table 11:

Table 11 Target reliability indices, USACE (1997)

Reliability Index, $\boldsymbol{\beta}$	Probability of failure, $\boldsymbol{P_f}$	Expected performance reliability level
1.0	0.16	Hazardous
1.5	0.07	Unsatisfactory
2.0	0.023	Poor
2.5	0.006	Below average
3.0	0.001	Above average
4.0	0.00003	Good
5.0	0.0000003	High

Low reliability indices indicate that system will perform poorly and the probability of failure of the structure or system under analyzes is in a hazardous situation; in the other hand, high reliability indices indicate that the system will perform their function in optimal conditions with high reliability.

2.4.3 Reliability Analysis Methods

It is relevant to consider the risk underlying in every pavement design. The first step in evaluating the reliability or probability of failure of a determine structure is to decide specific performance criteria such as loads and resistance parameters denoted as basic variables X_i, and the functional relationship among the corresponding to each performance criterion according to Haldar & Mahadevan (2000). The relationship or performance function can be described as:

$$Z = g(X_1, X_2, \dots, X_n) \tag{22}$$

The failure surface or limit state can be defined as Z=0 this is the boundary between safe and unsafe regions. Reliability analysis methods have been developed according to the limit states of different types and complexity.

When Z< 0 failure occurs and the probability of failure p_f can be obtained by:

(23)

$$p_f = \int \dots \int_{g()<0} f_x(X_1, X_2, \dots X_n)\, dx_1 dx_2 \dots dx_n$$

Where $f_x(X_1, X_2, \dots X_n)$ is the joint probability density function for the basic random variables that are $X_1, X_2, \dots X_n$ and the integration is performed over the failure region that is g ( )< 0 (see Figure 18).

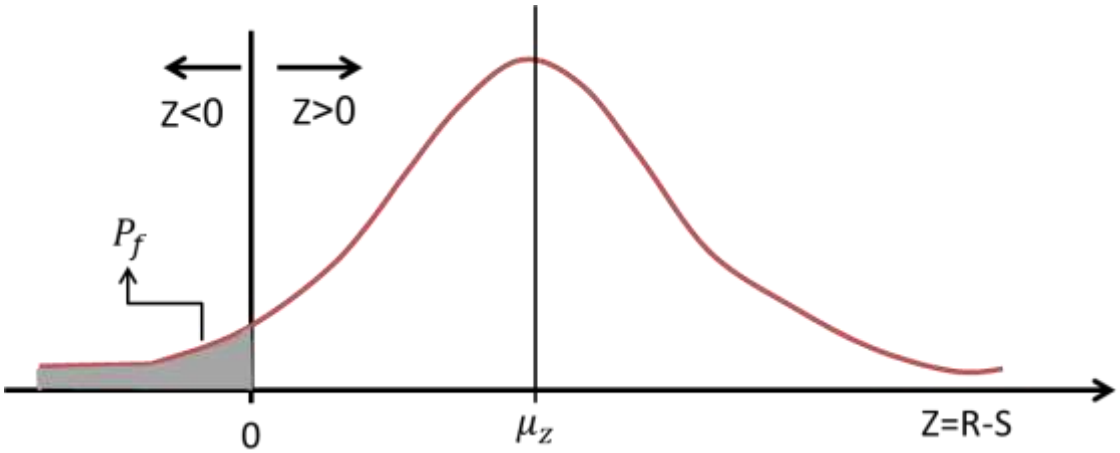

Figure 18: Probability density function, adapted from Borges et al. (1985).

The transformation of the limit state from the original to a reduced coordination system is presented in Figure 19:

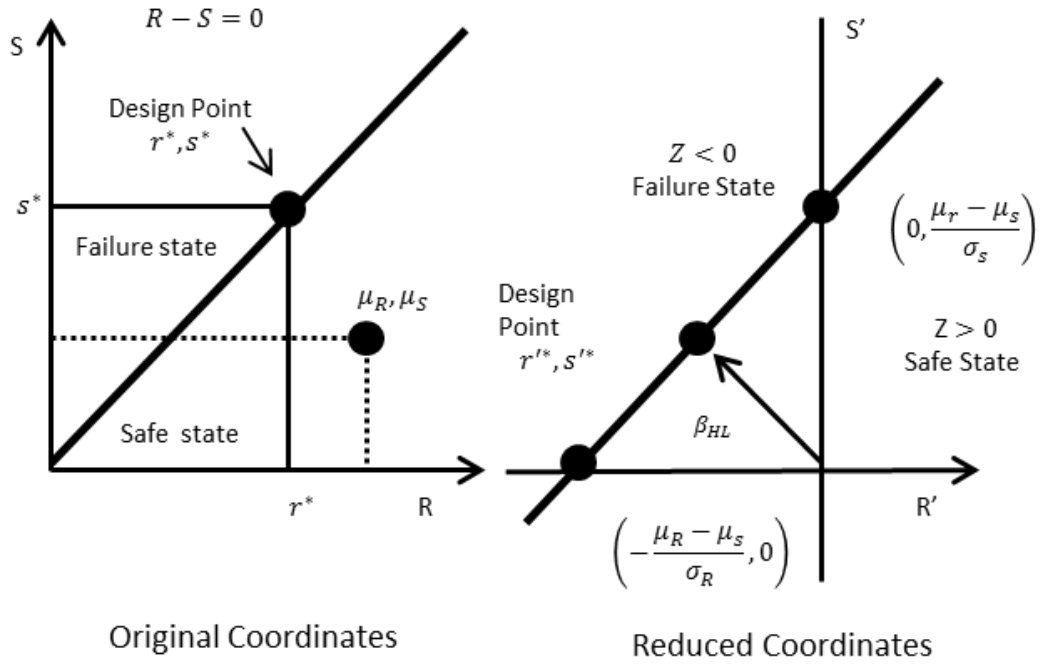

Figure 19: Hasofer-Lind Reliability Index for linear limit state function, Haldar & Mahadevan, 2000

It can clearly be observed the safe and failure state or region. In the reduced system it can be observed:

- That appear as the failure state is closer to the origin, the failure region is larger and if it is far away from the origin failure is smaller.
- The position of the limit state surface relative to the origin is measure of the reliability of the system.

The safety index denoted as β_{HL} (is the same as the reliability index) is the minimum distance from the origin of the axes in the reduced coordinate system to the limit state surface (failure state). The minimum distance point on the limit state surface is called the design point.

Variable techniques are available to help determine the probability distribution given in a function whether it is linear or nonlinear and varying in number of random variables. These methodologies can be grouped as:

- Simulation Techniques (Monte Carlos)
- First Order Reliability Method (FORM)
- First Order Second Moment Method (FOSM)
- Point Estimate Method (PEM)

2.4.3.1 Monte Carlos Simulation Technique

The estimation of probability of failures through the simulation technique of Monte Carlos, consists of performing a sufficiently large number of evaluations in such a way that it results, serve to perform a numerical integration. This technique has six essential elements cited by Haldar & Mahadevan (2000):

- The problem has to be defined in terms of random variables;
- Quantifying the probabilistic characteristics of all the random variables in terms of Probability Density Function (PDF) and Probability Mass Function (PMF) and the corresponding parameters;
- Generating the values of these random variables;
- Evaluating the problem deterministically for each set of realization of all the random variables, numerical experimentation;
- Extracting probabilistic information;
- Determining the accuracy and efficiency of the simulation.

2.4.3.2 First Order Reliability Method (FORM)

Historically traced to second-moment methods that used the information of first and second moments of random variables. The most commonly used reliability method is the first order, FORM. It consists of carrying out the project point search and making a linear approximation of the probability of failure around the project point**.**

As cited by Haldar & Mahadevan (2000) and Dalla (2015), in the FORM the limit state function of interest can be linear or nonlinear FORM can be used to evaluate the Equation 20. When it is linear function of uncorrelated ($\rho = 0$) normal variables or when the nonlinear limit state is can be represented by a first order (linear) approximation with equivalent normal variables.

Harr (1987) agrees that for N uncorrelated variables, F ($X_1, X_{2,\ldots\ldots,} X_N$), retaining only linear terms in Taylor series, them the expected value and variance can be expressed as:

$$E[F] = F\left(\overline{x_{1,}}\ \overline{x_2}, \ldots, \overline{x_N}\right) \tag{24}$$

$$\mathrm{V[F]} = \sum_{i=1}^{N} \left(\frac{\partial F}{\partial x_i}\right)^2 V[x_i] \tag{25}$$

$\overline{x_\iota} = E[x_i]$ and all the derivates are evaluated at the expected values of all variables contained their expressions.

As cited by Luo (2014), in most reliability approaches it is first determining the reliability index (β)i and them the equivalente probability of failure that can be computed as:

$$p_f = 1 - \Phi(\beta) \tag{26}$$

Where: Φ represents tha standard normal cumulative distribution function. The reliability index (β) can be efficientely evaluated using FORM, where (β) can be computed as the shortest distance between the limit state surface and the origin normalized variable space mentioned by Ditlevson (1981):

$$\beta = \overset{min}{x \epsilon F} \sqrt{\left[\frac{x_i - \mu_i}{\sigma_i}\right]^T [\rho]^{-1} \left[\frac{x_i - \mu_i}{\sigma_i}\right]} \tag{27}$$

Where:

- x_i is one of the uncertain variables in the vector x of input parameters in the reliability analysis;
- μ_i and $\sigma_i$are the mean value and standard deviation of valuable x_i;
- $[\rho]$ is the correlation matrix for all the input variables.

Retherford & McDonald (2010) acknowledge that in the FORM, the limit state function denoted as $g(x)$ to characterize the limit state of the system. The failure and safety domains are expressed as:

$$\{F\} = \{\boldsymbol{x}: g(x) \leq 0\} \tag{28}$$

$$\{S\} = \{\boldsymbol{x}: g(x) > 0\} \tag{29}$$

Where:

$\{F\}$ is the failure state;

$\{S\}$ is the safety state.

The limit state functions are consequent of the individual distress presented in the pavement. The probability of "failure" of the pavement section can be defined as:

$$P_F = P\{g(x) \leq 0\} = \int_{g(x)\leq 0} f_x(\boldsymbol{x})dx \tag{30}$$

Where:

$f_x(\boldsymbol{x})$ Is the joint probability density of the variables x_1, $x_{2,\ldots\ldots}$, x_n.

The reliability in pavement design is the probability that the design should not overdo or 1-P_F.

A four-step calculation process of the probability of failures for individual distress in the FORM can be done as cited by Retherford & McDonald (2010):

1. The transformation from the original $\boldsymbol{x}$- space to the standard uncorrelated normal $\boldsymbol{u}$- space.

$$u = \Phi^{-1}\big(F(x)\big) \tag{31}$$

2. Calculation of the most probable point of failure cab de defined as:

(32)

$$u^* = \arg\min(\| u\| \; g(x) = 0)$$

3. The calculation of the reliability index β is general is equal to αu^*, where α is the negative normalized grandient row vector of the limit state surface in the u-space that is pointing to the failure domain. In most cases $\beta > 0$, and in the cases where $\beta = \| u^* \|$. The magnitude of the elements α-vector is the information of the sensitivy.
4. In FORM the calculation of the probability of failure is presented as follows:

(33)

$$P_{F1} = \Phi(-\beta)$$

Where:

Φ (B,R) is the standard normal multivariate Cumulative Distribution Function (CDF)

Retherford & McDonald (2010) suggest that for pavements, the serial system failure probability is:

(34)

$$P_{F,SYS} = P\left\{\bigcup_i g_i(x) \leq 0\right\}$$

As cited by Haldar & Mahadevan (2000) the Hasofer-Lind reliability index can be used to calculate the FORM of the probability of failure as:

(35)

$$p(f) = P[G(x) \leq 0] = \Phi(-\beta_{HL}) = 1 \; - \Phi(\beta_{HL})$$

Where:

β_{HL} is the Hasofer-Lind realiability index and can be defined as the minimum distance from the origin to the design limit x'*on the limit state of the reduced coordinates presented above:

(36)

$$\beta_{HL} = \min_{g=0} \sqrt{(x'^*)^t * (x'^*)} \text{ for uncorrelated variables}$$

(37)

$$\beta_{HL} = \min_{g=0} \sqrt{(x'^*)^t * [R]^{-1}(x'^*)} \text{ for correlated variables}$$

Where:

x'^* is the vector of the random variable values at the design point reduced to standard normal space;

$[R]$ is the correlation matrix of the variables.

According to Dalla (2015), the advantage of the FORM is its accuracy for small probabilities factors and its ability to easily deal with complex nonlinear limit state function without the need to take any derivates. The FORM can also be used in the limit state function of correlated basic random variables. As expressed by Haldar & Mahadevan (2000), the orthogonal transformation is commonly used to transform correlated into uncorrelated variables.

2.4.3.3 First Order Second Moment Method (FOSM)

This method is based on a first-order Taylor series (finite difference method) approximation of the limit values, linearized in the mean values of the random variables, using only the second moments statistics up to (mean and standard deviation) of the random variables by Haldar & Mahadevan (2000).

The first order of Taylor series is expanded around the mean value of the factor of safety function, not in the design point, as mentioned by Phoon (2008). Also, the FOSM is the simple method to calculate the mean and variance of the F_s. For a function expressed as:

$$Y = g(X_1, .. X_n) \tag{38}$$

Where:

$X_1, \ldots X_n$ are random variables, the mean and variance are:

$$\bar{Y} = g\left[(\overline{X_1}, \ldots, \overline{X_n})\right] \tag{39}$$

$$V(Y) = \sum_i \left(\frac{\partial g}{\partial X_i}\right)^2 V(X_i) + \ldots \sum_i \sum_j \left(\frac{\partial g}{\partial X_i}\right)\left(\frac{\partial g}{\partial X_j}\right) \operatorname{cov}(X_i X_j) = \rho_{ij}\sigma(X_i)\sigma(X_j) \tag{40}$$

Where:

$\frac{\partial g}{\partial X_i}$ is the sensitivity of g to go X_i;

$\operatorname{cov}(X_i X_j)$ Covariance of $X_i X_j \rho_{ij}$= correlation coefficient

2.4.3.4 Point Estimate Method (PEM)

This method was developed by Rosenblueth (1975) and compiled by Harr (1987). Taylor series are not used instead uses measured values of the independent variables at different points to estimate the random dependent variables.

As mentioned by Dalla (2015), the method is capable to estimate a statistical moment of any order of a model input involving several stochastic variables that can be correlated or uncorrelated, symmetric or asymmetric. Despite the multivariate problems with more than two stochastic variables involved, the Rosenblueth method is not capable to provide a single solution, slightly an approximate solution to certain indeterminate problem.

3 METHODOLOGY AND DATA

This chapter provides information about the four types of pavement structures studied, as well as axle configurations; tire pressures; and loading and overloading conditions. All the information of the methodology used to complete all the analyses is described belong.

3.1 PAVEMENT STRUCTURES

A total of four pavement structures were studied in this research and each of them represents common structures used in Brazil. Structure “C” is usually used for pavement reconstruction of sections where structural deficiencies are presented. Table 12 indicates the number of pavement layers in each structure; the material type and their correspondent classification number in the software mePADS as well as layer thicknesses and material properties such as elastic modulus and Poisson ratios.

Table 12: Thickness and material properties of the four asphalt pavement structures

Structure	Layer	Material	Material Classification (mePADS)	Thickness (mm)	E (Mpa)	Poisson’s Ratio ν
A	1	SMA	AG	40	3750	0.35
	2	HMA +rubber	AC	90	3750	0.35
	3	Granular Base	G2	200	250	0.35
	4	Macadam (dry)	G4	150	250	0.35
	5	Soil	Soil (G9)	∞*	100	0.35
B	1	HMA	AC	75	4000	0.30
	2	Granular Base	G2	150	400	0.40
	3	Gravel Soil	G7	200	200	0.40
	4	Soil	Soil (G9)	∞*	70	0.45
C	1	HMA	AC	100	3450	0.30
	2	HMA	AC	120	2950	0.35
	3	Granular Base	G2	150	290	0.40
	4	Macadam (dry)	G4	550	250	0.40
	5	Soil	Soil(G9)	∞*	60	0.45
D	1	HMA	AC	125	4000	0.30
	2	Granular Base	G2	200	600	0.35
	3	Gravel Soil	G7	250	200	0.40
	4	Soil	Soil (G9)	∞*	60	0.45

*A value of zero was specified in mePADS software to assume that a rigid layer exists at 1000 mm below the defined pavement

3.2 AXLE CONFIGURATIONS

This research adopted a specific axles configuration for the simulations in mePADS software to obtain the structural responses of each pavement structure in terms of axle type, loading and overloading conditions, and tire pressure.

a) Axle Types:

Six types of axles were considered in this research: single (S); dual (D); tandem (Td); tandem-spaced (Tds); tridem (Tr); and tridem-spaced (Trs). Table 13 illustrates each standard axle and their correspondent axle load in kN.

Table 13: Axle configuration

	Axle Name	Axle Type	Axle Load (kN)
1	Single		59
2	Dual	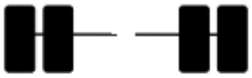	98
3	Tandem	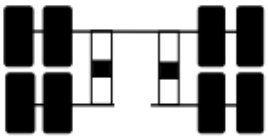	167
5	Tandem-spaced	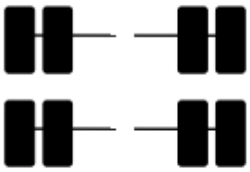	167
5	Tridem	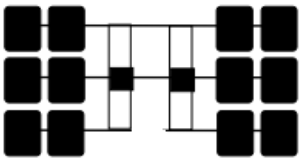	250
6	Tridem-spaced	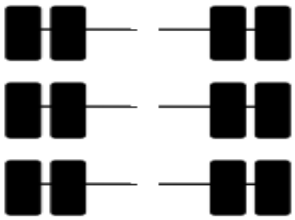	250

b) Load and Overload conditions:

Five overload percentages were adopted for each axle type: 0% (original axle load/no overload, Brazilian law 12/98); 7.5% (as stated in the Brazilian law 104/99); 10%; 20%; and 30%. Table 14 shows the different axle loads in kN and kg as well as the load by tire in kN that was used in the mePADS software for the simulations.

Table 14: Axle configuration used in the analysis

Axle Type	Axle Load (kg)	Axle Load (kN)	Load by tire (kN)
S0= Single (Resol. 12/98, 0%)	6000	59	29.4
S7.5= Single (Resol. 104/99, 7.5%)	6450	63	31.6
S10= Single (overload, 10%)	6600	65	32.4
S20= Single (overload, 20%)	7200	71	35.3
S30= Single (overload, 30%)	7800	76	38.2
D0= Dual (Resol. 12/98, 0%)	10000	98	24.5
D7.5= Dual (Resol. 104/99, 7.5%)	10750	105	26.4
D10= Dual (overload, 10%)	11000	108	27.0
D20= Dual (overload, 20%)	12000	118	29.4
D30= Dual (overload, 30%)	13000	127	31.9
Td0= Tandem (Resol. 12/98, 0%)	17000	167	20.8
Td7.5= Tandem (Resol. 104/99, 7.5%)	18275	179	22.4
Td10= Tandem (overload, 10%)	18700	183	22.9
Td20= Tandem (overload, 20%)	20400	200	25.0
Td30= Tandem (overload, 30%)	22100	217	27.1
Tds0= Tandem spaced (Resol. 12/98, 0%)	17000	167	20.8
Tds7.5= Tandem spaced (Resol. 104/99, 7.5%)	18275	179	22.4
Tds10= Tandem spaced (overload, 10%)	18700	183	22.9
Tds20= Tandem spaced (overload, 20%)	20400	200	25.0
Tds30= Tandem spaced (overload, 30%)	22100	217	27.1
Tr0= Tridem (Resol. 12/98, 0%)	25500	250	20.8
Tr7.5= Tridem (Resol. 104/99, 7.5%)	27412.5	269	22.4
Tr10= Tridem (overload, 10%)	28050	275	22.9
Tr20= Tridem (overload, 20%)	30600	300	25.0
Tr30= Tridem (overload, 30%)	33150	325	27.1
Trs0= Tridem spaced (Resol. 12/98, 0%)	25500	250	20.8
Trs7.5= Tridem spaced (Resol. 104/99, 7.5%)	27412.5	269	22.4
Trs10= Tridem spaced (overload, 10%)	28050	275	22.9
Trs20= Tridem spaced (overload, 20%)	30600	300	25.0
Trs30= Tridem spaced (overload, 30%)	33150	325	27.1

Note: charts presented along the thesis consider the overload percentage in the “x” axis and charts presented in the Appendices consider instead the load by tire in kN.

c) Axle Spacing:

Different axle spacing was considered for tandem and tridem and tandem-spaced and tridem-spaced axles, as follows:

- Tandem and Tridem = 1270 mm
- Tandem-paced and Tridem-spaced = 2400 mm

d) Tire Pressures:

Three different wheel pressures are taken in consideration:

- Low=550 KPa (80Psi)
- Medium=690 KPa (100 Psi)
- High=830 KPa (120 Psi)

3.3 STRUCTURAL RESPONSES

The mechanistical-empirical pavement design software mePADS (based on the practicality and low computational demand) was used to obtain four structures responses. This software allows data capturing associated with the design parameter of each structure such as the type of material, layer thickness (mm), elastic modulus (MPa), and Poisson's ratio. As cited in Table 12, a value of zero was specified in mePADS for subgrade thickness in order to assume that a rigid layer exists at 1000 mm below the defined pavement. MePADS have no provisions for semi-infinite pavements).

Figure 20 shows the mePADS software interface where the pavement structure characteristics are stablished. As can be seen, mePADS offers options to introduce climate region; terminal rut depth; road category; and design traffic class. Such options allow estimating the pavement life of each pavement layer based on certain equations inherent to the software itself define by the republic of South Africa. This research used mePADS software only to compute the pavement structural responses of interest and those options were not used. It is important to highlight that the user can omit these options and does not affect in the computation of the simulation results.

Figures 20 shows the input parameters for structure A while Figure 21 shows the loads and evaluation points interface to input the specifications of a certain axle type; the single load applied by each tire; tire pressure; and axle position/spacing distance in the

x-y axis. In addition, the same window showed in Figure 21 allows defining the position in X, Y, and Z where stresses and strain will be obtained.

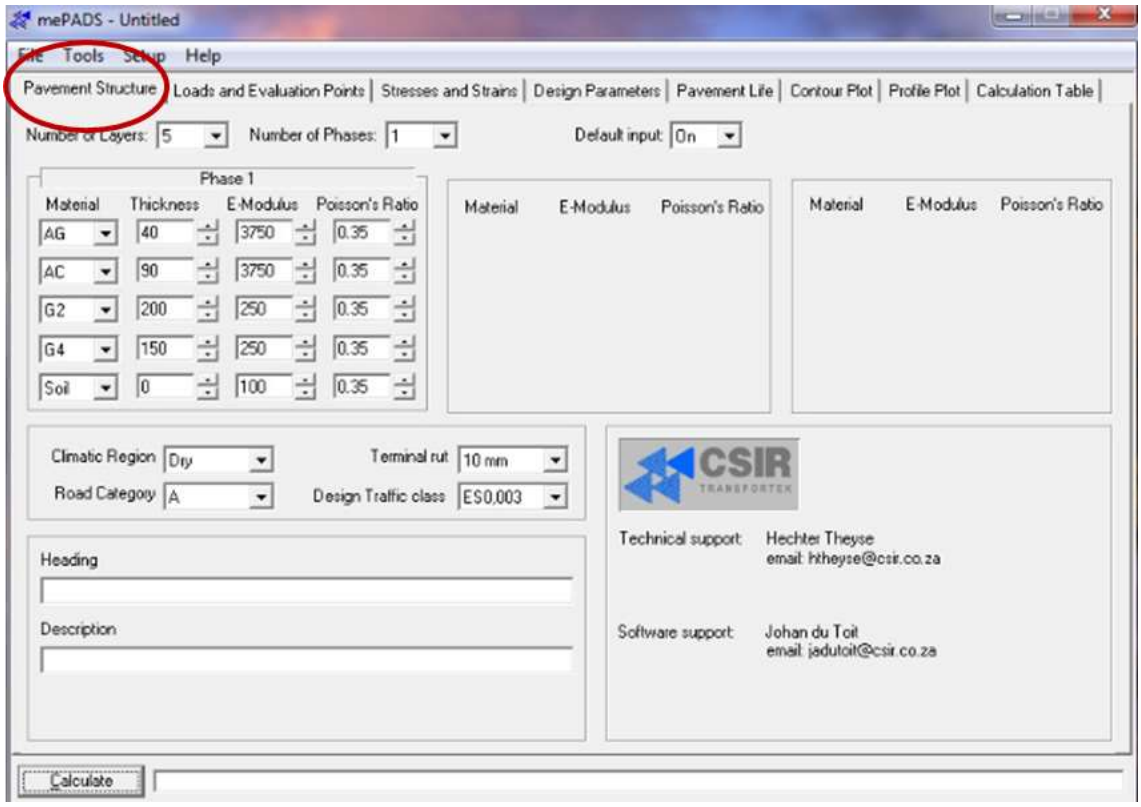

Figure 20 mePADS software interface where pavement structure characteristics are stablished

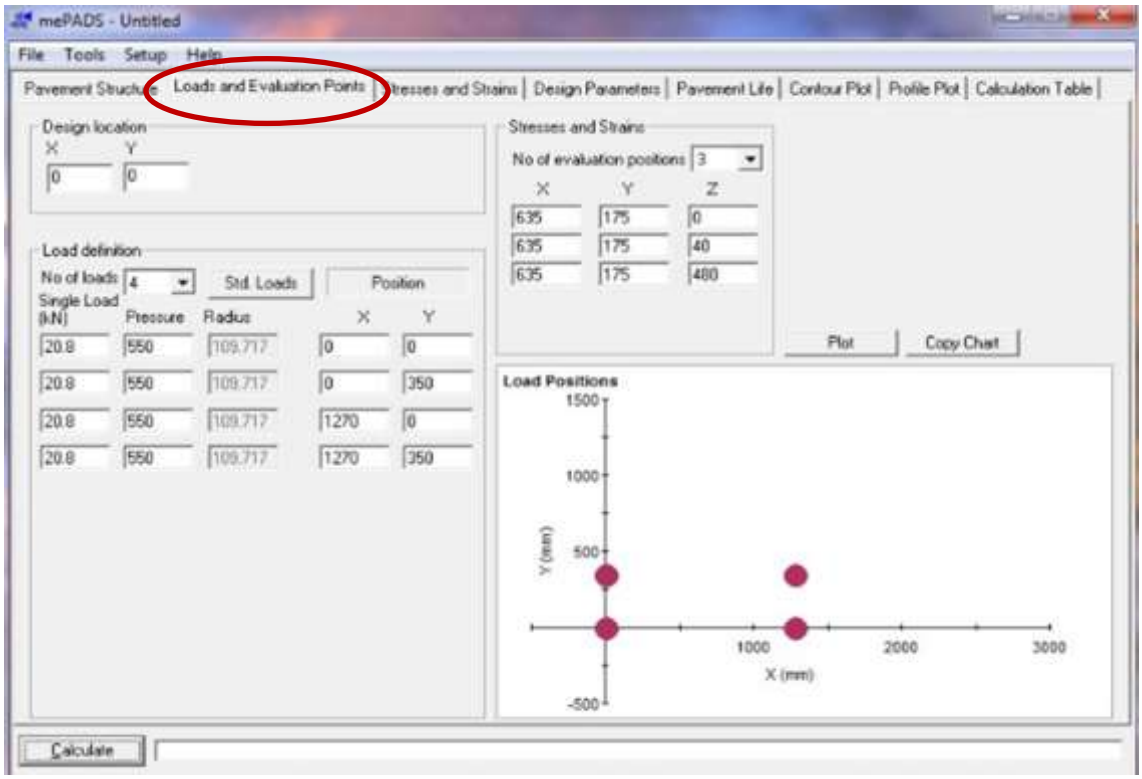

Figure 21 mePADS loads and evaluation points interface

By setting all input required to run the simulation it is possible to obtain stresses and strain. In this research only the following four structural responses were studied:

1) δ_1 = Surface displacements in mm (mePADS UZ=Displacement in Z);
2) εht_1= horizontal tensile strain at the bottom of the asphalt layer, in microstrain (mePADS Normal Strain in xx / PE1=Principal Normal Strain in X);
3) εvc_1= Vertical compression strain at the bottom of the asphalt layer, in microstrain (mePADS EZZ=Principal Normal Strain in Z / PE3=Principal Normal Strain in Z); and,
4) εvc_m= Vertical compression strain at the top of the subgrade, in microstrain (mePADS Principal Normal Strain in Z / PE3=Principal Normal Strain in Z).

Figure 22 illustrates the response points by axle type. Note that for single axle the response point was taken at the center of the tire; for dual axle, the point was taken between and at the center of the tires; and for the rest axles, this point was taken between the tires and at the center of the tandem or tridem system, depending on the case.

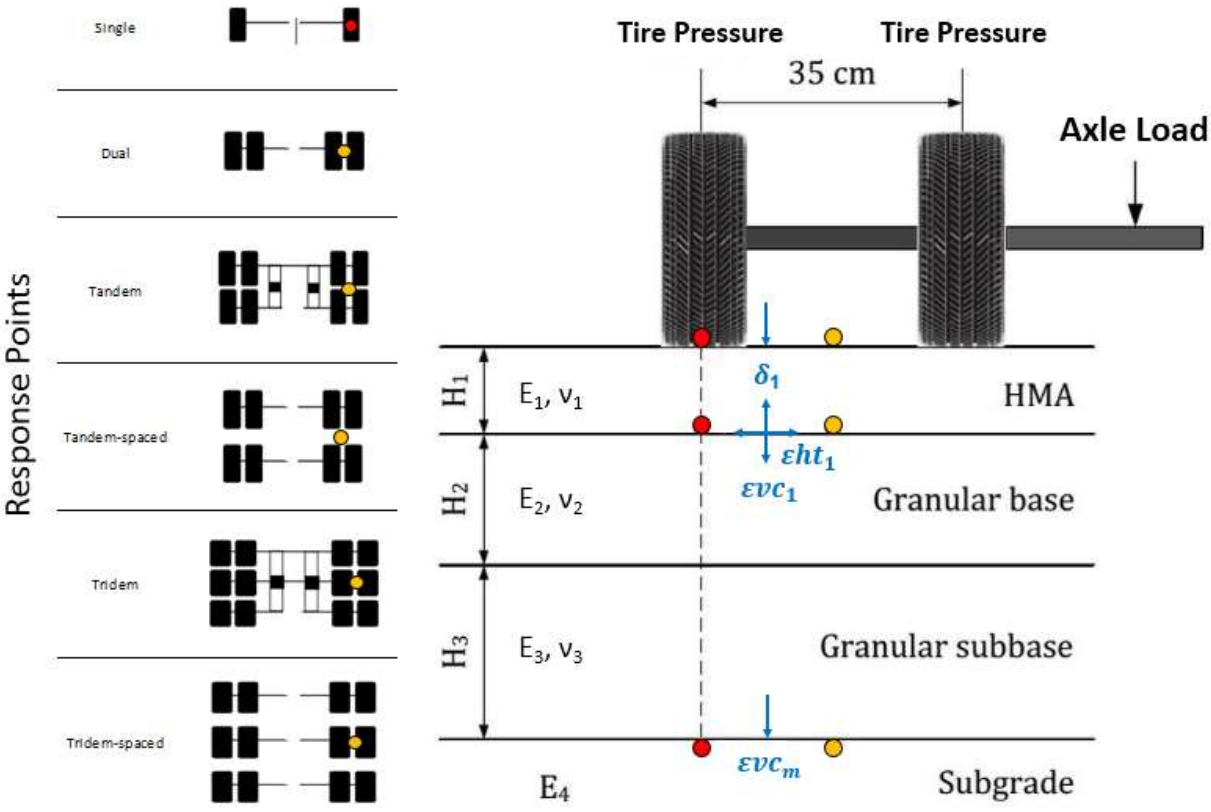

Figure 22 Response points in pavement structures according to the axle type

Figure 23 shows the mePADS output interface. Displacements are given in millimeters, stresses in kPa, and strain in microstrain. In addition, negative and positive values correspond to compressive or tensile responses, respectively. Result clipboards provided by mePADS were copied to an Excel sheet to extract the responses and stored them into a database that integrates all the simulation results.

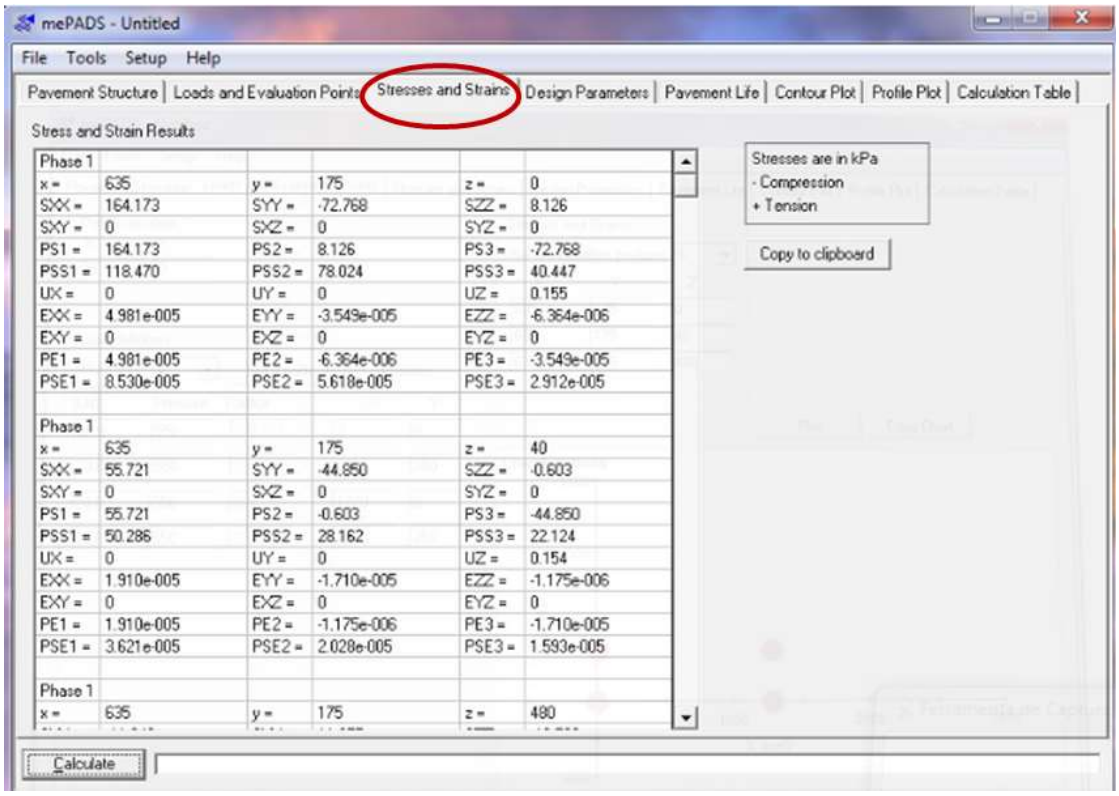

Figure 23 Stresses and Strain obtained by the mePADS software

To visualize strain and stress distributions in the structure surface or depth, mePADS provides a contour plot section that allows the user defining the plane of the contour plot; establishes plot ranges on X and Y-axis in millimeters; and select several plot parameters. As an example, Figure 24 shows normal strain in YY in a vertical plane parallel to X-Z, for the structure “A” and for a tandem axle with 550 KPa (80 psi) of tire pressure.

3.4 CYCLES TO FAILURE (“N” NUMBERS)

Empirical Asphalt Institute’s pavement life predictions in terms of the number of cycles to failure (N numbers) for both fatigue cracking and rutting pavement distresses were carried out.

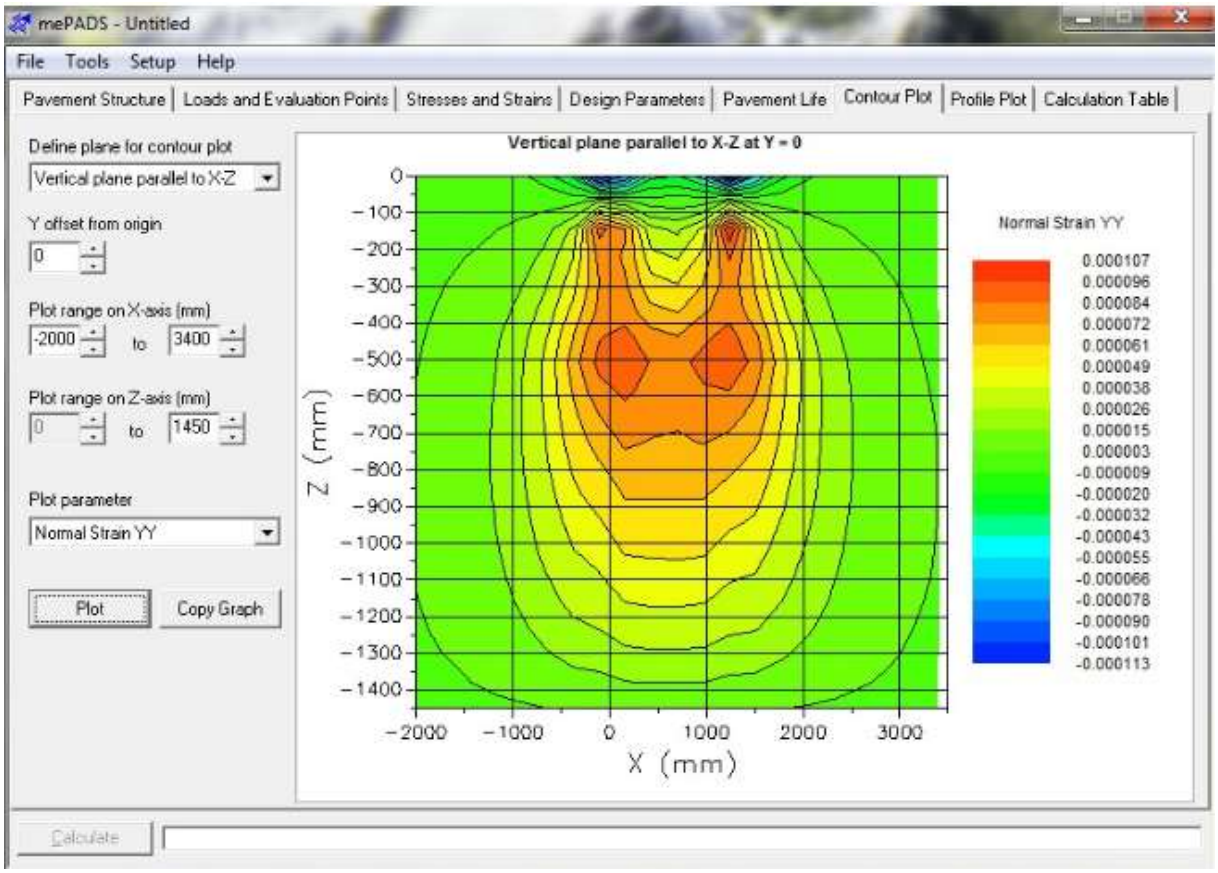

Figure 24: Contour Plot of the vertical plane of structure A, Tandem Axle

To calculate the number of load repetitions to fatigue cracking failure (Nf) and rutting failure (Nr) were used the horizontal tensile strain developed at the bottom of the asphalt layer (εht_1) and the vertical compressive strain developed at the top of the subgrade layer (εvc_m), respectively. Also, Nf requires the modulus of elasticity of the asphalt concrete. Equations 1 and 2 in Chapter 2 are the Nf and Nr formulas, respectively. Once Nf and Nr are calculated, the smaller value is adopted as a critical N value, referred in this research as “Critical Resistance”.

Note: this research assumes that critical N values are Critical Resistances and that solicitations are those defined from resistances varying as a function of the Safety Factors.

3.5 RELIABILITY ANALYSIS

To perform the reliability analyses the following steps were followed:

1) Nf and Nr were calculated for each structure, axle type, overload percentage, and tire pressure using the empirical model suggested by the Asphalt Institute. The lower values between Nf and Nr were adopted as critical resistances.

2) On the other hand, solicitations were determined based on several Safety Factors (SF). Thus, critical resistances were divided by a certain SF (SF=resistance/solicitation) and the resulting value was computed as solicitation. The SFs considered in this research were 0.20; 0.40; 0.60; 0.80; 1.00 (as a control parameter where the probability of failure always is 0.50); 2.0; 3.0; 4.0; and 5.0.
3) All resistances and solicitations were assumed as average values (μr and μs, respectively). In this context, the standard deviations of the resistances (σr) and solicitations (σs) were determined based on the standard deviations for each structure (A, B, C, and D), axle type (S, D, Td, Tds, Tr, and Trs), overload percentage (0, 7.5, 10, 20, and 30), and tire pressure (550 KPa, 690KPa, 830 KPa) configuration.

   As a result, a large set of μs-σs (solicitation curves) and μr-σr (resistance curves) values were obtained.
4) Margin curves (M) were calculated in order to determine the area where the probability of failure might occur. M curves were calculated for both averages and standard deviations, as follows:

$$\mu_M = (\mu r - \mu s) \tag{41}$$

$$\sigma_M = (\sigma r^2 + \sigma s^2)^{0.5} \tag{42}$$

5) Reliability index (β) is calculated from margin curves as follows:

$$\beta = \frac{\mu_M}{\sigma_M} \tag{43}$$

6) Therefore, with β values calculated it is possible to determine the probability of failure (Pf). Pf can be calculated easily through the NORM.DIST function in Excel which returns the normal distribution for the specified mean and standard deviation:

NORM.DIST(x,mean,standard_dev,cumulative) (44)

   Where:

   - X is the required value (the value for which we want the distribution, in our case β);
   - Mean is the arithmetic mean of the distribution;

- Standard_dev is the standard deviation of the distribution;

Cumulative is a logical value that determines the form of the function. If cumulative is TRUE, NORM.DIST returns the cumulative distribution function; if FALSE, it returns the probability density function. The equation for the normal density function (cumulative = FALSE) is:

(45)

$$f(x;\mu,\sigma) = \frac{1}{\sqrt{2\pi\sigma}} e^{-\left(\frac{(x-\mu^2)}{2\sigma^2}\right)}$$

When cumulative = TRUE, the formula is the integral from negative infinity to x of the given formula. In our case we need to select TRUE. Thus, the probability of failure Pf can be calculated as follows:

(46)

$$P_f = 1 - \text{NORM. DIST}(\beta, 0, 1, \text{TRUE})$$

If mean = 0, standard_dev = 1, and cumulative = TRUE, NORM.DIST returns the standard normal distribution, NORM.S.DIST.

Figure 25 illustrates the process to calculate the reliability index β and the probability of failure Pf.

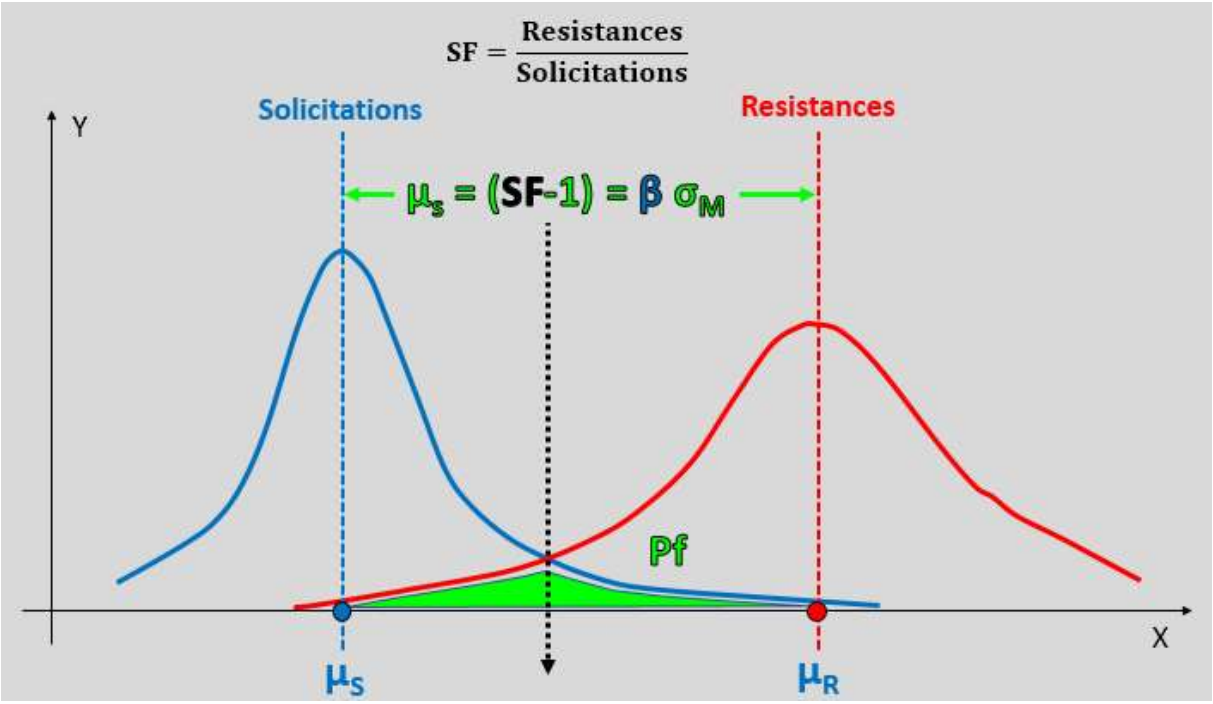

Figure 25 Reliability index concept

3.6 CRITICAL RESISTANCE VS OVERLOAD

Additional analysis of critical resistances versus overload percentages was conducted. All critical resistances of each structure were considered. A Root Mean Square (RMS) values – an arithmetic Mean that takes into account the standard deviation of the data – as well as the minimum and maximum values were also considered.

3.7 STATISTICS

Statistics for solicitations, resistances, reliability indices, and probabilities of failure were carried out as follows:

1. Descriptive statistics including histograms were obtain to verify the normality of the data. It was needed to improve normality of the data and was used the variable transformation by inverse distribution function of the IBM-SPSS software version 26. Normalized data histograms and residual statistics were obtained to verify the normal distribution.
2. Person's correlation analyses between variables were carried out using the normalized data;
3. Four multivariate linear regression models were carried out where probability of failure, resistance, solicitation, and reliability index were considered as dependent variables, separately, as shown in Table 15.

Table 15 Multivariate Linear Regression Models

Model	Dependent Variable	Independent Variables
1	Probability of failure	Resistance Solicitation
2	Resistance	Probability of failure Solicitation
3	Solicitation	Probability of failure Resistance
4	Reliability Index	Resistance Solicitation

Finally, Regression results were presented in the form of regression model summaries (including mainly R, R-squared, and level od significance); coefficients; and residual statistics (Histograms, Normal P-P plots, Scatterplots, and Partial Regression Plots of standardized residuals, that can be found in Appendix G).

4 RESULTS AND DATA ANALYSIS

This chapter presents the pavement data obtained from the simulations carried out in the MePads software for each of the four pavement structures studied in this research. The chapter is divided into three major sections, as listed below, and provides a brief analysis of the graphical information presented and the respective discussion of the findings.

1) Structural responses: surface displacements or deflections (δ_1); horizontal tensile strain at the bottom of the asphalt layer (εht_1); vertical compressive strain at the bottom of the asphalt layer (εvc_1); and vertical compressive strain at the top of the subgrade (εvc_m). All of them by axle type, axle load, and tire pressure;
2) Empirical Asphalt Institute's pavement life predictions in terms of the number of cycles to failure (N) for both fatigue cracking and rutting pavement distresses;
3) Reliability Index (β) and Probability of Failure (Pf) as a function of critical resistances (critical N) and solicitations defined by several safety factors (SF).

4.1 STRUCTURAL RESPONSES

4.1.1 Surface Displacements or Deflections (δ1)

Figure 26 to 29 presents the displacement values, in millimeters, of each structure by axle types (single, dual, tandem, tandem-spaced, tridem, and tridem-spaced); axle loads (0%, 7.5%, 10%, 20%, and 30% of overload); and tire pressures (550 KPa, 690 KPa, and 830 KPa).

As can be seen, surface displacements increase as both overload and tire pressure increase. As tire pressure increase, the surface contact area decreases and, consequently, the load applied become to be more concentrated. It is evident that tire pressure and overload does not only relate to fuel economy and vehicle efficiency but also to pavement deterioration.

According to Figures 26 to 29, dual, tridem, and tridem spaced axles have the highest surface displacements. However, it is evident that the structural configuration of the pavement (thicknesses and property materials) influences on the amount of this value. In this sense, structure B (asphalt layer equal to 75 mm) is the configuration that has

the highest values, ranging from 0.32 to 0.52 mm for single, dual, tridem, and tridem spaced axles.

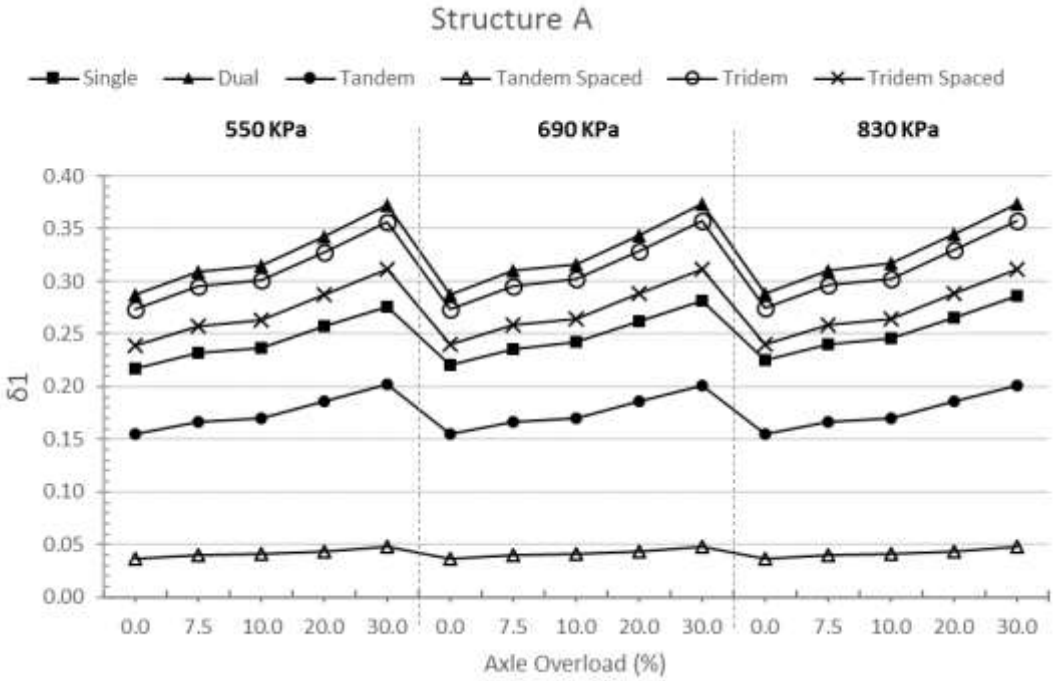

Figure 26 Surface displacements in Structure A

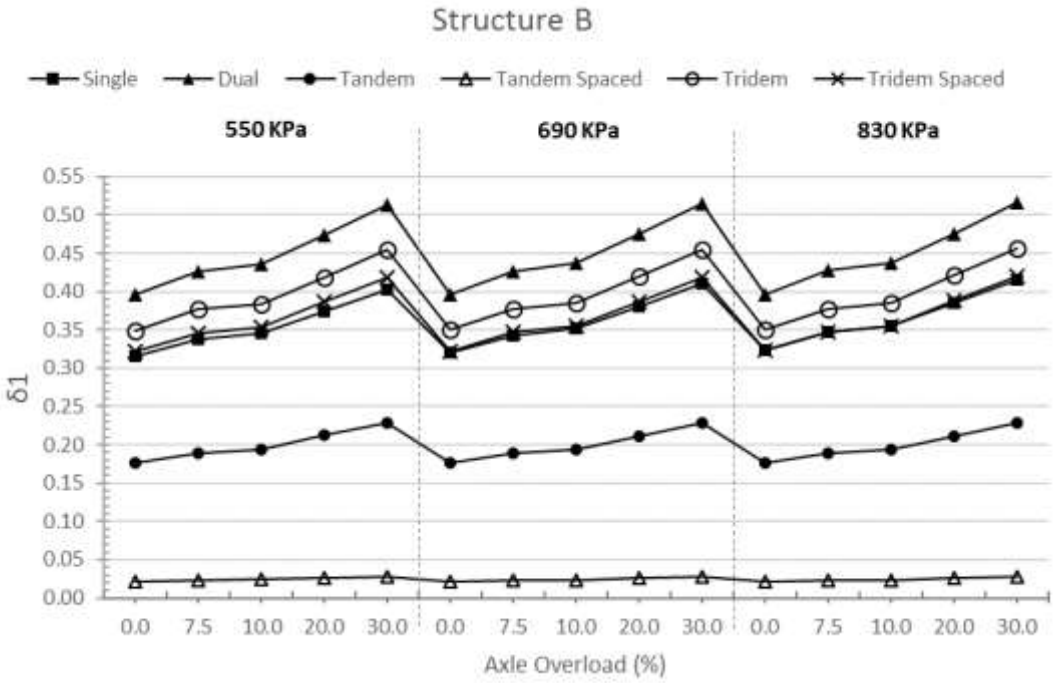

Figure 27 Surface displacements in Structure B

Data shows that pavement displacements range from 0.02 mm to 0.50 mm. In general, tandem spaced axles present the lowest displacements in all four structures. Single, dual, tridem, and tridem spaced axles have maximum values between 0.20 mm and

0.40 mm however, they may exceed 0.50 mm as in the case of the dual axle traveling the structure B.

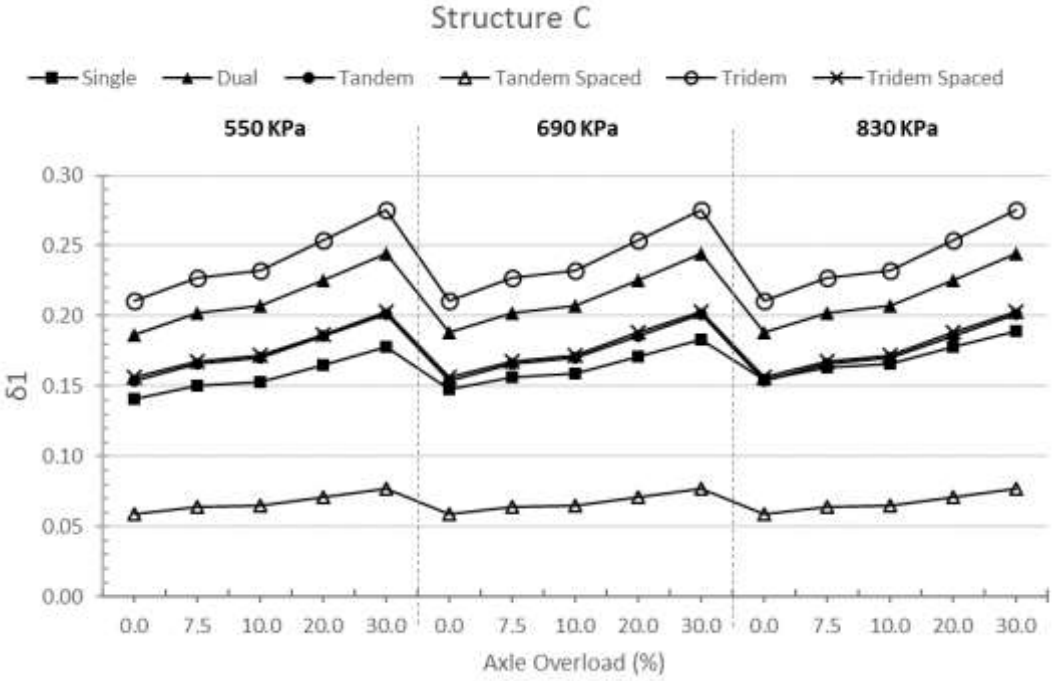

Figure 28 Surface displacements in Structure C

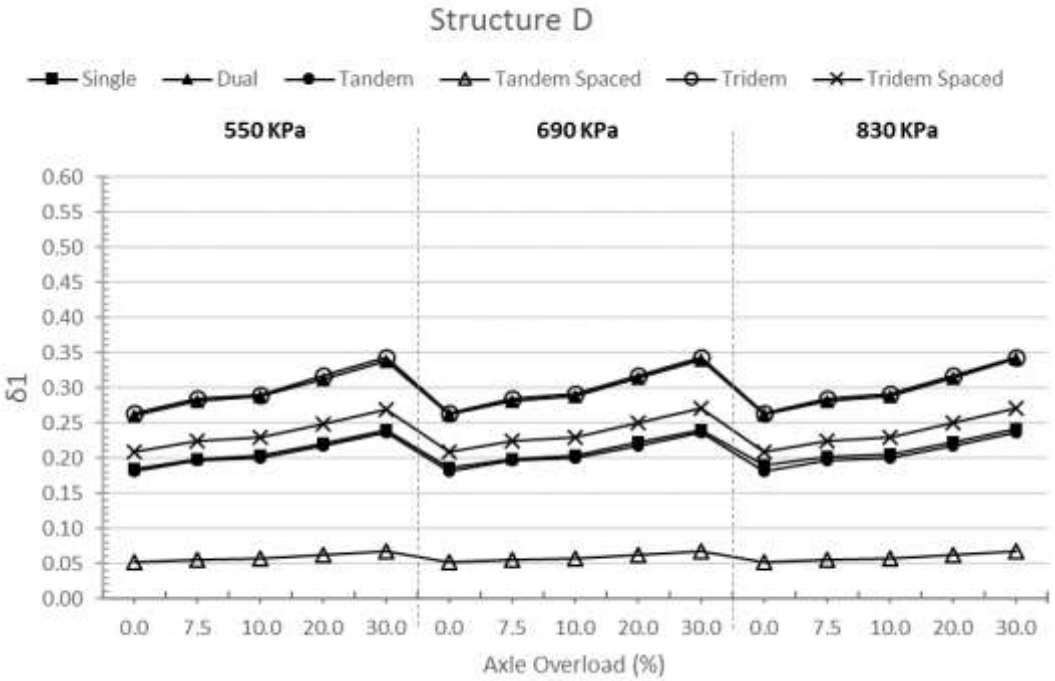

Figure 29 Surface displacements in Structure D

Figures 30 and 31 show the minimum and maximum surface displacements by structure and axle type. Note that, even Structure B is responsible for the highest

surface displacements, it presents the lowest maximum and minimum values for the tandem-spaced axle.

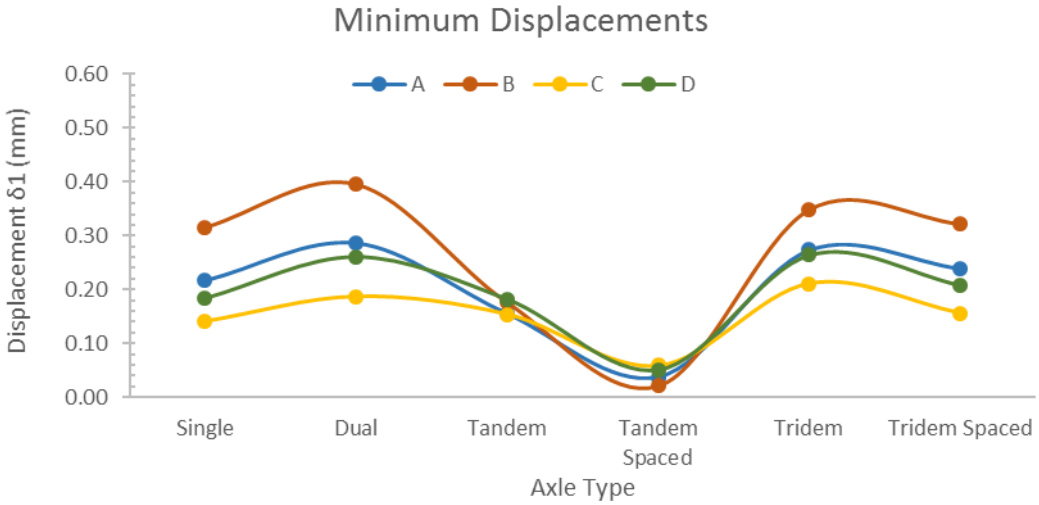

Figure 30 Minimum surface displacements by axle type

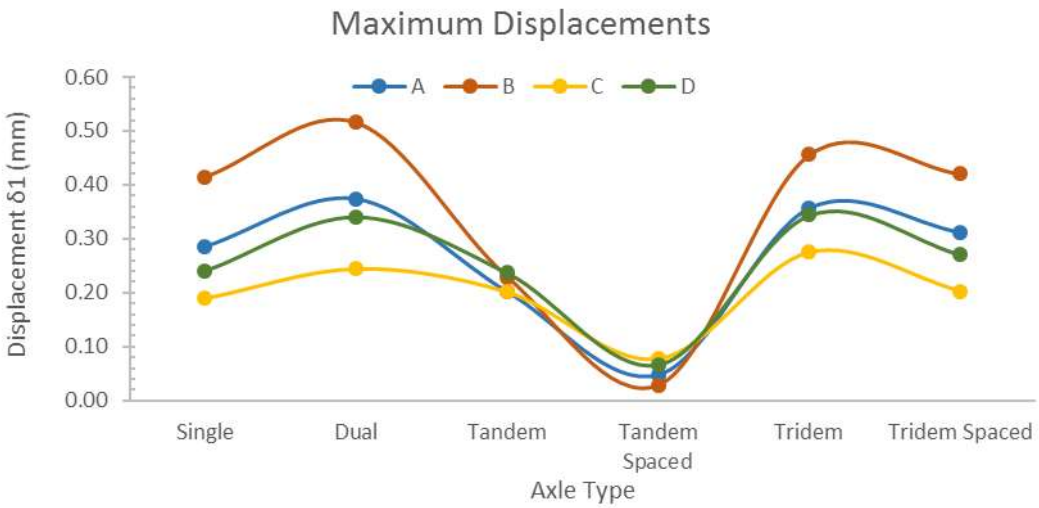

Figure 31 Maximum surface displacements by axle type

In order to identify displacements behavior, Figure 32 summarizes the average rate of increase for surface displacements as a function of the overload percentage and tire pressure. The first value corresponding to 0% overload and tire pressure of 550 KPa was taken as a reference to obtain the percentages of increase.

The figure shows a small rate of increase between tire pressures (about 0.41 %) directly proportional to the overload. Complementary graphs showing displacement data by axle overload and tire pressure can be found in Appendix A.

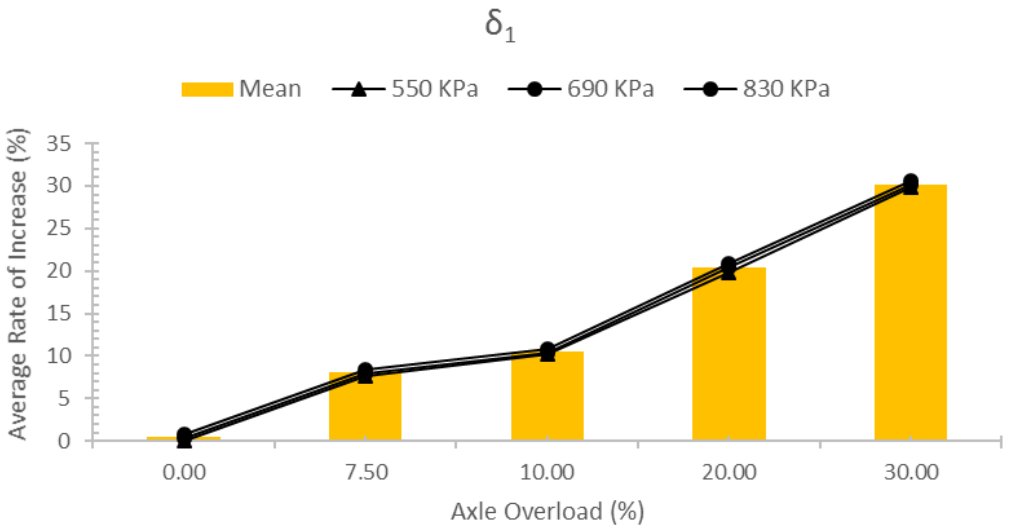

Figure 32 Average rate of increase for surface displacements

4.1.2 Horizontal Tensile Strain at the Bottom of the Asphalt Layer (εht$_1$)

Figure 33 to 36 presents the horizontal tensile strain at the bottom of the asphalt layer of each structure by axle type, overload percentage, and tire pressure, in the same format of surface displacements. Tensile strain are negative values and compressive strain positive values.

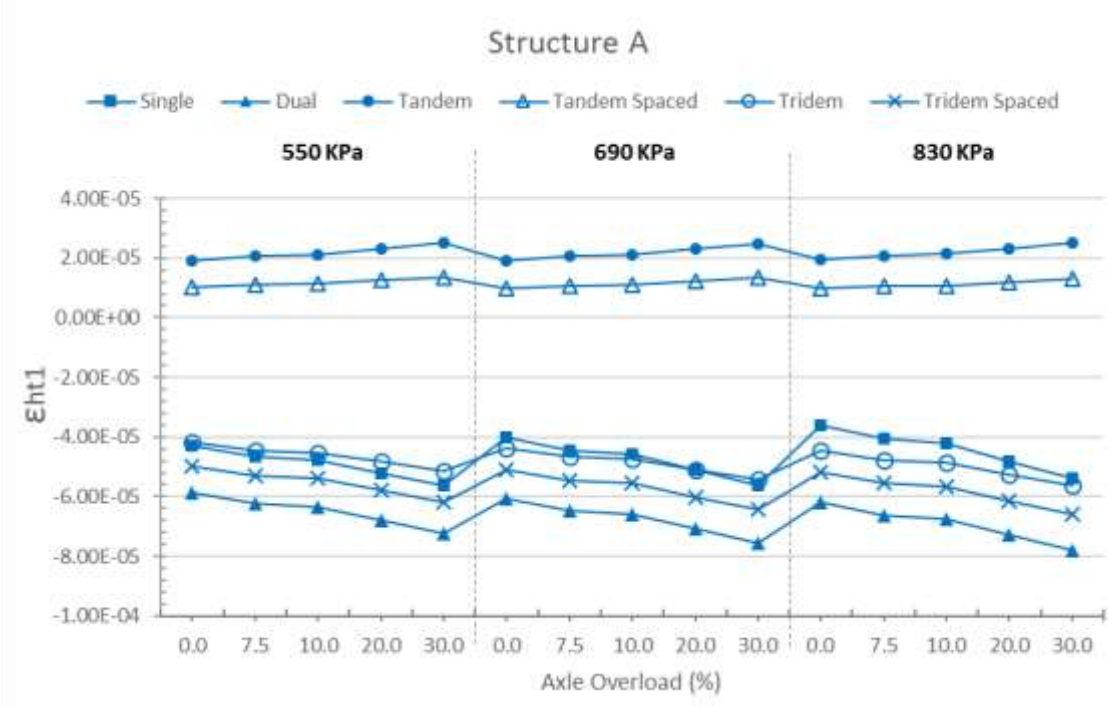

Figure 33 Horizontal strain at the bottom of the asphalt layer in Structure A

Figure 33, for example, shows that tandem and tandem-spaced axles in Structure A generate low compressive strain between 1E-05 to 2.5E-05, while the other axles

produce compressive strain ranging from -4.0E-05 to -8.0E-05. The opposite occurs in structure B (Figure 9), where only tandem and tandem-spaced axles produce tensile strain at the bottom of the asphalt layer.

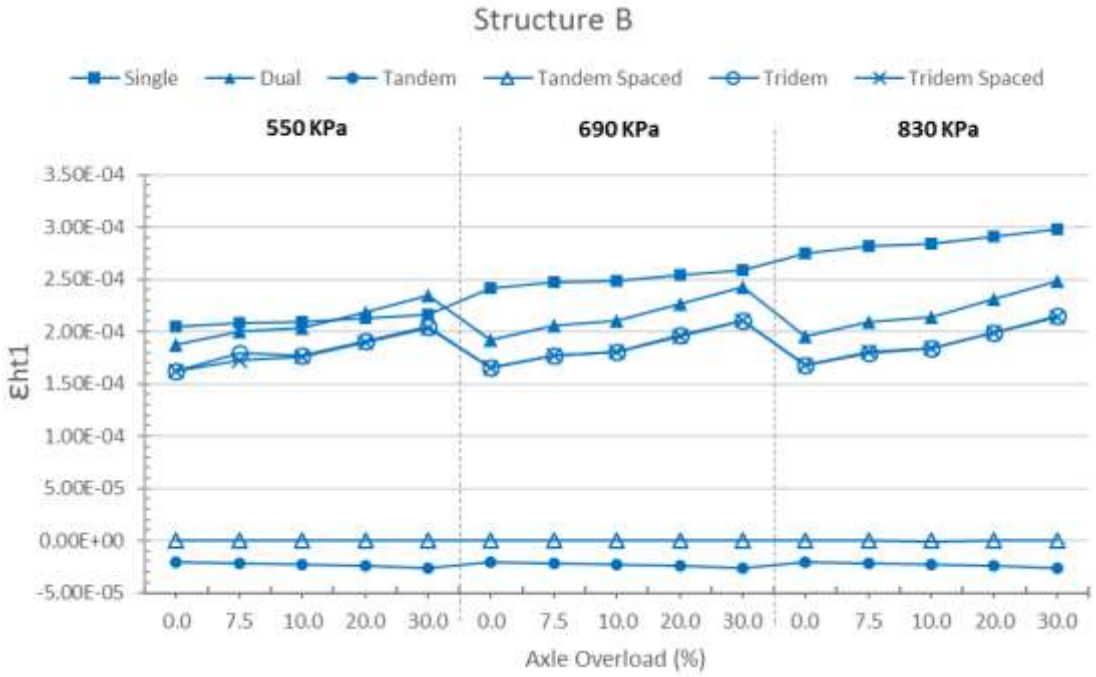

Figure 34 Horizontal strain at the bottom of the asphalt layer in Structure B

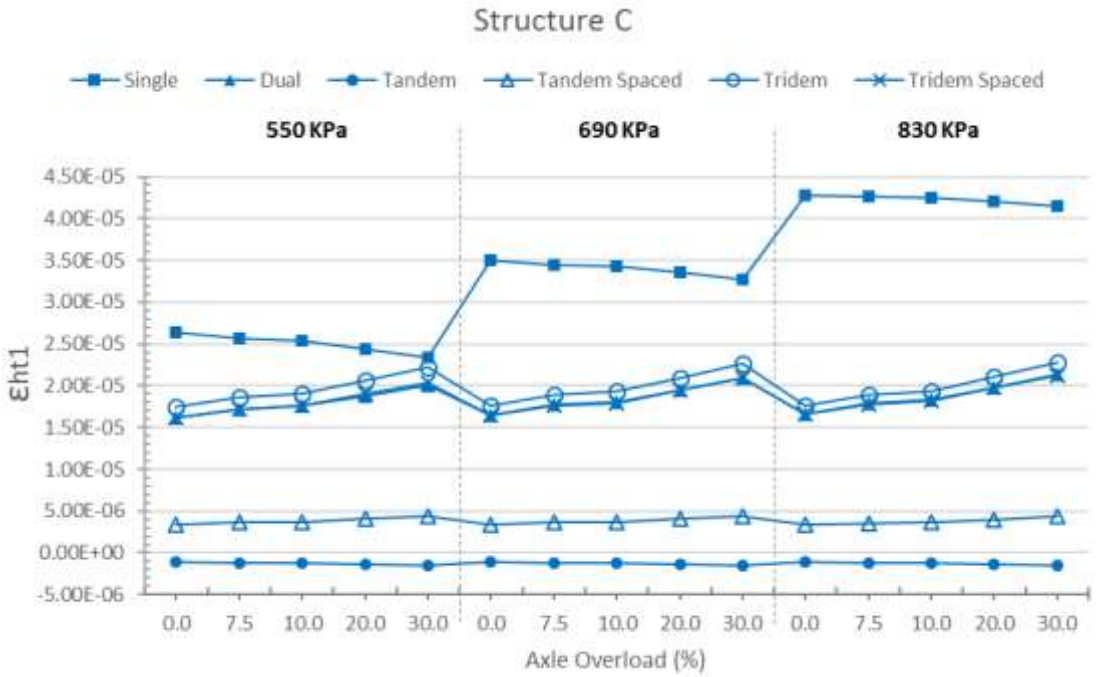

Figure 35 Horizontal strain at the bottom of the asphalt layer in Structure C

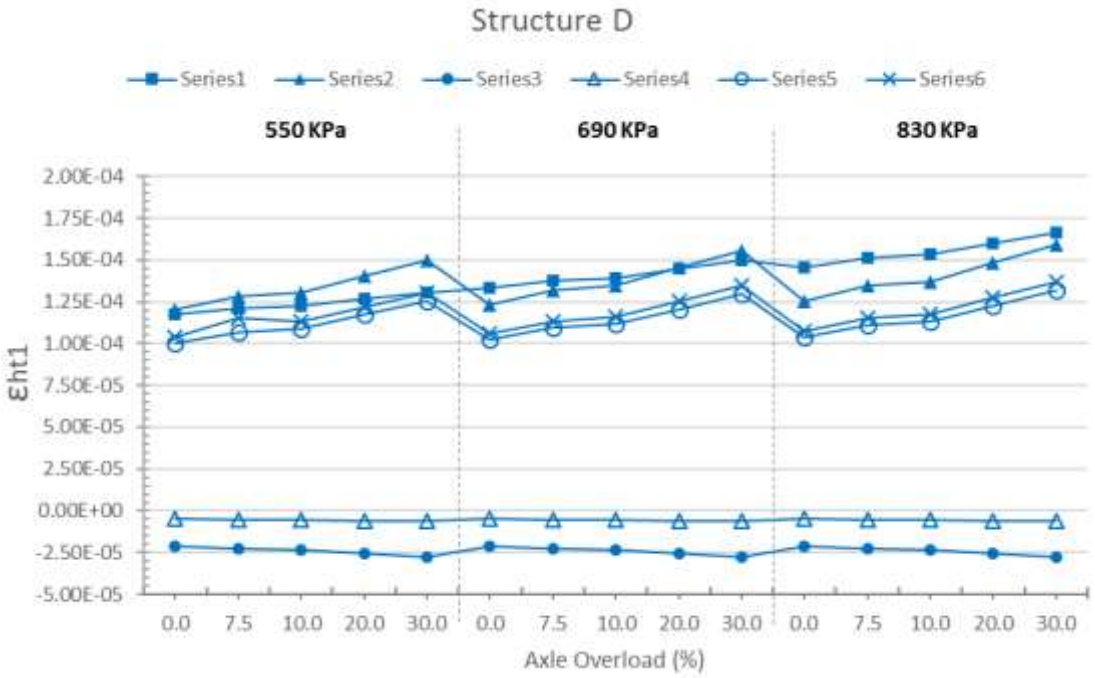

Figure 36 Horizontal strain at the bottom of the asphalt layer in Structure D

As can be seen, strain increase as both overload and tire pressure increase. Strain at the bottom of the asphalt layer shows the highest values in structure B, mainly for single, dual, tridem, and tridem spaced axles.

In Structure C, single, dual, tridem, and tridem-spaced axles produce compressive strain. Although single axle strain decreases as overload increases, these values showed more sensitivity to tire pressure, with a high increase rate compared to the other axles.

In general, tensile strain were generated only by single, dual, tridem, and tridem-spaced axles in structure A; tandem and tandem-spaced axles in structure B; tandem axle in structure C; and tandem and tandem-spaced axles in structure D. All other values are positive indicating that are compressive strain.

Figures 37 and 38 shows the minimum and maximum strain by structure and axle type. According with the data, horizontal strain at the bottom of the asphalt layer ranges from -7.80E-05 (dual axle in Structure A) to 2.98E-04 (single axle in Structure B). Observe that tandem and tandem spaced axles present the lowest strain in the four structures. However, the highest strain occurs in Structures B and D. In addition, Structure C has the lowest minimum and maximum strain in all axle types.

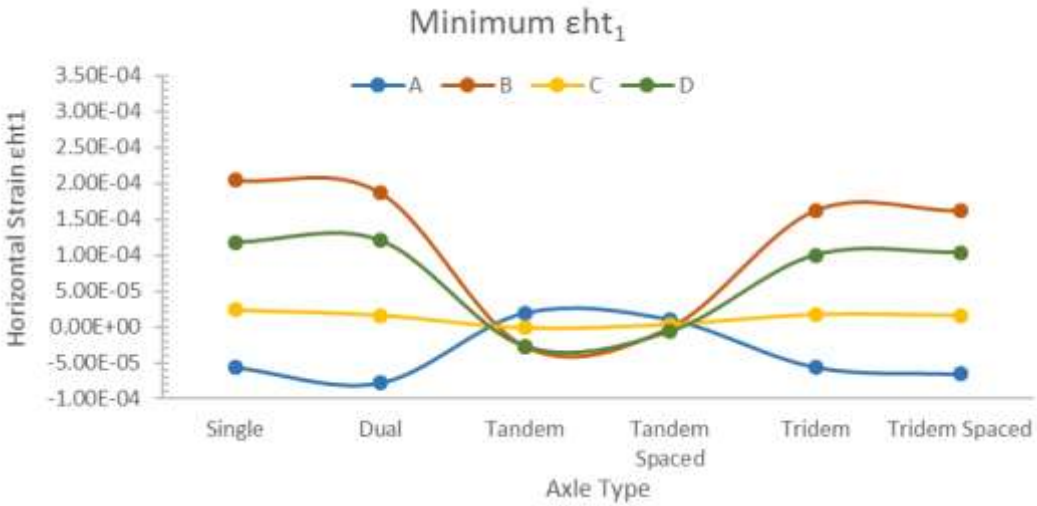

Figure 37 Minimum horizontal strain at the bottom of the asphalt layer by axle type

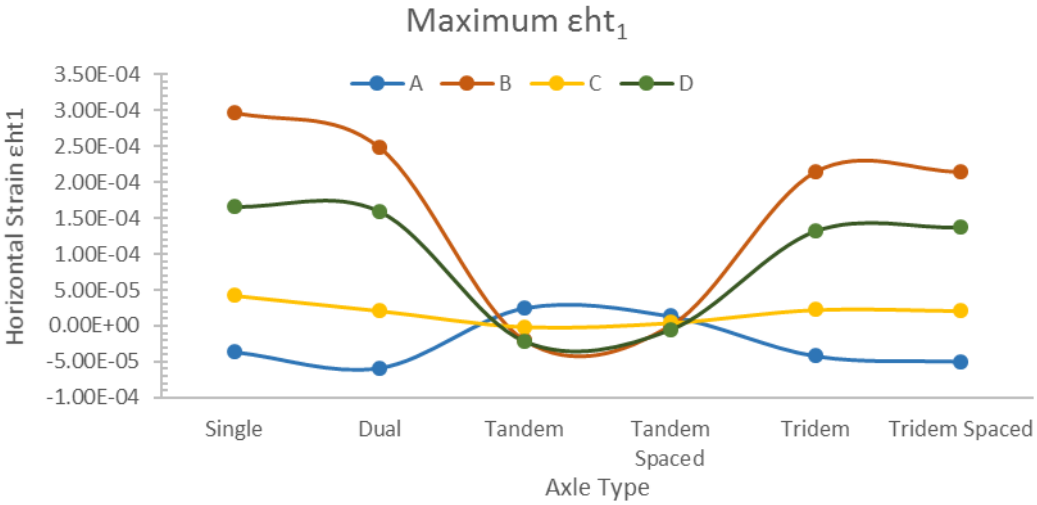

Figure 38 Maximum horizontal strain at the bottom of the asphalt layer by axle type

Figure 39 summarizes the average rate of increase for horizontal strain as a function of the overload percentage and tire pressure. The figure shows a moderate rate of increase between tire pressures (about 7.5 %) as overload increases.

As can be seen, the rate of increase in strain values at the bottom of the asphalt layer increase as tire pressure increase. At 0% of overload, strain increases up to 8% if the tire pressure increases from 550 KPa to 690 KPa and up to 12% from 690 KPa to 830 KPa. Likewise, at 30% of overload, strain increases up 28% if the tire pressure increases from 550 KPa to 690 KPa and up 37% if it reaches 830 KPa.

Complementary graphs showing horizontal strain data by axle overload and tire pressure can be found in Appendix B.

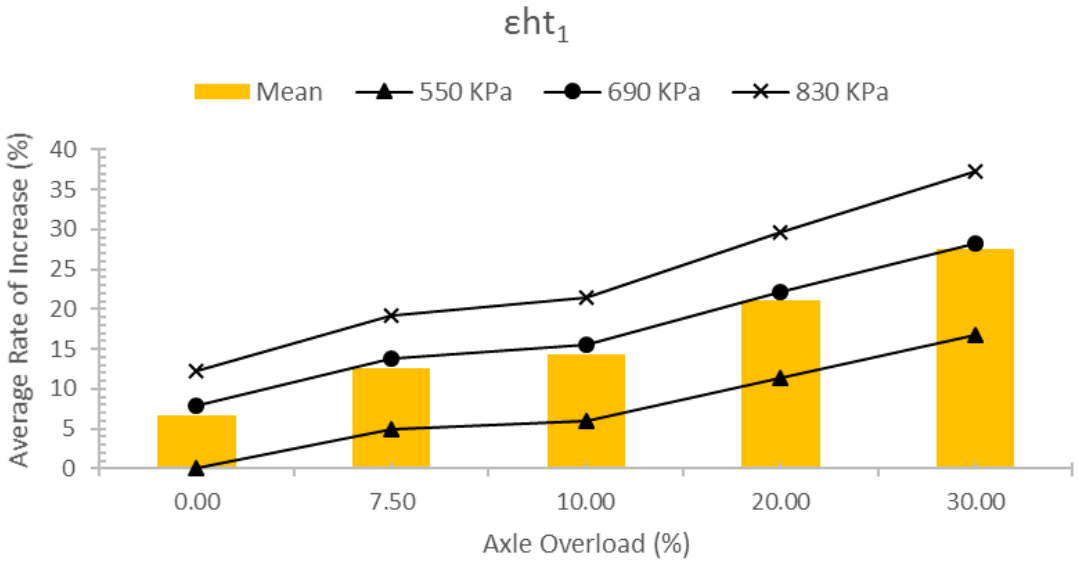

Figure 39 Average rate of increase for horizontal strain at the bottom of the asphalt layer

4.1.3 Vertical Compressive Strain at the Bottom of the Asphalt Layer (εvc_1)

Figure 40 to 43 presents the vertical compressive strain at the bottom of the asphalt layer of each structure by axle type, overload percentage, and tire pressure, in the same format of horizontal tensile strain.

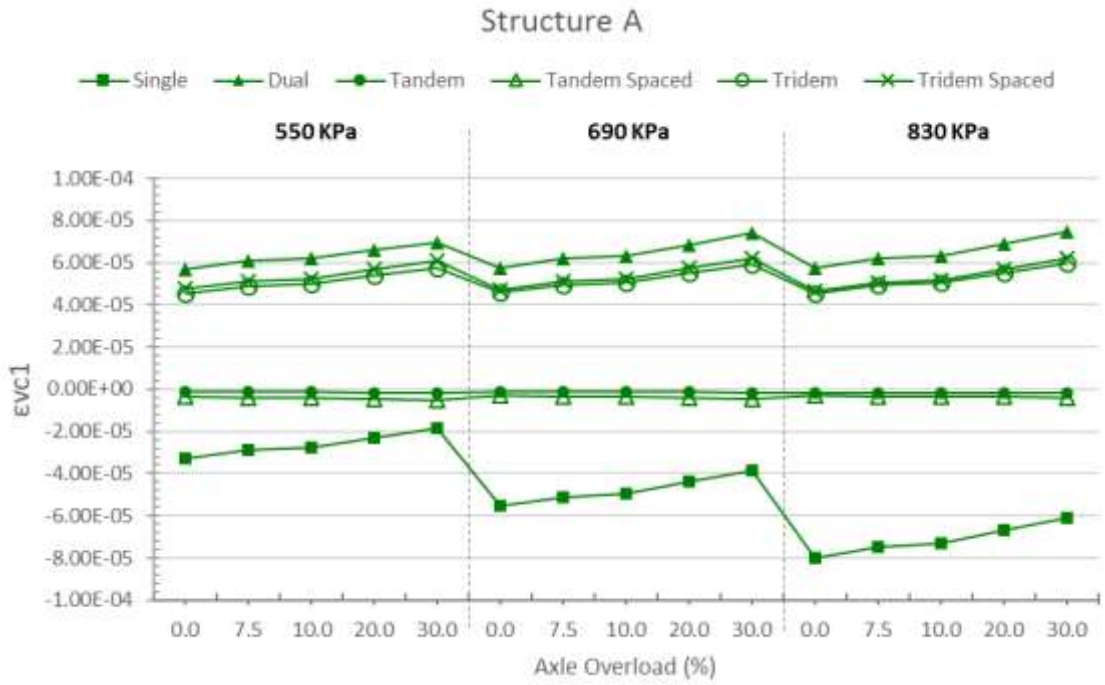

Figure 40 Vertical strain at the bottom of the asphalt layer in Structure A

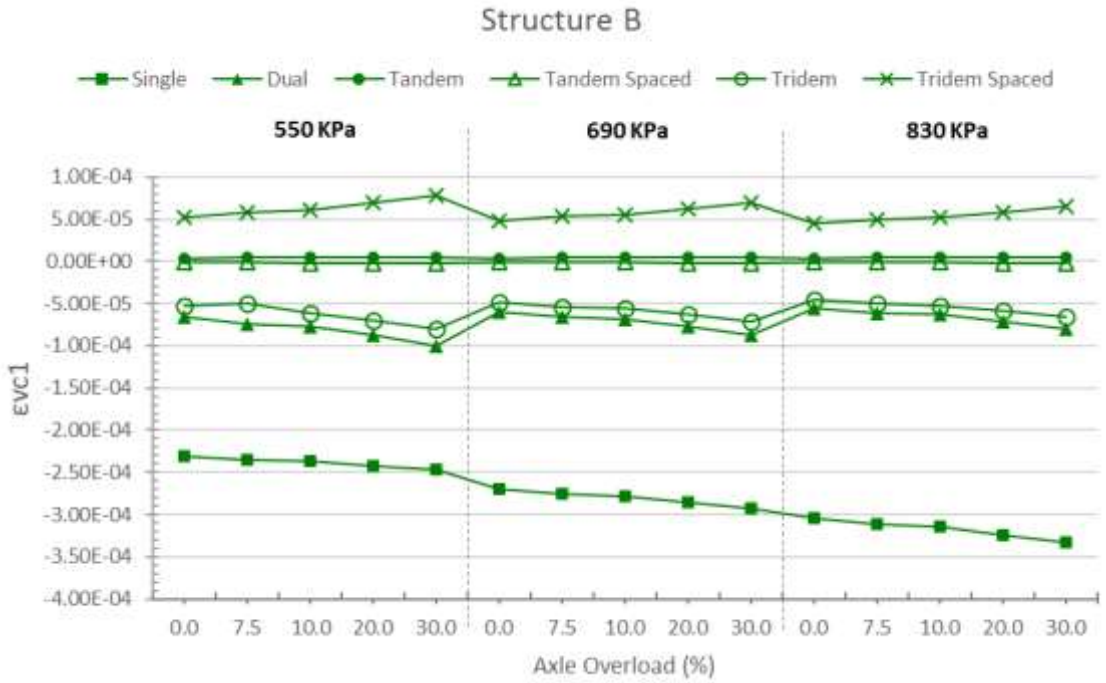

Figure 41 Vertical strain at the bottom of the asphalt layer in Structure B

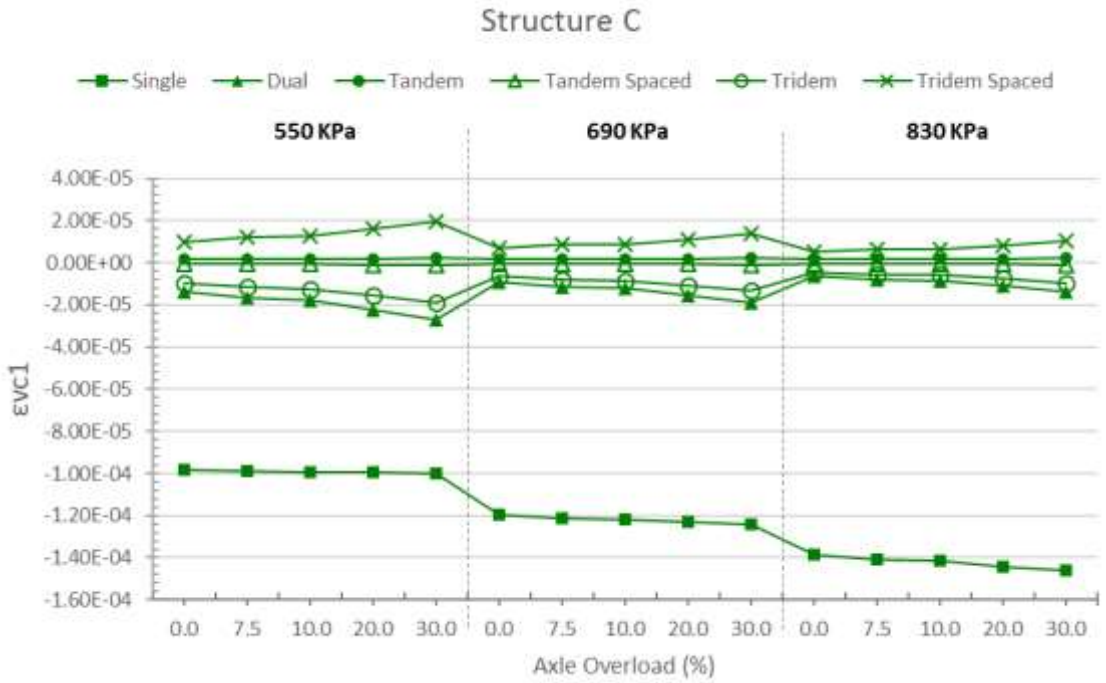

Figure 42 Vertical strain at the bottom of the asphalt layer in Structure C

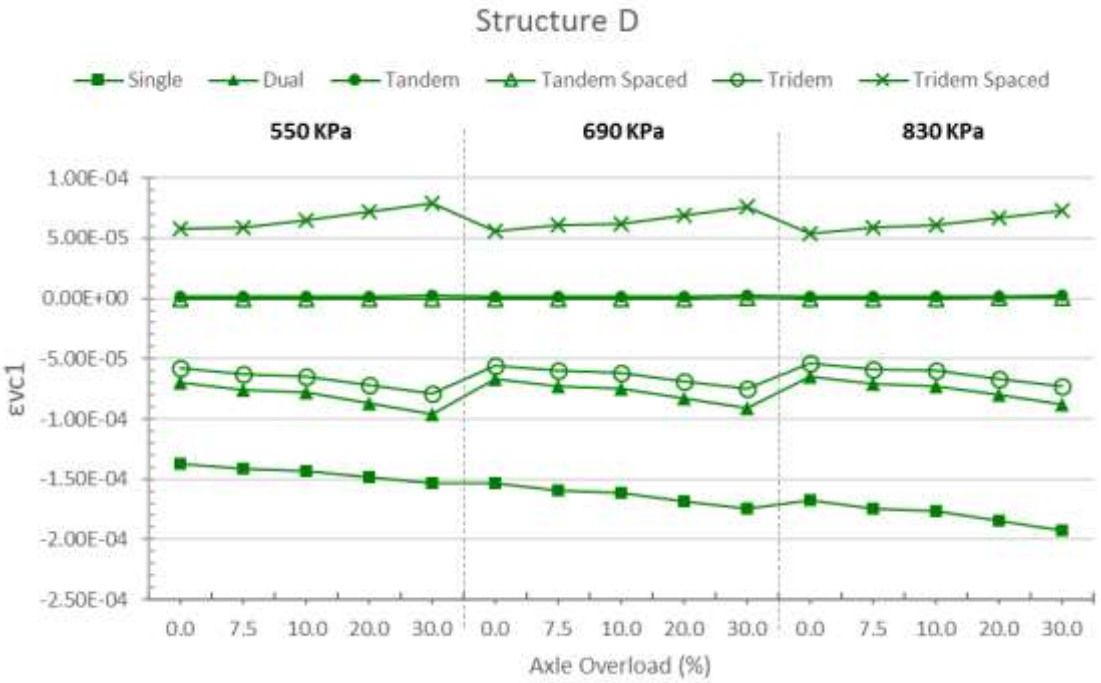

Figure 43 Vertical strain at the bottom of the asphalt layer in Structure D

As can be seen in the Figures above, vertical strain at the bottom of the asphalt layer also increases as overload percentage increase. However, these values present less sensitivity to tire pressure than the horizontal strain, in all axle types except single.

Single axle generates vertical compressive strain at the bottom of the four pavement structures, with average values ranging from -1.85E-05 to -3.33E-04.

Figures 44 and 45 shows the minimum and maximum vertical strain by structure and axle type.

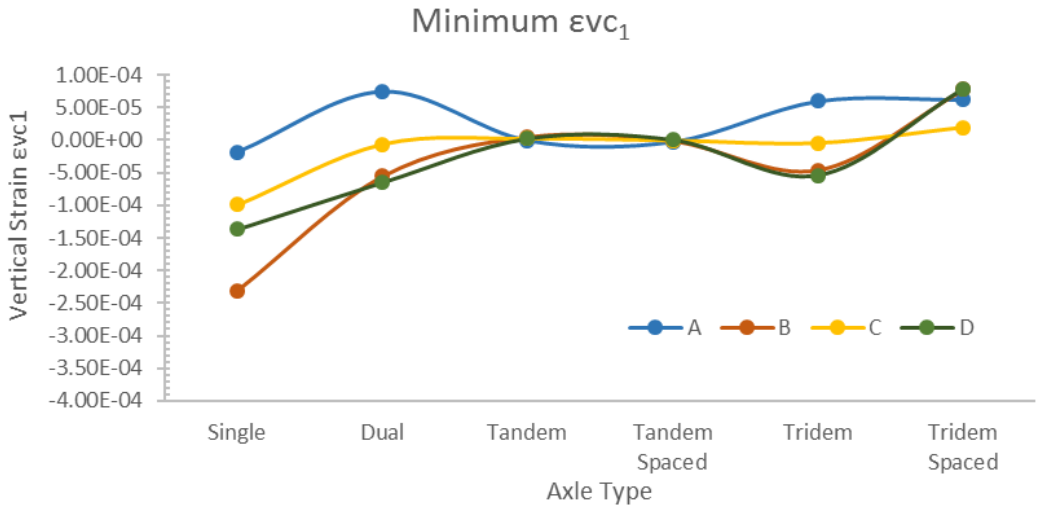

Figure 44 Minimum vertical strain at the bottom of the asphalt layer by axle type

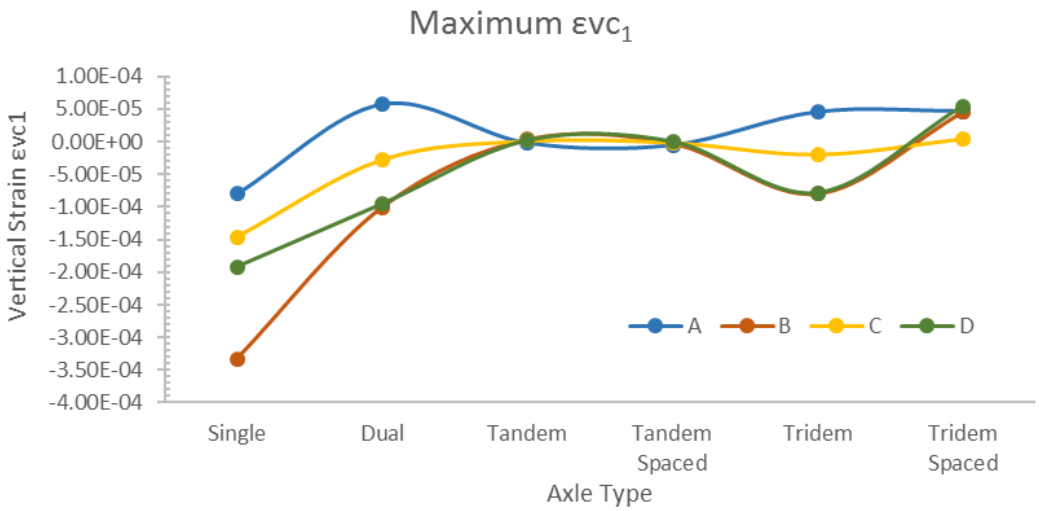

Figure 45 Minimum vertical strain at the bottom of the asphalt layer by axle type

According with the figures above, vertical strain at the bottom of the asphalt layer ranges from -3.33E-04 (single axle in Structure B) to 7.91E-05 (tridem-spaced axle in Structure D). Observe that tandem and tandem spaced axles also present the lowest strain in the four structures. However, the highest strain occurs in Structures A and B. In addition, Structure C has the lowest minimum and maximum strain in all axle types except single and tridem-spaced.

Figure 46 summarizes the average rate of increase for vertical strain as a function of the overload percentage and tire pressure. The figure shows a moderate rate of increase between tire pressures (about 8.0 %) as overload increases.

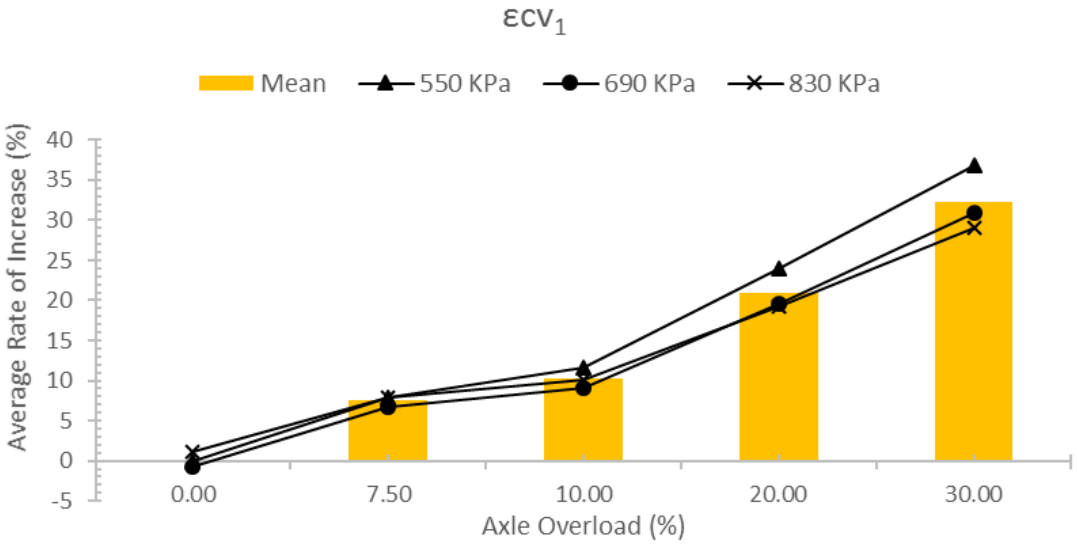

Figure 46 Average rate of increase for horizontal strain at the bottom of the asphalt layer

As can be seen, the rate of increase in strain values at the bottom of the asphalt layer increase as tire pressure increase. At 0% of overload, strain can decrease up to 0.73% if the tire pressure increases from 550 KPa to 690 KPa, but it increases up to 1.15% from 690 KPa to 830 KPa.

Likewise, at 30% of overload, strain at 550 KPa are about 36.86% higher; decreases up 30.91% if the tire pressure increases from 550 KPa to 690 KPa; and decrease up to 29.12% if it reaches 830 KPa. Complementary graphs showing horizontal strain data by axle overload and tire pressure can be found in Appendix C.

4.1.4 Vertical Compressive Strain at the Top of the Subgrade (εvc_m)

Figure 47 to 50 presents vertical compressive strain at the top of the subgrade for each structure by axle type, overload percentage, and tire pressure, in the same format of the previous structural responses. As can be seen, all the values are tensile strain, except those for tandem-spaced axle at Structures A and B. Tandem-spaced axle shows the lowest strain in the four structures, followed by the tandem axle only in Structures A and B. In general, vertical strain at the top the subgrade also increases as overload percentage increases. Average strain ranges from -5.53E-04 to 1.51E-05.

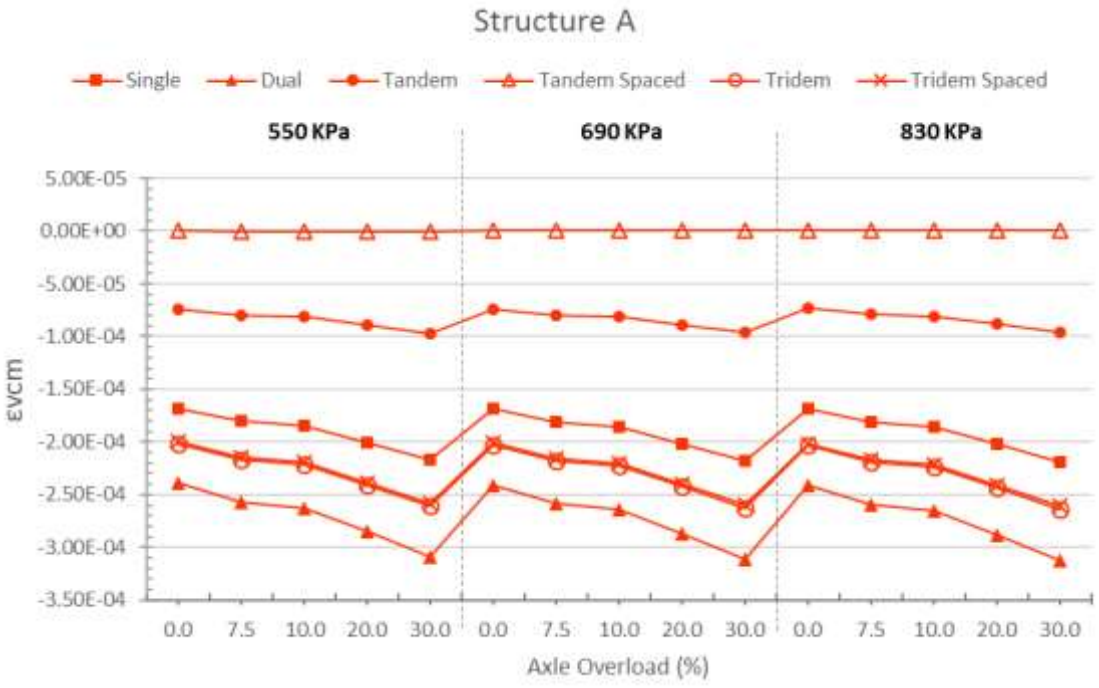

Figure 47 Vertical strain at the top of the subgrade in Structure A

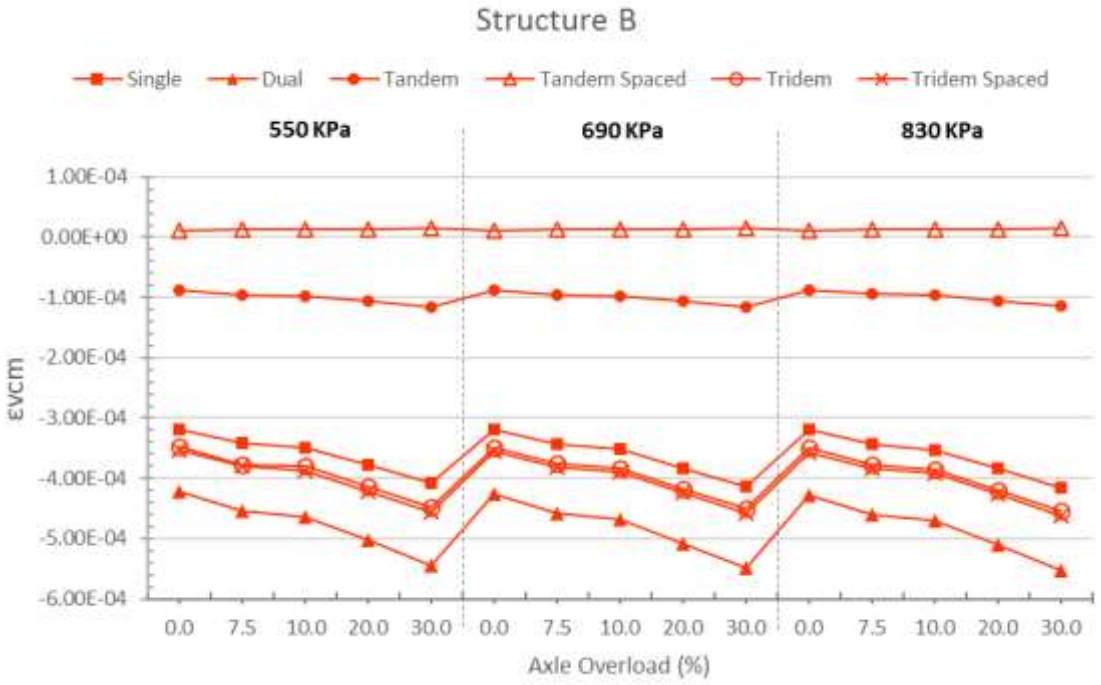

Figure 48 Vertical strain at the top of the subgrade in Structure B

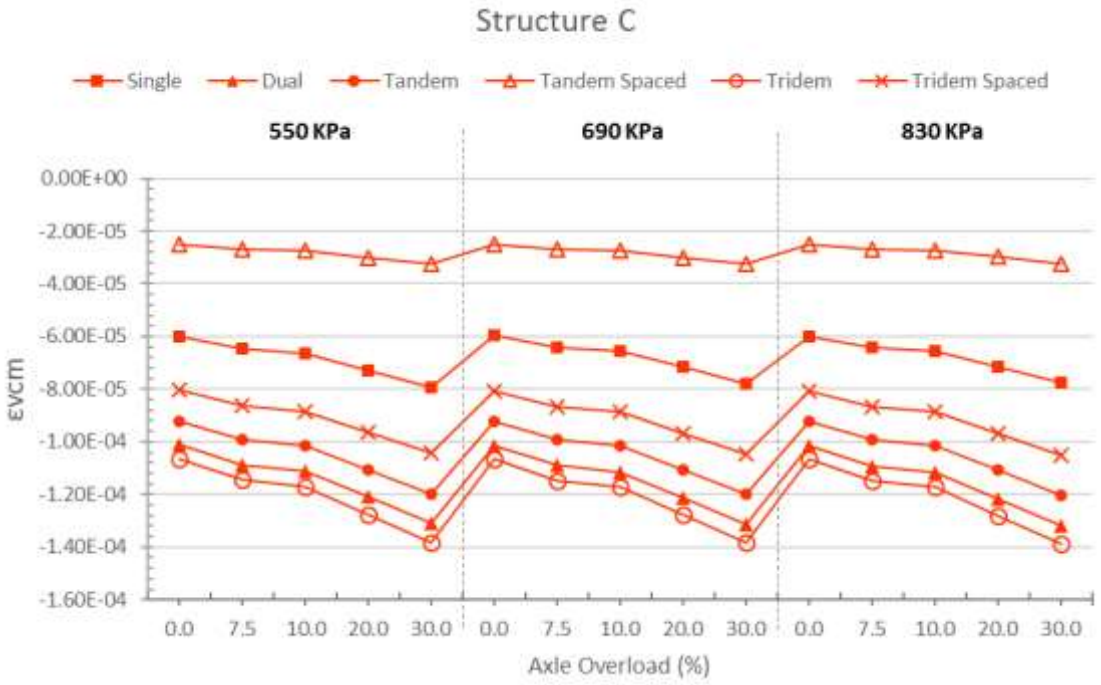

Figure 49 Vertical strain at the top of the subgrade in Structure C

Figures 51 and 52 shows the minimum and maximum vertical strain by structure and axle type.

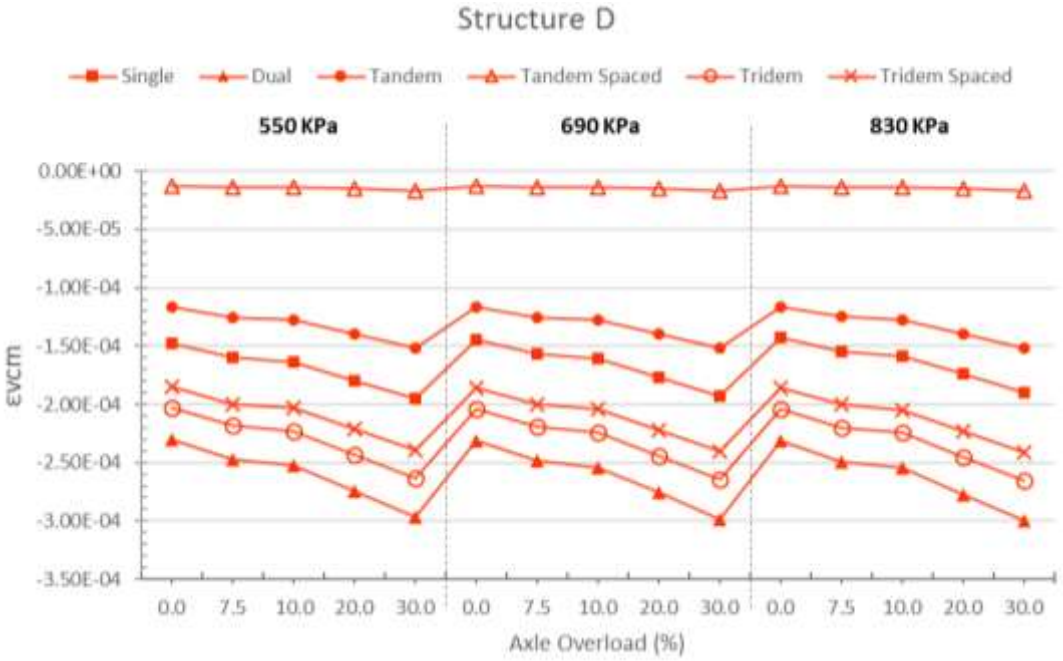

Figure 50 Vertical strain at the top of the subgrade in Structure D

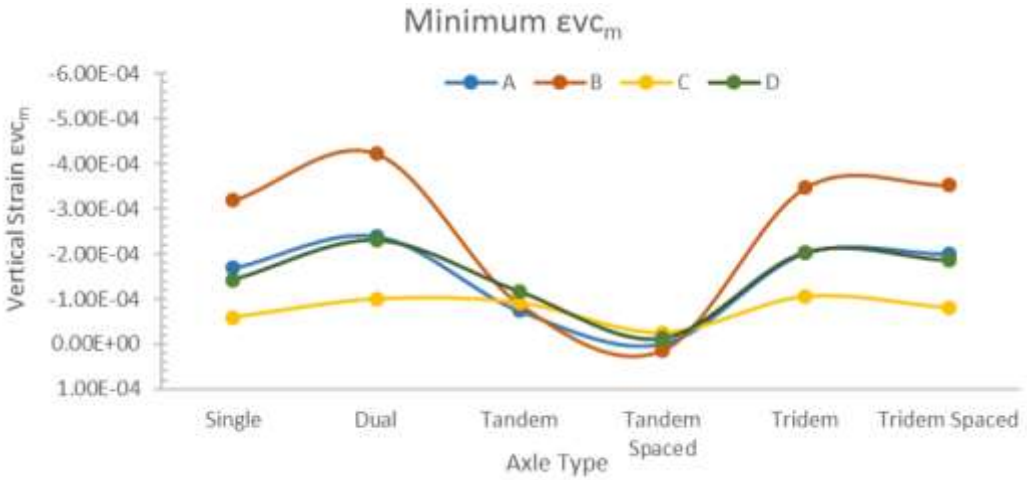

Figure 51 Minimum vertical strain at the top of the subgrade by axle type

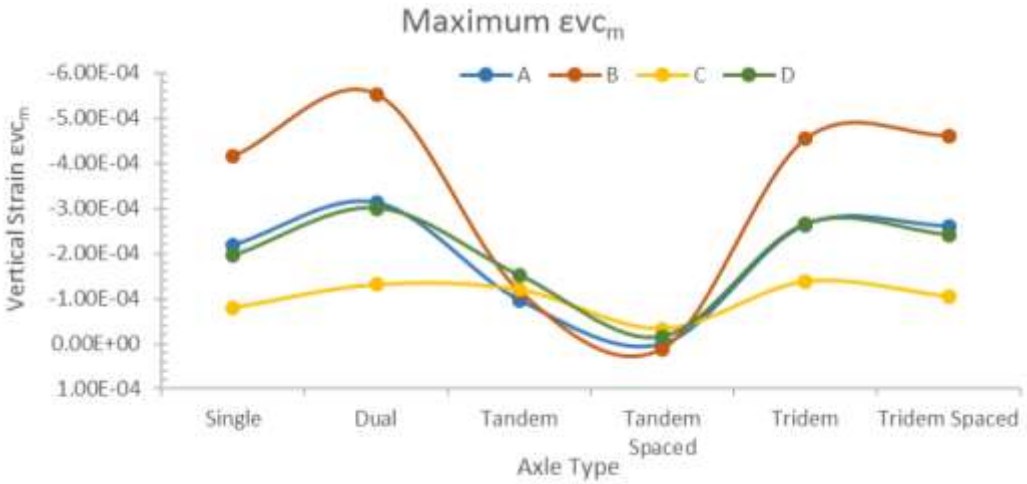

Figure 52 Maximum vertical strain at the top of the subgrade by axle type

According with the figures above, vertical strain at the top of the subgrade ranges from -5.53E-04 (dual axle in Structure B) to 1.51E-05 (tandem-spaced axle also in Structure B). Observe that tandem spaced axles present the lowest strain in the four structures. However, the highest strain occurs in Structure B. In this case, Structure C remains to have the lowest minimum and maximum strain.

Figure 28 summarizes the average rate of increase for vertical strain as a function of the overload percentage and tire pressure. Note that in this case some percentages can be negative as overload increase, but in general, when tire pressures are at 550 KPa for example, the average rate of increase can reach up to 43%.

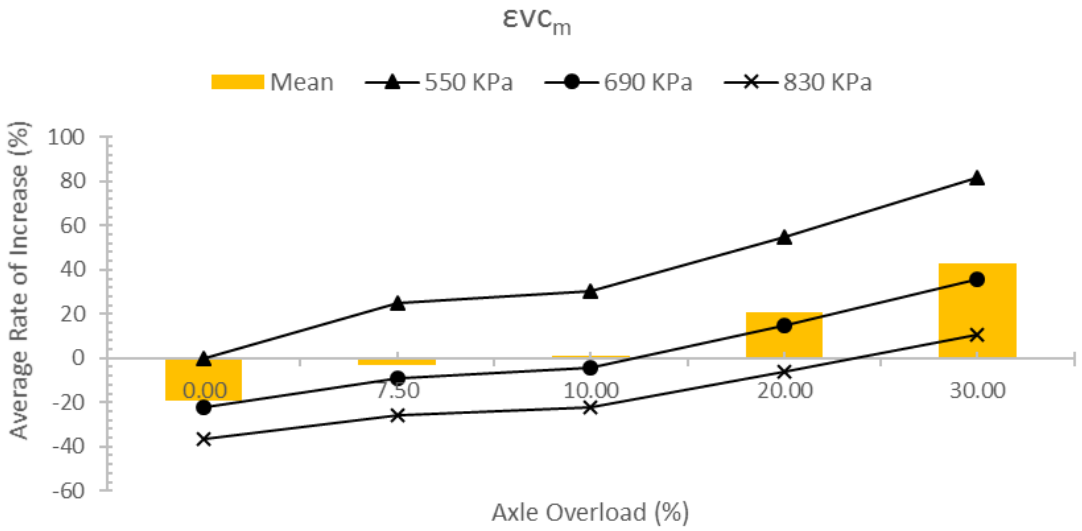

Figure 53 Average rate of increase for horizontal strain at the bottom of the asphalt layer

Complementary graphs showing horizontal strain data by axle overload and tire pressure can be found in Appendix D.

4.1.5 Structural Responses vs Thickness

Figures 54 to 57 shows minimum, maximum and root-mean-square structural responses in terms of the first asphalt layer thickness of each pavement structure studied (Structures A=40 mm; B=75 mm; C=100 mm; and D=125 mm).

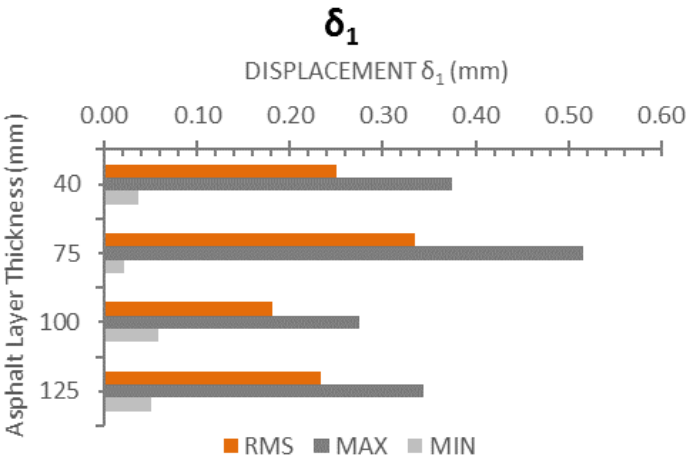

Figure 54 Surface displacements vs asphalt layer thicknesses

It is important to note that structures A and C have two asphalt layers which totalize 130 mm (40 + 90 mm) and 220 mm (100 + 120 mm) in depth, respectively. In this context, displacements decrease as asphalt thickness increases, at an average rate of 28%. Figure 54 shows that the lowest RMS surface displacements occur when the asphalt layer thickness is 100 mm (Structure C, whose layer is the thickest).

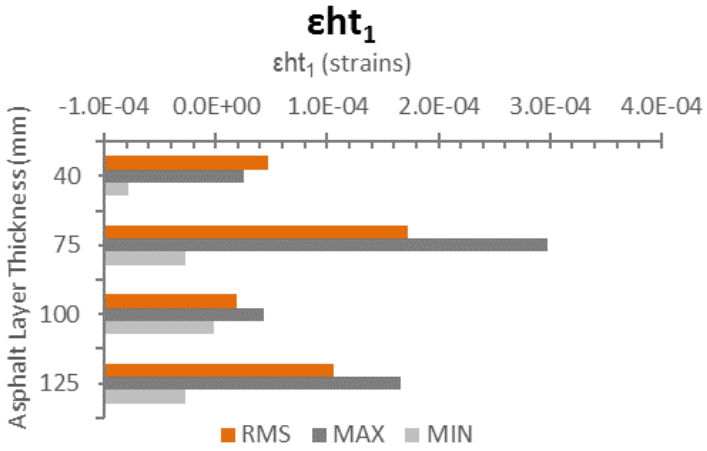

Figure 55 Horizontal strain at the bottom of the asphalt layer vs thicknesses

Figure 55 also shows that the effect of a second asphalt layer in Structures A and C may reduce the horizontal tensile strain up to 500%.

Figure 56 shows that Structure B remains to be the most affected by the structural responses due to its unique and thin asphalt layer of 75 mm. Vertical compressive strain at the bottom of the asphalt layer in Structure B are approximately 48% higher than the other structures.

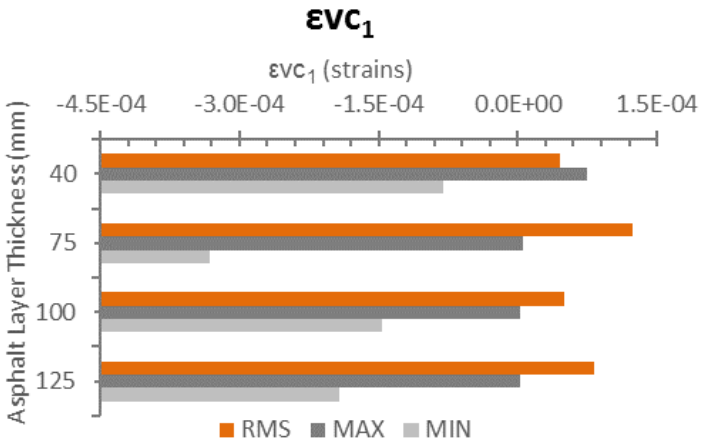

Figure 56 Vertical strain at the bottom of the asphalt layer vs thicknesses

Finally, Figure 57 shows that vertical compressive strain at the top of the subgrade have similar behavior than at the bottom of the asphalt layer. Here, RMS strain may be reach 3.40E-04, approximately 56% and 28% highest than in Structures A and D, and Structure C, respectively.

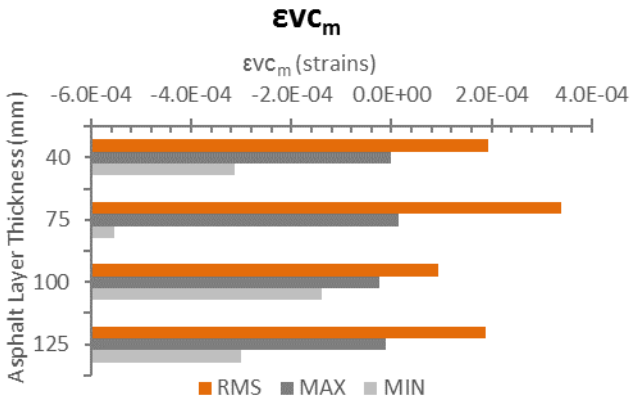

Figure 57 Vertical strain at the bottom of the asphalt layer vs thicknesses

4.2 PAVEMENT LIFE PREDICTIONS

4.2.1 Asphalt Institute's Cycles to Failure ("N" numbers)

Table 16 presents average N numbers for fatigue cracking and rutting distresses, according to the Asphalt Institute's criteria. Such average takes into account tire pressures and axle overloads variables. A red-yellow-green downgrade colored scale was used to improve data visualization.

Table 16 Average cycles to failure (N numbers) for fatigue cracking and rutting by axle type

Axle Type	Fatigue Cracking				Rutting			
	A	B	C	D	A	B	C	D
Single	1.98E+08	7.78E+05	7.81E+08	4.93E+06	6.74E+07	3.84E+06	6.85E+09	1.26E+08
Dual	5.69E+07	1.18E+06	4.32E+09	5.08E+06	1.37E+07	1.07E+06	6.54E+08	1.64E+07
Tandem	2.33E+09	1.81E+09	2.73E+13	1.62E+09	2.68E+09	1.21E+09	9.91E+08	3.51E+08
Tandem Spaced	1.99E+10	1.03E+20	7.82E+11	1.89E+11	4.62E+30	1.07E+13	3.49E+11	7.37E+12
Tridem	1.70E+08	1.88E+06	3.42E+09	9.38E+06	2.94E+07	2.59E+06	5.22E+08	2.86E+07
Tridem Spaced	9.85E+07	1.91E+06	4.35E+09	8.22E+06	3.08E+07	2.40E+06	1.82E+09	4.35E+07

According to Table 16, N numbers vary widely depending on the axle type, with values that can be low as 7.80E+05 and high as 4.60E+30. From the figure, it is evident that fatigue cracking N numbers are lower than rutting N numbers. The average for fatigue cracking is 4.30E+18 while for rutting is 1.90E+29.

Furthermore, the tandem-spaced axle shows the highest N numbers ranging from about 2.00E+10 to 4.60E+30 for all pavement structures, followed by the tandem axle who shows values approximately five times lower.

4.2.2 Critical Resistance

As described before in Chapter 3, resistance values are all those N numbers calculated from the structural responses obtained in the simulations carried out with the MePads software. Critical resistance values, consequently, were defined in this work as the minimum N number between fatigue cracking and rutting N numbers. Critical resistance data, then, is used from here in all data analyses presented.

Table 17 presents minimum, maximum, average, and standard deviation of critical resistances by pavement structure. All fatigue cracking and rutting N numbers as well as critical resistances can be found in Appendix E.

Table 17 Minimum, Maximum, and Average Critical N numbers by Structure

	A	B	C	D
MIN	6.72E+06	3.84E+05	2.56E+08	2.62E+06
MAX	3.08E+10	1.74E+13	5.63E+11	2.72E+11
MEAN	3.73E+09	1.79E+12	5.89E+10	3.15E+10
STD DEV	7.74E+09	4.33E+12	1.41E+11	7.36E+10

4.2.2.1 Resistances vs Overloads

Table 18 shows the RMS values of the critical resistances as a function of the overload percentages and by structure (tire pressure was taken into account in the calculation of the RMS). Note that tandem-spaced axles in all structures have the higher N numbers and single and dual axles the lowest. Furthermore, observe that tridem axle results in low N numbers in the structure C. Appendix F provides complementary charts for structure and axle types, separately.

Table 18 RMS Critical Resistances (N) vs Overload (%) by axle type and structure

Structure	Overload (&)	Single	Dual	Tandem	Tandem Spaced	Tridem	Tridem Spaced
A	0.00	1.07E+08	2.18E+07	3.32E+09	2.95E+10	4.68E+07	4.91E+07
	7.50	7.79E+07	1.57E+07	2.62E+09	2.26E+10	3.38E+07	3.55E+07
	10.00	6.98E+07	1.43E+07	2.44E+09	2.09E+10	3.07E+07	3.22E+07
	20.00	4.78E+07	9.86E+06	1.84E+09	1.53E+10	2.09E+07	2.20E+07
	30.00	3.38E+07	6.92E+06	1.30E+09	1.14E+10	1.47E+07	1.55E+07
B	0.00	9.22E+05	1.63E+06	1.96E+09	1.71E+13	2.66E+06	2.66E+06
	7.50	8.70E+05	1.23E+06	1.40E+09	1.24E+13	2.04E+06	2.14E+06
	10.00	8.53E+05	1.11E+06	1.27E+09	1.12E+13	1.99E+06	2.00E+06
	20.00	8.02E+05	7.70E+05	8.47E+08	7.65E+12	1.53E+06	1.55E+06
	30.00	7.61E+05	5.42E+05	5.86E+08	5.37E+12	1.21E+06	1.19E+06
C	0.00	8.01E+08	1.05E+09	1.59E+09	5.61E+11	8.37E+08	2.91E+09
	7.50	8.68E+08	7.52E+08	1.14E+09	4.02E+11	6.01E+08	2.09E+09
	10.00	8.96E+08	6.80E+08	1.03E+09	3.64E+11	5.45E+08	1.90E+09
	20.00	1.01E+09	4.66E+08	6.99E+08	2.45E+11	3.69E+08	1.29E+09
	30.00	1.16E+09	3.26E+08	4.88E+08	1.71E+11	2.58E+08	9.01E+08
D	0.00	6.10E+06	7.03E+06	5.65E+08	2.71E+11	1.31E+07	1.16E+07
	7.50	5.47E+06	5.66E+06	4.05E+08	2.12E+11	1.05E+07	8.85E+06
	10.00	5.28E+06	5.30E+06	3.67E+08	1.98E+11	9.81E+06	8.69E+06
	20.00	4.68E+06	4.15E+06	2.47E+08	1.48E+11	7.59E+06	6.73E+06
	30.00	4.21E+06	3.30E+06	1.72E+08	1.14E+11	6.01E+06	5.33E+06

As can be seen, critical pavement resistance decreases as tire pressure and axle overload increases. Figure 58 shows pavement life reduction in terms of decrease percentages of critical N numbers. The value corresponding to 0% of overload and 550 KPa has been taken as a reference value. Note that with 10% of axle overload pavement life reduces up to 34% and with 30% of axle overload this reduction exceeds 60%. Decrease percentages in N numbers by structure and axle type can be found in Appendix G.

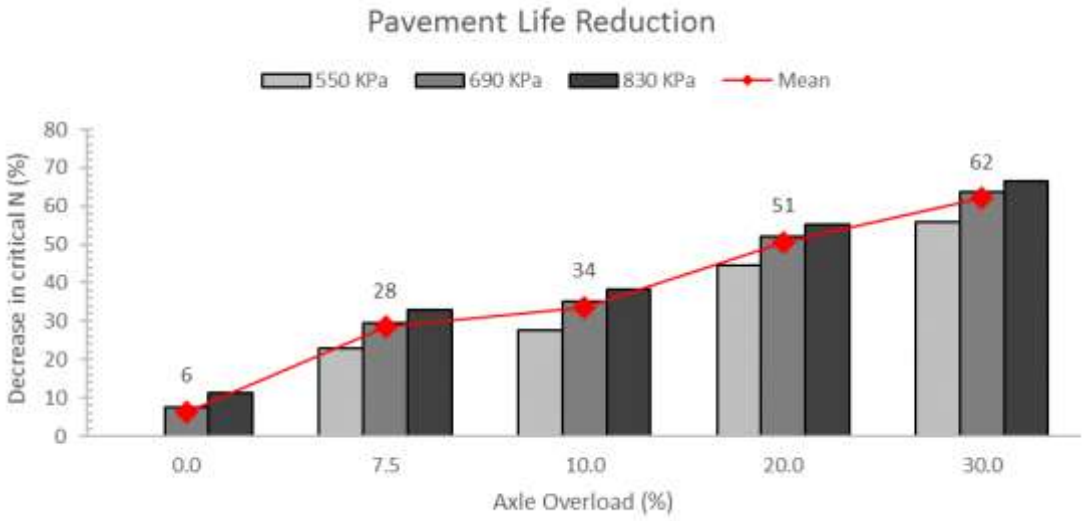

Figure 58 Pavement life reduction in terms of decrease percentages of critical N numbers

4.3 RELIABILITY INDEX AND PROBABILITY OF FAILURE

4.3.1 Descriptive Statistics

Table 19 provide a summary of the descriptive statistics for resistances, solicitations, reliability indices, and probabilities of failure. As shown in the Table, maximum resistances and solicitations range from 1.07E+13 to 5.37E+13, respectively. Mean values for reliability index (β) and probability of failure are 0.24 and 0.46, respectively.

In general, the data do not have a normal distribution. Skewness and kurtosis values for resistance and solicitation shows that the data is skewed left and distributed in a leptokurtic format. In this context, β data is slowly skewed right and Pf data is skewed right. Both β and Pf data has a platykurtic format curve. Figure 59 shows the histograms for the data presented in Table 19 in order to contribute to visualization of data distribution.

Table 19 Descriptive statistics for solicitations, reliability indices, and probabilities of failure

		RESISTANCE	SOLICITATION	β	Pf
N Statistic		216	216	216	216
Range Statistic		1.07E+13	5.37E+13	6	1
Minimum Statistic		7.78E+05	1.56E+05	-3	0
Maximum Statistic		1.07E+13	5.37E+13	3	1
Mean	Statistic	4.69E+11	6.65E+11	0.2432	0.4579
	Std. Error	1.46E+11	3.00E+11	0.11202	0.02678
Std. Deviation	Statistic	2.14E+12	4.41E+12	1.64633	0.39358
Variance Statistic		4.58E+24	1.95E+25	2.71	0.155
Skewness	Statistic	4.610	9.592	-0.095	0.07
	Std. Error	0.166	0.166	0.166	0.166
Kurtosis	Statistic	19.461	104.354	-1.246	-1.709
	Std. Error	0.33	0.33	0.33	0.33

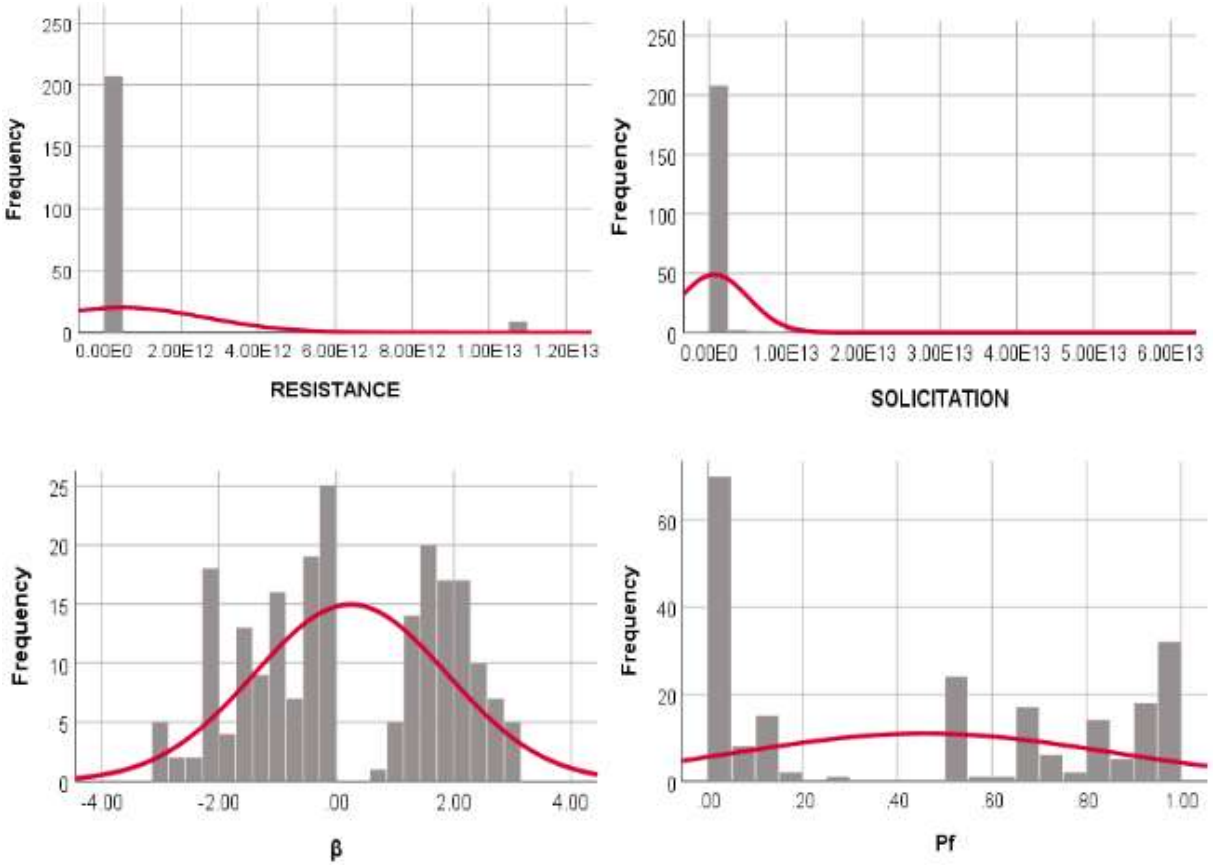

Figure 59 Histograms for resistance, solicitation, reliability index, and probability of failure data

Thereby, there was a need to improve normality. As described in Chapter 3, the software IBM-SPSS was used to normalize the data through the inverse distribution function (Idf.Normal). Table 20 presents the results of the Tests of normality for the transformed variables.

Table 20 Tests of normality for transformed variables

	Kolmogorov-Smirnov[a]			Shapiro-Wilk		
	Statistic	df	Sig.	Statistic	df	Sig.
NormRESISTANCE	0.031	213	.200*	0.986	213	0.039
NormSOLICITATION	0.008	213	.200*	0.999	213	1.000
Normβ	0.059	213	0.066	0.997	213	0.969
NormPf	0.059	213	0.073	0.997	213	0.946

* This is a lower bound of the true significance.
a Lilliefors Significance Correction

As can be seen, after variable transformation the significance level was improved and, except for resistance values, all of them were higher than 0.05. The significance level (Sig.) in Resistance values is less than 0.05 due to the nature of the data, which was taken as a reference to calculate the solicitations and, as a consequence of it, several resistance values are repeated and resulted in non-significative data. Figure 60 shows the histograms for the transformed data.

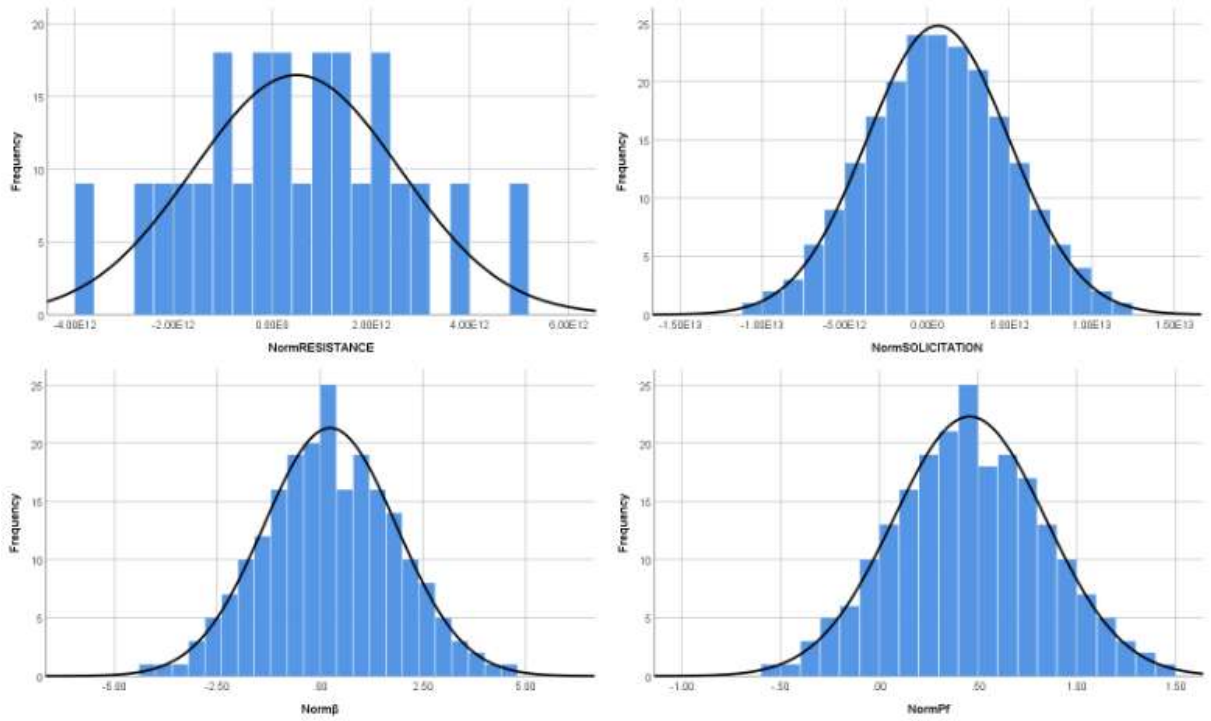

Figure 60 Histograms for resistance, solicitation, reliability index, and probability of failure data (transformed)

4.3.2 Pearson Correlations

Pearson product-moment correlation coefficients were computed to assess the relationship between the transformed variables studied. As shown in Table 21, results indicate strong and positive correlation between solicitations and resistances (r=0.941, n=215, p<0.001).

Table 21 Pearson correlations between transformed resistances, solicitations, reliability indices (β), and probabilities of failure (Pf)

		Norm RESISTANCE	Norm SOLICITATION	Norm β	Norm Pf
NormRESISTANCE	Pearson Correlation	**1**	**.941****	**-0.006**	**0.021**
	Sig. (2-tailed)		0	0.928	0.758
	N	216	215	215	215
NormSOLICITATION	Pearson Correlation	**.941****	**1**	**-.277****	**.292****
	Sig. (2-tailed)	0		0	0
	N	215	215	214	214
Normβ	Pearson Correlation	**-0.006**	**-.277****	**1**	**-.999****
	Sig. (2-tailed)	0.928	0		0
	N	215	214	215	214
NormPf	Pearson Correlation	**0.021**	**.292****	**-.999****	**1**
	Sig. (2-tailed)	0.758	0	0	
	N	215	214	214	215

** Correlation is significant at the 0.01 level (2-tailed).

According to the Table above, there is an extremely low correlation between resistance and β and Pf values. Solicitations, on the other hand, show higher correlations with

these variables but still are low and also negative in the case of β. Additionally, the reliability index β shows a low and positive correlation with solicitations (r=-0.277, n=214, p<0.001) but also a strong and negative correlation with the probability of failure Pf (r=-0.999, n=214, p<0.001). Figure 36 is a scatter plot that shows the correlation between β and Pf. According with the Figure, these variables have non-linear, negative, and perfect relationship with an R-squared value of 1.0, defined by a third-order polynomial trendline. Note that negative values of β are associated to high probabilities of failure and vice versa.

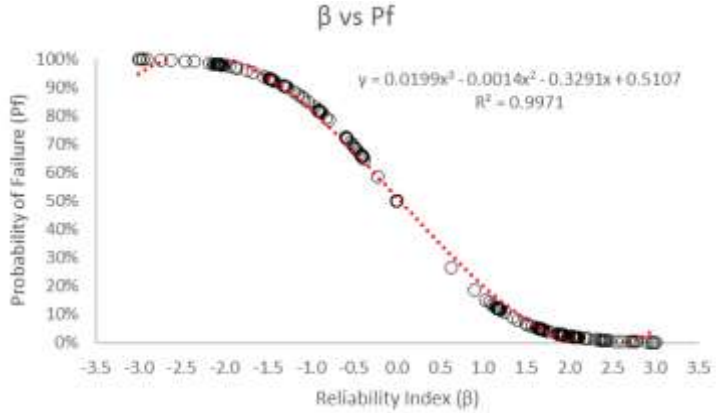

Figure 61 Reliability index (β) vs Probability of failure (Pf)

4.3.3 Regression Analysis

Table 22 presents the results of the multivariate linear regression analysis which considered solicitation, resistance, reliability index, and probability of failure values as dependent variables, separately. Likewise, Tables 23 and 24 show the regression coefficients with the respective levels of significance and the residuals statistics, respectively. Histograms, Normal P-P Plots, Scatterplots, and Partial Regression Plots of the Standardized residuals can be found in Appendix H.

Table 22 Regression models summary

Model	Dependent Variable	Predictors	R	R Square	Adjusted R Square	Std. Error of the Estimate	Durbin-Watson
1	NormPf	(Constant) NormSOLICITATION NormRESISTANCE	0.847	0.717	0.715	0.20505	0.850
2	NormRESISTANCE	(Constant) NormSOLICITATION NormPf	0.982	0.965	0.965	3.90881E+11	0.683
3	NormSOLICITATION	(Constant) NormRESISTANCE NormPf	0.984	0.968	0.968	7.78717E+11	0.721
4	Normβ	(Constant) NormSOLICITATION NormRESISTANCE	0.846	0.715	0.712	0.8617	0.825

Note that all the models indicate strong and positive correlations. However, according to Table 23, only models 1, 2, and 3 were significant (P-value < 0.05). Regression model 4 shows that the constant value is non-significative with an extremely high P-value of 0.80.

Table 23 Regression coefficients

Model	Dependent Variable	Coefficients	Unstandardized Coefficients		Standardized Coefficients	t	Sig.
			B	Std. Error	Beta		
1	NormPf	(Constant)	0.517	0.015		35.291	0.000
		NormRESISTANCE	-4.36E-13	0.000	-2.362	-21.728	0.000
		NormSOLICITATION	2.23E-13	0.000	2.515	23.142	0.000
2	NormRESISTANCE	(Constant)	8.75E+11	4.18E+10		20.897	0.000
		NormPf	-1.58E+12	7.29E+10	-0.293	-21.728	0.000
		NormSOLICITATION	4.93E-01	0.006	1.027	76.25	0.000
3	NormSOLICITATION	(Constant)	-1.7E+12	8.36E+10		-20.831	0.000
		NormPf	3.22E+12	1.39E+11	0.285	23.142	0.000
		NormRESISTANCE	1.96E+00	0.026	0.94	76.25	0.000
4	Normβ	(Constant)	0.016	0.061		0.253	0.800
		NormRESISTANCE	1.83E-12	0.000	2.371	21.738	0.000
		NormSOLICITATION	-9.35E-13	0.000	-2.51	-23.01	0.000

Table 24 Residual statistics

Model	Dependent Variable	Values	Minimum	Maximum	Mean	Std. Deviation
1	NormPf	Predicted Value	-0.3186	1.5562	0.4553	0.32515
		Residual	-0.65534	0.60490	0.00000	0.20408
		Std. Predicted Value	-2.380	3.386	0.000	1.000
		Std. Residual	-3.196	2.950	0.000	0.995
2	NormRESISTANCE	Predicted Value	-4.75E+12	5.52691E+12	4.83E+11	2.04223E+12
		Residual	-1.88E+12	9.45E+11	0.00113	3.89041E+11
		Std. Predicted Value	-2.561	2.47	0.000	1.000
		Std. Residual	-4.813	2.417	0.000	0.995
3	NormSOLICITATION	Predicted Value	-8.58E+12	1.06274E+13	6.7E+11	4.25994E+12
		Residual	-2.22E+12	3.51E+12	-2.08E-03	7.75052E+11
		Std. Predicted Value	-2.171	2.337	0.000	1.000
		Std. Residual	-2.851	4.507	0.000	0.995
3	Normβ	Predicted Value	-4.3583	3.5117	0.2538	1.35862
		Residual	-2.36911	2.78415	0.00000	0.85764
		Std. Predicted Value	-3.395	2.398	0.000	1.000
		Std. Residual	-2.749	3.231	0.000	0.995
N = 214 for all models						

4.3.4 Reliability Indices (β) and Probabilities of Failure (Pf) by Safety Factors (SF) and Axle Types

The reliability indices and the probabilities of failure based on resistances (critical N numbers) and solicitations (critical resistances varying as a function of different safety factors) are presented in the following figures by axle type and for each pavement structure. Such Figures present also RMS values and display the trendline and their respective equations (fifth degree polynomials) and R-squared values. In addition, data tables were put below each chart in order to complement data visualization and for comparative purposes.

It is important to highlight that safety factor equal to 1.00 was considered as a reference parameter. In this context, at SF=1.00, reliability indices always be equal to zero and, consequently, the probability of failure will be 0.50.

4.3.4.1 Structure A

As can be seen in Figures 62 and 63, tandem and tandem-spaced axles have the highest reliability indices and also the highest probabilities of failure when safety factors are less than 1.00. Note that positive reliability indices correspond to safety factors higher than 1.00. Note that RMS reliability indices ranges from -2.50 for a safety factor equal to 0.20 to 2.25 for a safety factor of 5.00.

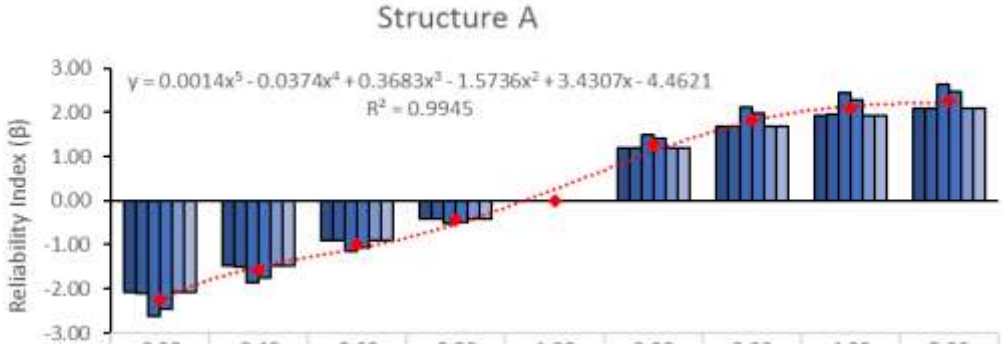

	0.20	0.40	0.60	0.80	1.00	2.00	3.00	4.00	5.00
Single	-2.0775	-1.4753	-0.9084	-0.4136	0.0000	1.1843	1.6749	1.9269	2.0775
Dual	-2.1007	-1.4918	-0.9185	-0.4182	0.0000	1.1976	1.6936	1.9484	2.1007
Tandem	-2.6226	-1.8624	-1.1467	-0.5221	0.0000	1.4951	2.1144	2.4325	2.6226
Tandem Spaced	-2.4648	-1.7504	-1.0777	-0.4907	0.0000	1.4052	1.9872	2.2862	2.4648
Tridem	-2.0835	-1.4796	-0.9110	-0.4148	0.0000	1.1878	1.6798	1.9325	2.0835
Tridem Spaced	-2.0862	-1.4815	-0.9122	-0.4153	0.0000	1.1893	1.6820	1.9350	2.0862
RMS	-2.2500	-1.5978	-0.9838	-0.4479	0.0000	1.2827	1.8140	2.0869	2.2500

Safety Factor (SF)

Figure 62 Reliability Indices vs Safety Factors for the Structure A

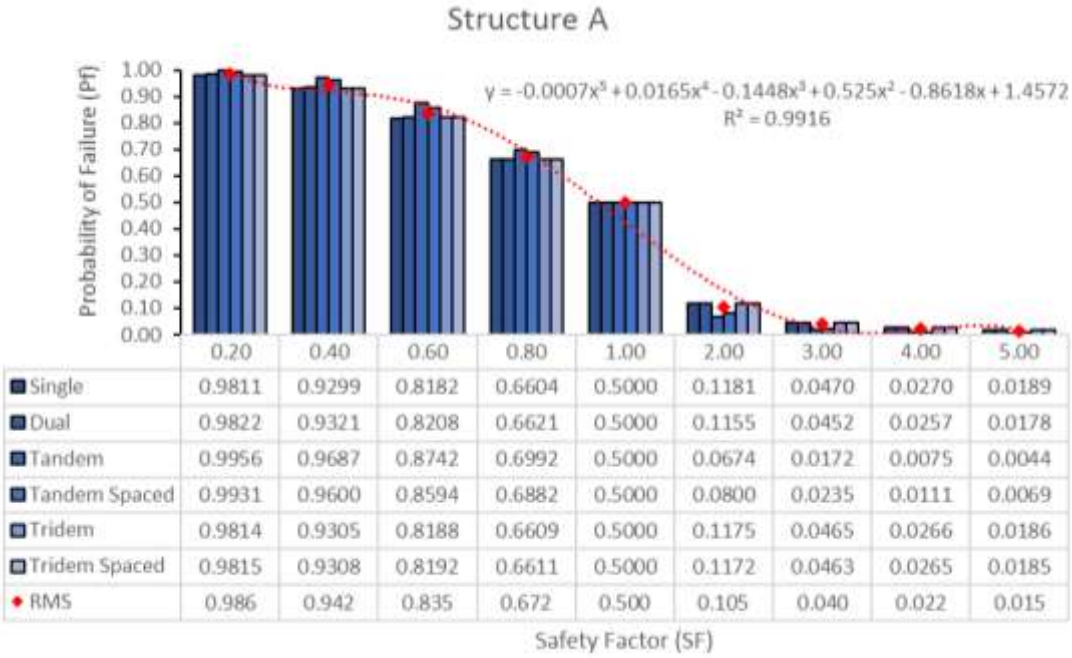

	0.20	0.40	0.60	0.80	1.00	2.00	3.00	4.00	5.00
Single	0.9811	0.9299	0.8182	0.6604	0.5000	0.1181	0.0470	0.0270	0.0189
Dual	0.9822	0.9321	0.8208	0.6621	0.5000	0.1155	0.0452	0.0257	0.0178
Tandem	0.9956	0.9687	0.8742	0.6992	0.5000	0.0674	0.0172	0.0075	0.0044
Tandem Spaced	0.9931	0.9600	0.8594	0.6882	0.5000	0.0800	0.0235	0.0111	0.0069
Tridem	0.9814	0.9305	0.8188	0.6609	0.5000	0.1175	0.0465	0.0266	0.0186
Tridem Spaced	0.9815	0.9308	0.8192	0.6611	0.5000	0.1172	0.0463	0.0265	0.0185
RMS	0.986	0.942	0.835	0.672	0.500	0.105	0.040	0.022	0.015

Figure 63 Probabilities of failure vs Safety Factors for the Structure A

4.3.4.2 Structure B

In Structure B, the highest reliability indices occur with tridem and tridem-spaced axles. As a consequence, these axles show the highest probabilities of failure for Safety Factors less than 1.00 (see Figures 64 and 65).

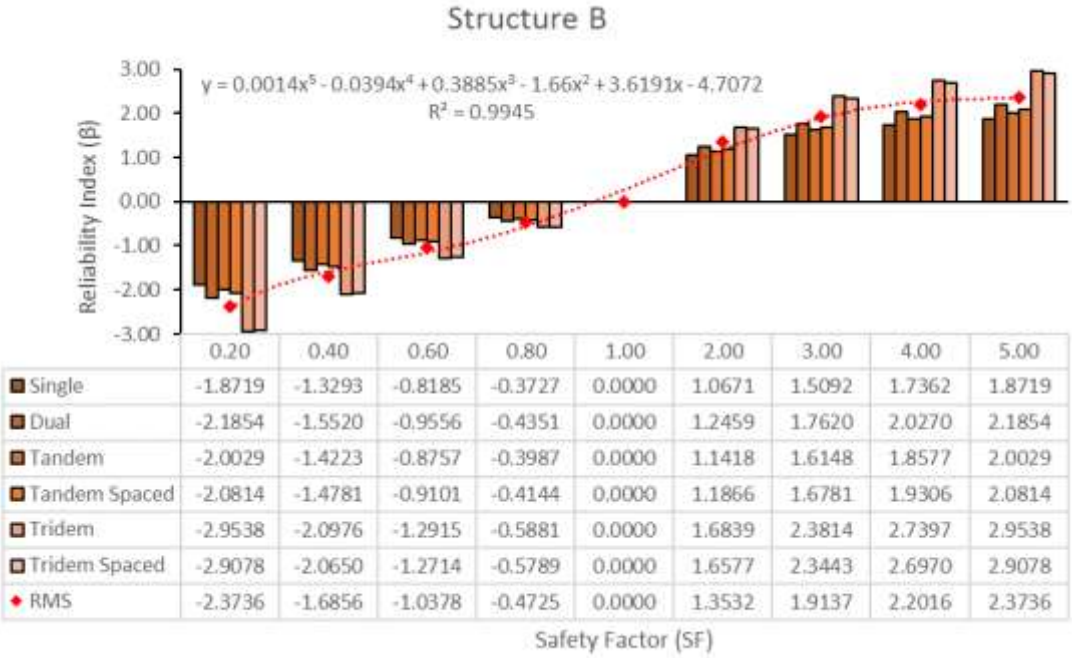

	0.20	0.40	0.60	0.80	1.00	2.00	3.00	4.00	5.00
Single	-1.8719	-1.3293	-0.8185	-0.3727	0.0000	1.0671	1.5092	1.7362	1.8719
Dual	-2.1854	-1.5520	-0.9556	-0.4351	0.0000	1.2459	1.7620	2.0270	2.1854
Tandem	-2.0029	-1.4223	-0.8757	-0.3987	0.0000	1.1418	1.6148	1.8577	2.0029
Tandem Spaced	-2.0814	-1.4781	-0.9101	-0.4144	0.0000	1.1866	1.6781	1.9306	2.0814
Tridem	-2.9538	-2.0976	-1.2915	-0.5881	0.0000	1.6839	2.3814	2.7397	2.9538
Tridem Spaced	-2.9078	-2.0650	-1.2714	-0.5789	0.0000	1.6577	2.3443	2.6970	2.9078
RMS	-2.3736	-1.6856	-1.0378	-0.4725	0.0000	1.3532	1.9137	2.2016	2.3736

Figure 64 Reliability Indices vs Safety Factors for the Structure B

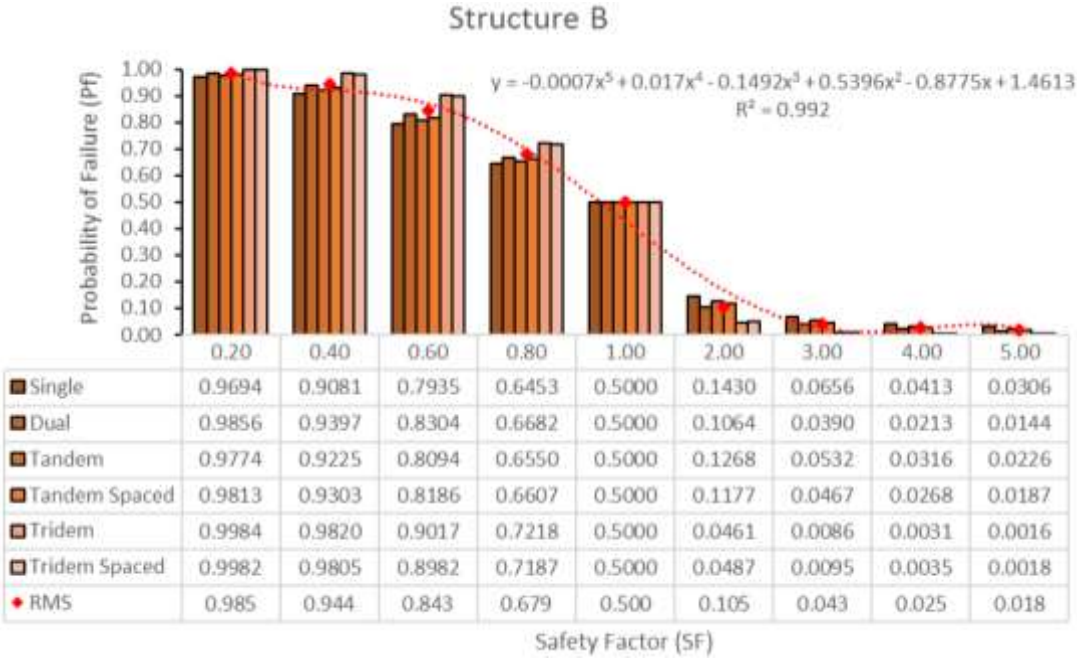

	0.20	0.40	0.60	0.80	1.00	2.00	3.00	4.00	5.00
Single	0.9694	0.9081	0.7935	0.6453	0.5000	0.1430	0.0656	0.0413	0.0306
Dual	0.9856	0.9397	0.8304	0.6682	0.5000	0.1064	0.0390	0.0213	0.0144
Tandem	0.9774	0.9225	0.8094	0.6550	0.5000	0.1268	0.0532	0.0316	0.0226
Tandem Spaced	0.9813	0.9303	0.8186	0.6607	0.5000	0.1177	0.0467	0.0268	0.0187
Tridem	0.9984	0.9820	0.9017	0.7218	0.5000	0.0461	0.0086	0.0031	0.0016
Tridem Spaced	0.9982	0.9805	0.8982	0.7187	0.5000	0.0487	0.0095	0.0035	0.0018
RMS	0.985	0.944	0.843	0.679	0.500	0.105	0.043	0.025	0.018

Figure 65 Probabilities of failure vs Safety Factors for the Structure B

4.3.4.3 Structure C

Structure C shows that both of the variables β and Pf become to be more homogeneous, except in the case of the Single axle who has the lowest β and Pf values (see Figures 66 and 67). In this case, the probabilities of failure for the single axle are about 12% lower than the RMS. However, note that when the Safety Factor is higher than 1.0, the Pf value for the single axle is approximately twice that of the other axle types.

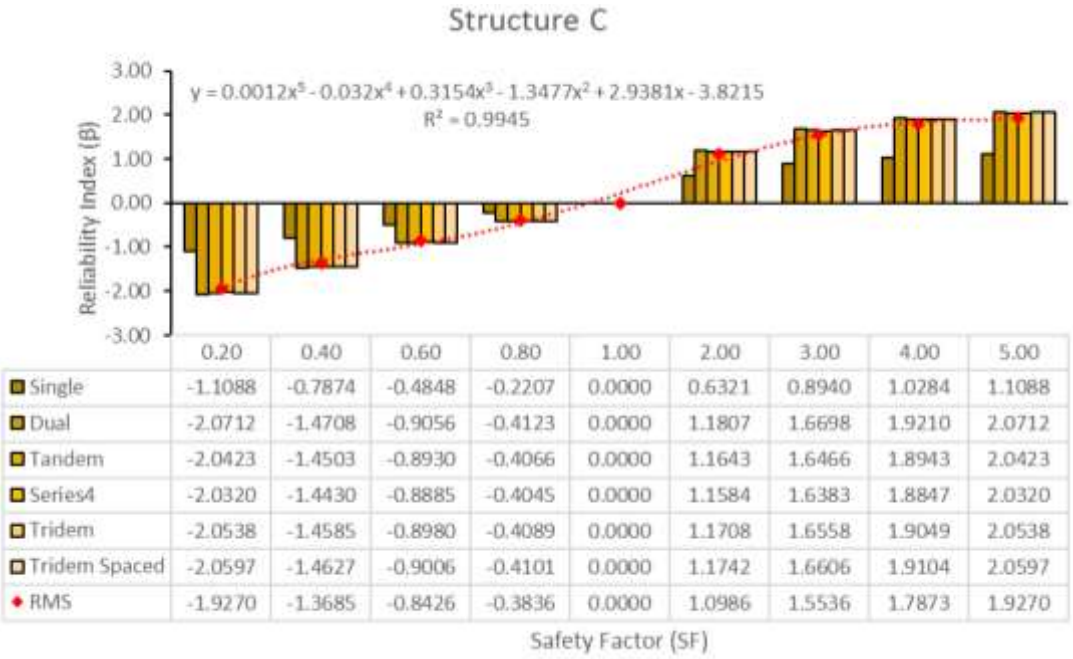

	0.20	0.40	0.60	0.80	1.00	2.00	3.00	4.00	5.00
Single	-1.1088	-0.7874	-0.4848	-0.2207	0.0000	0.6321	0.8940	1.0284	1.1088
Dual	-2.0712	-1.4708	-0.9056	-0.4123	0.0000	1.1807	1.6698	1.9210	2.0712
Tandem	-2.0423	-1.4503	-0.8930	-0.4066	0.0000	1.1643	1.6466	1.8943	2.0423
Series4	-2.0320	-1.4430	-0.8885	-0.4045	0.0000	1.1584	1.6383	1.8847	2.0320
Tridem	-2.0538	-1.4585	-0.8980	-0.4089	0.0000	1.1708	1.6558	1.9049	2.0538
Tridem Spaced	-2.0597	-1.4627	-0.9006	-0.4101	0.0000	1.1742	1.6606	1.9104	2.0597
RMS	-1.9270	-1.3685	-0.8426	-0.3836	0.0000	1.0986	1.5536	1.7873	1.9270

Figure 66 Reliability Indices vs Safety Factors for the Structure C

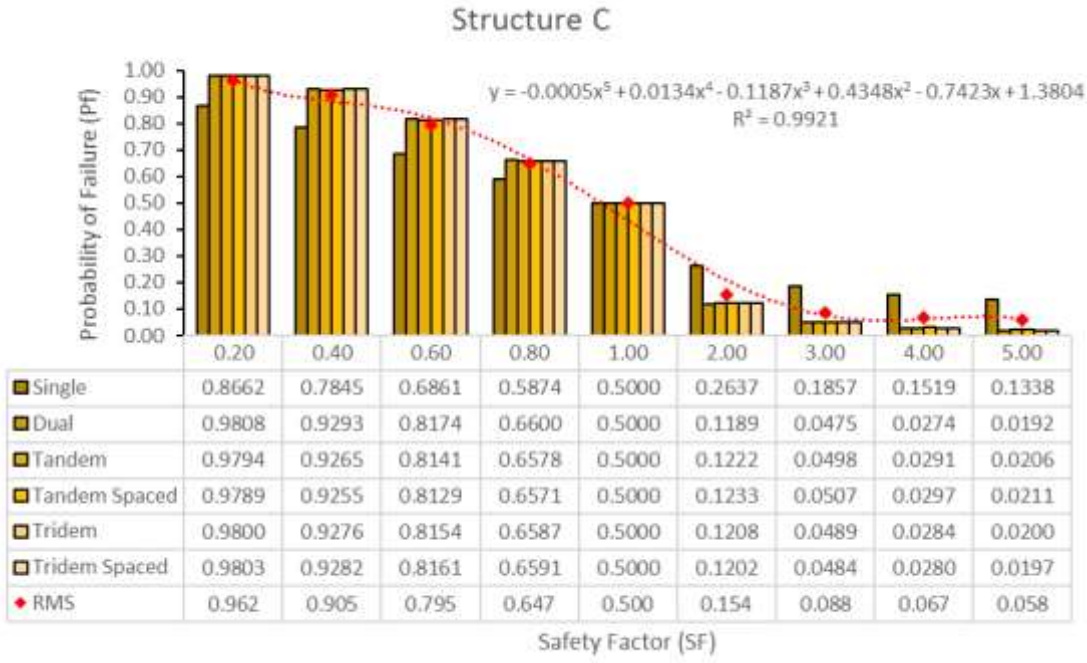

	0.20	0.40	0.60	0.80	1.00	2.00	3.00	4.00	5.00
Single	0.8662	0.7845	0.6861	0.5874	0.5000	0.2637	0.1857	0.1519	0.1338
Dual	0.9808	0.9293	0.8174	0.6600	0.5000	0.1189	0.0475	0.0274	0.0192
Tandem	0.9794	0.9265	0.8141	0.6578	0.5000	0.1222	0.0498	0.0291	0.0206
Tandem Spaced	0.9789	0.9255	0.8129	0.6571	0.5000	0.1233	0.0507	0.0297	0.0211
Tridem	0.9800	0.9276	0.8154	0.6587	0.5000	0.1208	0.0489	0.0284	0.0200
Tridem Spaced	0.9803	0.9282	0.8161	0.6591	0.5000	0.1202	0.0484	0.0280	0.0197
RMS	0.962	0.905	0.795	0.647	0.500	0.154	0.088	0.067	0.058

Figure 67 Probabilities of failure vs Safety Factors for the Structure C

4.3.4.4 Structure D

Structure D shows that dual, tridem, and tridem-spaced axles present the highest probabilities of failure (Figures 68 and 69). Here, RMS values range from -2.70 for SF=0.20 to 2.70 for SF=5.00.

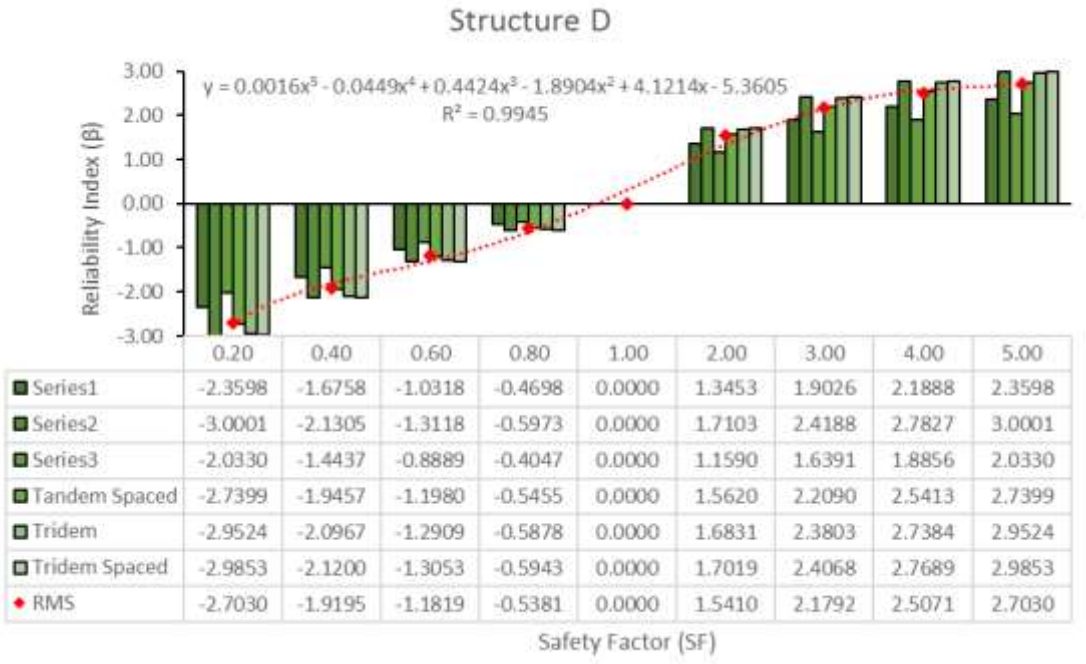

	0.20	0.40	0.60	0.80	1.00	2.00	3.00	4.00	5.00
Series1	-2.3598	-1.6758	-1.0318	-0.4698	0.0000	1.3453	1.9026	2.1888	2.3598
Series2	-3.0001	-2.1305	-1.3118	-0.5973	0.0000	1.7103	2.4188	2.7827	3.0001
Series3	-2.0330	-1.4437	-0.8889	-0.4047	0.0000	1.1590	1.6391	1.8856	2.0330
Tandem Spaced	-2.7399	-1.9457	-1.1980	-0.5455	0.0000	1.5620	2.2090	2.5413	2.7399
Tridem	-2.9524	-2.0967	-1.2909	-0.5878	0.0000	1.6831	2.3803	2.7384	2.9524
Tridem Spaced	-2.9853	-2.1200	-1.3053	-0.5943	0.0000	1.7019	2.4068	2.7689	2.9853
RMS	-2.7030	-1.9195	-1.1819	-0.5381	0.0000	1.5410	2.1792	2.5071	2.7030

Figure 68 Reliability Indices vs Safety Factors for the Structure D

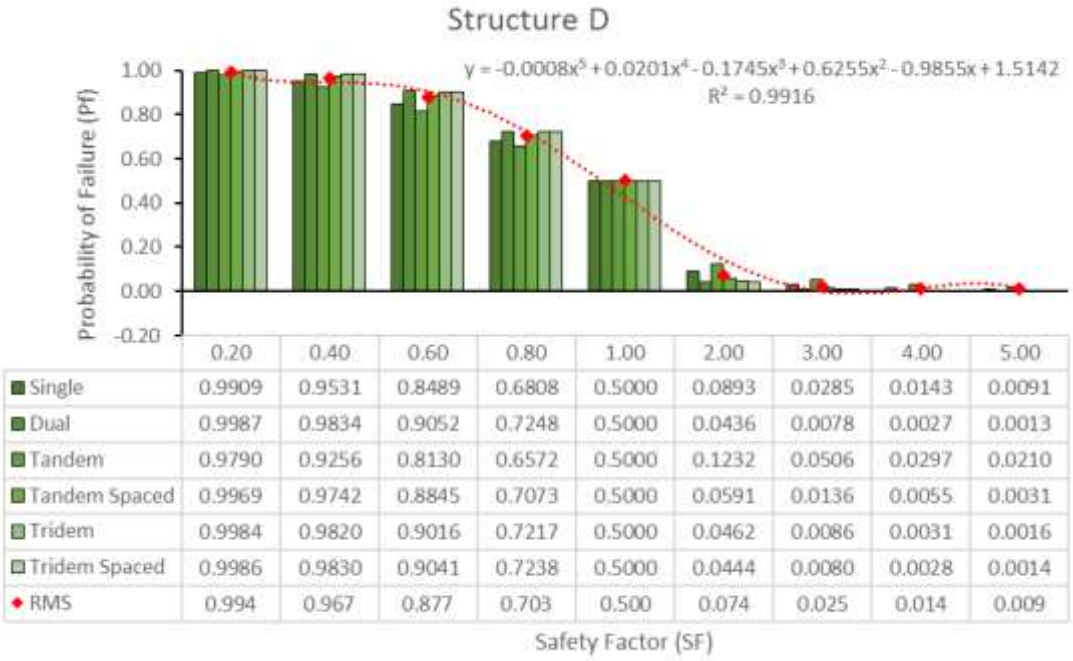

	0.20	0.40	0.60	0.80	1.00	2.00	3.00	4.00	5.00
Single	0.9909	0.9531	0.8489	0.6808	0.5000	0.0893	0.0285	0.0143	0.0091
Dual	0.9987	0.9834	0.9052	0.7248	0.5000	0.0436	0.0078	0.0027	0.0013
Tandem	0.9790	0.9256	0.8130	0.6572	0.5000	0.1232	0.0506	0.0297	0.0210
Tandem Spaced	0.9969	0.9742	0.8845	0.7073	0.5000	0.0591	0.0136	0.0055	0.0031
Tridem	0.9984	0.9820	0.9016	0.7217	0.5000	0.0462	0.0086	0.0031	0.0016
Tridem Spaced	0.9986	0.9830	0.9041	0.7238	0.5000	0.0444	0.0080	0.0028	0.0014
RMS	0.994	0.967	0.877	0.703	0.500	0.074	0.025	0.014	0.009

Figure 69 Probabilities of failure vs Safety Factors for the Structure D

Finally, as stated by Luo et al. (2014), in a reliability-based mechanistic-empirical pavement design, the required reliability level, or the equivalent probability of failure is first determined with the local design code or engineering judgement. The design is then performed through trial-and-error based on several proposed candidate designs. The material cost and the construction are also considered in each candidate design and the one that meets the required reliability level and meanwhile reduces the cost most will be selected as the final design.

In this context, reliability analysis depends basically on two extremely important values: resistances and solicitations. These values can be determined through any criteria that provide the cycles to failure of a certain pavement structure configuration. Thus, resistances can be calculated from any pavement analysis and design software and solicitations can be computed from field observations or traffic volume predictions.

5 METHOD APPLICATION EXAMPLE

In order to exemplify the developed method presented, a four-layer pavement structure commonly used in Brazil was adopted and layer properties and configurations were proposed as follows in Table 25:

Table 25 Thickness and material properties of the asphalt pavement structure

Layer	Material	Material Classification (mePADS)	Initial Thickness (mm)	E (MPa)	Poisson Ratio ν
1	Hot Mix Asphalt	AC	30*	4000	0.30
2	Granular Base	G2	100**	400	0.40
3	Gravel Soil	G7	200	200	0.40
4	Soil	Soil (G9)	∞***	70	0.45

*Layer 1 thickness variation (mm): 30, 40, 50, 60, 70, 80, 90, 100, 110, 120, 130, 140, and 150

**Layer 2 thickness variation (mm): 100, 150, 200, 250, 300, and 350

*** A value of zero was specified in mePADS software to assume that a rigid layer exists at 1000 mm below the defined pavement

Which indicates the material type of each layer, their correspondent classification number in the software mePADS, as well as layer thicknesses, elastic modulus and Poisson ratio. Note that the sub-base (layer 3) thickness was fixed while asphalt and base layer thicknesses were varied.

5.1 AXLE TYPE AND TIRE PRESSURE

For the example develop it was considered the effect of a standard axle (single axle, dual wheel spaced 350 mm from the center of each other) without overload conditions, and according to the specifications of the Brazilian National Department of Transport Infrastructure (DNIT, 2007), which indicates the correspondent axle load of 98 kN (24.5 kN by tire) at 550 kPa (80 psi) of tire pressure.

5.2 STRUCTURAL RESPONSES

The mechanistical-empirical pavement design software mePADS was used to obtain specific structural responses.

By setting all input required to run the simulation it is possible to obtain stresses, strain, and displacements. In this example only the following two structural responses were considered in order to satisfy the computation of the cycles to failure N numbers described later in item 5.3:

- εht1= horizontal tensile strain at the bottom of the asphalt layer, in microstrain (mePADS Normal Strain in xx / PE1=Principal Normal Strain in X);
- εvcm= Vertical compressive strain at the top of the subgrade, in microstrain (mePADS Principal Normal Strain in Z / PE3=Principal Normal Strain in Z).

5.3 CYCLES TO FAILURE

The empirical Asphalt Institute pavement life prediction in terms of the number of cycles to failure (N numbers) for both fatigue cracking and rutting pavement distresses, were carried out, since in this example the most important is the relative/ comparative effect.

To calculate the number of load repetitions to fatigue cracking failure (N_F) and rutting failure (N_R) were used the horizontal tensile strain at the bottom of the asphalt layer (εht_1) and the vertical compressive strain at the top of the subgrade layer (εvcm), respectively.

The empirical fatigue equation for NF suggested by the Asphalt Institute (Asphalt Institute, 1999) and used for hot mix asphalt is presented in Equation 47 as a function of:

$$N_F = 0.0796 * \left(\frac{1}{\varepsilon ht_1}\right)^{3.291} * \left(\frac{1}{E_1}\right)^{0.854} \quad (47)$$

εht_1 (horizontal tensile strain developed at the bottom of the asphalt layer due to traffic load) and E_1 (modulus of elasticity of the asphalt layer).

Accordingly, the number of standard axle load repetitions sustained by the pavement before reaching the rutting failure (N_R) is known as rutting life. The empirical model suggested by Asphalt Institute (1999) is shown below in Equation 48, as a function of:

$$N_R = (1.365 * 10^{-9}) * \left(\frac{1}{\varepsilon vc_m}\right)^{4.477} \quad (48)$$

εvc_m (vertical compression strain at the top of the subgrade).

In general, stress and strain and displacement values induced by traffic loads can be calculated using several approaches, such as elastic solution, finite element method, and response of surface method, among others.

Once N_F and N_R are calculated, the smaller value is adopted as a critical N value, referred in this example as “Critical Resistance”. In this context, it is assumed that critical N values are Critical Resistances and that Solicitations are those derived from resistances varying as a function of the Safety Factors (SF).

To perform the reliability analyses the following steps are followed:

1. N_F and N_R were calculated for each structure configuration using the empirical model suggested by the Asphalt Institute. The lower values between N_F and N_R were adopted as critical resistances.
2. On the other hand, solicitations were determined based on several Safety Factors (SF). Thus, critical resistances were divided by a certain SF (SF=resistance/solicitation) and the resulting value was computed as solicitation. The SF considered in this example were 0.20; 0.40; 0.60; 0.80; 1.00 (as a control parameter where the probability of failure is always <0.50); 2.0; 3.0; 4.0; and 5.0.
3. All resistances and solicitations were assumed as average values (μ_R and μ_S, respectively). In this context, the standard deviations of the resistances (σ_R) and solicitations (σ_S) were determined based on the standard deviation of the structural configurations proposed as a whole. As a result, a large set of μ_S-σ_S (solicitation curves) and μ_R-σ_R (resistance curves) values were obtained.
4. Margin curves (M) were calculated in order to determine the area where the probability of failure might occur. M curves were calculated for both averages and standard deviations, as follows:

$$\mu_M = (\mu r - \mu s) \tag{49}$$

$$\sigma_M = (\sigma r^2 + \sigma s^2)^{0.5} \tag{50}$$

5. Reliability index (β) is calculated from margin curves as follows:

$$\beta = \frac{\mu_M}{\sigma_M} \tag{51}$$

6. Therefore, with β values calculated it is possible to determine the probability of failure (Pf). Pf can be calculated easily through the NORM.DIST function in Excel which returns the normal distribution for the specified mean and standard deviation:

$$NORM.DIST(x, mean, standard_{dev}, cumulative) \quad (52)$$

where:

- X is the required value (the value for which the distribution β, is calculated);
- Mean is the arithmetic mean of the distribution;
- Standard_dev is the standard deviation of the distribution

Cumulative is a logical value that determines the form of the function. If cumulative is TRUE, NORM.DIST returns the cumulative distribution function; if FALSE, it returns the probability density function. The equation for the normal density function (cumulative = FALSE) is:

$$f(x;\mu,\sigma) = \frac{1}{\sqrt{2\pi\sigma}} e^{-\left(\frac{(x-\mu^2)}{2\sigma^2}\right)} \quad (53)$$

When cumulative = TRUE, the formula is the integral from negative infinity to x of the given formula. In this example it is necessary to select TRUE. Thus, the probability of failure Pf can be calculated as follows:

$$P_f = 1 - \text{NORM. DIST}(\beta, 0, 1, \text{TRUE}) \quad (54)$$

If mean = 0, standard_dev = 1, and cumulative = TRUE, NORM.DIST returns the standard normal distribution, NORM.S.DIST. Figure 25 in Chapter 3 illustrates the process to calculate the reliability index β and the probability of failure Pf.

7. Data obtained from the method is compiled in an Excel spreadsheet to process it and carry out analyses. A red-yellow-green downgrade-colored-scale matrix can be useful to improve data visualization and facilitate the decision-making process in pavement design.

5.4 EXAMPLE RESULTS

5.4.1 mePADS Output Data & N numbers

Figures 70 to 72 shows the resulted εht_1 and εvc_m values and the critical resistances for the pavement structure configuration proposed. In addition, As can be seen in

Figure 70, horizontal tensile strain at the bottom of the asphalt layer (εht_1) decrease as base layer thickness increases. However, note that when the asphalt layer thickness is between 30 and 70 mm, εht_1 values, that begin about 7.50E-05, increases as asphalt layer thickness increases up to approximately 2.0E-04, as in the case of the thinnest base layer (100 mm). For asphalt layer thickness bigger than 80mm, strain begin to decrease as the thickness increases. It means that horizontal tensile is indicating that pavement design is “bad” if the asphalt layer is between 50 and 120 mm in depth, taking into account a pavement design based on fatigue cracking failure criteria, for example.

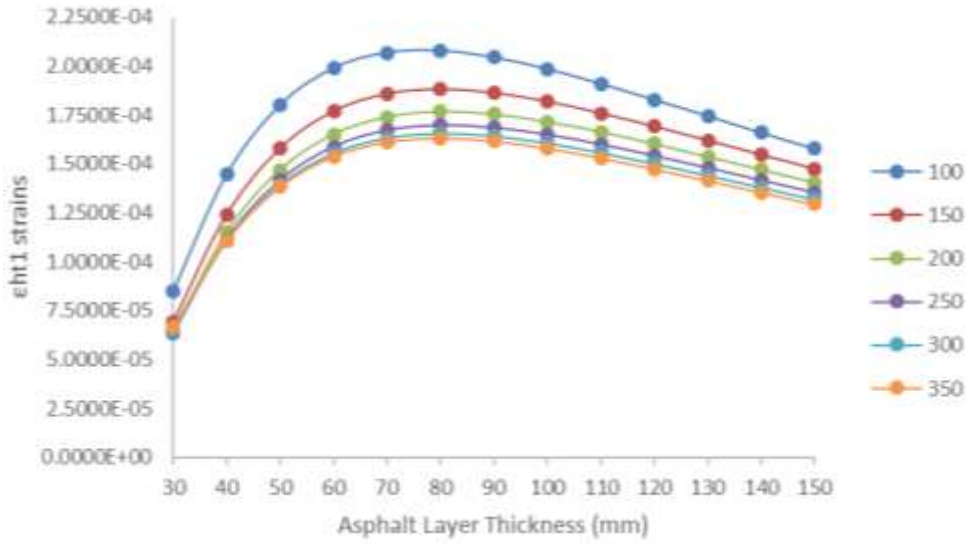

Figure 70 εht1 Strain by Asphalt & Base Layer Thicknesses

The same occurs at the top of the subgrade (Figure 71), where vertical compressive strain decrease as the base layer thickness increases and decreases as the asphalt layer thickness decrease. Note that to maintain a good pavement design based on both fatigue cracking and rutting failure criteria, the best base layer thickness should be between 250 and 350 mm, approximately.

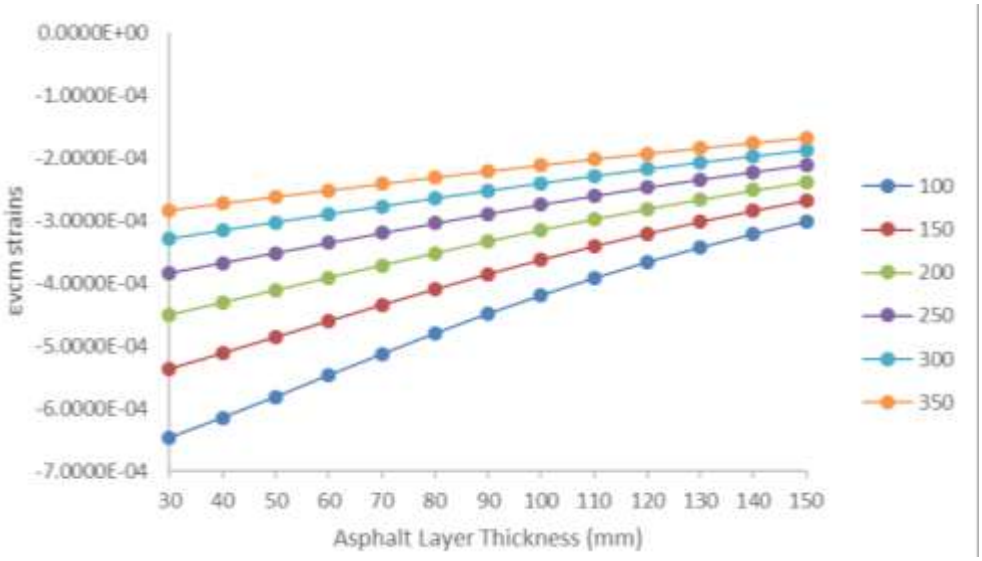

Figure 71 εvc_m Strain by Asphalt & Base Layer Thicknesses

In general, Figure 72 shows that critical resistances (minimum values between N_F and N_R) decrease as both asphalt and base layer thickness increases.

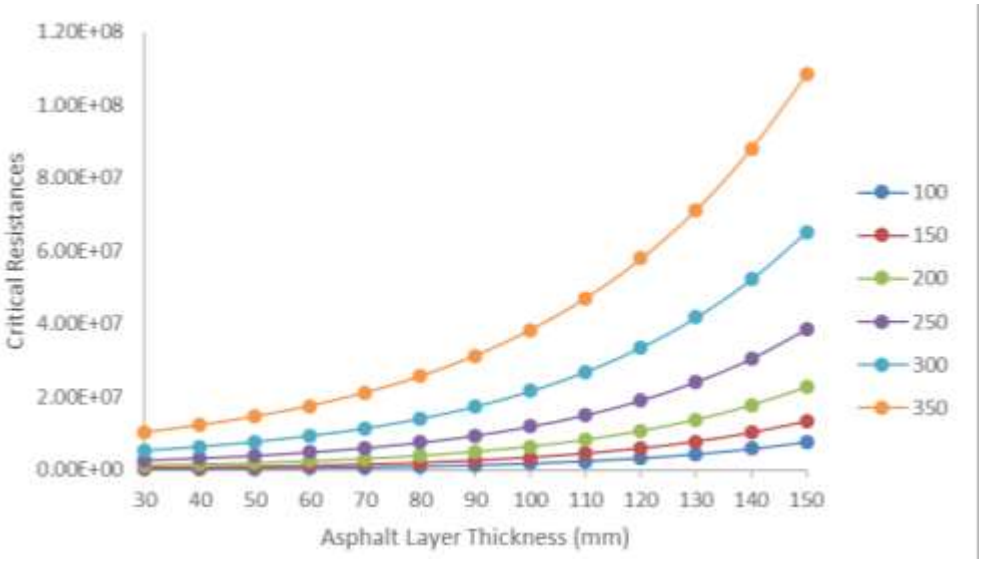

Figure 72 Critical Resistances by Asphalt & Base Layer Thicknesses

Observe that with a base layer thickness of 350 mm the cycles to failure of the pavement structure can be from about 1.0E07 up to about 1.1E08 as the thickness of the asphalt layer increases. This means that the deepest the structure, the longer the pavement life. However, here is the problem, because there is a potential risk of the pavement design be undersized or oversized.

The strong relationship between resistances and solicitations as well as the uncertainty of the different variables involved in the pavement design process makes it difficult to identify the ideal configuration that avoids excessive costs and guarantees an optimal service life capable to resist future solicitations.

Thus, there is a need for a complementary analysis that allow to measure this risk. In this context, a reliability-based method can be useful for design engineers to know the probability of failure of their proposed configurations and, consequently, allow them to make decisions in a reliability-based scenario.

Table 26 shows the statistics of the critical resistances. Observe that critical cycles to failure ranges from 2.59E+05 up to 1.09E+08. To begin with the reliability analysis, the first step is to determine the standard deviation of the overall critical resistance data corresponding to the example developed in this paper (2.08E+07).

Table 26 Critical Resistance Statistics

Statistics			
N Valid	78	Skewness	2.3930
Mean	1.56E+07	Std. Error of Skewness	0.2720
Median	7.76E+06	Kurtosis	6.4450
Std. Error of Mean	2.36E+06	Std. Error of Kurtosis	0.5380
Mode[a]	2.59E+05	Range	1.09E+08
Std. Deviation	**2.08E+07**	Minimum	2.59E+05
Variance	4.33E+14	Maximum	1.09E+08
		Root Mean Square (RMS)	2.60E+07

[a] Multiple modes exist. The smallest value is shown

5.4.2 Reliability Analysis

At this stage, critical resistances were calculated from the two structural parameters obtained through the simulations in the mePADS software, and also the standard deviation of the data is known. Figure 73 is a sample spreadsheet for the calculation of the probability-of-failure (Pf) corresponding to a pavement configuration with an asphalt layer thickness of 70 mm and a base layer thickness of 300 mm. Thus, each proposed structural configuration corresponds to a specific spreadsheet where the Pf values are calculated.

Parameter	Asphalt Layer thickness = 70 mm and Base layer thickness = 300 mm								
	SF=0.2	SF=0.4	SF=0.6	SF=0.8	SF=1	SF=2	SF=3	SF=4	SF=5
μR	1.14E+07	1.14E+07	1.14E+07	1.14E+07	**1.14E+07**	1.14E+07	1.14E+07	1.14E+07	1.14E+07
σR	2.08E+07	2.08E+07	2.08E+07	2.08E+07	**2.08E+07**	2.08E+07	2.08E+07	2.08E+07	2.08E+07
μS	5.71E+07	2.86E+07	1.90E+07	1.43E+07	1.14E+07	5.71E+06	3.81E+06	2.86E+06	2.29E+06
σS	1.04E+08	5.20E+07	3.47E+07	2.60E+07	2.08E+07	1.04E+07	6.93E+06	5.20E+06	4.16E+06
μM	-4.57E+07	-1.71E+07	-7.62E+06	-2.86E+06	0.00E+00	5.71E+06	7.62E+06	8.57E+06	9.14E+06
σM	1.06E+08	5.60E+07	4.04E+07	3.33E+07	2.94E+07	2.33E+07	2.19E+07	2.14E+07	2.12E+07
β	**-0.4309**	**-0.3060**	**-0.1884**	**-0.0858**	**0.0000**	**0.2457**	**0.3474**	**0.3997**	**0.4309**
PF	**0.6667**	**0.6202**	**0.5747**	**0.5342**	**0.5000**	**0.4030**	**0.3641**	**0.3447**	**0.3333**
PS	**0.3333**	**0.3798**	**0.4253**	**0.4658**	**0.5000**	**0.5970**	**0.6359**	**0.6553**	**0.6667**

Figure 73 Sample spreadsheet to calculate the Pf of a certain pavement structure configuration

In line with Figure 73, the first column contains the reliability-based method parameters:

- μR corresponds to the mean of the critical resistances. Note that is the same value for all Safety Factors (SF);
- σR is the standard deviation of the critical resistances and remains the same for all SF values;
- μS corresponds to the mean solicitations in terms of each SF value. Note that when SF=1.0 → μS=μR, consequently, successive μS values are obtained as follows:

$$\mu_S = \frac{\mu_S \; when \; SF = 1.0}{each \; SF} \tag{55}$$

- σS is the standard deviation of the solicitations in terms of each SF value. Observe that when SF=1.0 → σS= σR, consequently, successive σS values are obtained as follows:

$$\sigma_S = \frac{\sigma_S \; at \; SF = 1.0}{each \; SF} \tag{56}$$

- μM is the margin curve of both average resistances and solicitations and it is obtained by subtracting μR from μS:

$$\mu_M = \mu_R - \mu_S \tag{57}$$

- σM is the margin curve of both resistances and solicitations standard deviations and it is obtained as follows:

$$\sigma_M = \sqrt{{\sigma_R}^2 + {\sigma_S}^2} \tag{58}$$

- β is the reliability index, obtained by dividing the average margin curve by the deviation margin curve:

$$\beta = \frac{\mu_M}{\sigma_M} \tag{59}$$

- Pf is the correspondent probability-of-failure. It can be computed easily in Excel as follows (note that when SF=1.0 → Pf=0.5000):

$$Pf = 1 - NORMDIST(\beta, 0, 1, TRUE) \tag{60}$$

- Ps is the probability of success:

$$PS = 1 - Pf \quad (61)$$

Once all Pf values are calculated, results should be concentrated in a downgrade-colored-scale matrix in order to improve data visualization and facilitate the decision-making process in pavement design. It can be easily done in Excel using the color scale option of the conditional formatting tool that applies a color gradient to a range of cells. The color indicates where each value falls within that range.

Figures 74 and 75 concentrates all the probabilities-of-failure obtained from the reliability process by asphalt layer thickness, base layer thickness, and safety factors, it is meaningful to consider SF≤1 (only as academic specification, in general conditions SF≤1 should never be use). In this case, it was used a red-yellow-green color scale to improve data visualization. As can be seen in Figure 74, SF values range from 0.20 to 0.80, meaning that solicitations are about 5.0 to 1.2 times higher than the resistances, respectively. Observe that Pf values result higher than 0.50 and also reach 1.0 as safety factors decrease. In general, Pf values increase as both asphalt and base layer thicknesses increases, but gradually decreases as safety factors increase.

Base (mm)	SF	Asphalt Layer Thickness													SF	Base (mm)
		30.0	40.0	50.0	60.0	70.0	80.0	90.0	100.0	110.0	120.0	130.0	140.0	150.0		
100	0.2	0.5039	0.5049	0.5063	0.5082	0.5110	0.5147	0.5199	0.5270	0.5365	0.5491	0.5658	0.5876	0.6155	0.2	100
150		0.5089	0.5111	0.5140	0.5178	0.5230	0.5300	0.5393	0.5517	0.5678	0.5888	0.6157	0.6498	0.6918		150
200		0.5194	0.5238	0.5294	0.5367	0.5463	0.5589	0.5753	0.5963	0.6231	0.6570	0.6984	0.7480	0.8038		200
250		0.5402	0.5487	0.5592	0.5727	0.5898	0.6116	0.6393	0.6734	0.7150	0.7639	0.8186	0.8751	0.9273		250
300		0.5795	0.5955	0.6145	0.6381	0.6667	0.7021	0.7438	0.8447	0.8968	0.9425	0.9756	0.9930	0.9964		300
350		0.6505	0.6780	0.7094	0.7461	0.7876	0.8334	0.8813	0.9260	0.9622	0.9855	0.9964	0.9996	1.0000		350
100	0.4	0.5028	0.5035	0.5045	0.5058	0.5078	0.5105	0.5142	0.5192	0.5259	0.5349	0.5468	0.5625	0.5826	0.4	100
150		0.5063	0.5079	0.5099	0.5126	0.5163	0.5213	0.5279	0.5367	0.5483	0.5634	0.5828	0.6077	0.6390		150
200		0.5138	0.5169	0.5209	0.5261	0.5329	0.5419	0.5536	0.5687	0.5881	0.6130	0.6440	0.6824	0.7282		200
250		0.5285	0.5346	0.5421	0.5518	0.5641	0.5798	0.5999	0.6252	0.6566	0.6952	0.7410	0.7932	0.8494		250
300		0.5566	0.5681	0.5819	0.5990	0.6202	0.6468	0.6791	0.7643	0.8152	0.8684	0.9190	0.9594	0.9717		300
350		0.6082	0.6286	0.6524	0.6809	0.7146	0.7541	0.7993	0.8479	0.8965	0.9395	0.9720	0.9909	0.9982		350
100	0.6	0.5017	0.5021	0.5027	0.5036	0.5048	0.5064	0.5087	0.5118	0.5160	0.5215	0.5289	0.5386	0.5511	0.6	100
150		0.5039	0.5049	0.5061	0.5078	0.5101	0.5131	0.5172	0.5226	0.5298	0.5391	0.5512	0.5668	0.5867		150
200		0.5085	0.5104	0.5129	0.5161	0.5203	0.5258	0.5331	0.5424	0.5545	0.5701	0.5899	0.6149	0.6458		200
250		0.5176	0.5213	0.5260	0.5319	0.5395	0.5493	0.5619	0.5779	0.5981	0.6234	0.6547	0.6926	0.7378		250
300		0.5349	0.5421	0.5507	0.5614	0.5747	0.5917	0.6127	0.6713	0.7097	0.7546	0.8054	0.8585	0.8798		300
350		0.5671	0.5801	0.5953	0.6139	0.6364	0.6639	0.6973	0.7365	0.7814	0.8301	0.8802	0.9269	0.9632		350
100	0.8	0.5008	0.5010	0.5013	0.5016	0.5022	0.5029	0.5040	0.5054	0.5073	0.5098	0.5132	0.5176	0.5233	0.8	100
150		0.5018	0.5022	0.5028	0.5035	0.5046	0.5060	0.5078	0.5103	0.5136	0.5178	0.5234	0.5305	0.5397		150
200		0.5039	0.5047	0.5059	0.5073	0.5092	0.5118	0.5151	0.5193	0.5249	0.5321	0.5412	0.5529	0.5676		200
250		0.5080	0.5097	0.5118	0.5146	0.5180	0.5225	0.5283	0.5356	0.5450	0.5569	0.5719	0.5906	0.6140		250
300		0.5159	0.5192	0.5231	0.5280	0.5342	0.5421	0.5519	0.5800	0.5993	0.6231	0.6525	0.6875	0.7035		300
350		0.5307	0.5367	0.5437	0.5524	0.5631	0.5764	0.5930	0.6133	0.6382	0.6681	0.7039	0.7459	0.7924		350

Figure 74 Downgrade-colored-scale matrix for Pf values with SF between 0.20 and 0.80

As an example, Pf values in Figure 74 shows that, when SF=0.8 and the base layer thickness is 100 mm, the Pf for an asphalt layer of 30 mm in depth is 0.50 and gradually increase to reach 0.52 when the asphalt layer thickness is five times higher (150 mm). However, observe that if the base layer thickness increases up to 350 mm and the asphalt layer thickness remains to be 150 mm in depth, the corresponding Pf value is 0.7924 (approximately 50% higher). In other words, it means that if the pavement structure involves an asphalt layer thickness of 150 mm and a base layer thickness of 350 mm, but solicitation exceeds 20% of the calculated resistance (SF=0.80), then probably exists a problem of oversizing, meaning that the concept of a pavement life be higher as layer thicknesses increase is a false belief because it will depend, among several factors, on the proportions between resistances and solicitations.

Figure 75, on the other hand, shows SF values ranging from 2.0 to 5.0. It means that now solicitations are about 20% to 50% times lower than resistances, respectively.

Base (mm)	SF	Asphalt Layer Thickness (mm)													SF	Base (mm)
		30.0	40.0	50.0	60.0	70.0	80.0	90.0	100.0	110.0	120.0	130.0	140.0	150.0		
100	2.0	0.4978	0.4972	0.4964	0.4953	0.4938	0.4916	0.4886	0.4846	0.4792	0.4719	0.4624	0.4498	0.4335	2.0	100
150		0.4949	0.4937	0.4920	0.4899	0.4869	0.4829	0.4776	0.4705	0.4612	0.4491	0.4334	0.4132	0.3876		150
200		0.4889	0.4864	0.4832	0.4791	0.4736	0.4664	0.4569	0.4448	0.4290	0.4089	0.3835	0.3517	0.3130		200
250		0.4771	0.4722	0.4661	0.4584	0.4485	0.4358	0.4195	0.3989	0.3731	0.3409	0.3019	0.2558	0.2033		250
300		0.4545	0.4452	0.4341	0.4202	0.4030	0.3812	0.3544	0.2816	0.2356	0.1845	0.1308	0.0808	0.0629		300
350		0.4128	0.3961	0.3766	0.3529	0.3246	0.2906	0.2503	0.2047	0.1555	0.1066	0.0626	0.0291	0.0098		350
100	3.0	0.4969	0.4961	0.4949	0.4934	0.4912	0.4881	0.4839	0.4783	0.4706	0.4604	0.4469	0.4291	0.4064	3.0	100
150		0.4928	0.4911	0.4887	0.4857	0.4815	0.4758	0.4683	0.4583	0.4452	0.4282	0.4063	0.3782	0.3431		150
200		0.4843	0.4808	0.4763	0.4704	0.4626	0.4525	0.4392	0.4221	0.4002	0.3723	0.3375	0.2951	0.2453		200
250		0.4676	0.4607	0.4522	0.4413	0.4274	0.4096	0.3869	0.3585	0.3235	0.2811	0.2315	0.1767	0.1202		250
300		0.4358	0.4228	0.4072	0.3879	0.3641	0.3344	0.2987	0.2068	0.1541	0.1020	0.0562	0.0239	0.0152		300
350		0.3776	0.3547	0.3283	0.2967	0.2600	0.2176	0.1704	0.1217	0.0760	0.0392	0.0150	0.0037	0.0005		350
100	4.0	0.4964	0.4955	0.4942	0.4924	0.4898	0.4863	0.4815	0.4750	0.4662	0.4544	0.4390	0.4186	0.3926	4.0	100
150		0.4917	0.4897	0.4871	0.4835	0.4787	0.4722	0.4636	0.4521	0.4370	0.4175	0.3925	0.3606	0.3210		150
200		0.4820	0.4779	0.4727	0.4659	0.4570	0.4454	0.4301	0.4106	0.3855	0.3539	0.3148	0.2677	0.2139		200
250		0.4627	0.4549	0.4450	0.4325	0.4166	0.3963	0.3704	0.3384	0.2992	0.2524	0.1993	0.1428	0.0884		250
300		0.4262	0.4113	0.3936	0.3716	0.3447	0.3113	0.2717	0.1735	0.1206	0.0719	0.0339	0.0114	0.0064		300
350		0.3599	0.3341	0.3044	0.2695	0.2296	0.1847	0.1366	0.0898	0.0497	0.0214	0.0063	0.0010	0.0001		350
100	5.0	0.4961	0.4951	0.4937	0.4918	0.4890	0.4853	0.4801	0.4730	0.4635	0.4509	0.4342	0.4124	0.3845	5.0	100
150		0.4911	0.4889	0.4860	0.4822	0.4770	0.4700	0.4607	0.4483	0.4322	0.4112	0.3843	0.3502	0.3082		150
200		0.4806	0.4762	0.4706	0.4633	0.4537	0.4411	0.4247	0.4037	0.3769	0.3430	0.3016	0.2520	0.1962		200
250		0.4598	0.4513	0.4408	0.4273	0.4102	0.3884	0.3607	0.3266	0.2850	0.2361	0.1814	0.1249	0.0727		250
300		0.4205	0.4045	0.3855	0.3619	0.3333	0.2979	0.2562	0.1553	0.1032	0.0575	0.0244	0.0070	0.0036		300
350		0.3495	0.3220	0.2906	0.2539	0.2124	0.1666	0.1187	0.0740	0.0378	0.0145	0.0036	0.0004	0.0000		350

Figure 75 Downgrade-colored-scale matrix for Pf values with SF between 2.0 and 5.0

Observe, in this case, that Pf values decrease as both asphalt and base layer thicknesses and SF values increases. As an example, Pf values in Figure 75 shows that, when SF=2.0 and the base layer thickness is 100 mm, the Pf for an asphalt layer

of 30 mm in depth is 0.4978 and gradually decrease to reach 0.4335 when the asphalt layer thickness is five times higher (150 mm). Additionally, observe that if the base layer thickness increases up to 350 mm and the asphalt layer thickness remains to be 150 mm in depth, so the corresponding Pf value is close to zero (0.0098, approximately 43% lower).

5.5 EXAMPLE CONCLUSIONS

From the percentages shown in Figure 75, some relevant assumptions can be made:

- If a safety factor of 2.0 is adopted and the structural configuration involves thicker asphalt and base layers ranging from 70 to 110 mm and 250 to 350 mm in depth, respectively, then the risk of failure can be reduced from about 9% up to 68%. This risk scenario gradually becomes to be less restrictive as safety factor increases, ranging from about 13% up to 84% when the SF=3.0; 16% up to 90% when the SF=4.0; and 17% up to 92% when the SF=5.0;
- In general, pavement structures with asphalt layers less than 70 mm in depth and with base layer thicknesses between 250 and 350 mm in depth, can only reduce the risk of failure from about 17% up to 49%, depending on the safety factor used. Certainly, a poor combination of thinner asphalt and base layers will result in risk reductions less than 6%. Likewise, combinations of thicker asphalt and base layers will result in risk reductions ranging from 28% up to 100% as safety factor increases;
- On the other hand, pavement structures subjected to more solicitations than resistances ($0.2 \leq FS \leq 0.8$) will show that probably thicker configurations are not the best option. In this context, the risk of pavement failure increases as layer thicknesses increase. This information can be useful for pavements that are already built and operable but that exceeds the expected solicitations, in order to identify a variety of probabilities of failure to propose eventual structural modifications;

It is important to note that the example proposed in this paper only took into account the thickness variation of the asphalt and base layers, without varying the material properties, and also without considering the possibility of additional layers or different axle types, overload conditions, and tire pressures. However, for any case or set of

structural configurations the process to determine the probability of failure will be the same as presented in this research.

In general, it was observed that a reliability-based analysis can be performed from accurate resistances and solicitations data that can be obtained from any criteria that provide the cycles to failure of the pavement structure configuration. The approach developed in this research is a practical tool to be adopted in the engineering practice and thus has the potential to become a practical tool in the reliability-based mechanistic-empirical pavement design.

6 CONCLUSIONS

The main objective of this research was to evaluate the probability of failure of different flexible pavement structures through the reliability concept, taking into account six axle types which were subjected to five overload conditions and three tire pressures. To achieve this objective, several tasks were conducted. Firstly, simulations were carried out in the software MePADS to obtain four structural pavement responses for each pavement structure, varying the axle type, load applied and tire pressure. A structural response vs thickness analysis was done for each structure. Secondly, pavement life predictions in terms of cycles to failure (N numbers) were obtained for Fatigue Cracking and Rutting pavement distresses. Critical resistance values, consequently, were determined from the minimum N value (Fatigue Cracking and Rutting). Thirdly, solicitations were defined from several safety factors. Thus, resistances and solicitations allow to calculate the reliability indices and the probabilities of failure. Statistical analyses were also done to verify the normality of the data and a transformation by inverse distribution function was conducted to normalize it. In addition, Pearson's Correlations were carried out and four regression models were obtained. Finally, reliability indices and probabilities of failure associated with different safety factors and axle types were acquired for each structure.

The main conclusions of this research are the following:

1. Comparison between structural responses: surface displacement by axle type, horizontal tensile strain at the bottom of the asphalt layer, vertical tensile compression strain at the bottom of the asphalt layer, vertical compressive strain at the top of the subgrade;
2. Pavement life predictions; comparison between critical resistance vs overload;
3. Reliability index and probability of failure statistics data analysis;
4. Reliability Indices and Probabilities of Failure by Safety Factors and Axle type;

6.1 STRUCTURAL RESPONSES

The main conclusions about the four structural responses obtained for the four pavement structures are the following:

a) Displacement of the Surface of Pavements

Of the four structures analyzed in this research, structure B present the highest values of displacement, ranging from 0.32 to 0.52 mm for single, dual, tridem and tridem spaced axles;

Data obtained clearly indicates that pavement displacements occur from 0.02 m to 0.50 mm in all the structures studied and that single, dual, tridem and tridem-spaced axles have the maximum values ranging from 0.20 mm to 0.40 mm. Surface displacements increase as both overload and tire pressures create a vertical contact pressure at the tire edge and longitudinal contact stress increase;

Structure B has the highest surface displacements but tandem-spaced axle showed the lowest values;

The average rate of increase surface displacement as a function of the overload percentage and tire pressure exist a relation of about 0.41% directly proportionally to the overload percentage.

b) Horizontal Tensile Strain at the Bottom of the Asphalt Layer

It was clearly observed that tandem and tandem-spaced axles present the lowest strain in the four structures. The highest strain occurs in Structures B and D, and Structure C presents the lowest minimum and maximum strain for all the axle types analyzed.

The rate of increasing of the strain values increase up to 8% as tire pressure increase 550 KPa to 690 KPa and 12% up to tire pressure increases from 690 KPa to 830 KPa.

Strain values increase as tire pressure and overload increases, due to the vertical contact causing longitudinal stresses increase. For instance, at 30% of overload, Eht, increases up to 28%.

c) Vertical Compressive Strain at the Bottom of the Asphalt Layer

Vertical Compressive Strain at the Bottom of the Asphalt Layer values presented less sensitivity to tire pressure than horizontal strain, in all axle types

except for the single axle. Single axle generates only vertical compressive strain at the bottom of the asphalt layer of the four structures studied.

Structures A and B have the highest strain considering that these two structures are the thinner ones, structure C (thinner structure) presented the lowest minimum and maximum strain in all axle types, except in the single and tridem-spaced axles.

At 0% of overload, strain decrease up to 0.73% when tire pressure increases from 550 KPa to 690 KPa and strain can increase up to 1.15% when tire pressure varies from 690 KPa to 830 KPa.

When axles are under 30% of overload, strain at 550 KPa are about 36.86% higher than at 0% and 550 KPa of tire pressure. Still at 30% of overload, strain decrease up 30.91% if the tire pressure increases from 550 KPa to 690 KPa; and decrease up to 29.12% if it reaches 830 KPa.

d) Vertical Compressive Strain at the Top of the Subgrade

Tandem-spaced axle showed the lowest strain in the four pavement structures, followed by the tandem axle only in Structure A and B. Vertical Strain at the top of the subgrade increased as overload percentage increased.

For all four structures, Tandem-spaced presented the lowest strain, but the highest strain occurs in Structure B. As Structure C remains to have the lowest minimum and maximum strain.

f) Structural Responses vs Thickness

For all pavement structures analyzed, the asphalt layer thicknesses (Structures A= 40 mm; B= 75 mm; C= 100 mm; and D= 125 mm), with the only difference that structure A is 130 mm (40 + 90 mm) and C 220 mm (100 + 120 mm) because have two asphalt layers, displacements registered are decreases as the asphalt thickness increase, in an average of 28%.;

Structures A and C reflect how a second asphalt layer can reduce the horizontal tensile strain up to 500%;

Vertical compressive strain at the bottom of the asphalt layer for Structure B are approximately 48% higher than for the other 3 Structures;

Structure B presented the highest vertical strain at the top of the subgrade, approximately 56% higher than Structure A and D; and 28% higher than Structure C.

6.2 PAVEMENT LIFE PREDICTIONS

Average N numbers for fatigue cracking and rutting distresses according to the Asphalt Institute criteria were calculated for the four Structures, considering axle types, tire pressures and axle overloads.

a) Fatigue Cracking

For all four Structures analyzed the average cycles to Failure (N numbers) for this distress are:

- Structure A, the lowest values were observed for Dual and Tridem-spaced axles;
- Structure B, the lowest values where observed for single and dual axles;
- Structure C, the lowest values where observed for single axle; and,
- Structure D, the lowest values where observed for single and dual axles.

As can be seen, single and dual axles presented the lowest values being adopted as critical values, being the ones responsible to cause Fatigue cracking due to the punctual load acting in the pavement structure. The damage is much lower when considering Tandem, Tandem-spaced, Tridem and Tridem-spaced (expect in Structure A) because the reduction stress is less under multiple axles.

b) Rutting

Rutting affects pavement performance the most significantly, of the four pavement structures analyzed the result for this failure are presented as follow:

- Structure A, lowest values where achieved by Dual, Tridem and Tridem-spaced axles;
- Structure B, lowest values where for Dual, Tridem and Tridem-spaced axles;
- Structure C, lowest values where for Tridem, Dual, and Tandem axles;

- Structure D, lowest values where for Dual, Tridem and Tridem-spaced axles.

This result may be due to the position of the load distribution applied to each axle type, being the best scene the simulation due with the tandem spaced as being the one that presented the highest N numbers for all pavement structures, followed by the tandem axle with values are about five times lower.

c) Critical Resistances vs. Overloads

The main conclusions about the comparison of critical resistances vs overload of this research are:

- It was observed that tandem-spaced axles presented the higher N numbers and that single and dual axles showed the lowest and more critical values between fatigue cracking and rutting. The only variation was observed at the Structure C where tridem axles presented the lower N number;
- Results confirms that single and dual axle causes the greatest damage on pavement structures independent of the asphalt layer thickness;
- Additionally, critical pavement resistance decreases as tire pressure and axle overload increases. In all four structures analyzed it was observed that when overload and tire pressure increase, the pavement life reduces for 34% with axle overload of 10% and 550 KPa tire pressure. In the highest overload condition analyzed in this research (30% of axle overload with tire pressure of 830 KPa) pavement life reduction increased up to 60%.

6.3 RELIABILITY INDEX AND PROBABILITY OF FAILURE

In order to obtain the reliability indices and the probabilities of failure in the four structures, it was necessary first analyze the data information. Data did not have a normal distribution so it was crucial to improve normality, using the software IBM-SPSS was used to normalize the data through the inverse distribution.

The main conclusions through the Pearson Correlations are the following:

- Results indicate strong and positive coefficient of determination between solicitations and resistances (average r= 0.941) with significant values (p<0.001).
- Reliability index β demonstrate a low and positive correlation with solicitation with coefficient of determination (r= -0.277) and a significant value of (p<0.001),
- Strong and negative correlation with the probability of failure Pf (r= -0.99) and significant value of (p<0.001).
- Correlation between β and Pf have non-linear, negative and perfect relation with an R square value of 1.0 defined by a third-order polynomial trend line.

All regression models indicate strong and positive correlation. However, according to models 1, 2 and 3 were significant (P-value <0.05), regression model of 4 model indicate that the constant value is non-significative with an extremely high value of 0.80.

6.4 RELIABILITY INDICES AND PROBABILITIES OF FAILURE BY SAFETY FACTORS AND AXLE TYPES

The results for reliability indices and probabilities of failure based in the resistance (critical N numbers) and solicitation (critical resistance varying a function of different safety factors) are the following:

Structure A

For this type of structure, the tandem and tandem-Spaced axles presented the highest reliability indices and also the highest probability of failure when safety factors are less than 1.00.

Structure B

The highest reliability indices occur with tridem and tridem-spaced axles as well as the probabilities of failure for this type of axle, for those Safety Factors less than 1.00

Structure C

The highest reliability indices in this structure are for single axle as well as the probability of failure that for this type of axe is about 12% lower that the RMS.

For Safety Factors greater than 1.00 the PF value for the single axle is approximately twice than the other axle types.

Structure D

For this structure the dual, tridem, and tridem-spaced axle present the highest probability of failure. For a Pf value greater than 1.00 single axle is nearly twice that the other axles.

6.5 FINAL REMARKS

As safety factors increase, the reliability index decreases as well as the probability of failure for all four structures. In general, Safety Factors are associated to the Reliability Index and to the Probability of Failure, and they should take into consideration in pavement design analysis because in most cases Safety Factors are adopted as measurements of safety, independent from the Reliability Index and the Probability of Failure.

The process developed in this research to calculate the probability of failure of flexible pavements was based only on resistances and solicitations as well as on their variations as a function of several Safety Factors. In this context, this research can contribute to the decision-making process that a design engineer faces, bringing a practical and easy way to evaluate a certain structural configuration and avoid, as far as possible, the risk of oversizing or undersizing the pavement structure.

7 REFERENCES

AASHTO. (1986). *Guide for Design of Pavement Structures.* Washington, D.C.: American Association of State Highway and Transportation Officials.

AASHTO. (1993). *Guide for Design of Pavement Structures.* Washington, D.C.: American Association of State Highway and Transportation Officials.

Aguiar-Moya, J., & Prozzi, J. (2011). Effect of field variability of design inputs on the MEPDG. *Transportation Research Board 90th Annual Meeting*.

Albano, J. (2005). *Efeitos dos Excessos de Carga Sobre a Durabilidade de Pavimentos.* Porto Alegre: Pós-graduação em Engenharia de Produção da Universidade Federal do Rio Grande do Sul.

Alhasan, A., Ali, A., Offenbacker, D., Smadi, O., & Lewis-Beck, C. (2018). Incorporating Spatial Variability of Pavement Foundation Layers Stiffness in Reliability-Based Mechanistic-Empirical Pavement Performance Prediction. *Transportation Geotechnics, 17 Part A*, 1-13. doi:https://doi.org/10.1016/j.trgeo.2018.08.001

Al-Qadi, I., & Yoo, P. (2007). Effect of Surface Tangential Contact Stress on Flexible Pavement Response. *Journal of the Association of Asphalt Pavement Technologist, 76*, 663-692.

Al-Qadi, I., Elseifi, M., & Yoo, P.J., P. (2005). Characterization of Pavement Damage due to Different Tire Configurations. *Journal of the Association of Asphalt Paving Technologist, 84*, 921-962.

Asphalt Institute. (1999). *Thickness Design-Asphalt Pavements for Highways and Streets* (9th Ed. ed.). Lexington, KY: Asphalt Institute.

Ayres, J. (1997). *Development of a Rational Probabilistic Approach for Flexible Pavement Analysis.* Maryland: University of Maryland, College Park.

Banerjee, A., Aguiar-Moya, J., & Prozzi, J. (n.d.). Calibration of Mechanistic–Empirical Pavement Design Guide Permanent Deformation Models: Texas Experience with Long-Term Pavement Performance. *Transportation Research Record:*

Journal of the Transportation Research Board, 2094. doi:https://doi.org/10.3141/2094-02

Bekele, A. (2011). *Implementation of the AASHTO Pavement Design Procedures into Multi-Pave.* Stockholm-Sweden: Division of Highway and Railway Engineering, School if Architecture and the Built Environment, Royal Institute of Technology (KTH).

Boussinesq, J. (1885). *Application des potentiels à l'étude de l'équilibre et du mouvement des solides élastiques, principalement au calcul des déformations et des pressions que produisent, dans les solides, des efforts quelquonques exercés sur une petite partie de...* Paris: Gauthier-Villars.

Burmister, D. (1943). The General Theory of Stresses and Displacement in Layered Soils Systems. *Journal of Applied Physics, 16*.

Dalla, V. (2015). *Reliability in pavement design.* The University of Nottingham. Retrieved from http://eprints.nottingham.ac.uk/28999/1/Thesis%20report_final%20issue.pdf

Ditlevson, O. (1981). *Uncertainty Modeling with Applications to Multidimensional Civil Engineering System.* New York: McGraw-Hill.

DNIT. (2005). *Contagem Volumetrica do Trafego - Relatorio do Volume Medio Diario Anual.* Brasilia: Brazilian National Department of Transport Infrastructure.

DNIT. (2006a). *Manual de Pavimentacao* (Third Ed. ed.). Rio de Janeiro: Departamento Nacional de Infraestrutura de Transportes.

DNIT. (2006b). *Manual de Restauracao de Pavimentos Asfalticos* (2nd Ed. ed.). Rio de Janeiro: Departamento Nacional de Infraestrutura de Transportes.

DNIT. (2007). *Limites Legais.* Rio de Janeiro: Departamento Nacional de Infraestrutura de Transportes - Conselho Nacional de Transito CONTRAN. Retrieved from http://www1.dnit.gov.br/Pesagem/qfv%20pdf.pdf

Douglas, R., Woodward, W., & Woodside, A. (2000). Road Contact Stresses and Forces under Tires with Low Inflation Pressure. *Canadian Journal of Civil Engineering, 27*, 1248-1258.

Elliott, R., & Thompson, M. (1985). *Mechanistic design concepts for conventional flexible pavements.* Interim Report Illinois University, Urbana-Champaign, Department of Civil Engineering.

Feng, W. (2005). *Mechanistic-Empirical Study of Effects of Truck Tire Pressure on Asphalt Pavement Performance.* Austin, TX: The University of Texas at Austin.

Fernandes Jr., J. (1994). *Investigação dos Efeitos das Solicitações do Tráfego sobre o Desempenho de Pavimentos.* Sao Carlos, SP: Sao Carlos School of Engineering, University of Sao Paulo.

Fernandes Jr., J., & Soria, M. (1996). Investigação dos Efeitos das Solicitações do Tráfego sobre o Desempenho de Pavimentos. *Anais da 30ª Reunião anual de Pavimentação.* Salvador, BA, Brazil: Asociacao Brasileira de Pavimentacao - ABPv.

Fernandes Jr., J., Pais, J., & Pereira, P. (2006). Effects of traffic loading on Portuguese and Brazilian pavements performance. *85th Transportation Research Board Annual Meeting*.

Fernandes Jr., J., Soria, M., & Widmer, J. (2007). Efeitos das solicitações de trafego sobre os custos de construção, manutenção e utilização das rodovias. *Reuniao anual de pavimentação*, 266-284.

FHWA. (2006). *Geotechnical Aspects of Pavements Reference Manual.* Washington, D.C.: U.S. Department of Transportation Publication No. FHWA NHI-05-037. Retrieved from https://www.fhwa.dot.gov/engineering/geotech/pubs/05037/index.cfm

Fontenele, H. (2011). *Representação do Trafego de Veículos Rodoviários de Carga através de Espectros de Carga por Eixo e seu Efeito no Desempenho dos Pavimentos.* Sao Carlos, SP: Pós-graduação em Engenharia de Transportes. Escola de Engenharia de São Carlos, Universidade de Sao Paulo.

Franco , F. (2000). *Um Sistema para Analise Mecanistica de Pavimentos Asfalticos.* Rio de Janeiro: Programa de Pos-Graduacao de Engenharia, Universidad Federal do Rio de Janeiro.

Franco, F. (2007). *Metodo de Dimensionamiento Mecanistico-Empirico de Pavimentos Asfalticos-SISPAV.* Rio de Janeiro: Programa de Pos-Graduacao de Engenharia, Universidade Federal do Rio de Janeiro.

Haldar, A., & Mahadevan, S. (2000). *Probability, Reliability and Statistical Methods in Engineering Design.* New York: John Wiley & Sos, Inc.

Hall, K., Xiao, D., Pohl, E., & Wang, K. (2012). *Reliability-Based Mechanistic–Empirical Pavement Design with Statistical Methods.* Washington D.C.: Transportation Research Record: Journal of the Transportation Research Board. doi:https://doi.org/10.3141/2305-13

Hall, K., Xiao, D., Pohl, E., & Wang, K. (2014). Reliability based mechanistic empirical pavement design with statistical methods. *Transportation Research Record: Journal of the Transportation Research Board 2305:121-30*.

Harr, M. (1987). *Reliability-based Design in Civil Engineering.* Department of Civil Engineering, School of Engineering, North Carolina State University.

Hu, S., Zhou, F., Scullion, T., & Leidy, J. (2014). Reliability-Based Mechanistic-Empirical Flexible Pavement Design. *Transportation Research Record: Journal of the Transportation Research Board*, 85-95.

Huang, Y. (1993). *Pavement Analysis and Design.* New Jersey, USA: Prentice Hall.

Huang, Y. (2003). *Pavement Analysis and Design* (2nd Ed. ed.). New Jersey, USA: Prentice Hall, Englewood Cliffs. doi:ISBN-10:0131424734

Huang, Y. (2004). *Pavement Analysis and Design.* Upper Saddle River, N.J.: Prentice Hall.

Jiang, X., Zeng, C., Gao, X., Liu, Z., & Qiu, Y. (2017). 3D FEM Analysis of Flexible Base Asphalt Pavement Structure Under Non-Uniform Tyre Contact Pressure. *International Journal of Pavement Engineering*. doi:https://doi.org/10.1080/10298435.2017.1380803

Kenis, W., & Wang, W. (2004). *Pavement variability and reliability.* Kansas State University. Retrieved September 2019, from http://www.ksu.edu/pavements/TRB/A2B09/CS13-12.pdf

Kulkarni, R. (1994). Rational Approach in Applying Reliability Theory to Pavement Structural Design. *Transportation Research Record 1449*, 13-17.

Li, Q., Mills, L., & McNeil, S. (2011). *The Implications of Climate Change on Pavement Performance and Design.* Newark, DE: University of Delaware Transportation Center.

Luo, Z., Xiao, F., & Sharma, R. (2014). Efficient Reliability-Based Approach for Mechanistic Empirical Asphalt Pavement Design. *Construction and Building Materials*, 157-165.

Luo, Z., Xiao, F., Hu, S., & Yang, Y. (2013). Probabilistic Analysis of Fatigue Life of Rubberized Asphalt Concrete Mixtures Containing Reclaimed Asphalt Pavement. *Construction Building Materials*.

McInvale, H., Retherford, J., & McDonal, M. (2012). Load and Resistance Factorsd and Design Parameter Offsets for Mechanisti-Empirical Pavement Design Guide. *Transportation Research Record: Journal of the Transportation Research Board 2305*, 162-169.

Medina, J., & Motta, L. (2005). Resilient behavior of Brazilian tropical soils in pavement design. *ABPV Mecânica dos pavimentos. 2. ed., 1 Part 1*, 1-22.

Mehta, Y., Sauber, R., Owad, J., & Krause, J. (2008). Lessons learned during implementation of mechanistic-empirical pavement design guide. *Transportation Research Record: Journal of the Transportation Research Board*.

Moreno, M., Navarro, T., & Zeballos, G. (2017). Including Reliability in the AASHTO-93 Flexible Pavement Design Method Integrating Pavement Deterioration Models. *Revista de la Construcción, 16*(2). doi:http://dx.doi.org/10.7764/rdlc.16.2.284

Motta, L. (1991). *Metodo de Dimensionamento de Pavimentos Flexiveis; Criterio de Confiabilidade e Ensaios de Carga Repetidas.* Rio de Janeiro: Coordenacao dos Programas de Pos-Graduacao de Engenharia, Universidad Federal do Rio de Janeiro.

Murphy, V. (2002). *Geotechnical Engineering. Principles and Practices of Soil Mechanics and Foundation Engineering.* New York: Marcel Dekker, Inc.

Myers, L., Roque, R., & Birisson, B. (2001). Propagation Mechanism for Surface-Iniciated longitudinal Wheelpath Cracks. *Transportation Research Board: Transportation Research Record No. 1778, Design and Rehabilitation of Pavements, Transportation Research Board*, 113-122.

NCHRP. (1993). *Effects of Heavy Vehicle Characteristics on Pavement Response and Performance.* National Cooperative Highway Research Program Report 353.

NCHRP. (2000). *Assessing Pavement Layer Condition Using Deflection Data.* National Cooperative Highway Research Program.

NCHRP. (2004a). *Guide for Mechanistic-Empirical Design of New and Rehabilitated Pavement Structures.* Washington D.C.: National Cooperative Highway Research Program.

NCHRP. (2004b). *Mechanistic-empirical design of new and rehabilitated pavement structures.* Washington, D.C.: National Cooperative Highway Research Program, NCHRP Project 1-37A, National Research Council.

NCHRP. (2009). *Document 108: Guide for Pavement Friction.* National Cooperative Highway Research Program. Retrieved from http://onlinepubs.trb.org/onlinepubs/nchrp/nchrp_w108.pdf

Oliveira, A. (2013). *Avaliação do Risco Associado ao Dimensionamento de Pavimentos Flexíveis.* Minho, Portugal: Pós-graduação em Engenharia Civil, Universidade do Minho, Escola de Engenharia.

Peng, C., Jin, F., Zhou, C., & Fan, X. (2016). Tire-Pavement Contact Stress with 3D Finite Element Model: Part 1: Semi-Steel Radial Tires on Light Vehicles. *Journal of Testing and Evaluation*. doi:10.1520/JTE20150234

Phoon, K.-K. (2008). *Reliability Based Design in Geotechnical Engineering Computation and Applications.* New York, USA: Taylor and Francis e-library.

Pinto, S., & Preussler, E. (2002). *Pavimentação Rodoviária: conceitos fundamentais sobre pavimentos flexíveis* (2ª ed.). Rio de Janeiro, Brazil: Copiarte Copiadora e Artes Gráficas Ltda.

Priest, A., & Timm, D. (2006). *Methodology And Calibration of Fatigue Transfer Functions For Mechanistic-Empirical Flexible Pavement Design.* Alabama.: NCAT Report 06-03. National Center for Asphalt Technology, Auburn University.

Prozzi, J., & Hong, F. (2005). Hierarchical axle load data for mechanistic-empirical design. *Transportation Research Record: Journal of the Transportation Research Board*.

Prozzi, J., Gossain, V., & Manuel, L. (2005). Reliability of pavement structures using empirical-mechanistic models. *Transportation Research Board Annual Meeting*.

Qin, J. (2010). *Predicting Flexible Pavement Structural Response Using Falling Weight Deflectometer Deflections.* Ohio University, Civil Engineering (Engineering and Technology).

Read, J., & Whiteoak, D. (2003). *The Shell Bitumen Handbook* (Fifth Edition ed.). London, UK.: Thomas Telford Publishing.

Retherford, J., & McDonald, M. (2010). Reliability Methods Applicable to Mechanistic Empirical Pavement Design Method. *Transportation Research Record: Journal of the Transportation Research Board*.

Rogness, R. (1988). Reliability and Statistical Issues of the AASHTO Pavement Design Guide. *Transportation Research Record: Journal of the Transportation Researcn Board 1200*, 213-231.

Rosenblueth, E. (1975). Point estimates for probability moments. *Proceedings of the National Academy of Sciences of the United States of America - PNAS*, *72 no. 10.* doi:https://doi.org/10.1073/pnas.72.10.3812

Sánchez-Silva, M., Arroyo, O., Junca, M., Caro, S., & Caicedo, B. (2005). Reliability-based Design Optimization of Asphalt Pavements. *International Journal of Pavement Engineering*, 281-294.

Santos, C. (2011). *Dimensionamento e Analise do Ciclo de Vida de Pavimentos Rodoviários; Uma Abordagem Probabilística.* São Paulo, SP: Departamento de Engenharia de Transportes, Escola Politécnica da Universidade de São Paulo.

Santos, C., Suzuki, C., & Bernucci, L. (2016). A Probabilistic Approach for Asphaltic Pavements Design in Brazil. *Proceedings of the Eighth International Conference on Maintenance and Rehabilitation of Pavements.* Research Publishing, Singapore. doi:ISBN: 978-981-11-0449-7, doi:10.3850/978-981-11-0449-7-104-cd

Southgate, H. (1991). *Sensitivity Study of 1986 AASHTO Guide for Design of Pavement Structures.* Lexington, Kentucky: Research Report KTC-91-15. Kentucky Transportation Center Collegue of Engineering.

Suzuki, C., Kabbach Junior, F., & Azevedo, A. (2004). Introdução do conceito de confiabilidade nos métodos de dimensionamento de pavimentos flexíveis utilizados no Brasil. *RAPv Reuniao Anual de Pavimentacao.* Rio de Janeiro, RJ, Brazil.

Suzuki, C., Nagao, E., Osório, C., & Azevedo, A. (2001). Considerações sobre o conceito de confiabilidade na análise mecanística de estruturas de pavimentos flexíveis. *RAPv Reuniao Anual de Pavimentacao*, (pp. 695-705). Florianópolis, SC, Brazil.

Tarefder, R., Saha, N., & Stormont, J. (2010). Evaluation of Subgrade Strength and Pavement Design for Reliability. *Journal of Transportation Engineering. ASCE American Society of Civil Engineers, 136*(4). doi:https://doi.org/10.1061/(ASCE)TE.1943-5436.0000103

Thyagarajan, S., Muhunthan, B., Sivaneswaran, N., & Petros, K. (2011). Efficient Simulation Techniques for Reliability Analysis of Flexible Pavements Using the Mechanistic Empirical Pavement Design Guide. *Journal of Transportation Engineering. ASCE American Society of Civil Engineers, 137*(11). doi:https://doi.org/10.1061/(ASCE)TE.1943-5436.0000272

Turnbull, W., Foster, C., & Ahlvin, R. (1962). Design of flexible pavements considering mixed loads and traffic volume. *International Conference on Structural Design Asphalt Pavements* (pp. 821-825). Transportation Research Board.

Ullidta, P. (1987). *Pavement Analysis.* Amsterdam, The Netherlands: Elsevier.

USACE. (1996). *Development of a Reliability-Based Design Procedure for Rigid and Flexible Airfield Pavements.* Opelika, AL: US Army Corps of Engineers, Waterways Experiment Station.

USACE. (1997). *Engineering and design: Introduction to probability and reliability methods for use in geotechnical engineering.* Washington, D.C.: U.S. Army Corps of Engineers, Engineer Technical Letter 1110-2-547, Dept. of the Army.

Vale, A., Caio, M., Merighi, C., Negrao, D., Machado, P., & Chiariello, F. (2018). Overload impacts on pavement design and performance– Brazilian Traffic Load Law Change and it's Consequenses. *ISAP Conference. International Society for Asphalt Pavements.*

Wang, S. (2011). *Risk Analysis and Reliability Improvement of Mechanistic Empirical Pavement.* Fayetteville: University of Arkansas.

Weismann, S. (1999). Influence of tire pavement contact stress distribution on development of distress mechanisms in pavement. *Transportation Research Record. Journal of the Transportation Research Board. No.1655*, 161-167.

Xiao, X. (2012). *Risk Analysis and Reliability Improvement of Mechanistic-Empirical Pavement Design.* University of Arkansas.

Yoder, E., & Witczak, M. (1991). *Principles of Pavement Design* (2nd Edition ed.). New York: John Wiley & Sons Inc. doi:ISBN: 978-0-471-97780-3

Zaghloul, S., & White, T. (1993). The Use of a Three Dimensional Dynamic Finite Element Program for Analysis of Flexible Pavement. *Transportation Research Record, No. 1388, Journal of the Transportation Research Board*, 60-69.

APPENDIX A – SURFACE DISPLACEMENTS

Pavement surface displacements (δ_1) by axle overload (0%, 7.5%, 10%, 20%, and 30%) and tire pressure (550 KPa, 690 KPa, and 830 KPa).

STRUCTURE A

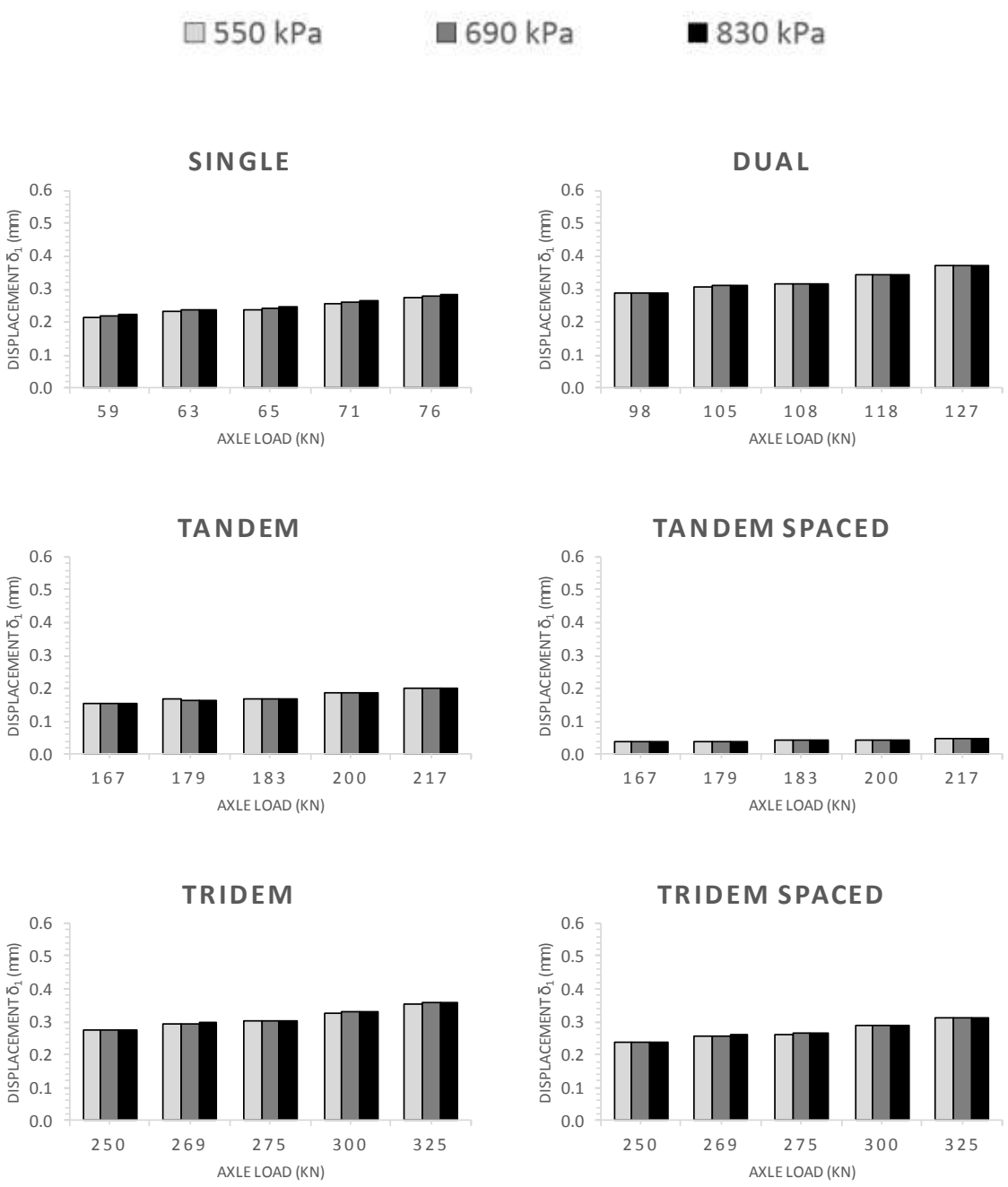

STRUCTURE B

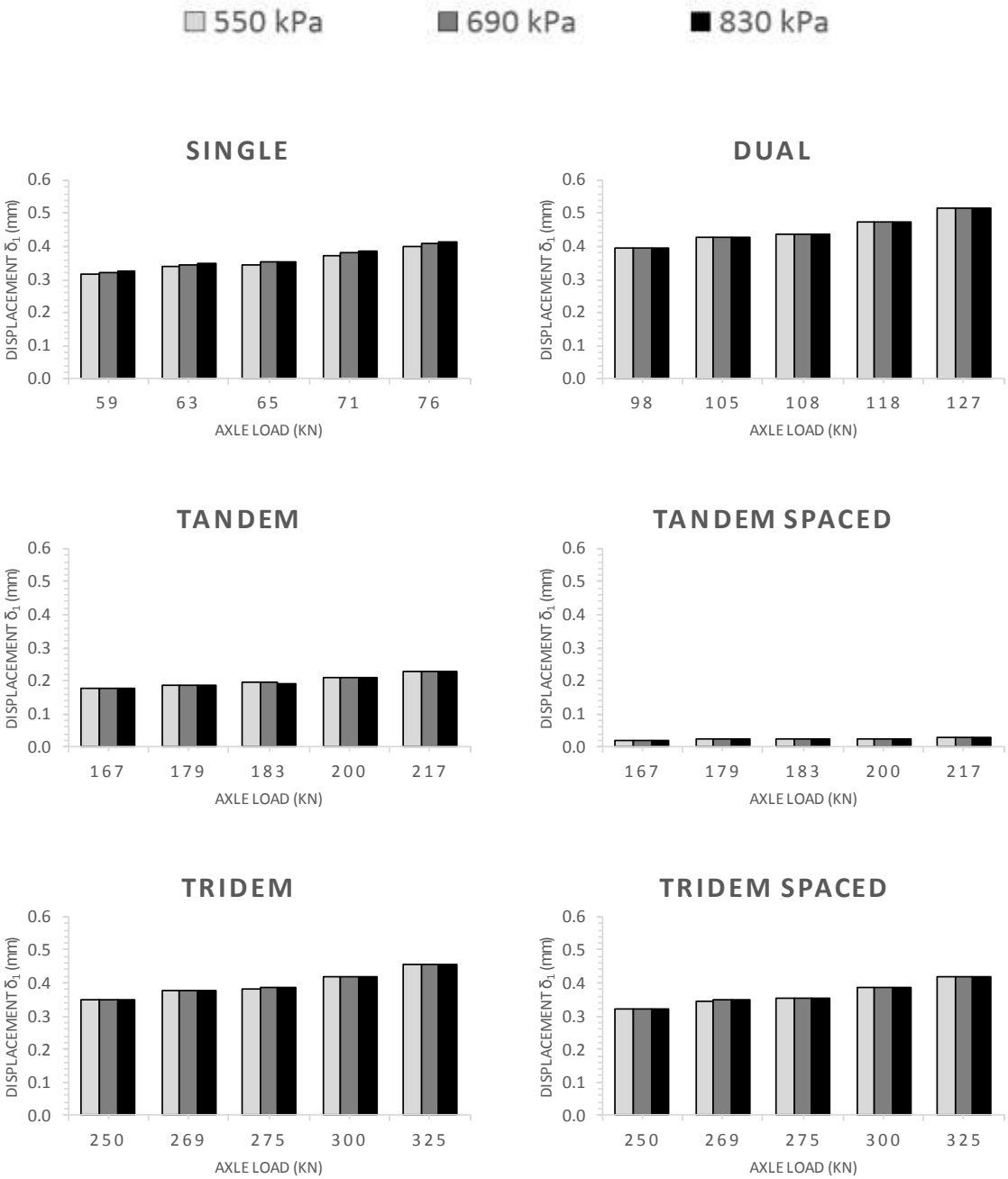
550 kPa
690 kPa
830 kPa
SINGLE
DUAL
TANDEM
TANDEM SPACED
TRIDEM
TRIDEM SPACED
DISPLACEMENT δ1 (mm)
0.0
0.1
0.2
0.3
0.4
0.5
0.6
59 63 65 71 76
98 105 108 118 127
167 179 183 200 217
250 269 275 300 325
AXLE LOAD (KN)

STRUCTURE C

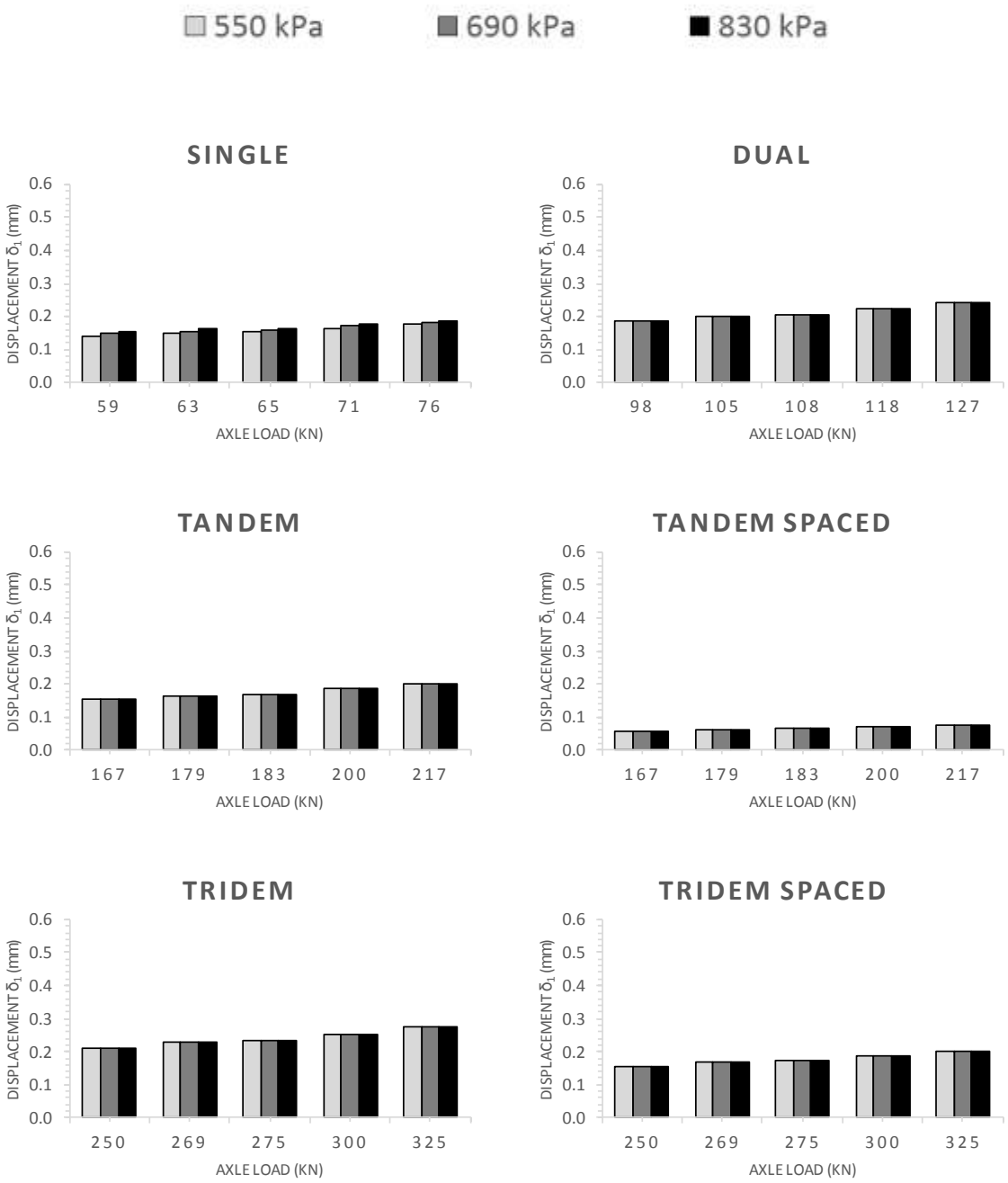
550 kPa
690 kPa
830 kPa
SINGLE
DISPLACEMENT δ1 (mm)
0.0
0.1
0.2
0.3
0.4
0.5
0.6
59
63
65
71
76
AXLE LOAD (KN)
DUAL
98
105
108
118
127
TANDEM
167
179
183
200
217
TANDEM SPACED
TRIDEM
250
269
275
300
325
TRIDEM SPACED

STRUCTURE D

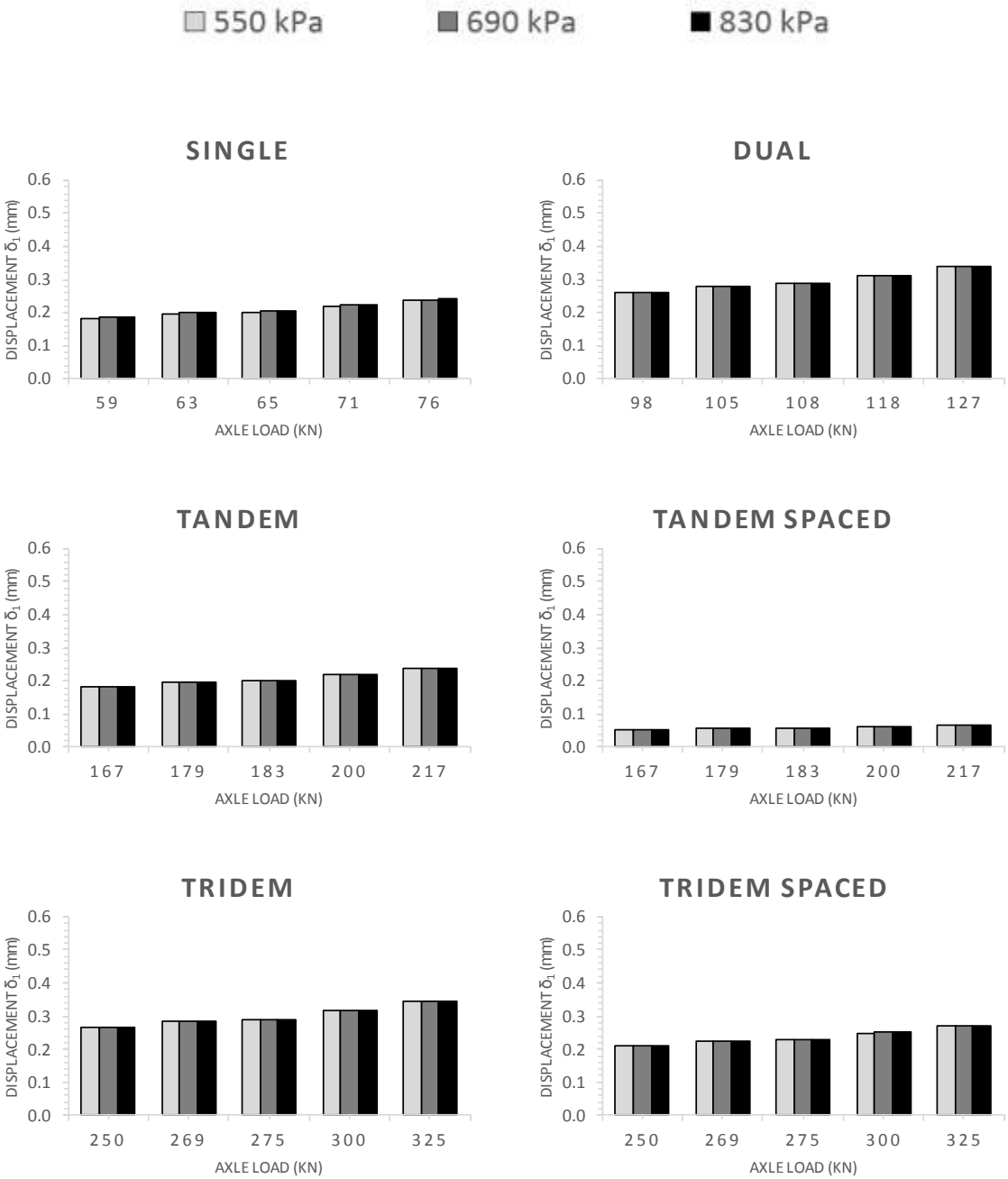
550 kPa
690 kPa
830 kPa
SINGLE
DUAL
TANDEM
TANDEM SPACED
TRIDEM
TRIDEM SPACED
DISPLACEMENT δ1 (mm)
0.0
0.1
0.2
0.3
0.4
0.5
0.6
59 63 65 71 76
98 105 108 118 127
167 179 183 200 217
250 269 275 300 325
AXLE LOAD (KN)

Surface displacements for single (left) and dual (right) axles:

Tire Pressure (Kpa)	Overload (&)	SINGLE			
		A	B	C	D
550	0.0	0.2170	0.3160	0.1410	0.1840
	7.5	0.2320	0.3380	0.1500	0.1980
	10.0	0.2370	0.3460	0.1530	0.2030
	20.0	0.2570	0.3740	0.1650	0.2210
	30.0	0.2760	0.4020	0.1780	0.2400
690	0.0	0.2210	0.3210	0.1480	0.1860
	7.5	0.2360	0.3430	0.1560	0.1990
	10.0	0.2420	0.3520	0.1590	0.2040
	20.0	0.2620	0.3810	0.1710	0.2220
	30.0	0.2810	0.4100	0.1830	0.2390
830	0.0	0.2250	0.3240	0.1550	0.1890
	7.5	0.2400	0.3470	0.1630	0.2020
	10.0	0.2460	0.3550	0.1660	0.2060
	20.0	0.2660	0.3850	0.1780	0.2230
	30.0	0.2860	0.4150	0.1890	0.2410

Tire Pressure (Kpa)	Overload (&)	DUAL			
		A	B	C	D
550	0.0	0.2870	0.3960	0.1870	0.2610
	7.5	0.3090	0.4260	0.2020	0.2810
	10.0	0.3150	0.4360	0.2070	0.2880
	20.0	0.3430	0.4740	0.2250	0.3130
	30.0	0.3720	0.5140	0.2440	0.3390
690	0.0	0.2870	0.3970	0.1880	0.2620
	7.5	0.3100	0.4270	0.2020	0.2820
	10.0	0.3160	0.4370	0.2070	0.2880
	20.0	0.3440	0.4750	0.2250	0.3140
	30.0	0.3730	0.5150	0.2440	0.3400
830	0.0	0.2880	0.3970	0.1880	0.2620
	7.5	0.3100	0.4280	0.2020	0.2820
	10.0	0.3170	0.4380	0.2070	0.2890
	20.0	0.3450	0.4760	0.2250	0.3140
	30.0	0.3740	0.5160	0.2440	0.3410

Surface displacements for tandem (left) and tandem spaced (right) axles:

Tire Pressure (Kpa)	Overload (&)	TANDEM			
		A	B	C	D
550	0.0	0.1550	0.1760	0.1540	0.1820
	7.5	0.1670	0.1890	0.1660	0.1960
	10.0	0.1700	0.1940	0.1700	0.2000
	20.0	0.1860	0.2120	0.1860	0.2180
	30.0	0.2020	0.2290	0.2010	0.2370
690	0.0	0.1550	0.1760	0.1540	0.1820
	7.5	0.1660	0.1890	0.1660	0.1960
	10.0	0.1700	0.1940	0.1700	0.2000
	20.0	0.1860	0.2110	0.1860	0.2180
	30.0	0.2010	0.2290	0.2010	0.2370
830	0.0	0.1550	0.1760	0.1540	0.1820
	7.5	0.1660	0.1890	0.1660	0.1960
	10.0	0.1700	0.1930	0.1700	0.2000
	20.0	0.1860	0.2110	0.1860	0.2180
	30.0	0.2010	0.2290	0.2010	0.2370

Tire Pressure (Kpa)	Overload (&)	TANDEM SPACED			
		A	B	C	D
550	0.0	0.0370	0.0210	0.0590	0.0520
	7.5	0.0400	0.0230	0.0640	0.0560
	10.0	0.0410	0.0240	0.0650	0.0570
	20.0	0.0440	0.0260	0.0710	0.0620
	30.0	0.0480	0.0280	0.0770	0.0670
690	0.0	0.0370	0.0210	0.0590	0.0510
	7.5	0.0400	0.0230	0.0640	0.0550
	10.0	0.0410	0.0230	0.0650	0.0570
	20.0	0.0440	0.0260	0.0710	0.0620
	30.0	0.0480	0.0280	0.0770	0.0670
830	0.0	0.0370	0.0210	0.0590	0.0510
	7.5	0.0400	0.0230	0.0640	0.0550
	10.0	0.0410	0.0230	0.0650	0.0570
	20.0	0.0440	0.0260	0.0710	0.0620
	30.0	0.0480	0.0280	0.0770	0.0670

Surface displacements for tridem (left) and tridem spaced (right) axles:

Tire Pressure (Kpa)	Overload (&)	TRIDEM			
		A	B	C	D
550	0.0	0.2740	0.3490	0.2110	0.2640
	7.5	0.2950	0.3770	0.2270	0.2840
	10.0	0.3010	0.3840	0.2320	0.2900
	20.0	0.3280	0.4190	0.2540	0.3170
	30.0	0.3560	0.4540	0.2750	0.3430
690	0.0	0.2740	0.3500	0.2110	0.2640
	7.5	0.2950	0.3770	0.2270	0.2840
	10.0	0.3020	0.3850	0.2320	0.2910
	20.0	0.3290	0.4200	0.2540	0.3170
	30.0	0.3570	0.4550	0.2750	0.3440
830	0.0	0.2750	0.3500	0.2110	0.2640
	7.5	0.2960	0.3770	0.2270	0.2850
	10.0	0.3020	0.3850	0.2320	0.2910
	20.0	0.3300	0.4210	0.2540	0.3180
	30.0	0.3570	0.4560	0.2750	0.3440

Tire Pressure (Kpa)	Overload (&)	TRIDEM SPACED			
		A	B	C	D
550	0.0	0.2390	0.3220	0.1560	0.2080
	7.5	0.2570	0.3460	0.1680	0.2240
	10.0	0.2630	0.3540	0.1720	0.2290
	20.0	0.2870	0.3860	0.1870	0.2490
	30.0	0.3110	0.4180	0.2030	0.2700
690	0.0	0.2400	0.3220	0.1560	0.2080
	7.5	0.2580	0.3470	0.1680	0.2240
	10.0	0.2640	0.3550	0.1720	0.2290
	20.0	0.2880	0.3870	0.1880	0.2500
	30.0	0.3120	0.4190	0.2030	0.2710
830	0.0	0.2400	0.3230	0.1560	0.2080
	7.5	0.2590	0.3470	0.1680	0.2240
	10.0	0.2640	0.3550	0.1720	0.2290
	20.0	0.2880	0.3880	0.1880	0.2500
	30.0	0.3120	0.4200	0.2030	0.2710

APPENDIX B – HORIZONTAL TENSILE STRAIN AT THE BOTTOM OF THE ASPHALT LAYER

Horizontal tensile strainat the bottom of the asphalt layer (εht_1) by axle overload (0%, 7.5%, 10%, 20%, and 30%) and tire pressure (550 KPa, 690 KPa, and 830 KPa).

STRUCTURE A

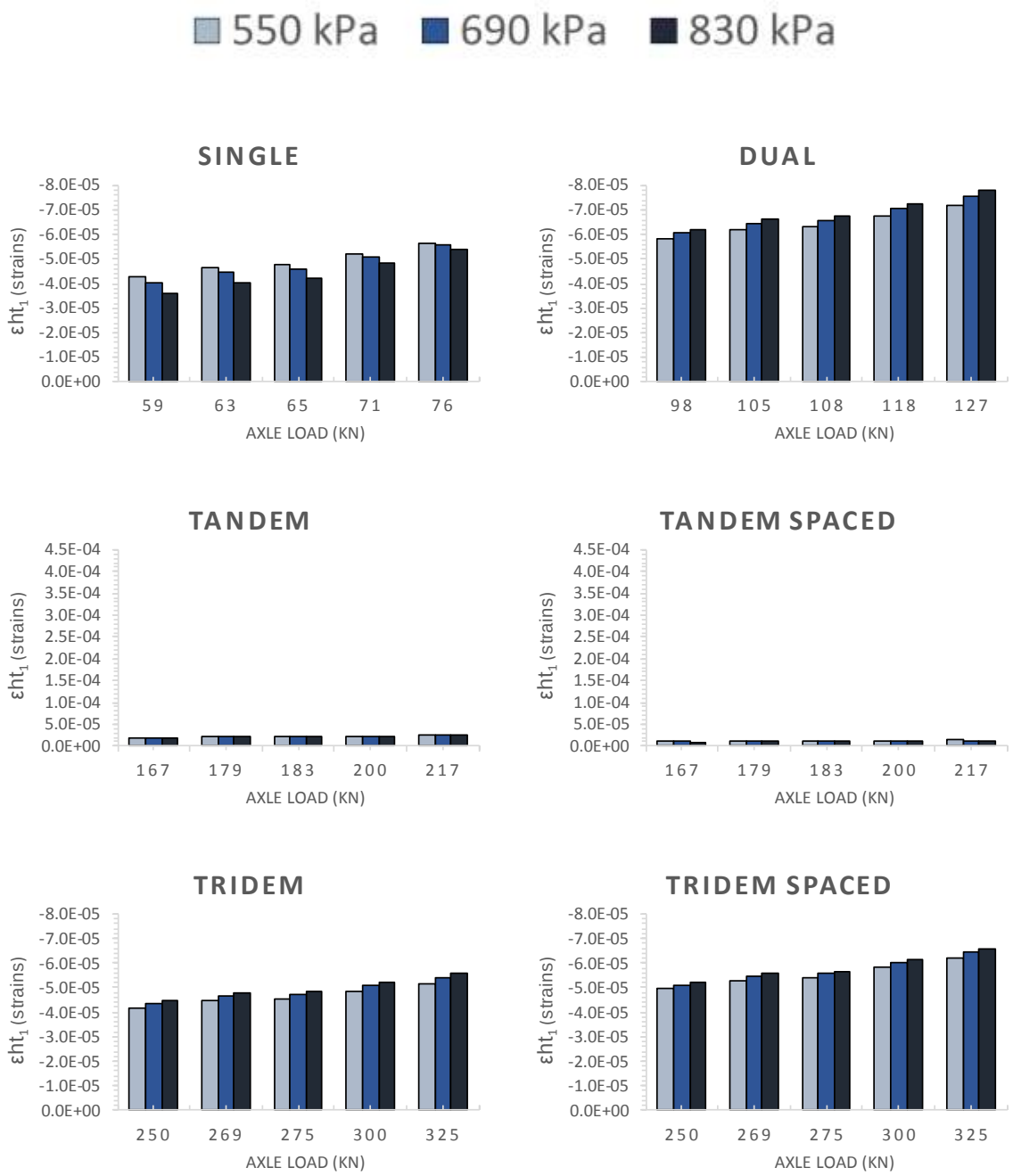

STRUCTURE B

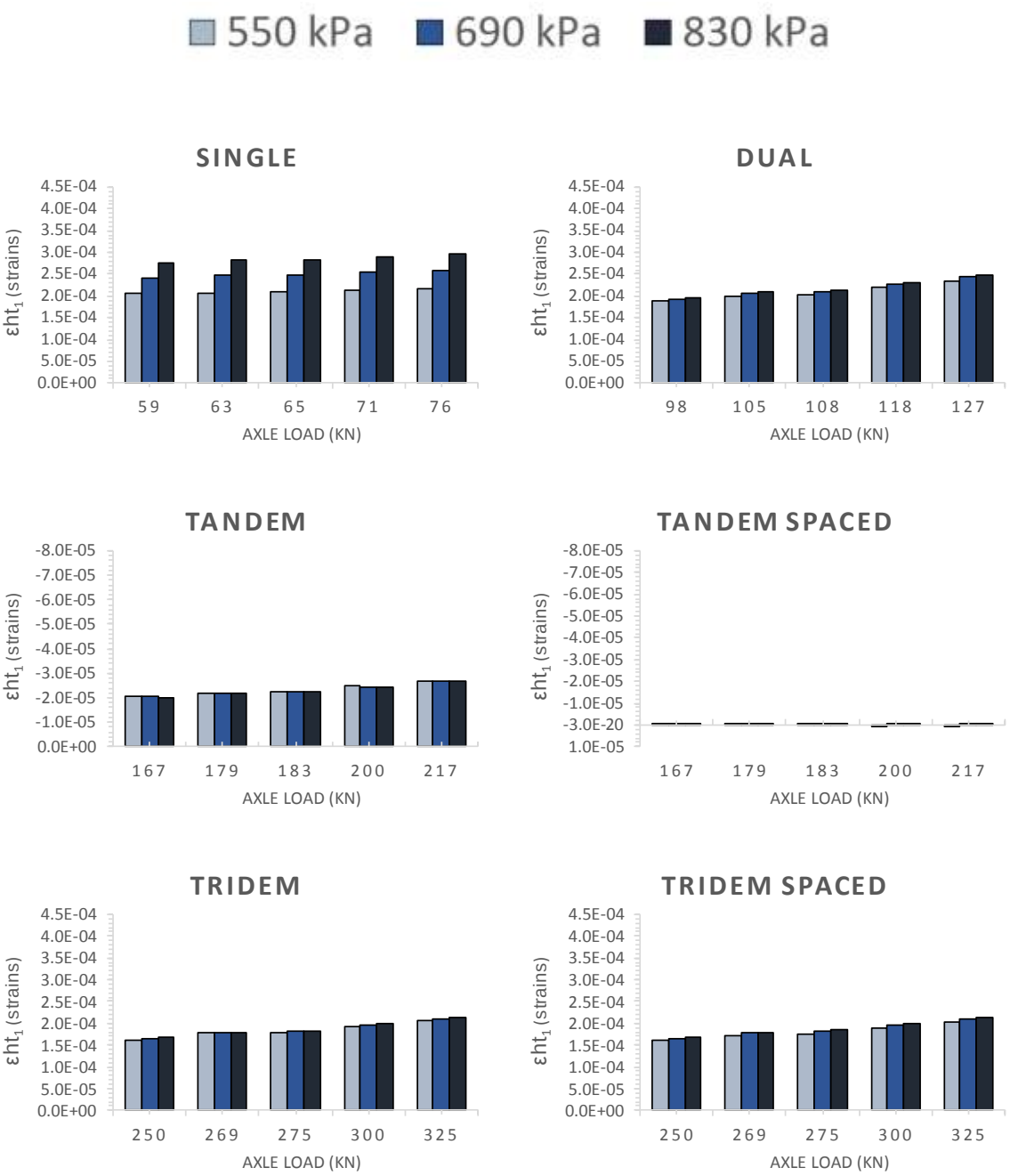
550 kPa
690 kPa
830 kPa
SINGLE
εht1 (strains)
4.5E-04
4.0E-04
3.5E-04
3.0E-04
2.5E-04
2.0E-04
1.5E-04
1.0E-04
5.0E-05
0.0E+00
59
63
65
71
76
AXLE LOAD (KN)
DUAL
εht1 (strains)
4.5E-04
4.0E-04
3.5E-04
3.0E-04
2.5E-04
2.0E-04
1.5E-04
1.0E-04
5.0E-05
0.0E+00
98
105
108
118
127
AXLE LOAD (KN)
TANDEM
εht1 (strains)
-8.0E-05
-7.0E-05
-6.0E-05
-5.0E-05
-4.0E-05
-3.0E-05
-2.0E-05
-1.0E-05
0.0E+00
167
179
183
200
217
AXLE LOAD (KN)
TANDEM SPACED
εht1 (strains)
-8.0E-05
-7.0E-05
-6.0E-05
-5.0E-05
-4.0E-05
-3.0E-05
-2.0E-05
-1.0E-05
-3.0E-20
1.0E-05
167
179
183
200
217
AXLE LOAD (KN)
TRIDEM
εht1 (strains)
4.5E-04
4.0E-04
3.5E-04
3.0E-04
2.5E-04
2.0E-04
1.5E-04
1.0E-04
5.0E-05
0.0E+00
250
269
275
300
325
AXLE LOAD (KN)
TRIDEM SPACED
εht1 (strains)
4.5E-04
4.0E-04
3.5E-04
3.0E-04
2.5E-04
2.0E-04
1.5E-04
1.0E-04
5.0E-05
0.0E+00
250
269
275
300
325
AXLE LOAD (KN)

STRUCTURE C

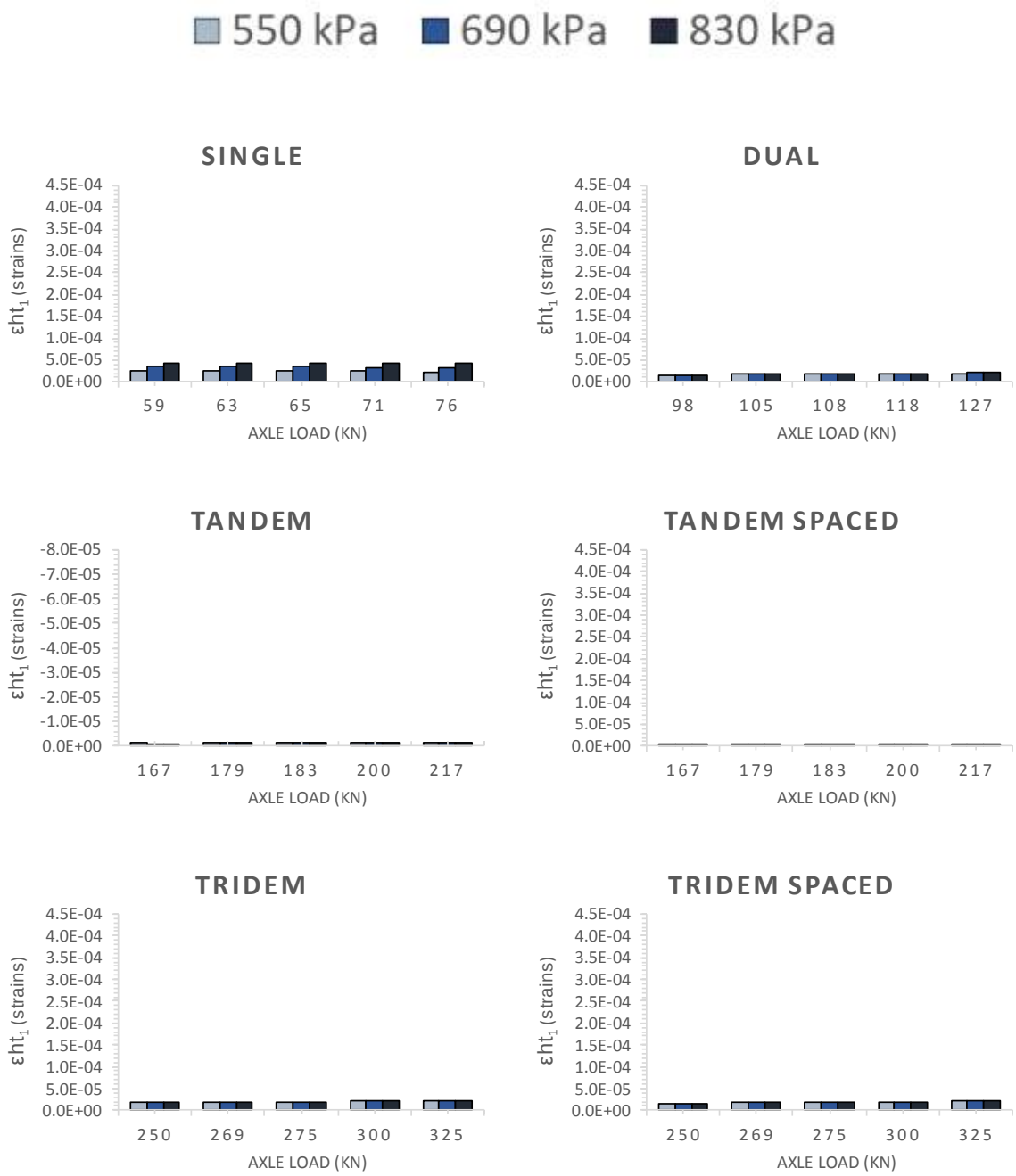
550 kPa
690 kPa
830 kPa
SINGLE
DUAL
TANDEM
TANDEM SPACED
TRIDEM
TRIDEM SPACED
εht1 (strains)
AXLE LOAD (KN)
59
63
65
71
76
98
105
108
118
127
167
179
183
200
217
250
269
275
300
325

STRUCTURE D

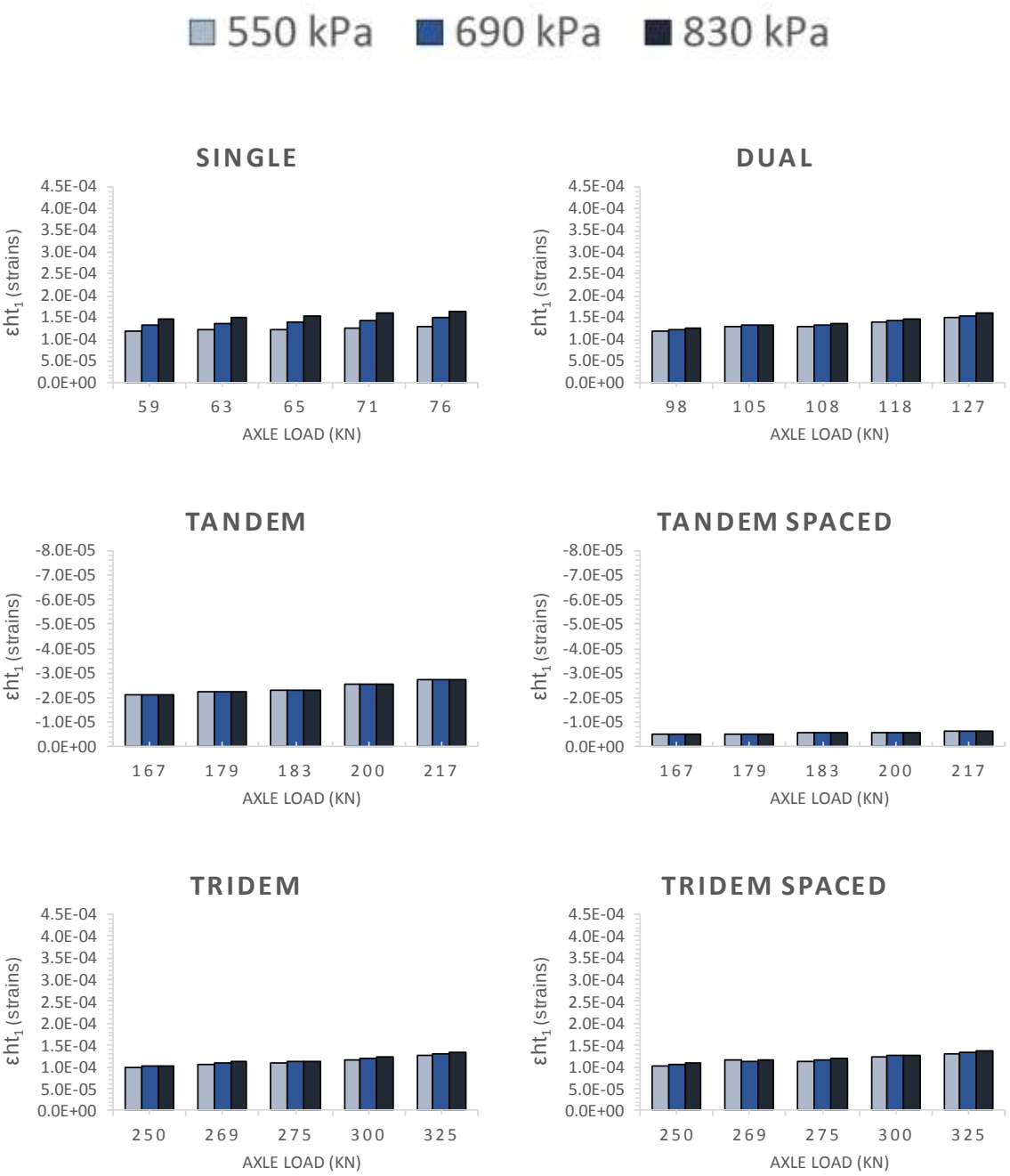
550 kPa
690 kPa
830 kPa
SINGLE
DUAL
TANDEM
TANDEM SPACED
TRIDEM
TRIDEM SPACED
εht1 (strains)
AXLE LOAD (KN)
59 63 65 71 76
98 105 108 118 127
167 179 183 200 217
250 269 275 300 325

Horizontal Strain at the bottom of the asphalt layer for single (left) and dual (right) axles (red and bold values are negative – tensile strain):

Tire Pressure (Kpa)	Overload (&)	SINGLE			
		A	B	C	D
550	0.0	**4.29E-05**	2.05E-04	2.64E-05	1.18E-04
	7.5	**4.65E-05**	2.08E-04	2.57E-05	1.21E-04
	10.0	**4.78E-05**	2.09E-04	2.54E-05	1.23E-04
	20.0	**5.22E-05**	2.13E-04	2.44E-05	1.27E-04
	30.0	**5.64E-05**	2.16E-04	2.34E-05	1.31E-04
690	0.0	**4.02E-05**	2.42E-04	3.50E-05	1.33E-04
	7.5	**4.44E-05**	2.47E-04	3.45E-05	1.38E-04
	10.0	**4.59E-05**	2.49E-04	3.43E-05	1.39E-04
	20.0	**5.11E-05**	2.54E-04	3.36E-05	1.45E-04
	30.0	**5.60E-05**	2.59E-04	3.27E-05	1.50E-04
830	0.0	**3.59E-05**	2.75E-04	4.27E-05	1.46E-04
	7.5	**4.06E-05**	2.82E-04	4.26E-05	1.51E-04
	10.0	**4.23E-05**	2.84E-04	4.25E-05	1.53E-04
	20.0	**4.82E-05**	2.91E-04	4.21E-05	1.60E-04
	30.0	**5.38E-05**	2.98E-04	4.15E-05	1.66E-04

Tire Pressure (Kpa)	Overload (&)	DUAL			
		A	B	C	D
550	0.0	**5.85E-05**	1.88E-04	1.62E-05	1.20E-04
	7.5	**6.22E-05**	2.00E-04	1.72E-05	1.28E-04
	10.0	**6.33E-05**	2.04E-04	1.76E-05	1.31E-04
	20.0	**6.77E-05**	2.19E-04	1.88E-05	1.40E-04
	30.0	**7.22E-05**	2.34E-04	2.01E-05	1.50E-04
690	0.0	**6.06E-05**	1.92E-04	1.65E-05	1.24E-04
	7.5	**6.46E-05**	2.06E-04	1.77E-05	1.32E-04
	10.0	**6.58E-05**	2.10E-04	1.81E-05	1.35E-04
	20.0	**7.07E-05**	2.26E-04	1.95E-05	1.45E-04
	30.0	**7.56E-05**	2.43E-04	2.09E-05	1.56E-04
830	0.0	**6.20E-05**	1.95E-04	1.67E-05	1.26E-04
	7.5	**6.62E-05**	2.09E-04	1.79E-05	1.35E-04
	10.0	**6.75E-05**	2.14E-04	1.83E-05	1.37E-04
	20.0	**7.27E-05**	2.31E-04	1.98E-05	1.48E-04
	30.0	**7.80E-05**	2.49E-04	2.14E-05	1.59E-04

Tandem (left) and tandem-spaced (right) axles:

Tire Pressure (Kpa)	Overload (&)	TANDEM			
		A	B	C	D
550	0.0	1.91E-05	**2.04E-05**	**1.15E-06**	**2.11E-05**
	7.5	2.06E-05	**2.21E-05**	**1.25E-06**	**2.27E-05**
	10.0	2.10E-05	**2.26E-05**	**1.28E-06**	**2.32E-05**
	20.0	2.30E-05	**2.47E-05**	**1.41E-06**	**2.53E-05**
	30.0	2.50E-05	**2.68E-05**	**1.54E-06**	**2.75E-05**
690	0.0	1.92E-05	**2.04E-05**	**1.13E-06**	**2.11E-05**
	7.5	2.06E-05	**2.20E-05**	**1.22E-06**	**2.27E-05**
	10.0	2.11E-05	**2.25E-05**	**1.25E-06**	**2.32E-05**
	20.0	2.30E-05	**2.46E-05**	**1.38E-06**	**2.53E-05**
	30.0	2.49E-05	**2.67E-05**	**1.50E-06**	**2.75E-05**
830	0.0	1.95E-05	**2.03E-05**	**1.11E-06**	**2.11E-05**
	7.5	2.09E-05	**2.19E-05**	**1.21E-06**	**2.27E-05**
	10.0	2.13E-05	**2.24E-05**	**1.23E-06**	**2.32E-05**
	20.0	2.31E-05	**2.45E-05**	**1.36E-06**	**2.53E-05**
	30.0	2.50E-05	**2.66E-05**	**1.48E-06**	**2.75E-05**

Tire Pressure (Kpa)	Overload (&)	TANDEM SPACED			
		A	B	C	D
550	0.0	1.01E-05	**1.26E-07**	3.36E-06	**4.97E-06**
	7.5	1.10E-05	**7.81E-08**	3.63E-06	**5.35E-06**
	10.0	1.13E-05	**6.24E-08**	3.71E-06	**5.46E-06**
	20.0	1.24E-05	5.40E-09	4.06E-06	**5.96E-06**
	30.0	1.36E-05	7.05E-08	4.41E-06	**6.46E-06**
690	0.0	9.87E-06	**2.61E-07**	3.34E-06	**4.98E-06**
	7.5	1.07E-05	**2.41E-07**	3.60E-06	**5.36E-06**
	10.0	1.10E-05	**2.33E-07**	3.69E-06	**5.47E-06**
	20.0	1.21E-05	**1.87E-07**	4.03E-06	**5.97E-06**
	30.0	1.32E-05	**1.29E-07**	4.38E-06	**6.47E-06**
830	0.0	9.78E-06	**3.10E-07**	3.34E-06	**4.98E-06**
	7.5	1.06E-05	**3.21E-07**	3.59E-06	**5.36E-06**
	10.0	1.08E-05	**3.22E-07**	3.68E-06	**5.48E-06**
	20.0	1.19E-05	**3.14E-07**	4.02E-06	**5.98E-06**
	30.0	1.30E-05	**2.88E-07**	4.36E-06	**6.48E-06**

Tridem (left) and tridem spaced (right) axles:

Tire Pressure (Kpa)	Overload (&)	TRIDEM			
		A	B	C	D
550	0.0	**4.19E-05**	1.63E-04	1.74E-05	1.00E-04
	7.5	**4.44E-05**	1.80E-04	1.87E-05	1.07E-04
	10.0	**4.52E-05**	1.77E-04	1.90E-05	1.09E-04
	20.0	**4.83E-05**	1.91E-04	2.06E-05	1.17E-04
	30.0	**5.12E-05**	2.05E-04	2.22E-05	1.26E-04
690	0.0	**4.36E-05**	1.66E-04	1.76E-05	1.02E-04
	7.5	**4.64E-05**	1.78E-04	1.89E-05	1.09E-04
	10.0	**4.73E-05**	1.81E-04	1.93E-05	1.12E-04
	20.0	**5.08E-05**	1.96E-04	2.10E-05	1.21E-04
	30.0	**5.42E-05**	2.11E-04	2.26E-05	1.30E-04
830	0.0	**4.46E-05**	1.68E-04	1.76E-05	1.04E-04
	7.5	**4.77E-05**	1.80E-04	1.90E-05	1.11E-04
	10.0	**4.86E-05**	1.84E-04	1.94E-05	1.13E-04
	20.0	**5.24E-05**	1.99E-04	2.11E-05	1.23E-04
	30.0	**5.61E-05**	2.15E-04	2.28E-05	1.32E-04

Tire Pressure (Kpa)	Overload (&)	TRIDEM SPACED			
		A	B	C	D
550	0.0	**4.97E-05**	1.62E-04	1.61E-05	1.04E-04
	7.5	**5.29E-05**	1.73E-04	1.72E-05	1.15E-04
	10.0	**5.39E-05**	1.76E-04	1.76E-05	1.13E-04
	20.0	**5.80E-05**	1.90E-04	1.90E-05	1.22E-04
	30.0	**6.20E-05**	2.04E-04	2.03E-05	1.30E-04
690	0.0	**5.10E-05**	1.66E-04	1.64E-05	1.06E-04
	7.5	**5.45E-05**	1.77E-04	1.76E-05	1.14E-04
	10.0	**5.56E-05**	1.81E-04	1.80E-05	1.16E-04
	20.0	**6.00E-05**	1.96E-04	1.95E-05	1.25E-04
	30.0	**6.44E-05**	2.10E-04	2.09E-05	1.35E-04
830	0.0	**5.19E-05**	1.68E-04	1.66E-05	1.08E-04
	7.5	**5.56E-05**	1.80E-04	1.78E-05	1.15E-04
	10.0	**5.67E-05**	1.84E-04	1.82E-05	1.18E-04
	20.0	**6.14E-05**	1.99E-04	1.97E-05	1.28E-04
	30.0	**6.59E-05**	2.14E-04	2.13E-05	1.37E-04

APPENDIX C – VERTICAL TENSILE STRAIN AT THE BOTTOM OF THE ASPHALT LAYER

Vertical compressive strain at the bottom of the asphalt layer (εvc_1) by axle overload (0%, 7.5%, 10%, 20%, and 30%) and tire pressure (550 KPa, 690 KPa, and 830 KPa).

STRUCTURE A

STRUCTURE B

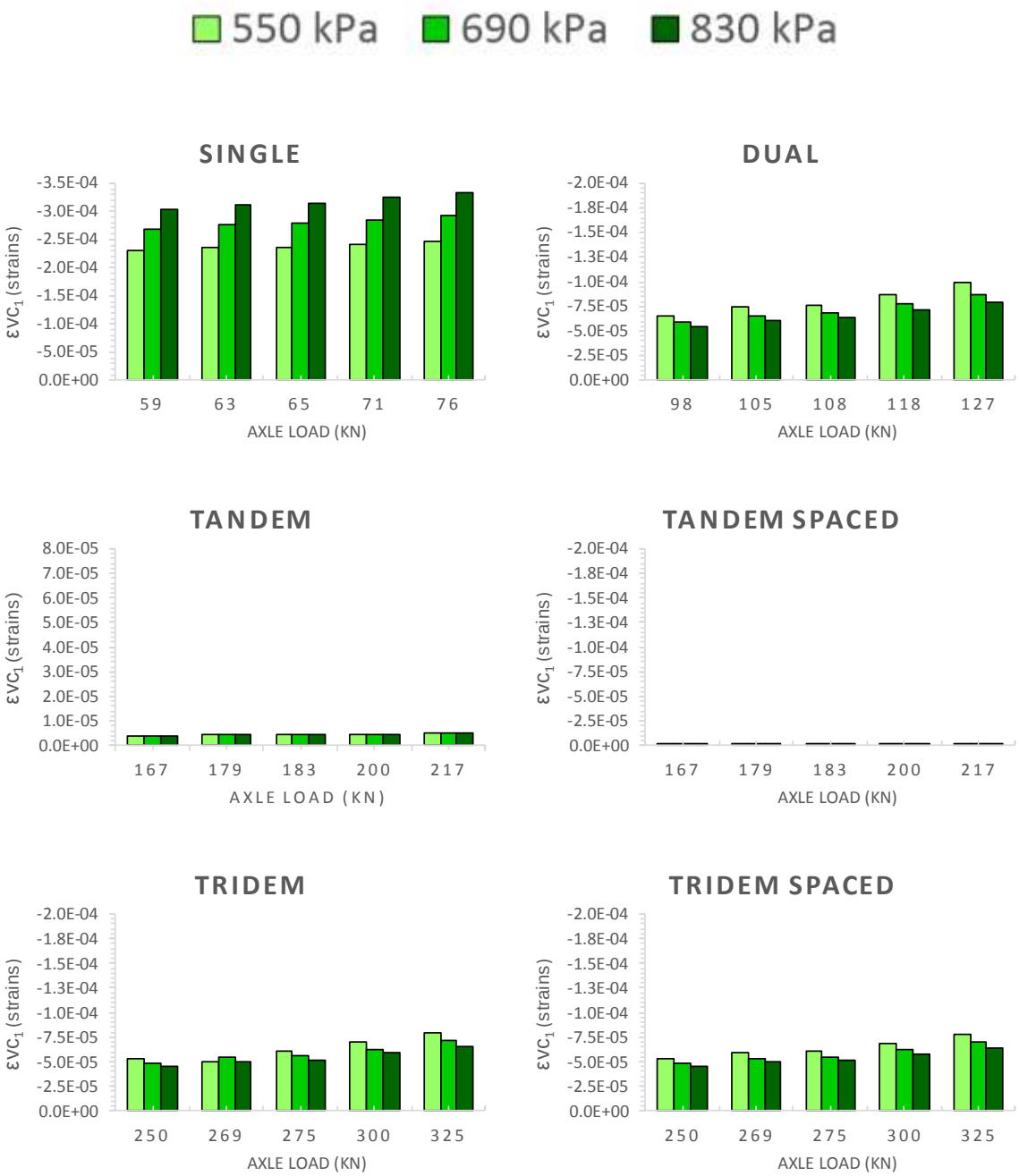
550 kPa
690 kPa
830 kPa
SINGLE
εVC1 (strains)
-3.5E-04
-3.0E-04
-2.5E-04
-2.0E-04
-1.5E-04
-1.0E-04
-5.0E-05
0.0E+00
59
63
65
71
76
AXLE LOAD (KN)
DUAL
εVC1 (strains)
-2.0E-04
-1.8E-04
-1.5E-04
-1.3E-04
-1.0E-04
-7.5E-05
-5.0E-05
-2.5E-05
0.0E+00
98
105
108
118
127
AXLE LOAD (KN)
TANDEM
εVC1 (strains)
8.0E-05
7.0E-05
6.0E-05
5.0E-05
4.0E-05
3.0E-05
2.0E-05
1.0E-05
0.0E+00
167
179
183
200
217
AXLE LOAD (KN)
TANDEM SPACED
εVC1 (strains)
-2.0E-04
-1.8E-04
-1.5E-04
-1.3E-04
-1.0E-04
-7.5E-05
-5.0E-05
-2.5E-05
0.0E+00
167
179
183
200
217
AXLE LOAD (KN)
TRIDEM
εVC1 (strains)
-2.0E-04
-1.8E-04
-1.5E-04
-1.3E-04
-1.0E-04
-7.5E-05
-5.0E-05
-2.5E-05
0.0E+00
250
269
275
300
325
AXLE LOAD (KN)
TRIDEM SPACED
εVC1 (strains)
-2.0E-04
-1.8E-04
-1.5E-04
-1.3E-04
-1.0E-04
-7.5E-05
-5.0E-05
-2.5E-05
0.0E+00
250
269
275
300
325
AXLE LOAD (KN)

STRUCTURE C

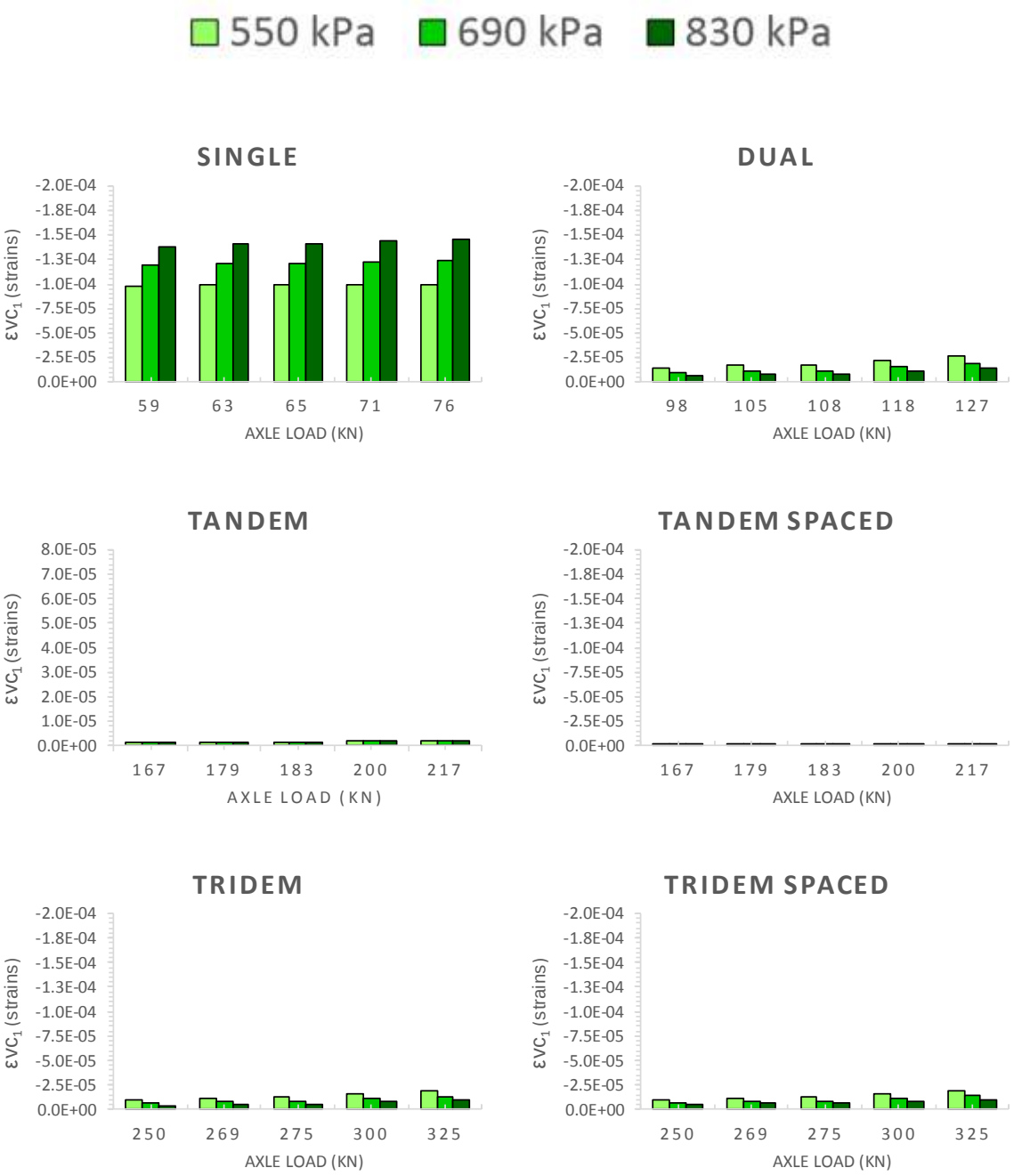
550 kPa
690 kPa
830 kPa
SINGLE
DUAL
TANDEM
TANDEM SPACED
TRIDEM
TRIDEM SPACED
εVC1 (strains)
AXLE LOAD (KN)
59
63
65
71
76
98
105
108
118
127
167
179
183
200
217
250
269
275
300
325

STRUCTURE D

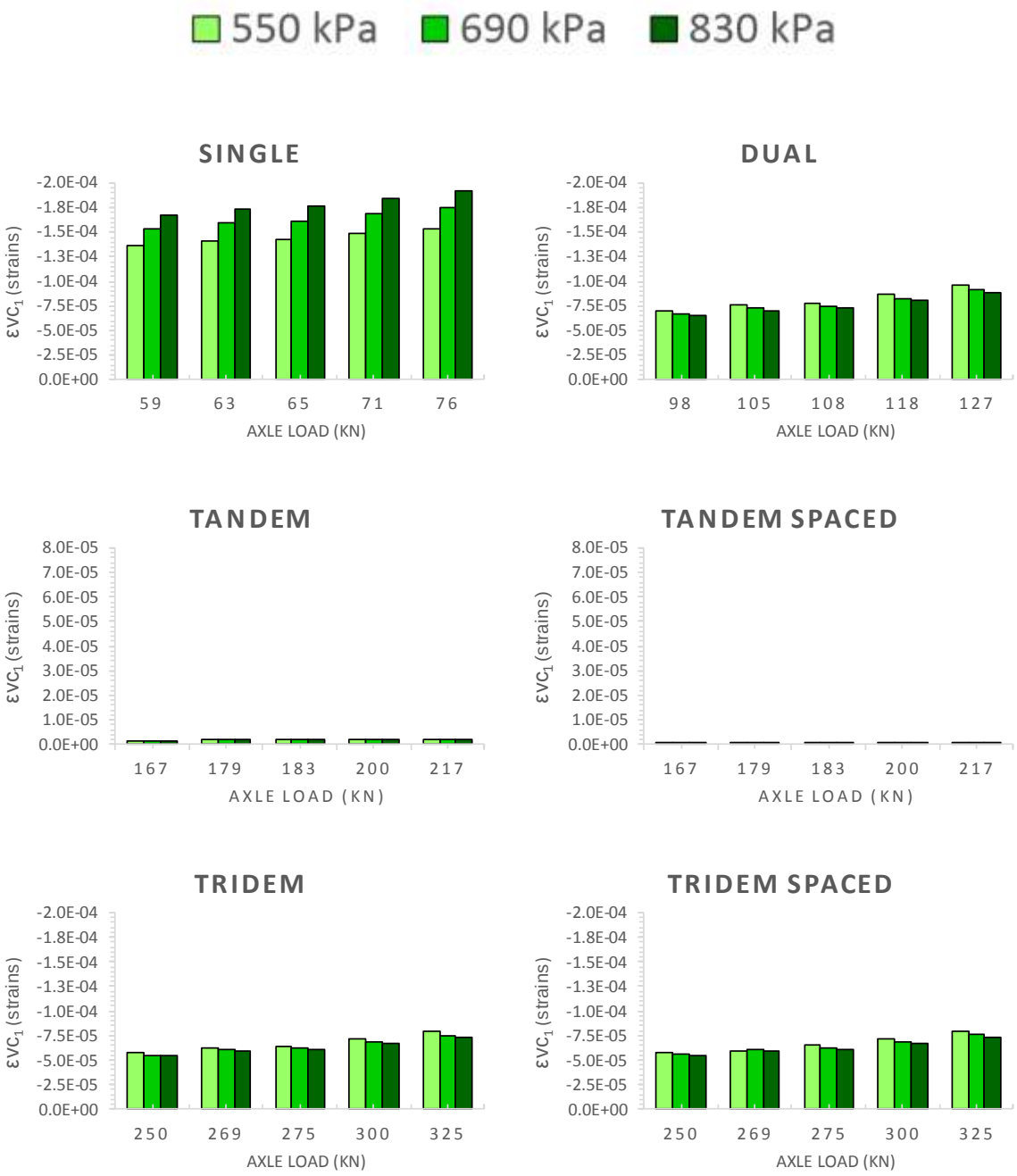
550 kPa
690 kPa
830 kPa
SINGLE
DUAL
TANDEM
TANDEM SPACED
TRIDEM
TRIDEM SPACED
εVC1 (strains)
AXLE LOAD (KN)
59 63 65 71 76
98 105 108 118 127
167 179 183 200 217
250 269 275 300 325

Vertical strain at the bottom of the asphalt layer for single (left) and dual (right) axles:

Tire Pressure (Kpa)	Overload (&)	SINGLE			
		A	B	C	D
550	0.0	-3.27E-05	-2.31E-04	-9.84E-05	-1.37E-04
	7.5	-2.88E-05	-2.35E-04	-9.90E-05	-1.42E-04
	10.0	-2.75E-05	-2.37E-04	-9.92E-05	-1.43E-04
	20.0	-2.28E-05	-2.42E-04	-9.96E-05	-1.49E-04
	30.0	-1.85E-05	-2.47E-04	-9.98E-05	-1.54E-04
690	0.0	-5.54E-05	-2.70E-04	-1.20E-04	-1.54E-04
	7.5	-5.10E-05	-2.76E-04	-1.21E-04	-1.60E-04
	10.0	-4.94E-05	-2.78E-04	-1.22E-04	-1.62E-04
	20.0	-4.39E-05	-2.86E-04	-1.23E-04	-1.68E-04
	30.0	-3.87E-05	-2.92E-04	-1.24E-04	-1.75E-04
830	0.0	-7.98E-05	-3.04E-04	-1.39E-04	-1.68E-04
	7.5	-7.48E-05	-3.12E-04	-1.41E-04	-1.74E-04
	10.0	-7.30E-05	-3.15E-04	-1.42E-04	-1.77E-04
	20.0	-6.68E-05	-3.24E-04	-1.44E-04	-1.85E-04
	30.0	-6.09E-05	-3.33E-04	-1.46E-04	-1.92E-04

Tire Pressure (Kpa)	Overload (&)	DUAL			
		A	B	C	D
550	0.0	5.70E-05	-6.61E-05	-1.38E-05	-6.97E-05
	7.5	6.08E-05	-7.41E-05	-1.68E-05	-7.62E-05
	10.0	6.19E-05	-7.68E-05	-1.78E-05	-7.83E-05
	20.0	6.60E-05	-8.78E-05	-2.21E-05	-8.68E-05
	30.0	6.93E-05	-1.00E-04	-2.71E-05	-9.58E-05
690	0.0	5.75E-05	-5.94E-05	-9.14E-06	-6.69E-05
	7.5	6.19E-05	-6.61E-05	-1.13E-05	-7.30E-05
	10.0	6.33E-05	-6.84E-05	-1.21E-05	-7.50E-05
	20.0	6.86E-05	-7.76E-05	-1.53E-05	-8.29E-05
	30.0	7.38E-05	-8.78E-05	-1.91E-05	-9.14E-05
830	0.0	5.74E-05	-5.52E-05	-6.24E-06	-6.49E-05
	7.5	6.19E-05	-6.12E-05	-7.90E-06	-7.08E-05
	10.0	6.34E-05	-6.31E-05	-8.46E-06	-7.26E-05
	20.0	6.90E-05	-7.12E-05	-1.09E-05	-8.02E-05
	30.0	7.48E-05	-8.01E-05	-1.38E-05	-8.83E-05

Tandem (left) and tandem-spaced (right) axles:

Tire Pressure (Kpa)	Overload (&)	TANDEM			
		A	B	C	D
550	0.0	-1.18E-06	4.00E-06	1.59E-06	1.66E-06
	7.5	-1.30E-06	4.31E-06	1.71E-06	1.78E-06
	10.0	-1.34E-06	4.41E-06	1.75E-06	1.82E-06
	20.0	-1.54E-06	4.83E-06	1.91E-06	1.98E-06
	30.0	-1.76E-06	5.24E-06	2.07E-06	2.14E-06
690	0.0	-1.29E-06	3.97E-06	1.59E-06	1.67E-06
	7.5	-1.31E-06	4.29E-06	1.71E-06	1.79E-06
	10.0	-1.33E-06	4.39E-06	1.75E-06	1.83E-06
	20.0	-1.41E-06	4.80E-06	1.91E-06	1.99E-06
	30.0	-1.55E-06	5.21E-06	2.07E-06	2.16E-06
830	0.0	-1.51E-06	3.95E-06	1.59E-06	1.67E-06
	7.5	-1.52E-06	4.26E-06	1.71E-06	1.80E-06
	10.0	-1.53E-06	4.36E-06	1.75E-06	1.84E-06
	20.0	-1.55E-06	4.77E-06	1.91E-06	2.00E-06
	30.0	-1.58E-06	5.19E-06	2.07E-06	2.17E-06

Tire Pressure (Kpa)	Overload (&)	TANDEM SPACED			
		A	B	C	D
550	0.0	-3.47E-06	-1.55E-06	-6.76E-07	9.74E-08
	7.5	-3.87E-06	-1.69E-06	-7.38E-07	1.03E-07
	10.0	-4.00E-06	-1.74E-06	-7.57E-07	1.04E-07
	20.0	-4.54E-06	-1.94E-06	-8.39E-07	1.11E-07
	30.0	-5.08E-06	-2.13E-06	-9.21E-07	1.18E-07
690	0.0	-3.15E-06	-1.48E-06	-6.54E-07	1.03E-07
	7.5	-3.48E-06	-1.61E-06	-7.11E-07	1.09E-07
	10.0	-3.59E-06	-1.65E-06	-7.29E-07	1.11E-07
	20.0	-4.08E-06	-1.84E-06	-8.07E-07	1.19E-07
	30.0	-4.60E-06	-2.03E-06	-8.87E-07	1.26E-07
830	0.0	-3.02E-06	-1.45E-06	-6.45E-07	1.05E-07
	7.5	-3.29E-06	-1.57E-06	-6.97E-07	1.12E-07
	10.0	-3.38E-06	-1.61E-06	-7.14E-07	1.15E-07
	20.0	-3.78E-06	-1.77E-06	-7.86E-07	1.24E-07
	30.0	-4.22E-06	-1.95E-06	-8.61E-07	1.32E-07

Tridem (left) and tridem spaced (right) axles:

Tire Pressure (Kpa)	Overload (&)	TRIDEM			
		A	B	C	D
550	0.0	4.56E-05	-5.34E-05	-9.55E-06	-5.74E-05
	7.5	4.89E-05	-5.06E-05	-1.17E-05	-6.27E-05
	10.0	4.99E-05	-6.15E-05	-1.24E-05	-6.43E-05
	20.0	5.38E-05	-7.02E-05	-1.55E-05	-7.14E-05
	30.0	5.74E-05	-7.94E-05	-1.91E-05	-7.87E-05
690	0.0	4.58E-05	-4.88E-05	-6.34E-06	-5.53E-05
	7.5	4.93E-05	-5.40E-05	-7.85E-06	-6.02E-05
	10.0	5.04E-05	-5.57E-05	-8.36E-06	-6.18E-05
	20.0	5.50E-05	-6.30E-05	-1.07E-05	-6.85E-05
	30.0	5.93E-05	-7.08E-05	-1.33E-05	-7.53E-05
830	0.0	4.56E-05	-4.59E-05	-4.35E-06	-5.39E-05
	7.5	4.92E-05	-5.06E-05	-5.48E-06	-5.86E-05
	10.0	5.03E-05	-5.21E-05	-5.86E-06	-6.01E-05
	20.0	5.51E-05	-5.86E-05	-7.61E-06	-6.65E-05
	30.0	5.97E-05	-6.55E-05	-9.60E-06	-7.29E-05

Tire Pressure (Kpa)	Overload (&)	TRIDEM SPACED			
		A	B	C	D
550	0.0	4.76E-05	5.26E-05	1.00E-05	5.78E-05
	7.5	5.12E-05	5.86E-05	1.21E-05	5.91E-05
	10.0	5.23E-05	6.05E-05	1.28E-05	6.47E-05
	20.0	5.68E-05	6.89E-05	1.59E-05	7.18E-05
	30.0	6.09E-05	7.79E-05	1.94E-05	7.91E-05
690	0.0	4.73E-05	4.82E-05	6.92E-06	5.57E-05
	7.5	5.11E-05	5.33E-05	8.43E-06	6.07E-05
	10.0	5.23E-05	5.49E-05	8.93E-06	6.23E-05
	20.0	5.72E-05	6.21E-05	1.12E-05	6.89E-05
	30.0	6.20E-05	6.97E-05	1.38E-05	7.58E-05
830	0.0	4.68E-05	4.54E-05	5.01E-06	5.44E-05
	7.5	5.06E-05	5.00E-05	6.16E-06	5.91E-05
	10.0	5.18E-05	5.15E-05	6.55E-06	6.06E-05
	20.0	5.68E-05	5.79E-05	8.30E-06	6.70E-05
	30.0	6.18E-05	6.46E-05	1.03E-05	7.35E-05

APPENDIX D – VERTICAL COMPRESSIVE STRAIN AT THE TOP OF THE SUBGRADE

Vertical compressive strain at the top of the subgrade (εvc_m) by axle overload (0%, 7.5%, 10%, 20%, and 30%) and tire pressure (550 KPa, 690 KPa, and 830 KPa).

STRUCTURE A

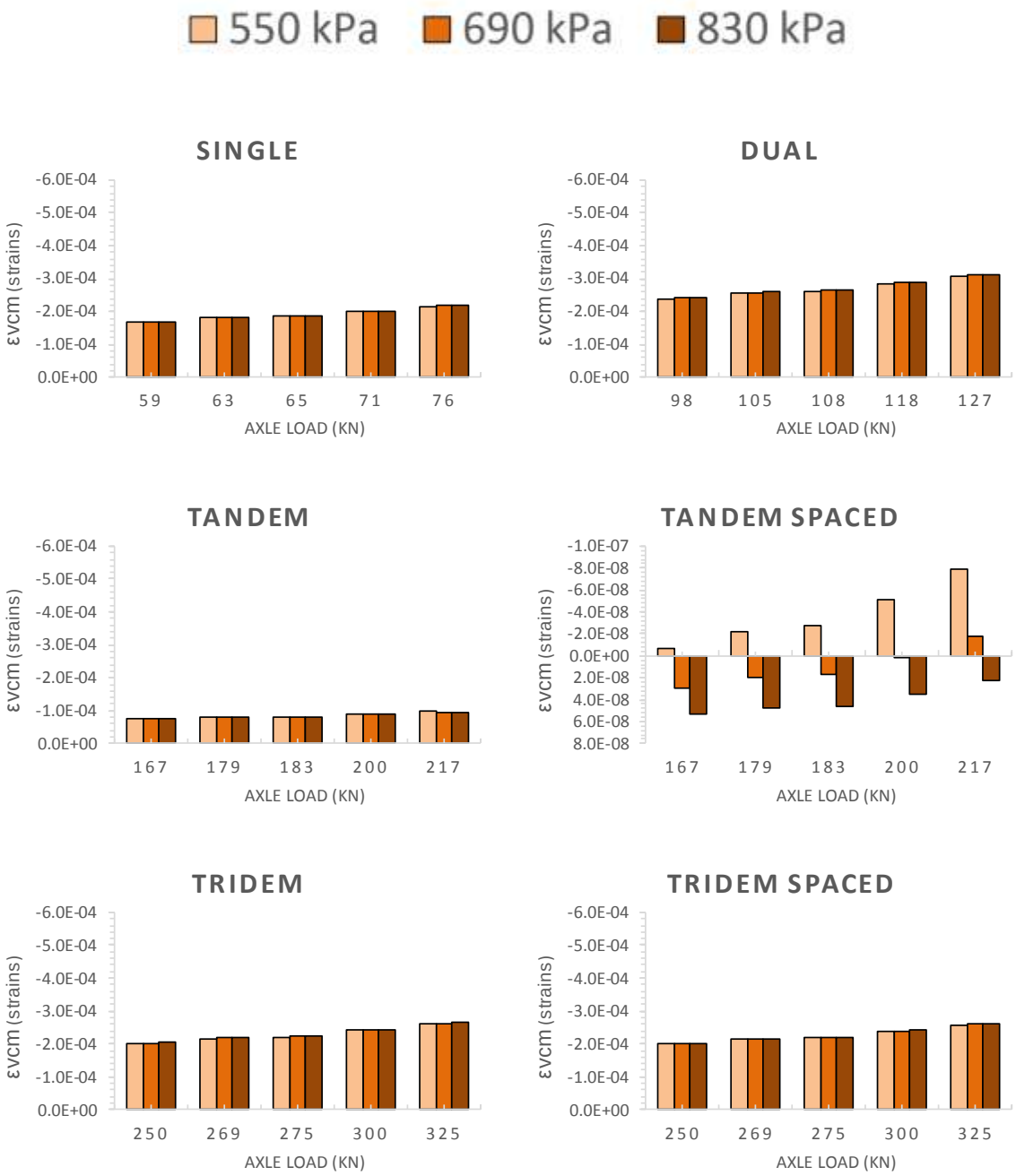

STRUCTURE B

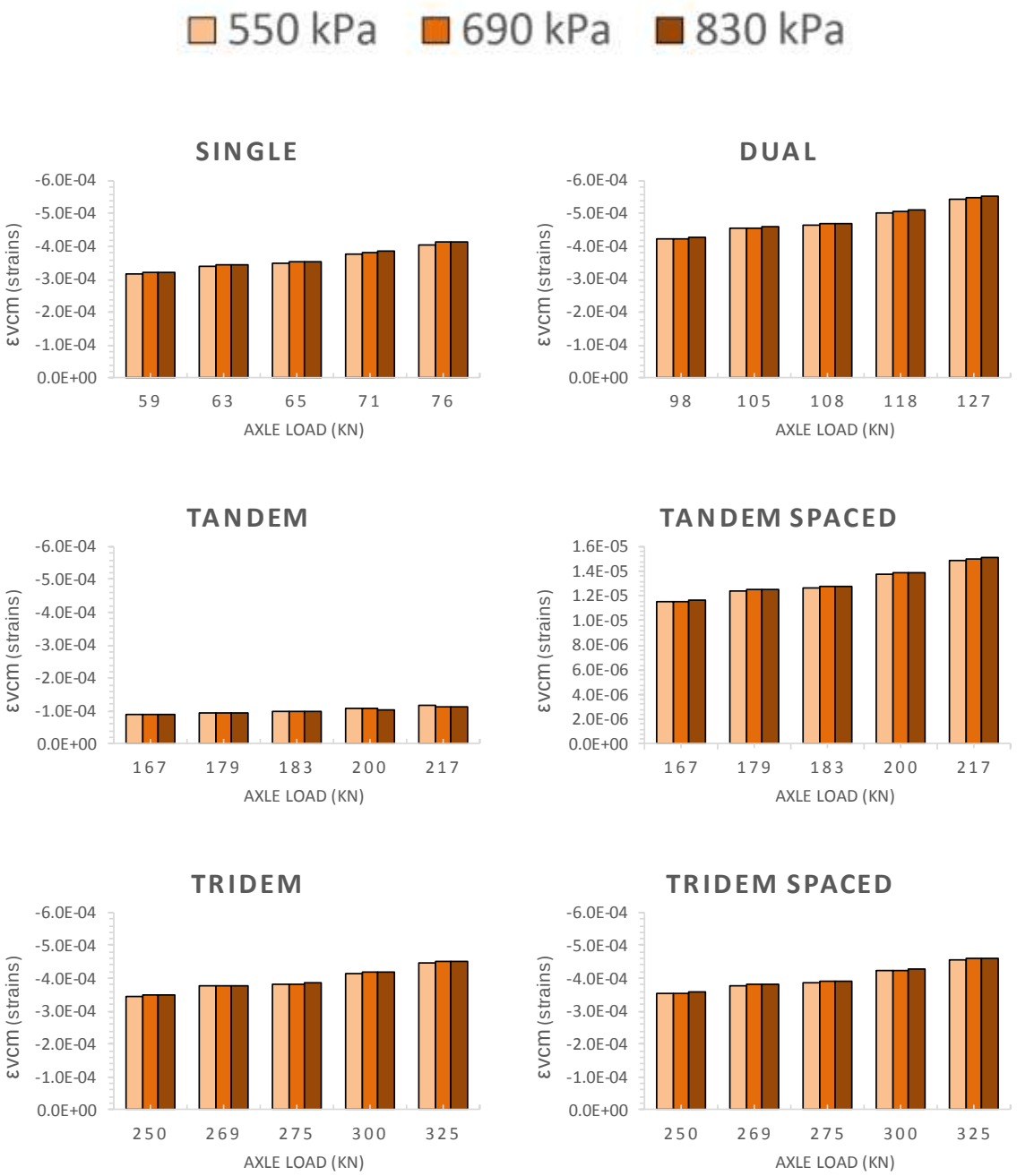
550 kPa
690 kPa
830 kPa
SINGLE
DUAL
TANDEM
TANDEM SPACED
TRIDEM
TRIDEM SPACED
εvcm (strains)
AXLE LOAD (KN)
-6.0E-04
-5.0E-04
-4.0E-04
-3.0E-04
-2.0E-04
-1.0E-04
0.0E+00
1.6E-05
1.4E-05
1.2E-05
1.0E-05
8.0E-06
6.0E-06
4.0E-06
2.0E-06
59 63 65 71 76
98 105 108 118 127
167 179 183 200 217
250 269 275 300 325

STRUCTURE C

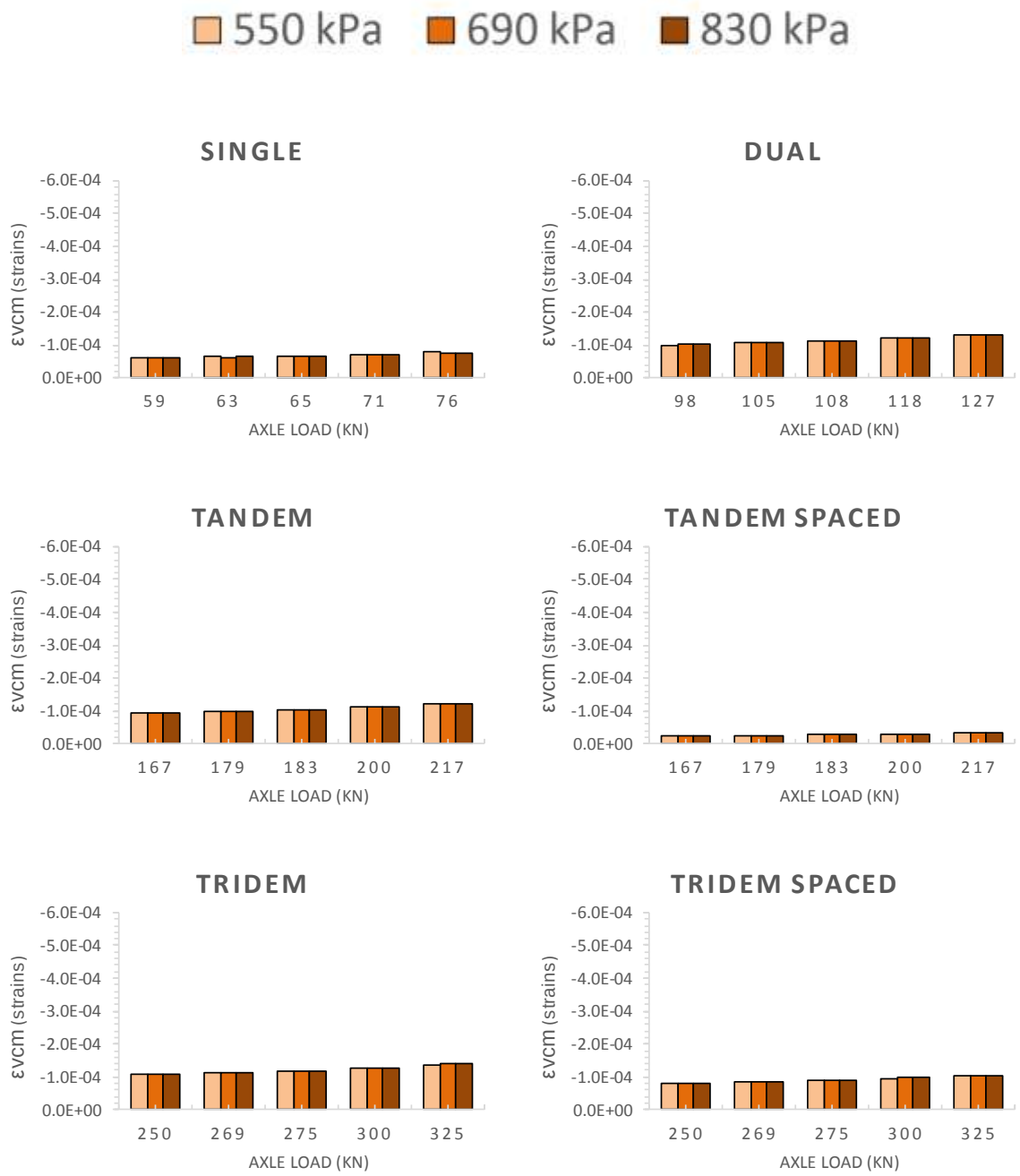
550 kPa
690 kPa
830 kPa
SINGLE
DUAL
TANDEM
TANDEM SPACED
TRIDEM
TRIDEM SPACED
εvcm (strains)
-6.0E-04
-5.0E-04
-4.0E-04
-3.0E-04
-2.0E-04
-1.0E-04
0.0E+00
59 63 65 71 76
98 105 108 118 127
167 179 183 200 217
250 269 275 300 325
AXLE LOAD (KN)

STRUCTURE D

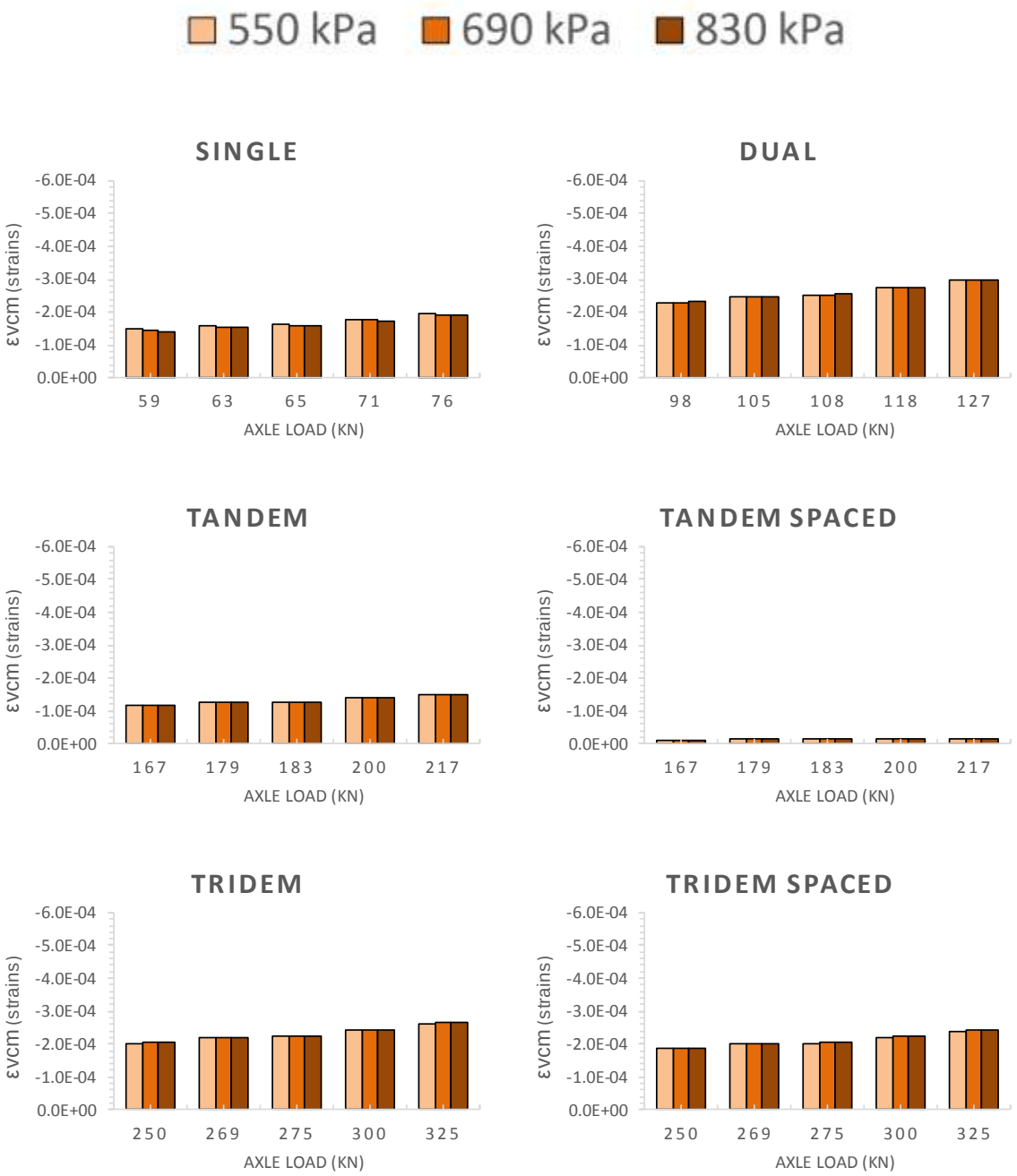
550 kPa
690 kPa
830 kPa
SINGLE
DUAL
TANDEM
TANDEM SPACED
TRIDEM
TRIDEM SPACED
εvcm (strains)
-6.0E-04
-5.0E-04
-4.0E-04
-3.0E-04
-2.0E-04
-1.0E-04
0.0E+00
59 63 65 71 76
98 105 108 118 127
167 179 183 200 217
250 269 275 300 325
AXLE LOAD (KN)

Vertical strain at the top of the subgrade for single (left) and dual (right) axles:

Tire Pressure (Kpa)	Overload (&)	SINGLE			
		A	B	C	D
550	0.0	-1.68E-04	-3.18E-04	-5.99E-05	-1.48E-04
	7.5	-1.80E-04	-3.41E-04	-6.47E-05	-1.60E-04
	10.0	-1.85E-04	-3.49E-04	-6.65E-05	-1.64E-04
	20.0	-2.01E-04	-3.78E-04	-7.29E-05	-1.80E-04
	30.0	-2.17E-04	-4.07E-04	-7.95E-05	-1.95E-04
690	0.0	-1.68E-04	-3.20E-04	-5.95E-05	-1.45E-04
	7.5	-1.81E-04	-3.44E-04	-6.40E-05	-1.57E-04
	10.0	-1.86E-04	-3.52E-04	-6.57E-05	-1.61E-04
	20.0	-2.02E-04	-3.83E-04	-7.18E-05	-1.77E-04
	30.0	-2.18E-04	-4.13E-04	-7.80E-05	-1.93E-04
830	0.0	-1.68E-04	-3.20E-04	-5.99E-05	-1.43E-04
	7.5	-1.81E-04	-3.44E-04	-6.42E-05	-1.54E-04
	10.0	-1.86E-04	-3.53E-04	-6.57E-05	-1.59E-04
	20.0	-2.02E-04	-3.84E-04	-7.15E-05	-1.74E-04
	30.0	-2.19E-04	-4.15E-04	-7.74E-05	-1.90E-04

Tire Pressure (Kpa)	Overload (&)	DUAL			
		A	B	C	D
550	0.0	-2.39E-04	-4.22E-04	-1.01E-04	-2.30E-04
	7.5	-2.57E-04	-4.54E-04	-1.09E-04	-2.47E-04
	10.0	-2.63E-04	-4.64E-04	-1.11E-04	-2.53E-04
	20.0	-2.85E-04	-5.03E-04	-1.21E-04	-2.74E-04
	30.0	-3.08E-04	-5.44E-04	-1.31E-04	-2.97E-04
690	0.0	-2.41E-04	-4.26E-04	-1.01E-04	-2.31E-04
	7.5	-2.59E-04	-4.58E-04	-1.09E-04	-2.48E-04
	10.0	-2.64E-04	-4.68E-04	-1.12E-04	-2.54E-04
	20.0	-2.87E-04	-5.08E-04	-1.21E-04	-2.76E-04
	30.0	-3.11E-04	-5.49E-04	-1.31E-04	-2.99E-04
830	0.0	-2.42E-04	-4.28E-04	-1.01E-04	-2.32E-04
	7.5	-2.60E-04	-4.60E-04	-1.09E-04	-2.49E-04
	10.0	-2.66E-04	-4.70E-04	-1.12E-04	-2.55E-04
	20.0	-2.89E-04	-5.11E-04	-1.22E-04	-2.77E-04
	30.0	-3.13E-04	-5.53E-04	-1.32E-04	-3.00E-04

Tandem (left) and tandem-spaced (right) axles:

Tire Pressure (Kpa)	Overload (&)	TANDEM			
		A	B	C	D
550	0.0	-7.39E-05	-8.83E-05	-9.21E-05	-1.16E-04
	7.5	-7.97E-05	-9.52E-05	-9.92E-05	-1.25E-04
	10.0	-8.15E-05	-9.74E-05	-1.01E-04	-1.28E-04
	20.0	-8.91E-05	-1.07E-04	-1.11E-04	-1.40E-04
	30.0	-9.67E-05	-1.16E-04	-1.20E-04	-1.52E-04
690	0.0	-7.37E-05	-8.79E-05	-9.22E-05	-1.16E-04
	7.5	-7.94E-05	-9.48E-05	-9.93E-05	-1.25E-04
	10.0	-8.12E-05	-9.70E-05	-1.02E-04	-1.28E-04
	20.0	-8.88E-05	-1.06E-04	-1.11E-04	-1.40E-04
	30.0	-9.64E-05	-1.15E-04	-1.20E-04	-1.52E-04
830	0.0	-7.35E-05	-8.77E-05	-9.22E-05	-1.16E-04
	7.5	-7.92E-05	-9.45E-05	-9.93E-05	-1.25E-04
	10.0	-8.10E-05	-9.67E-05	-1.02E-04	-1.28E-04
	20.0	-8.86E-05	-1.06E-04	-1.11E-04	-1.40E-04
	30.0	-9.61E-05	-1.15E-04	-1.20E-04	-1.51E-04

Tire Pressure (Kpa)	Overload (&)	TANDEM SPACED			
		A	B	C	D
550	0.0	-6.83E-09	1.15E-05	-2.49E-05	-1.26E-05
	7.5	-2.22E-08	1.24E-05	-2.68E-05	-1.36E-05
	10.0	-2.74E-08	1.27E-05	-2.74E-05	-1.39E-05
	20.0	-5.17E-08	1.38E-05	-3.00E-05	-1.52E-05
	30.0	-7.96E-08	1.49E-05	-3.25E-05	-1.65E-05
690	0.0	2.94E-08	1.16E-05	-2.49E-05	-1.26E-05
	7.5	1.99E-08	1.25E-05	-2.68E-05	-1.35E-05
	10.0	1.66E-08	1.27E-05	-2.74E-05	-1.39E-05
	20.0	8.09E-10	1.39E-05	-2.99E-05	-1.51E-05
	30.0	-1.79E-08	1.50E-05	-3.24E-05	-1.64E-05
830	0.0	5.34E-08	1.16E-05	-2.49E-05	-1.25E-05
	7.5	4.77E-08	1.25E-05	-2.68E-05	-1.35E-05
	10.0	4.57E-08	1.28E-05	-2.74E-05	-1.38E-05
	20.0	3.55E-08	1.39E-05	-2.99E-05	-1.51E-05
	30.0	2.29E-08	1.51E-05	-3.24E-05	-1.64E-05

Tridem (left) and tridem spaced (right) axles:

Tire Pressure (Kpa)	Overload (&)	TRIDEM			
		A	B	C	D
550	0.0	-2.02E-04	-3.47E-04	-1.06E-04	-2.03E-04
	7.5	-2.17E-04	-3.77E-04	-1.14E-04	-2.18E-04
	10.0	-2.22E-04	-3.80E-04	-1.17E-04	-2.23E-04
	20.0	-2.41E-04	-4.14E-04	-1.28E-04	-2.43E-04
	30.0	-2.61E-04	-4.47E-04	-1.38E-04	-2.63E-04
690	0.0	-2.03E-04	-3.49E-04	-1.06E-04	-2.04E-04
	7.5	-2.18E-04	-3.75E-04	-1.15E-04	-2.19E-04
	10.0	-2.23E-04	-3.83E-04	-1.17E-04	-2.24E-04
	20.0	-2.43E-04	-4.17E-04	-1.28E-04	-2.44E-04
	30.0	-2.63E-04	-4.51E-04	-1.38E-04	-2.64E-04
830	0.0	-2.04E-04	-3.50E-04	-1.07E-04	-2.04E-04
	7.5	-2.19E-04	-3.77E-04	-1.15E-04	-2.20E-04
	10.0	-2.24E-04	-3.85E-04	-1.17E-04	-2.25E-04
	20.0	-2.44E-04	-4.19E-04	-1.28E-04	-2.45E-04
	30.0	-2.64E-04	-4.53E-04	-1.39E-04	-2.65E-04

Tire Pressure (Kpa)	Overload (&)	TRIDEM SPACED			
		A	B	C	D
550	0.0	-2.00E-04	-3.53E-04	-8.04E-05	-1.85E-04
	7.5	-2.15E-04	-3.79E-04	-8.65E-05	-2.00E-04
	10.0	-2.19E-04	-3.87E-04	-8.84E-05	-2.03E-04
	20.0	-2.39E-04	-4.21E-04	-9.64E-05	-2.21E-04
	30.0	-2.58E-04	-4.55E-04	-1.04E-04	-2.39E-04
690	0.0	-2.01E-04	-3.55E-04	-8.06E-05	-1.86E-04
	7.5	-2.16E-04	-3.82E-04	-8.67E-05	-2.00E-04
	10.0	-2.20E-04	-3.90E-04	-8.86E-05	-2.04E-04
	20.0	-2.40E-04	-4.25E-04	-9.67E-05	-2.22E-04
	30.0	-2.60E-04	-4.59E-04	-1.05E-04	-2.41E-04
830	0.0	-2.01E-04	-3.57E-04	-8.07E-05	-1.86E-04
	7.5	-2.17E-04	-3.83E-04	-8.69E-05	-2.00E-04
	10.0	-2.21E-04	-3.92E-04	-8.88E-05	-2.05E-04
	20.0	-2.41E-04	-4.27E-04	-9.69E-05	-2.23E-04
	30.0	-2.61E-04	-4.62E-04	-1.05E-04	-2.41E-04

APPENDIX E – CRITICAL N NUMBERS

STRUCTURE A													
Type	Load (Kg)	Load by Tire (kN)	Pressure (kPa)	Asphalt Institute		Critical Resistance	Type	Load (Kg)	Load by Tire (kN)	Pressure (kPa)	Asphalt Institute		Critical Resistance
				Fatigue	Rutting						Fatigue	Rutting	
S_0	6000	29.4	550	2.38E+08	1.08E+08	1.08E+08	Tds_0	17000	20.8	550	2.76E+10	4.93E+27	2.76E+10
S_0	6000	29.4	690	2.95E+08	1.07E+08	1.07E+08	Tds_0	17000	20.8	690	2.99E+10	7.13E+24	2.99E+10
S_0	6000	29.4	830	4.28E+08	1.07E+08	1.07E+08	Tds_0	17000	20.8	830	3.08E+10	4.94E+23	3.08E+10
$S_{7.5}$	6450	31.6	550	1.82E+08	7.87E+07	7.87E+07	$Tds_{7.5}$	18275	22.4	550	2.10E+10	2.53E+25	2.10E+10
$S_{7.5}$	6450	31.6	690	2.12E+08	7.75E+07	7.75E+07	$Tds_{7.5}$	18275	22.4	690	2.29E+10	4.10E+25	2.29E+10
$S_{7.5}$	6450	31.6	830	2.84E+08	7.75E+07	7.75E+07	$Tds_{7.5}$	18275	22.4	830	2.40E+10	8.18E+23	2.40E+10
S_{10}	6600	32.4	550	1.67E+08	7.06E+07	7.06E+07	Tds_{10}	18700	22.9	550	1.94E+10	9.79E+24	1.94E+10
S_{10}	6600	32.4	690	1.90E+08	6.95E+07	6.95E+07	Tds_{10}	18700	22.9	690	2.12E+10	9.32E+25	2.12E+10
S_{10}	6600	32.4	830	2.49E+08	6.93E+07	6.93E+07	Tds_{10}	18700	22.9	830	2.22E+10	9.96E+23	2.22E+10
S_{20}	7200	35.3	550	1.24E+08	4.87E+07	4.87E+07	Tds_{20}	20400	25	550	1.40E+10	5.73E+23	1.40E+10
S_{20}	7200	35.3	690	1.34E+08	4.74E+07	4.74E+07	Tds_{20}	20400	25	690	1.54E+10	6.93E+31	1.54E+10
S_{20}	7200	35.3	830	1.62E+08	4.72E+07	4.72E+07	Tds_{20}	20400	25	830	1.63E+10	3.07E+24	1.63E+10
S_{30}	7800	38.2	550	9.68E+07	3.48E+07	3.48E+07	Tds_{30}	22100	27.1	550	1.04E+10	8.27E+22	1.04E+10
S_{30}	7800	38.2	690	9.88E+07	3.36E+07	3.36E+07	Tds_{30}	22100	27.1	690	1.14E+10	6.63E+25	1.14E+10
S_{30}	7800	38.2	830	1.13E+08	3.32E+07	3.32E+07	Tds_{30}	22100	27.1	830	1.22E+10	2.18E+25	1.22E+10
D_0	10000	24.5	550	8.59E+07	2.23E+07	2.23E+07	Tr_0	25500	20.8	550	2.57E+08	4.77E+07	4.77E+07
D_0	10000	24.5	690	7.64E+07	2.17E+07	2.17E+07	Tr_0	25500	20.8	690	2.26E+08	4.66E+07	4.66E+07
D_0	10000	24.5	830	7.08E+07	2.13E+07	2.13E+07	Tr_0	25500	20.8	830	2.09E+08	4.59E+07	4.59E+07
$D_{7.5}$	10750	26.4	550	7.02E+07	1.62E+07	1.62E+07	$Tr_{7.5}$	27413	22.4	550	2.12E+08	3.46E+07	3.46E+07
$D_{7.5}$	10750	26.4	690	6.19E+07	1.57E+07	1.57E+07	$Tr_{7.5}$	27413	22.4	690	1.84E+08	3.36E+07	3.36E+07
$D_{7.5}$	10750	26.4	830	5.70E+07	1.54E+07	1.54E+07	$Tr_{7.5}$	27413	22.4	830	1.68E+08	3.31E+07	3.31E+07
D_{10}	11000	27	550	6.62E+07	1.47E+07	1.47E+07	Tr_{10}	28050	22.9	550	2.01E+08	3.14E+07	3.14E+07
D_{10}	11000	27	690	5.81E+07	1.42E+07	1.42E+07	Tr_{10}	28050	22.9	690	1.73E+08	3.06E+07	3.06E+07
D_{10}	11000	27	830	5.34E+07	1.39E+07	1.39E+07	Tr_{10}	28050	22.9	830	1.58E+08	3.00E+07	3.00E+07
D_{20}	12000	29.4	550	5.30E+07	1.02E+07	1.02E+07	Tr_{20}	30600	25	550	1.61E+08	2.14E+07	2.14E+07
D_{20}	12000	29.4	690	4.59E+07	9.81E+06	9.81E+06	Tr_{20}	30600	25	690	1.36E+08	2.09E+07	2.09E+07
D_{20}	12000	29.4	830	4.19E+07	9.60E+06	9.60E+06	Tr_{20}	30600	25	830	1.23E+08	2.04E+07	2.04E+07
D_{30}	13000	31.9	550	4.30E+07	7.14E+06	7.14E+06	Tr_{30}	33150	27.1	550	1.33E+08	1.51E+07	1.51E+07
D_{30}	13000	31.9	690	3.68E+07	6.89E+06	6.89E+06	Tr_{30}	33150	27.1	690	1.11E+08	1.47E+07	1.47E+07
D_{30}	13000	31.9	830	3.33E+07	6.72E+06	6.72E+06	Tr_{30}	33150	27.1	830	9.84E+07	1.44E+07	1.44E+07
Td_0	17000	20.8	550	3.41E+09	4.28E+09	3.41E+09	Trs_0	25500	20.8	550	1.47E+08	5.02E+07	5.02E+07
Td_0	17000	20.8	690	3.33E+09	4.34E+09	3.33E+09	Trs_0	25500	20.8	690	1.34E+08	4.89E+07	4.89E+07
Td_0	17000	20.8	830	3.21E+09	4.38E+09	3.21E+09	Trs_0	25500	20.8	830	1.27E+08	4.81E+07	4.81E+07
$Td_{7.5}$	18275	22.4	550	2.67E+09	3.05E+09	2.67E+09	$Trs_{7.5}$	27413	22.4	550	1.19E+08	3.63E+07	3.63E+07
$Td_{7.5}$	18275	22.4	690	2.64E+09	3.10E+09	2.64E+09	$Trs_{7.5}$	27413	22.4	690	1.08E+08	3.54E+07	3.54E+07
$Td_{7.5}$	18275	22.4	830	2.56E+09	3.13E+09	2.56E+09	$Trs_{7.5}$	27413	22.4	830	1.02E+08	3.48E+07	3.48E+07
Td_{10}	18700	22.9	550	2.48E+09	2.76E+09	2.48E+09	Trs_{10}	28050	22.9	550	1.12E+08	3.30E+07	3.30E+07
Td_{10}	18700	22.9	690	2.46E+09	2.80E+09	2.46E+09	Trs_{10}	28050	22.9	690	1.01E+08	3.21E+07	3.21E+07
Td_{10}	18700	22.9	830	2.39E+09	2.83E+09	2.39E+09	Trs_{10}	28050	22.9	830	9.51E+07	3.15E+07	3.15E+07
Td_{20}	20400	25	550	1.85E+09	1.85E+09	1.85E+09	Trs_{20}	30600	25	550	8.81E+07	2.25E+07	2.25E+07
Td_{20}	20400	25	690	1.86E+09	1.88E+09	1.86E+09	Trs_{20}	30600	25	690	7.87E+07	2.19E+07	2.19E+07
Td_{20}	20400	25	830	1.82E+09	1.90E+09	1.82E+09	Trs_{20}	30600	25	830	7.33E+07	2.15E+07	2.15E+07
Td_{30}	22100	27.1	550	1.41E+09	1.28E+09	1.28E+09	Trs_{30}	33150	27.1	550	7.09E+07	1.59E+07	1.59E+07
Td_{30}	22100	27.1	690	1.43E+09	1.30E+09	1.30E+09	Trs_{30}	33150	27.1	690	6.26E+07	1.54E+07	1.54E+07
Td_{30}	22100	27.1	830	1.41E+09	1.32E+09	1.32E+09	Trs_{30}	33150	27.1	830	5.79E+07	1.51E+07	1.51E+07

STRUCTURE B													
Type	Load (Kg)	Load by Tire (kN)	Pressure (kPa)	Asphalt Institute		Critical Resistance	Type	Load (Kg)	Load by Tire (kN)	Pressure (kPa)	Asphalt Institute		Critical Resistance
				Fatigue	Rutting						Fatigue	Rutting	
S_0	6000	29.4	550	1.32E+06	6.20E+06	1.32E+06	Tds_0	17000	20.8	550	4.87E+16	1.74E+13	1.74E+13
S_0	6000	29.4	690	7.58E+05	6.05E+06	7.58E+05	Tds_0	17000	20.8	690	4.41E+15	1.70E+13	1.70E+13
S_0	6000	29.4	830	4.97E+05	6.04E+06	4.97E+05	Tds_0	17000	20.8	830	2.51E+15	1.68E+13	1.68E+13
$S_{7.5}$	6450	31.6	550	1.25E+06	4.56E+06	1.25E+06	$Tds_{7.5}$	18275	22.4	550	2.34E+17	1.26E+13	1.26E+13
$S_{7.5}$	6450	31.6	690	7.09E+05	4.40E+06	7.09E+05	$Tds_{7.5}$	18275	22.4	690	5.71E+15	1.23E+13	1.23E+13
$S_{7.5}$	6450	31.6	830	4.61E+05	4.36E+06	4.61E+05	$Tds_{7.5}$	18275	22.4	830	2.22E+15	1.22E+13	1.22E+13
S_{10}	6600	32.4	550	1.22E+06	4.10E+06	1.22E+06	Tds_{10}	18700	22.9	550	4.90E+17	1.15E+13	1.15E+13
S_{10}	6600	32.4	690	6.94E+05	3.94E+06	6.94E+05	Tds_{10}	18700	22.9	690	6.44E+15	1.12E+13	1.12E+13
S_{10}	6600	32.4	830	4.49E+05	3.90E+06	4.49E+05	Tds_{10}	18700	22.9	830	2.20E+15	1.10E+13	1.10E+13
S_{20}	7200	35.3	550	1.16E+06	2.86E+06	1.16E+06	Tds_{20}	20400	25	550	1.54E+21	7.83E+12	7.83E+12
S_{20}	7200	35.3	690	6.46E+05	2.71E+06	6.46E+05	Tds_{20}	20400	25	690	1.32E+16	7.63E+12	7.63E+12
S_{20}	7200	35.3	830	4.13E+05	2.66E+06	4.13E+05	Tds_{20}	20400	25	830	2.40E+15	7.49E+12	7.49E+12
S_{30}	7800	38.2	550	1.11E+06	2.06E+06	1.11E+06	Tds_{30}	22100	27.1	550	3.28E+17	5.51E+12	5.51E+12
S_{30}	7800	38.2	690	6.07E+05	1.93E+06	6.07E+05	Tds_{30}	22100	27.1	690	4.52E+16	5.36E+12	5.36E+12
S_{30}	7800	38.2	830	3.84E+05	1.88E+06	3.84E+05	Tds_{30}	22100	27.1	830	3.20E+15	5.25E+12	5.25E+12
D_0	10000	24.5	550	1.75E+06	1.74E+06	1.74E+06	Tr_0	25500	20.8	550	2.81E+06	4.24E+06	2.81E+06
D_0	10000	24.5	690	1.61E+06	1.69E+06	1.61E+06	Tr_0	25500	20.8	690	2.63E+06	4.12E+06	2.63E+06
D_0	10000	24.5	830	1.53E+06	1.65E+06	1.53E+06	Tr_0	25500	20.8	830	2.53E+06	4.04E+06	2.53E+06
$D_{7.5}$	10750	26.4	550	1.42E+06	1.27E+06	1.27E+06	$Tr_{7.5}$	27413	22.4	550	2.01E+06	2.92E+06	2.01E+06
$D_{7.5}$	10750	26.4	690	1.29E+06	1.22E+06	1.22E+06	$Tr_{7.5}$	27413	22.4	690	2.10E+06	2.98E+06	2.10E+06
$D_{7.5}$	10750	26.4	830	1.22E+06	1.19E+06	1.19E+06	$Tr_{7.5}$	27413	22.4	830	2.01E+06	2.92E+06	2.01E+06
D_{10}	11000	27	550	1.33E+06	1.15E+06	1.15E+06	Tr_{10}	28050	22.9	550	2.11E+06	2.80E+06	2.11E+06
D_{10}	11000	27	690	1.21E+06	1.11E+06	1.11E+06	Tr_{10}	28050	22.9	690	1.97E+06	2.70E+06	1.97E+06
D_{10}	11000	27	830	1.14E+06	1.08E+06	1.08E+06	Tr_{10}	28050	22.9	830	1.88E+06	2.65E+06	1.88E+06
D_{20}	12000	29.4	550	1.05E+06	7.98E+05	7.98E+05	Tr_{20}	30600	25	550	1.64E+06	1.91E+06	1.64E+06
D_{20}	12000	29.4	690	9.44E+05	7.66E+05	7.66E+05	Tr_{20}	30600	25	690	1.51E+06	1.85E+06	1.51E+06
D_{20}	12000	29.4	830	8.85E+05	7.46E+05	7.46E+05	Tr_{20}	30600	25	830	1.44E+06	1.81E+06	1.44E+06
D_{30}	13000	31.9	550	8.44E+05	5.63E+05	5.63E+05	Tr_{30}	33150	27.1	550	1.30E+06	1.35E+06	1.30E+06
D_{30}	13000	31.9	690	7.47E+05	5.39E+05	5.39E+05	Tr_{30}	33150	27.1	690	1.19E+06	1.30E+06	1.19E+06
D_{30}	13000	31.9	830	6.95E+05	5.23E+05	5.23E+05	Tr_{30}	33150	27.1	830	1.13E+06	1.27E+06	1.13E+06
Td_0	17000	20.8	550	2.58E+09	1.93E+09	1.93E+09	Trs_0	25500	20.8	550	2.83E+06	3.91E+06	2.83E+06
Td_0	17000	20.8	690	2.62E+09	1.97E+09	1.97E+09	Trs_0	25500	20.8	690	2.63E+06	3.80E+06	2.63E+06
Td_0	17000	20.8	830	2.65E+09	1.99E+09	1.99E+09	Trs_0	25500	20.8	830	2.51E+06	3.72E+06	2.51E+06
$Td_{7.5}$	18275	22.4	550	2.01E+09	1.37E+09	1.37E+09	$Trs_{7.5}$	27413	22.4	550	2.29E+06	2.84E+06	2.29E+06
$Td_{7.5}$	18275	22.4	690	2.04E+09	1.40E+09	1.40E+09	$Trs_{7.5}$	27413	22.4	690	2.11E+06	2.75E+06	2.11E+06
$Td_{7.5}$	18275	22.4	830	2.06E+09	1.42E+09	1.42E+09	$Trs_{7.5}$	27413	22.4	830	2.00E+06	2.69E+06	2.00E+06
Td_{10}	18700	22.9	550	1.87E+09	1.24E+09	1.24E+09	Trs_{10}	28050	22.9	550	2.15E+06	2.58E+06	2.15E+06
Td_{10}	18700	22.9	690	1.89E+09	1.27E+09	1.27E+09	Trs_{10}	28050	22.9	690	1.98E+06	2.50E+06	1.98E+06
Td_{10}	18700	22.9	830	1.92E+09	1.29E+09	1.29E+09	Trs_{10}	28050	22.9	830	1.87E+06	2.45E+06	1.87E+06
Td_{20}	20400	25	550	1.39E+09	8.30E+08	8.30E+08	Trs_{20}	30600	25	550	1.67E+06	1.77E+06	1.67E+06
Td_{20}	20400	25	690	1.41E+09	8.51E+08	8.51E+08	Trs_{20}	30600	25	690	1.52E+06	1.71E+06	1.52E+06
Td_{20}	20400	25	830	1.43E+09	8.62E+08	8.62E+08	Trs_{20}	30600	25	830	1.44E+06	1.67E+06	1.44E+06
Td_{30}	22100	27.1	550	1.06E+09	5.73E+08	5.73E+08	Trs_{30}	33150	27.1	550	1.33E+06	1.25E+06	1.25E+06
Td_{30}	22100	27.1	690	1.08E+09	5.88E+08	5.88E+08	Trs_{30}	33150	27.1	690	1.20E+06	1.20E+06	1.20E+06
Td_{30}	22100	27.1	830	1.09E+09	5.98E+08	5.98E+08	Trs_{30}	33150	27.1	830	1.13E+06	1.17E+06	1.13E+06

STRUCTURE C													
Type	Load (Kg)	Load by Tire (kN)	Pressure (kPa)	Asphalt Institute		Critical Resistance	Type	Load (Kg)	Load by Tire (kN)	Pressure (kPa)	Asphalt Institute		Critical Resistance
				Fatigue	Rutting						Fatigue	Rutting	
S_0	6000	29.4	550	1.27E+09	1.10E+10	1.27E+09	Tds_0	17000	20.8	550	1.12E+12	5.59E+11	5.59E+11
S_0	6000	29.4	690	5.01E+08	1.13E+10	5.01E+08	Tds_0	17000	20.8	690	1.14E+12	5.62E+11	5.62E+11
S_0	6000	29.4	830	2.59E+08	1.09E+10	2.59E+08	Tds_0	17000	20.8	830	1.14E+12	5.63E+11	5.63E+11
$S_{7.5}$	6450	31.6	550	1.38E+09	7.76E+09	1.38E+09	$Tds_{7.5}$	18275	22.4	550	8.68E+11	4.01E+11	4.01E+11
$S_{7.5}$	6450	31.6	690	5.23E+08	8.14E+09	5.23E+08	$Tds_{7.5}$	18275	22.4	690	8.86E+11	4.03E+11	4.03E+11
$S_{7.5}$	6450	31.6	830	2.62E+08	8.06E+09	2.62E+08	$Tds_{7.5}$	18275	22.4	830	8.94E+11	4.04E+11	4.04E+11
S_{10}	6600	32.4	550	1.43E+09	6.88E+09	1.43E+09	Tds_{10}	18700	22.9	550	8.06E+11	3.62E+11	3.62E+11
S_{10}	6600	32.4	690	5.32E+08	7.26E+09	5.32E+08	Tds_{10}	18700	22.9	690	8.23E+11	3.65E+11	3.65E+11
S_{10}	6600	32.4	830	2.63E+08	7.24E+09	2.63E+08	Tds_{10}	18700	22.9	830	8.31E+11	3.66E+11	3.66E+11
S_{20}	7200	35.3	550	1.64E+09	4.54E+09	1.64E+09	Tds_{20}	20400	25	550	5.99E+11	2.44E+11	2.44E+11
S_{20}	7200	35.3	690	5.74E+08	4.88E+09	5.74E+08	Tds_{20}	20400	25	690	6.12E+11	2.45E+11	2.45E+11
S_{20}	7200	35.3	830	2.73E+08	4.97E+09	2.73E+08	Tds_{20}	20400	25	830	6.20E+11	2.47E+11	2.47E+11
S_{30}	7800	38.2	550	1.89E+09	3.08E+09	1.89E+09	Tds_{30}	22100	27.1	550	4.57E+11	1.70E+11	1.70E+11
S_{30}	7800	38.2	690	6.26E+08	3.36E+09	6.26E+08	Tds_{30}	22100	27.1	690	4.66E+11	1.71E+11	1.71E+11
S_{30}	7800	38.2	830	2.86E+08	3.48E+09	2.86E+08	Tds_{30}	22100	27.1	830	4.73E+11	1.71E+11	1.71E+11
D_0	10000	24.5	550	6.35E+09	1.06E+09	1.06E+09	Tr_0	25500	20.8	550	4.97E+09	8.40E+08	8.40E+08
D_0	10000	24.5	690	5.93E+09	1.04E+09	1.04E+09	Tr_0	25500	20.8	690	4.82E+09	8.37E+08	8.37E+08
D_0	10000	24.5	830	5.75E+09	1.04E+09	1.04E+09	Tr_0	25500	20.8	830	4.76E+09	8.33E+08	8.33E+08
$D_{7.5}$	10750	26.4	550	5.14E+09	7.60E+08	7.60E+08	$Tr_{7.5}$	27413	22.4	550	3.95E+09	6.05E+08	6.05E+08
$D_{7.5}$	10750	26.4	690	4.71E+09	7.51E+08	7.51E+08	$Tr_{7.5}$	27413	22.4	690	3.81E+09	6.00E+08	6.00E+08
$D_{7.5}$	10750	26.4	830	4.54E+09	7.45E+08	7.45E+08	$Tr_{7.5}$	27413	22.4	830	3.75E+09	5.98E+08	5.98E+08
D_{10}	11000	27	550	4.83E+09	6.89E+08	6.89E+08	Tr_{10}	28050	22.9	550	3.70E+09	5.49E+08	5.49E+08
D_{10}	11000	27	690	4.40E+09	6.78E+08	6.78E+08	Tr_{10}	28050	22.9	690	3.55E+09	5.45E+08	5.45E+08
D_{10}	11000	27	830	4.23E+09	6.73E+08	6.73E+08	Tr_{10}	28050	22.9	830	3.49E+09	5.43E+08	5.43E+08
D_{20}	12000	29.4	550	3.84E+09	4.72E+08	4.72E+08	Tr_{20}	30600	25	550	2.84E+09	3.72E+08	3.72E+08
D_{20}	12000	29.4	690	3.42E+09	4.65E+08	4.65E+08	Tr_{20}	30600	25	690	2.69E+09	3.68E+08	3.68E+08
D_{20}	12000	29.4	830	3.25E+09	4.62E+08	4.62E+08	Tr_{20}	30600	25	830	2.63E+09	3.67E+08	3.67E+08
D_{30}	13000	31.9	550	3.12E+09	3.30E+08	3.30E+08	Tr_{30}	33150	27.1	550	2.25E+09	2.60E+08	2.60E+08
D_{30}	13000	31.9	690	2.71E+09	3.25E+08	3.25E+08	Tr_{30}	33150	27.1	690	2.10E+09	2.58E+08	2.58E+08
D_{30}	13000	31.9	830	2.54E+09	3.22E+08	3.22E+08	Tr_{30}	33150	27.1	830	2.04E+09	2.56E+08	2.56E+08
Td_0	17000	20.8	550	3.81E+13	1.59E+09	1.59E+09	Trs_0	25500	20.8	550	6.39E+09	2.94E+09	2.94E+09
Td_0	17000	20.8	690	4.05E+13	1.59E+09	1.59E+09	Trs_0	25500	20.8	690	6.04E+09	2.91E+09	2.91E+09
Td_0	17000	20.8	830	4.23E+13	1.59E+09	1.59E+09	Trs_0	25500	20.8	830	5.86E+09	2.88E+09	2.88E+09
$Td_{7.5}$	18275	22.4	550	2.92E+13	1.14E+09	1.14E+09	$Trs_{7.5}$	27413	22.4	550	5.13E+09	2.12E+09	2.12E+09
$Td_{7.5}$	18275	22.4	690	3.11E+13	1.14E+09	1.14E+09	$Trs_{7.5}$	27413	22.4	690	4.80E+09	2.09E+09	2.09E+09
$Td_{7.5}$	18275	22.4	830	3.26E+13	1.14E+09	1.14E+09	$Trs_{7.5}$	27413	22.4	830	4.65E+09	2.08E+09	2.08E+09
Td_{10}	18700	22.9	550	2.69E+13	1.04E+09	1.04E+09	Trs_{10}	28050	22.9	550	4.81E+09	1.92E+09	1.92E+09
Td_{10}	18700	22.9	690	2.88E+13	1.03E+09	1.03E+09	Trs_{10}	28050	22.9	690	4.49E+09	1.90E+09	1.90E+09
Td_{10}	18700	22.9	830	3.01E+13	1.03E+09	1.03E+09	Trs_{10}	28050	22.9	830	4.33E+09	1.88E+09	1.88E+09
Td_{20}	20400	25	550	1.96E+13	7.01E+08	7.01E+08	Trs_{20}	30600	25	550	3.74E+09	1.30E+09	1.30E+09
Td_{20}	20400	25	690	2.11E+13	6.98E+08	6.98E+08	Trs_{20}	30600	25	690	3.44E+09	1.29E+09	1.29E+09
Td_{20}	20400	25	830	2.21E+13	6.98E+08	6.98E+08	Trs_{20}	30600	25	830	3.30E+09	1.27E+09	1.27E+09
Td_{30}	22100	27.1	550	1.46E+13	4.88E+08	4.88E+08	Trs_{30}	33150	27.1	550	2.99E+09	9.11E+08	9.11E+08
Td_{30}	22100	27.1	690	1.58E+13	4.88E+08	4.88E+08	Trs_{30}	33150	27.1	690	2.71E+09	8.99E+08	8.99E+08
Td_{30}	22100	27.1	830	1.66E+13	4.86E+08	4.86E+08	Trs_{30}	33150	27.1	830	2.57E+09	8.91E+08	8.91E+08

STRUCTURE D													
Type	Load (Kg)	Load by Tire (kN)	Pressure (kPa)	Asphalt Institute		Critical Resistance	Type	Load (Kg)	Load by Tire (kN)	Pressure (kPa)	Asphalt Institute		Critical Resistance
				Fatigue	Rutting						Fatigue	Rutting	
S_0	6000	29.4	550	8.13E+06	1.93E+08	8.13E+06	Tds_0	17000	20.8	550	2.72E+11	1.17E+13	2.72E+11
S_0	6000	29.4	690	5.42E+06	2.10E+08	5.42E+06	Tds_0	17000	20.8	690	2.70E+11	1.19E+13	2.70E+11
S_0	6000	29.4	830	4.03E+06	2.24E+08	4.03E+06	Tds_0	17000	20.8	830	2.70E+11	1.21E+13	2.70E+11
$S_{7.5}$	6450	31.6	550	7.34E+06	1.36E+08	7.34E+06	$Tds_{7.5}$	18275	22.4	550	2.13E+11	8.36E+12	2.13E+11
$S_{7.5}$	6450	31.6	690	4.84E+06	1.48E+08	4.84E+06	$Tds_{7.5}$	18275	22.4	690	2.12E+11	8.53E+12	2.12E+11
$S_{7.5}$	6450	31.6	830	3.56E+06	1.58E+08	3.56E+06	$Tds_{7.5}$	18275	22.4	830	2.11E+11	8.61E+12	2.11E+11
S_{10}	6600	32.4	550	7.09E+06	1.21E+08	7.09E+06	Tds_{10}	18700	22.9	550	1.99E+11	7.56E+12	1.99E+11
S_{10}	6600	32.4	690	4.66E+06	1.31E+08	4.66E+06	Tds_{10}	18700	22.9	690	1.97E+11	7.71E+12	1.97E+11
S_{10}	6600	32.4	830	3.41E+06	1.40E+08	3.41E+06	Tds_{10}	18700	22.9	830	1.97E+11	7.81E+12	1.97E+11
S_{20}	7200	35.3	550	6.34E+06	8.01E+07	6.34E+06	Tds_{20}	20400	25	550	1.49E+11	5.07E+12	1.49E+11
S_{20}	7200	35.3	690	4.10E+06	8.63E+07	4.10E+06	Tds_{20}	20400	25	690	1.48E+11	5.17E+12	1.48E+11
S_{20}	7200	35.3	830	2.96E+06	9.25E+07	2.96E+06	Tds_{20}	20400	25	830	1.48E+11	5.23E+12	1.48E+11
S_{30}	7800	38.2	550	5.74E+06	5.50E+07	5.74E+06	Tds_{30}	22100	27.1	550	1.15E+11	3.50E+12	1.15E+11
S_{30}	7800	38.2	690	3.67E+06	5.88E+07	3.67E+06	Tds_{30}	22100	27.1	690	1.14E+11	3.58E+12	1.14E+11
S_{30}	7800	38.2	830	2.62E+06	6.30E+07	2.62E+06	Tds_{30}	22100	27.1	830	1.13E+11	3.63E+12	1.13E+11
D_0	10000	24.5	550	7.56E+06	2.66E+07	7.56E+06	Tr_0	25500	20.8	550	1.39E+07	4.64E+07	1.39E+07
D_0	10000	24.5	690	6.94E+06	2.61E+07	6.94E+06	Tr_0	25500	20.8	690	1.29E+07	4.56E+07	1.29E+07
D_0	10000	24.5	830	6.56E+06	2.57E+07	6.56E+06	Tr_0	25500	20.8	830	1.23E+07	4.51E+07	1.23E+07
$D_{7.5}$	10750	26.4	550	6.13E+06	1.92E+07	6.13E+06	$Tr_{7.5}$	27413	22.4	550	1.12E+07	3.35E+07	1.12E+07
$D_{7.5}$	10750	26.4	690	5.57E+06	1.88E+07	5.57E+06	$Tr_{7.5}$	27413	22.4	690	1.03E+07	3.29E+07	1.03E+07
$D_{7.5}$	10750	26.4	830	5.24E+06	1.85E+07	5.24E+06	$Tr_{7.5}$	27413	22.4	830	9.83E+06	3.25E+07	9.83E+06
D_{10}	11000	27	550	5.76E+06	1.74E+07	5.76E+06	Tr_{10}	28050	22.9	550	1.05E+07	3.04E+07	1.05E+07
D_{10}	11000	27	690	5.21E+06	1.70E+07	5.21E+06	Tr_{10}	28050	22.9	690	9.68E+06	2.99E+07	9.68E+06
D_{10}	11000	27	830	4.91E+06	1.68E+07	4.91E+06	Tr_{10}	28050	22.9	830	9.19E+06	2.95E+07	9.19E+06
D_{20}	12000	29.4	550	4.55E+06	1.20E+07	4.55E+06	Tr_{20}	30600	25	550	8.20E+06	2.07E+07	8.20E+06
D_{20}	12000	29.4	690	4.07E+06	1.17E+07	4.07E+06	Tr_{20}	30600	25	690	7.48E+06	2.03E+07	7.48E+06
D_{20}	12000	29.4	830	3.81E+06	1.15E+07	3.81E+06	Tr_{20}	30600	25	830	7.05E+06	2.00E+07	7.05E+06
D_{30}	13000	31.9	550	3.64E+06	8.45E+06	3.64E+06	Tr_{30}	33150	27.1	550	6.55E+06	1.46E+07	6.55E+06
D_{30}	13000	31.9	690	3.23E+06	8.21E+06	3.23E+06	Tr_{30}	33150	27.1	690	5.90E+06	1.42E+07	5.90E+06
D_{30}	13000	31.9	830	3.00E+06	8.06E+06	3.00E+06	Tr_{30}	33150	27.1	830	5.54E+06	1.40E+07	5.54E+06
Td_0	17000	20.8	550	2.33E+09	5.62E+08	5.62E+08	Trs_0	25500	20.8	550	1.23E+07	7.06E+07	1.23E+07
Td_0	17000	20.8	690	2.33E+09	5.66E+08	5.66E+08	Trs_0	25500	20.8	690	1.14E+07	6.93E+07	1.14E+07
Td_0	17000	20.8	830	2.33E+09	5.66E+08	5.66E+08	Trs_0	25500	20.8	830	1.09E+07	6.85E+07	1.09E+07
$Td_{7.5}$	18275	22.4	550	1.83E+09	4.04E+08	4.04E+08	$Trs_{7.5}$	27413	22.4	550	8.70E+06	4.94E+07	8.70E+06
$Td_{7.5}$	18275	22.4	690	1.83E+09	4.05E+08	4.05E+08	$Trs_{7.5}$	27413	22.4	690	9.16E+06	5.00E+07	9.16E+06
$Td_{7.5}$	18275	22.4	830	1.83E+09	4.07E+08	4.07E+08	$Trs_{7.5}$	27413	22.4	830	8.70E+06	4.94E+07	8.70E+06
Td_{10}	18700	22.9	550	1.70E+09	3.66E+08	3.66E+08	Trs_{10}	28050	22.9	550	9.32E+06	4.64E+07	9.32E+06
Td_{10}	18700	22.9	690	1.70E+09	3.67E+08	3.67E+08	Trs_{10}	28050	22.9	690	8.57E+06	4.55E+07	8.57E+06
Td_{10}	18700	22.9	830	1.70E+09	3.68E+08	3.68E+08	Trs_{10}	28050	22.9	830	8.13E+06	4.48E+07	8.13E+06
Td_{20}	20400	25	550	1.27E+09	2.46E+08	2.46E+08	Trs_{20}	30600	25	550	7.28E+06	3.17E+07	7.28E+06
Td_{20}	20400	25	690	1.27E+09	2.47E+08	2.47E+08	Trs_{20}	30600	25	690	6.63E+06	3.09E+07	6.63E+06
Td_{20}	20400	25	830	1.27E+09	2.48E+08	2.48E+08	Trs_{20}	30600	25	830	6.25E+06	3.05E+07	6.25E+06
Td_{30}	22100	27.1	550	9.77E+08	1.71E+08	1.71E+08	Trs_{30}	33150	27.1	550	5.80E+06	2.23E+07	5.80E+06
Td_{30}	22100	27.1	690	9.76E+08	1.72E+08	1.72E+08	Trs_{30}	33150	27.1	690	5.24E+06	2.17E+07	5.24E+06
Td_{30}	22100	27.1	830	9.76E+08	1.72E+08	1.72E+08	Trs_{30}	33150	27.1	830	4.91E+06	2.14E+07	4.91E+06

APPENDIX F – CRITICAL RESISTANCE VS OVERLOAD

Critical resistances (N numbers) vs Overload percentages by structure.

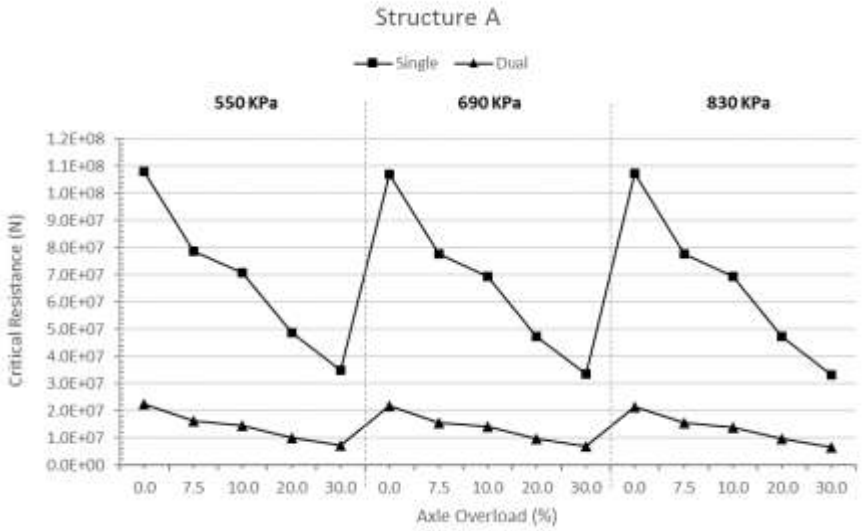

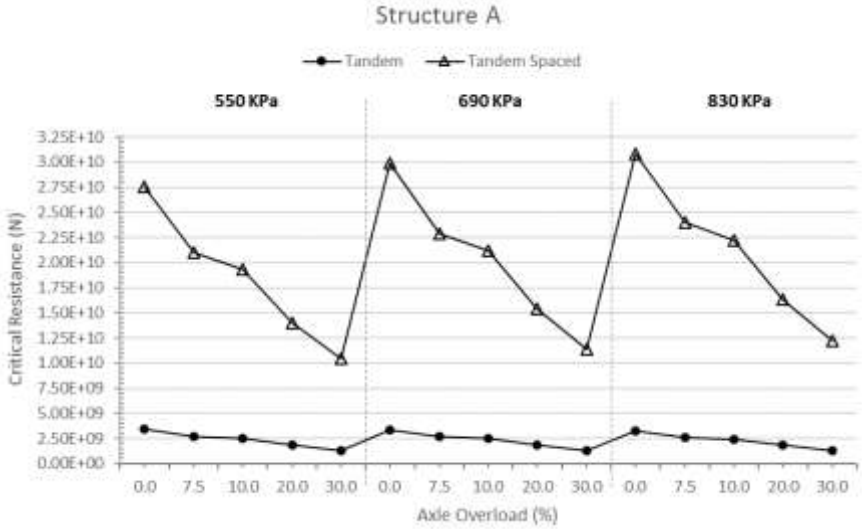

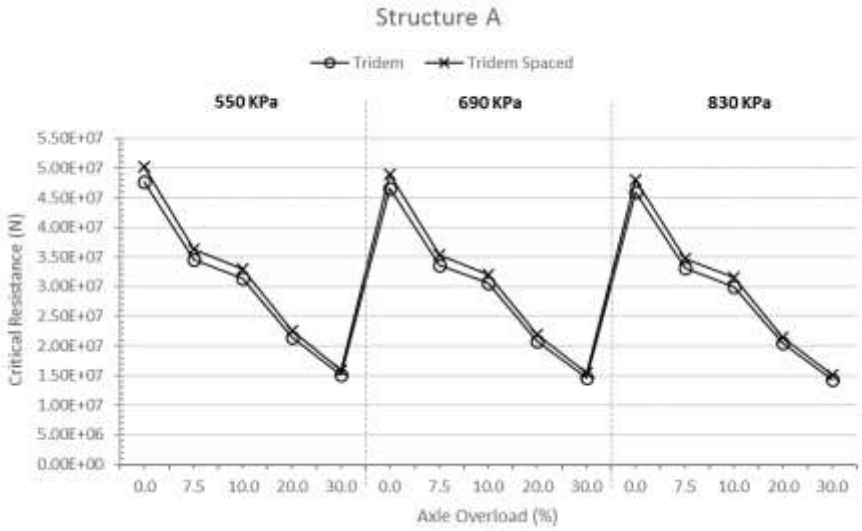

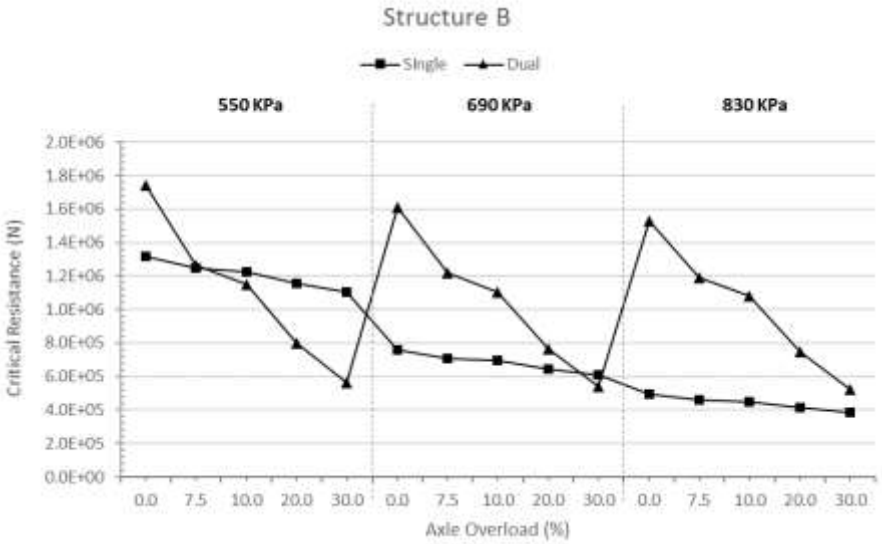
Structure B
Single
Dual
550 KPa
690 KPa
830 KPa
Critical Resistance (N)
2.0E+06
1.8E+06
1.6E+06
1.4E+06
1.2E+06
1.0E+06
8.0E+05
6.0E+05
4.0E+05
2.0E+05
0.0E+00
0.0 7.5 10.0 20.0 30.0 0.0 7.5 10.0 20.0 30.0 0.0 7.5 10.0 20.0 30.0
Axle Overload (%)

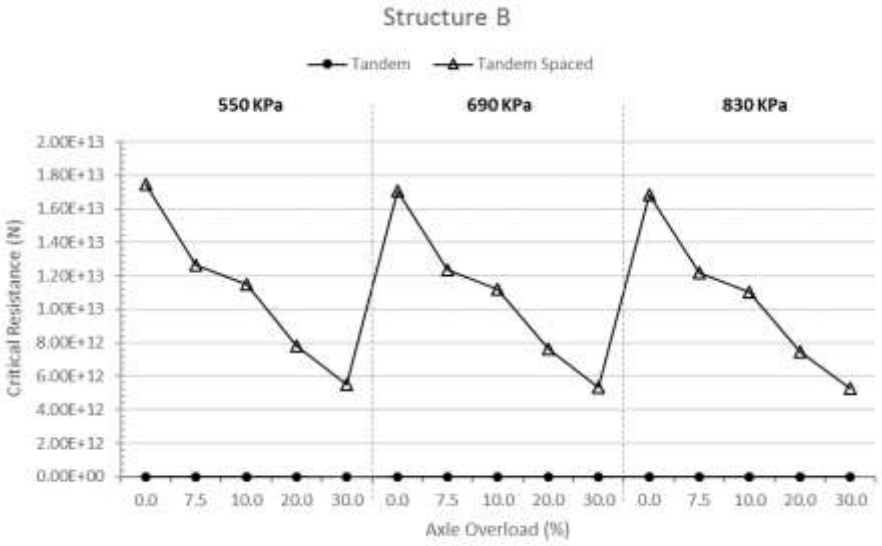
Structure B
Tandem
Tandem Spaced
550 KPa
690 KPa
830 KPa
Critical Resistance (N)
2.00E+13
1.80E+13
1.60E+13
1.40E+13
1.20E+13
1.00E+13
8.00E+12
6.00E+12
4.00E+12
2.00E+12
0.00E+00
0.0 7.5 10.0 20.0 30.0 0.0 7.5 10.0 20.0 30.0 0.0 7.5 10.0 20.0 30.0
Axle Overload (%)

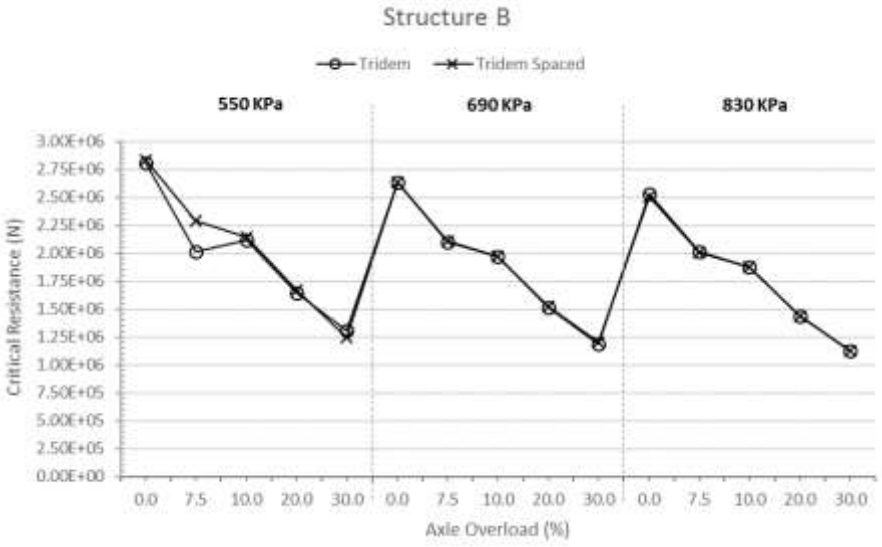
Structure B
Tridem
Tridem Spaced
550 KPa
690 KPa
830 KPa
Critical Resistance (N)
3.00E+06
2.75E+06
2.50E+06
2.25E+06
2.00E+06
1.75E+06
1.50E+06
1.25E+06
1.00E+06
7.50E+05
5.00E+05
2.50E+05
0.00E+00
0.0 7.5 10.0 20.0 30.0 0.0 7.5 10.0 20.0 30.0 0.0 7.5 10.0 20.0 30.0
Axle Overload (%)

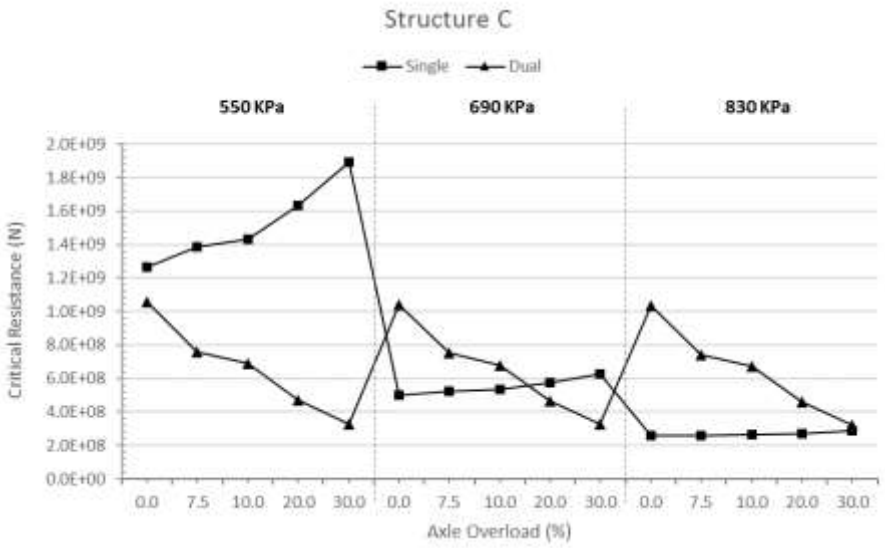
Structure C
Single
Dual
550 KPa
690 KPa
830 KPa
Critical Resistance (N)
2.0E+09
1.8E+09
1.6E+09
1.4E+09
1.2E+09
1.0E+09
8.0E+08
6.0E+08
4.0E+08
2.0E+08
0.0E+00
0.0 7.5 10.0 20.0 30.0 0.0 7.5 10.0 20.0 30.0 0.0 7.5 10.0 20.0 30.0
Axle Overload (%)

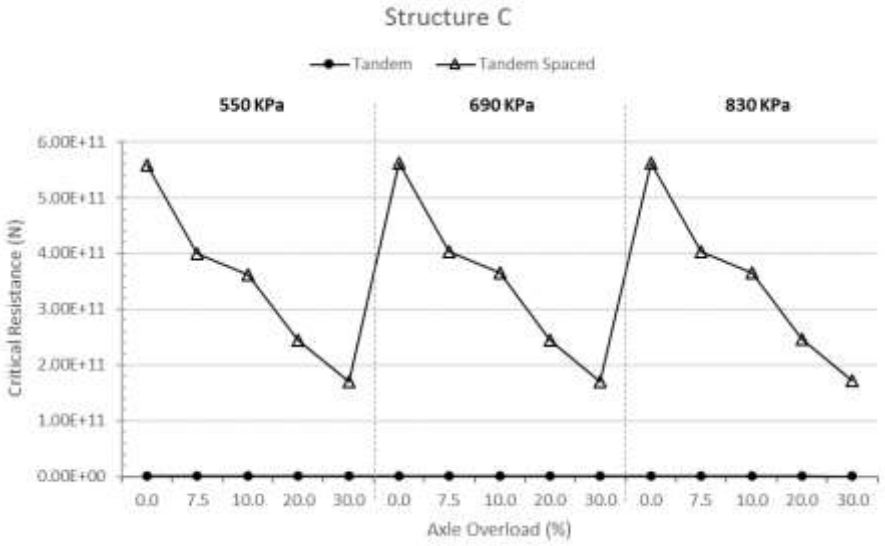
Structure C
Tandem
Tandem Spaced
550 KPa
690 KPa
830 KPa
Critical Resistance (N)
6.00E+11
5.00E+11
4.00E+11
3.00E+11
2.00E+11
1.00E+11
0.00E+00
0.0 7.5 10.0 20.0 30.0 0.0 7.5 10.0 20.0 30.0 0.0 7.5 10.0 20.0 30.0
Axle Overload (%)

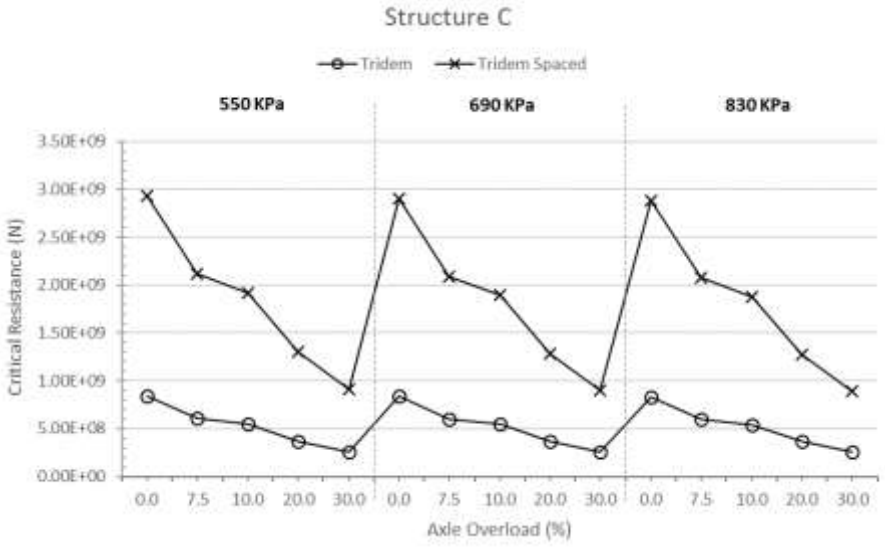
Structure C
Tridem
Tridem Spaced
550 KPa
690 KPa
830 KPa
Critical Resistance (N)
3.50E+09
3.00E+09
2.50E+09
2.00E+09
1.50E+09
1.00E+09
5.00E+08
0.00E+00
0.0 7.5 10.0 20.0 30.0 0.0 7.5 10.0 20.0 30.0 0.0 7.5 10.0 20.0 30.0
Axle Overload (%)

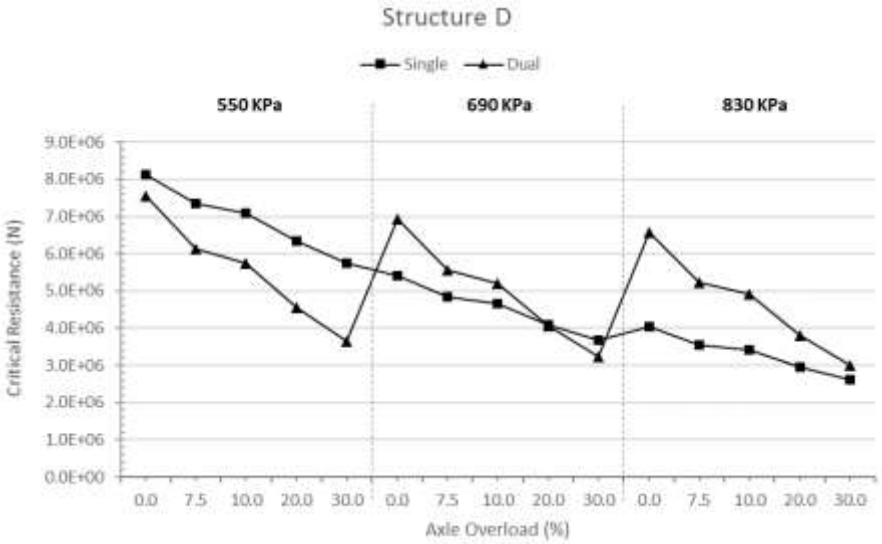
Structure D
Single
Dual
550 KPa
690 KPa
830 KPa
Critical Resistance (N)
9.0E+06
8.0E+06
7.0E+06
6.0E+06
5.0E+06
4.0E+06
3.0E+06
2.0E+06
1.0E+06
0.0E+00
0.0 7.5 10.0 20.0 30.0 0.0 7.5 10.0 20.0 30.0 0.0 7.5 10.0 20.0 30.0
Axle Overload (%)

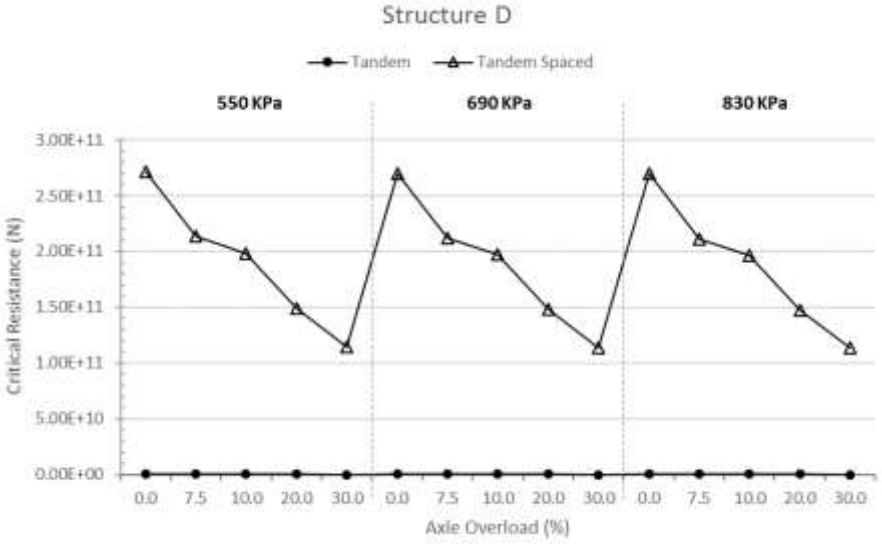
Structure D
Tandem
Tandem Spaced
550 KPa
690 KPa
830 KPa
Critical Resistance (N)
3.00E+11
2.50E+11
2.00E+11
1.50E+11
1.00E+11
5.00E+10
0.00E+00
0.0 7.5 10.0 20.0 30.0 0.0 7.5 10.0 20.0 30.0 0.0 7.5 10.0 20.0 30.0
Axle Overload (%)

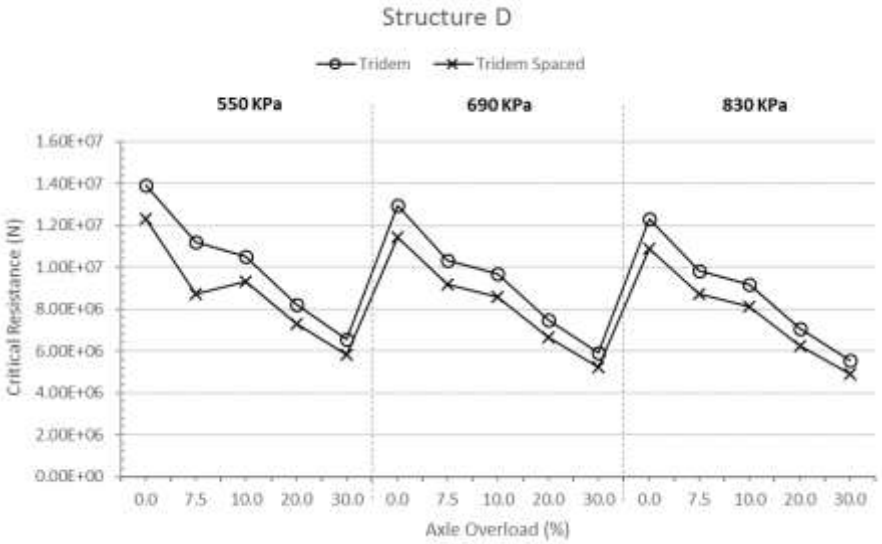
Structure D
Tridem
Tridem Spaced
550 KPa
690 KPa
830 KPa
Critical Resistance (N)
1.60E+07
1.40E+07
1.20E+07
1.00E+07
8.00E+06
6.00E+06
4.00E+06
2.00E+06
0.00E+00
0.0 7.5 10.0 20.0 30.0 0.0 7.5 10.0 20.0 30.0 0.0 7.5 10.0 20.0 30.0
Axle Overload (%)

Critical resistances (N numbers) vs Overload percentages by axle type.

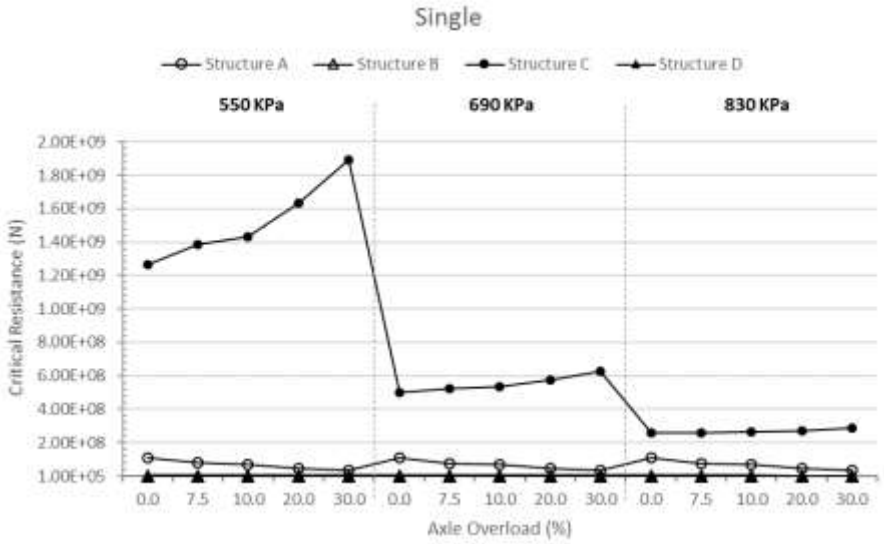

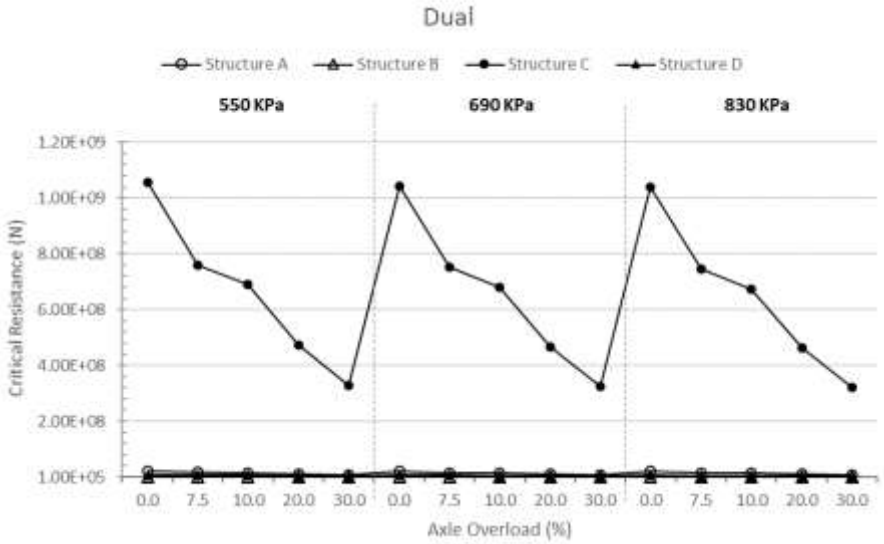

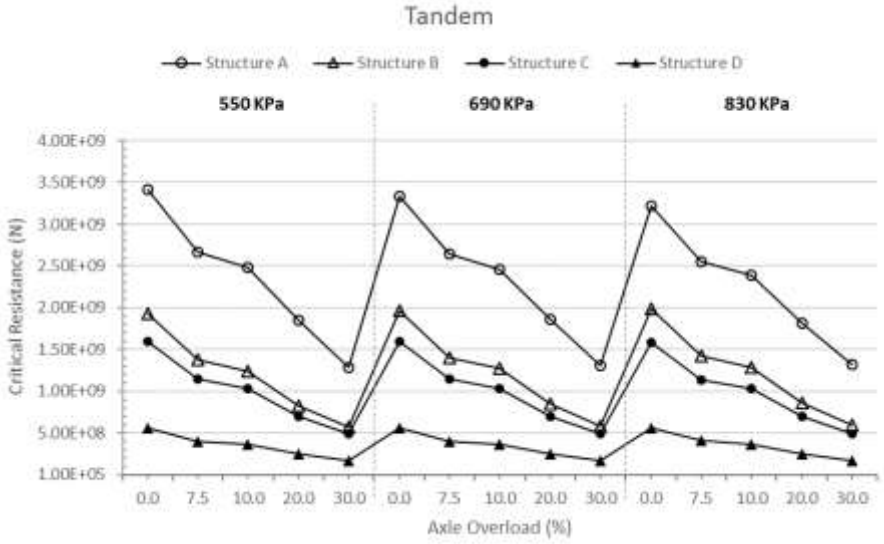

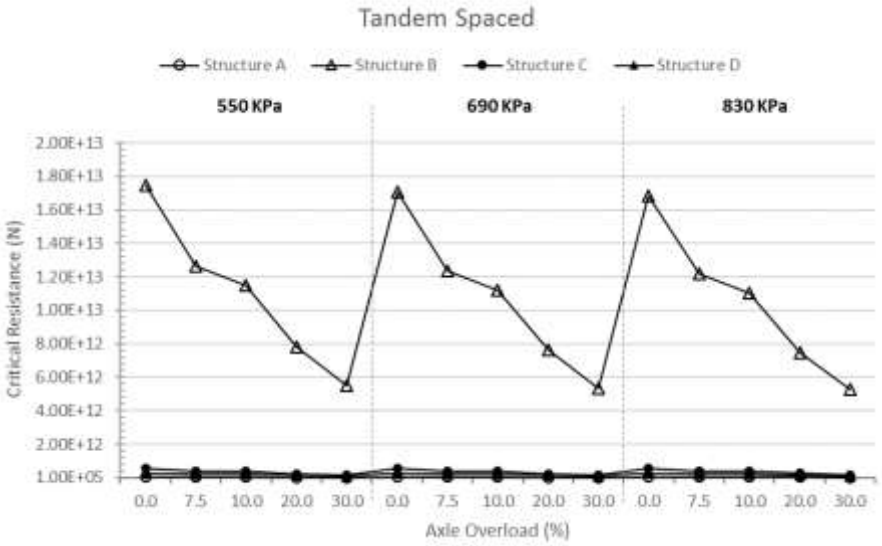
Tandem Spaced
Structure A
Structure B
Structure C
Structure D
550 KPa
690 KPa
830 KPa
Critical Resistance (N)
2.00E+13
1.80E+13
1.60E+13
1.40E+13
1.20E+13
1.00E+13
8.00E+12
6.00E+12
4.00E+12
2.00E+12
1.00E+05
0.0 7.5 10.0 20.0 30.0 0.0 7.5 10.0 20.0 30.0 0.0 7.5 10.0 20.0 30.0
Axle Overload (%)

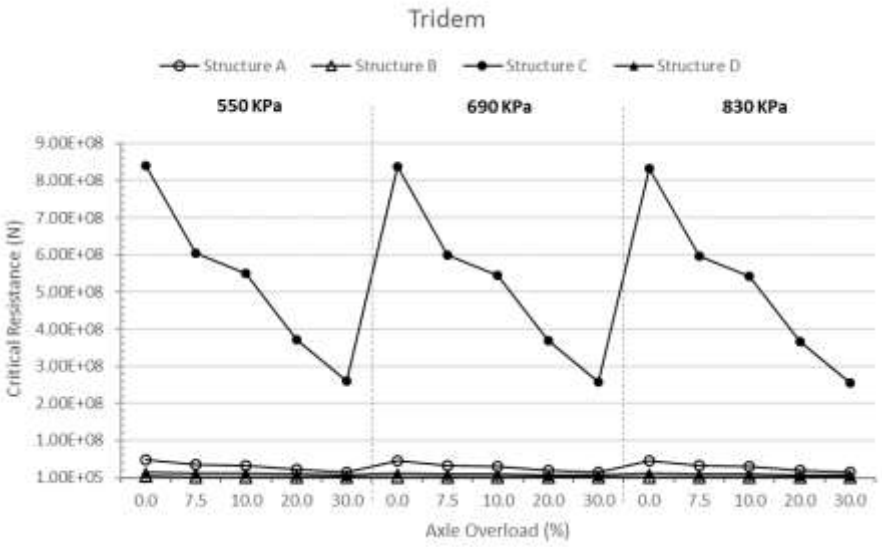
Tridem
Structure A
Structure B
Structure C
Structure D
550 KPa
690 KPa
830 KPa
Critical Resistance (N)
9.00E+08
8.00E+08
7.00E+08
6.00E+08
5.00E+08
4.00E+08
3.00E+08
2.00E+08
1.00E+08
1.00E+05
0.0 7.5 10.0 20.0 30.0 0.0 7.5 10.0 20.0 30.0 0.0 7.5 10.0 20.0 30.0
Axle Overload (%)

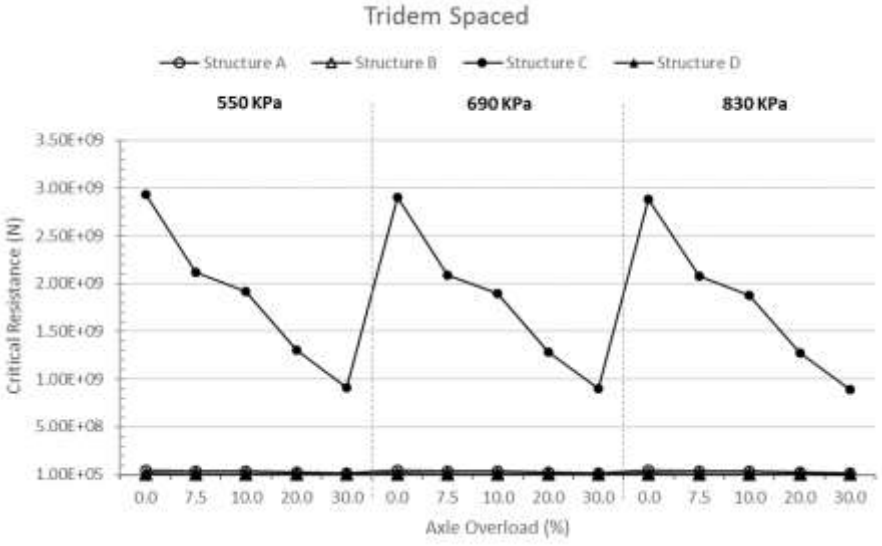
Tridem Spaced
Structure A
Structure B
Structure C
Structure D
550 KPa
690 KPa
830 KPa
Critical Resistance (N)
3.50E+09
3.00E+09
2.50E+09
2.00E+09
1.50E+09
1.00E+09
5.00E+08
1.00E+05
0.0 7.5 10.0 20.0 30.0 0.0 7.5 10.0 20.0 30.0 0.0 7.5 10.0 20.0 30.0
Axle Overload (%)

APPENDIX G – PAVEMENT LIFE REDUCTION

Pavement life reduction in terms of decrease percentages of critical N numbers, by structure and axle type. The value corresponding to 0% of overload and 550 KPa of tire pressure was taken as reference to obtain the percentages.

a) Percentages by structure:

STRUCTURE A

Pressure (Kpa)	Overload (%)	S	D	Td	Tds	Tr	Trs
550	0	0	0	0	0	0	0
	7.5	27	28	22	24	28	28
	10	35	34	27	30	34	34
	20	55	55	46	49	55	55
	30	68	68	62	62	68	68
690	0	1	3	2	-8	2	2
	7.5	28	30	23	17	30	29
	10	36	36	28	23	36	36
	20	56	56	46	44	56	56
	30	69	69	62	59	69	69
830	0	1	5	6	-12	4	4
	7.5	28	31	25	13	31	31
	10	36	38	30	20	37	37
	20	56	57	47	41	57	57
	30	69	70	61	56	70	70

STRUCTURE B

Pressure (Kpa)	Overload (%)	S	D	Td	Tds	Tr	Trs
550	0	0	0	0	0	0	0
	7.5	5	27	29	28	28	19
	10	7	34	36	34	25	24
	20	12	54	57	55	42	41
	30	16	68	70	68	54	56
690	0	42	8	-2	2	6	7
	7.5	46	30	27	29	25	26
	10	47	37	34	36	30	30
	20	51	56	56	56	46	46
	30	54	69	69	69	58	58
830	0	62	12	-3	3	10	11
	7.5	65	32	26	30	28	29
	10	66	38	33	37	33	34
	20	69	57	55	57	49	49
	30	71	70	69	70	60	60

STRUCTURE C

Pressure (Kpa)	Overload (%)	S	D	Td	Tds	Tr	Trs
550	0	0	0	0	0	0	0
	7.5	-9	28	28	28	28	28
	10	-13	35	35	35	35	35
	20	-29	55	56	56	56	56
	30	-49	69	69	70	69	69
690	0	60	1	0	-1	0	1
	7.5	59	29	28	28	29	29
	10	58	36	35	35	35	35
	20	55	56	56	56	56	56
	30	51	69	69	69	69	69
830	0	80	2	0	-1	1	2
	7.5	79	29	28	28	29	29
	10	79	36	35	35	35	36
	20	78	56	56	56	56	57
	30	77	70	69	69	70	70

STRUCTURE D

Pressure (Kpa)	Overload (%)	S	D	Td	Tds	Tr	Trs
550	0	0	0	0	0	0	0
	7.5	10	19	28	21	19	29
	10	13	24	35	27	24	24
	20	22	40	56	45	41	41
	30	29	52	70	58	53	53
690	0	33	8	-1	1	7	7
	7.5	40	26	28	22	26	26
	10	43	31	35	27	30	30
	20	50	46	56	45	46	46
	30	55	57	69	58	58	58
830	0	50	13	-1	1	11	12
	7.5	56	31	28	22	29	29
	10	58	35	34	28	34	34
	20	64	50	56	46	49	49
	30	68	60	69	58	60	60

b) Percentages by axle type:

Pressure (Kpa)	Overload (%)	Single				Dual				Tandem			
		A	B	C	D	A	B	C	D	A	B	C	D
550	0	0	0	0	0	0	0	0	0	0	0	0	0
	7.5	27	5	-9	10	28	27	28	19	22	29	28	28
	10	35	7	-13	13	34	34	35	24	27	36	35	35
	20	55	12	-29	22	55	54	55	40	46	57	56	56
	30	68	16	-49	29	68	68	69	52	62	70	69	70
690	0	1	42	60	33	3	8	1	8	2	-2	0	-1
	7.5	28	46	59	40	30	30	29	26	23	27	28	28
	10	36	47	58	43	36	37	36	31	28	34	35	35
	20	56	51	55	50	56	56	56	46	46	56	56	56
	30	69	54	51	55	69	69	69	57	62	69	69	69
830	0	1	62	80	50	5	12	2	13	6	-3	0	-1
	7.5	28	65	79	56	31	32	29	31	25	26	28	28
	10	36	66	79	58	38	38	36	35	30	33	35	34
	20	56	69	78	64	57	57	56	50	47	55	56	56
	30	69	71	77	68	70	70	70	60	61	69	69	69

Pressure (Kpa)	Overload (%)	Tandem Spaced				Tridem				Tridem Spaced			
		A	B	C	D	A	B	C	D	A	B	C	D
550	0	0	0	0	0	0	0	0	0	0	0	0	0
	7.5	24	28	28	21	28	28	28	19	28	19	28	29
	10	30	34	35	27	34	25	35	24	34	24	35	24
	20	49	55	56	45	55	42	56	41	55	41	56	41
	30	62	68	70	58	68	54	69	53	68	56	69	53
690	0	-8	2	-1	1	2	6	0	7	2	7	1	7
	7.5	17	29	28	22	30	25	29	26	29	26	29	26
	10	23	36	35	27	36	30	35	30	36	30	35	30
	20	44	56	56	45	56	46	56	46	56	46	56	46
	30	59	69	69	58	69	58	69	58	69	58	69	58
830	0	-12	3	-1	1	4	10	1	11	4	11	2	12
	7.5	13	30	28	22	31	28	29	29	31	29	29	29
	10	20	37	35	28	37	33	35	34	37	34	36	34
	20	41	57	56	46	57	49	56	49	57	49	57	49
	30	56	70	69	58	70	60	70	60	70	60	70	60

Summary of the percentages of decrease in critical N:

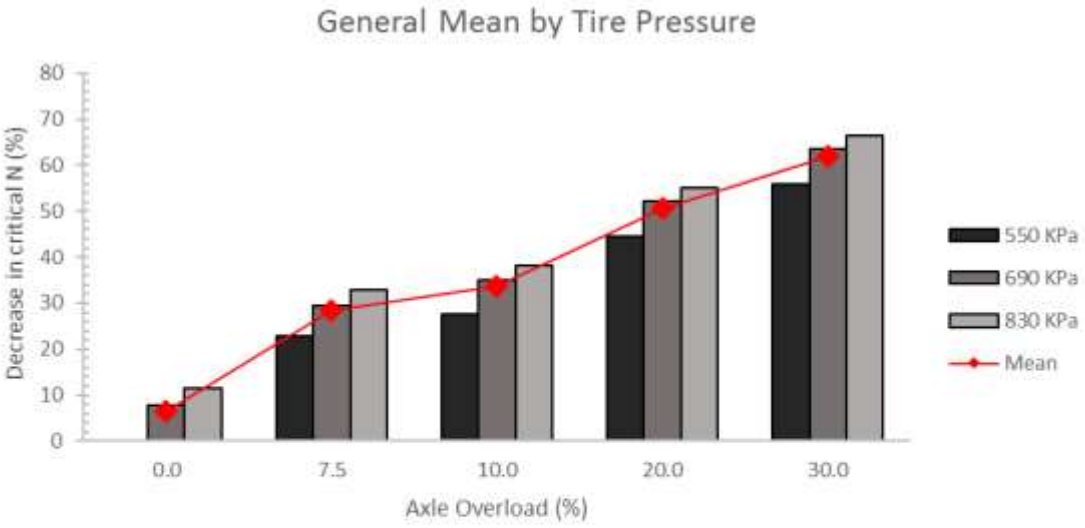

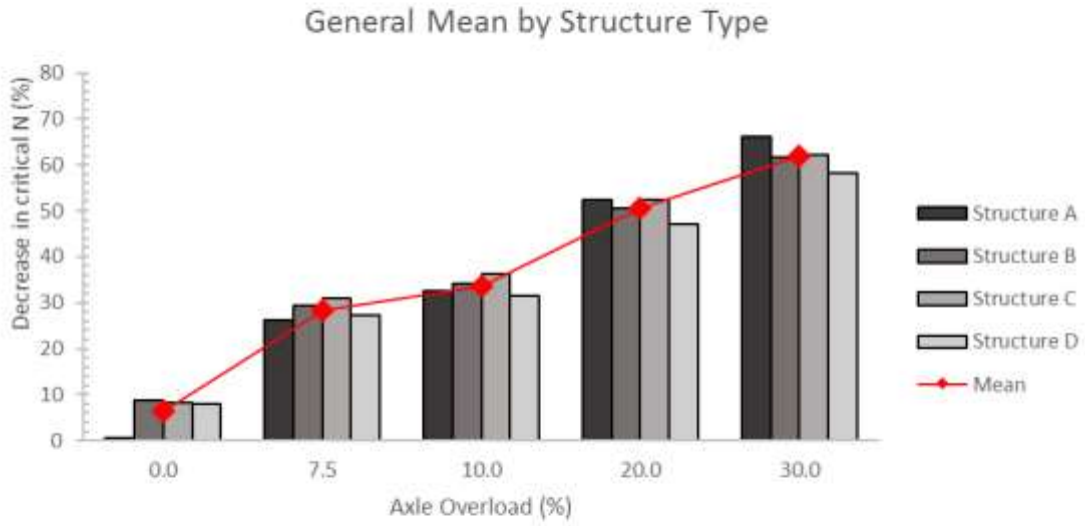

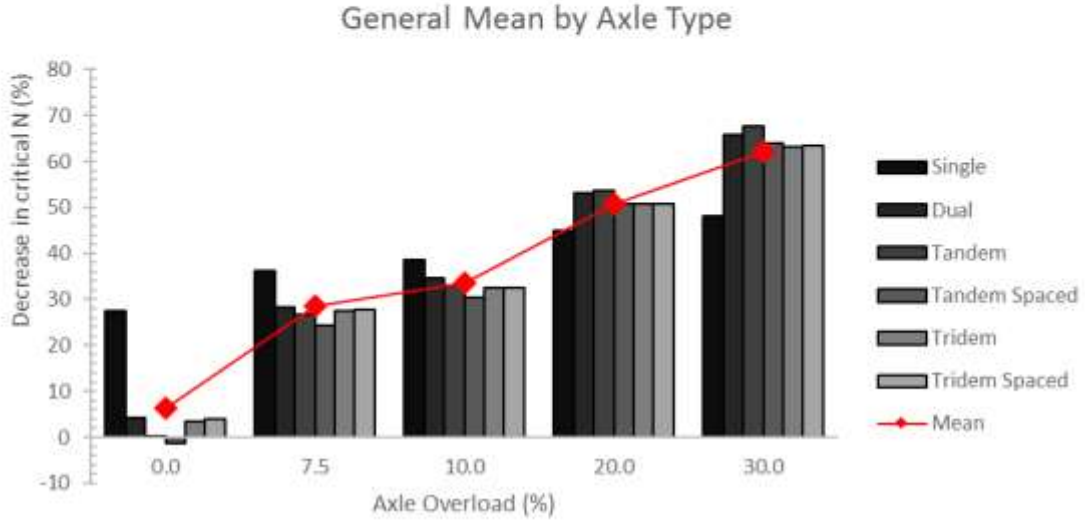

APPENDIX H – RESIDUALS STATISTICS

MODEL 1

a) Histogram -Standardized residual

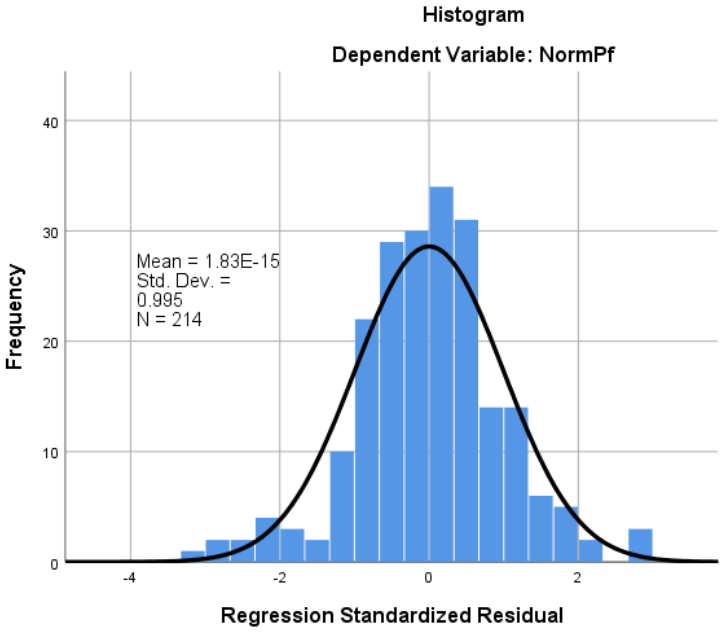

b) Normal P-P Plot of Regression Standardized residual

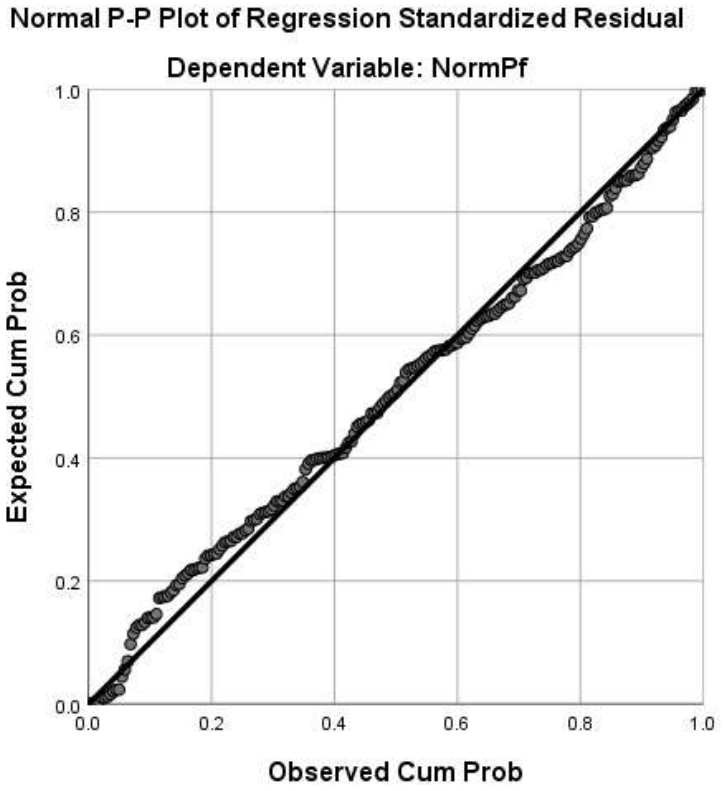

c) Scatterplot – Dependent variable

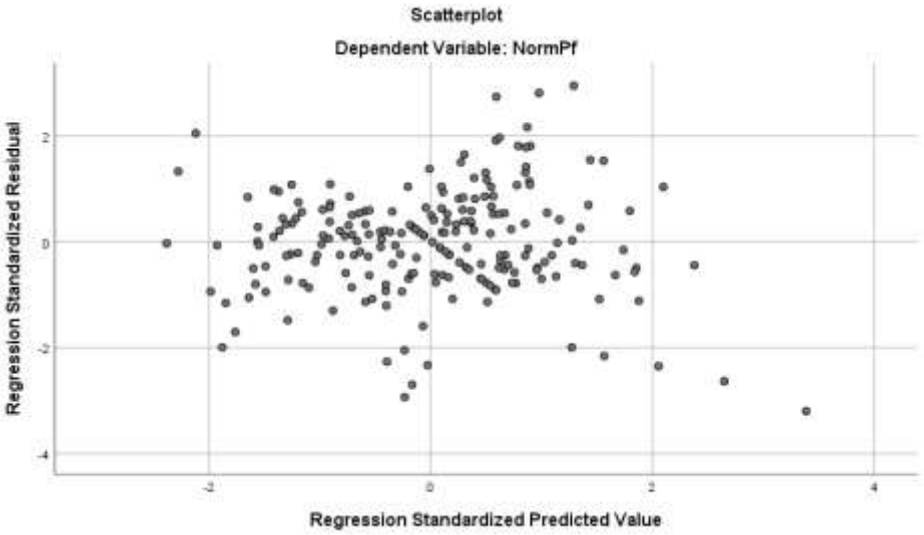

d) Partial Regression Plots

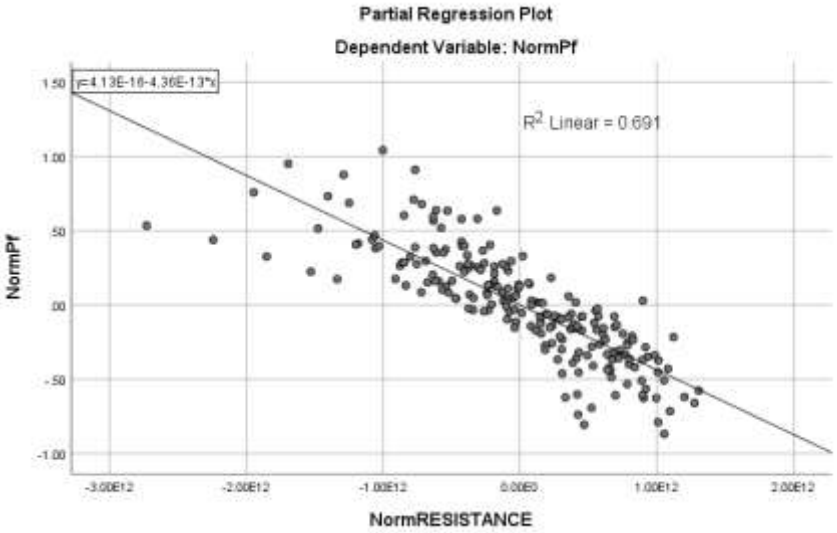

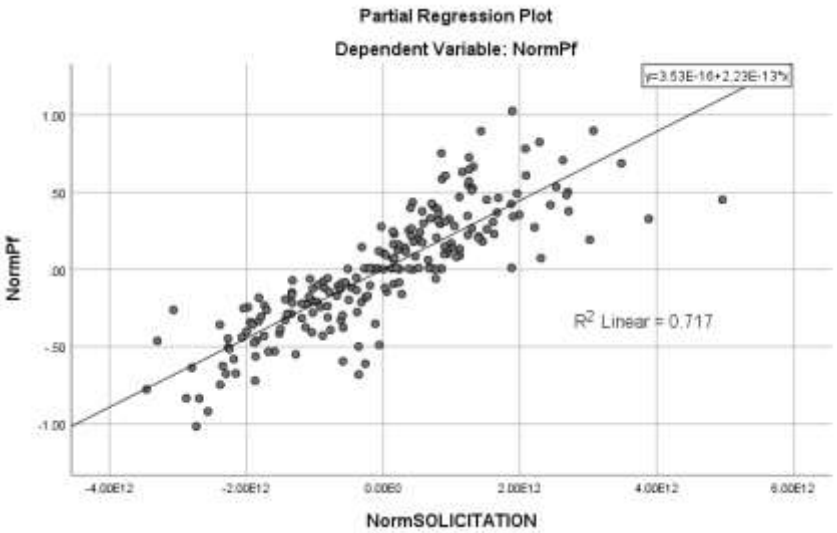

MODEL 2

a) Histogram -Standardized residual

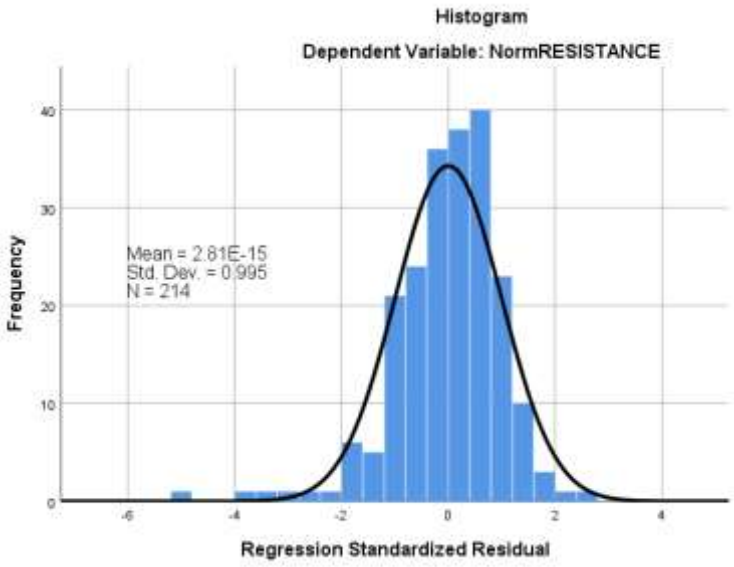

b) Normal P-P Plot of Regression Standardized residual

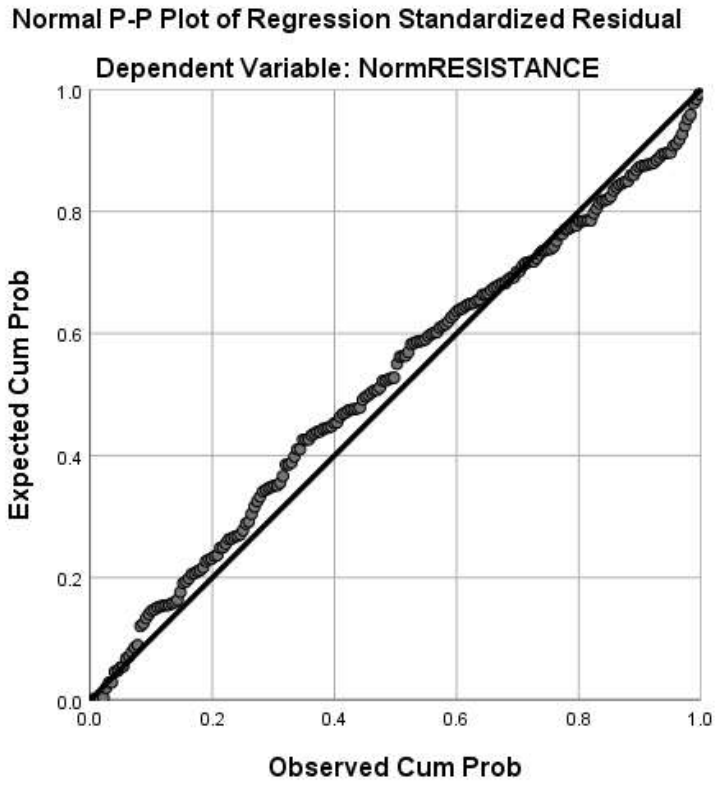

c) Scatterplot – Dependent variable

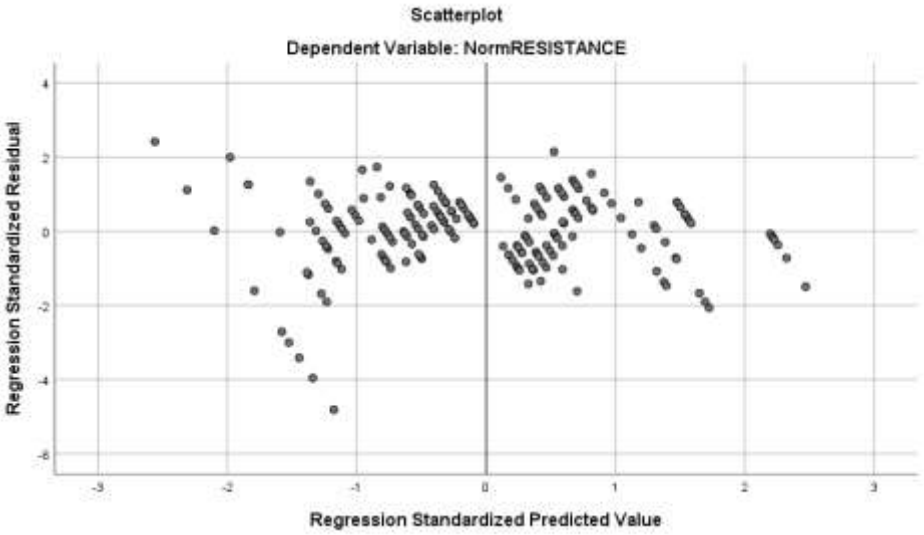

d) Partial Regression Plots

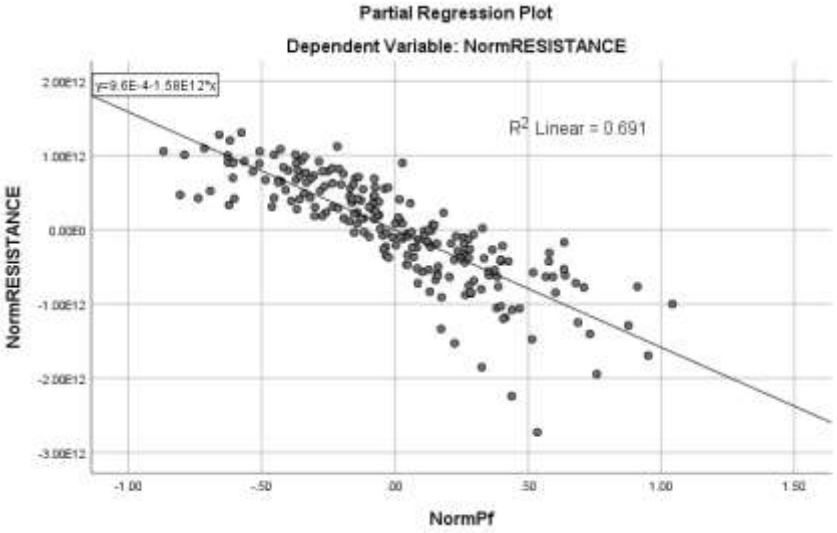

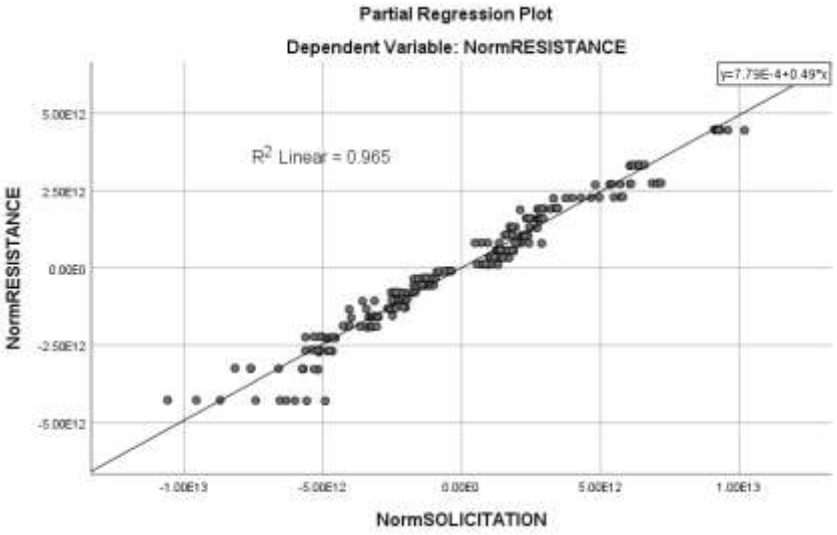

MODEL 3

a) Histogram -Standardized residual

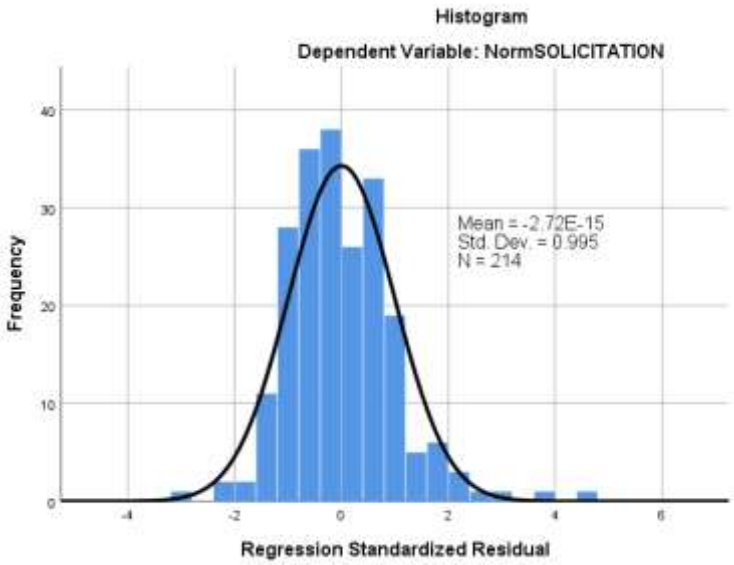

b) Normal P-P Plot of Regression Standardized residual

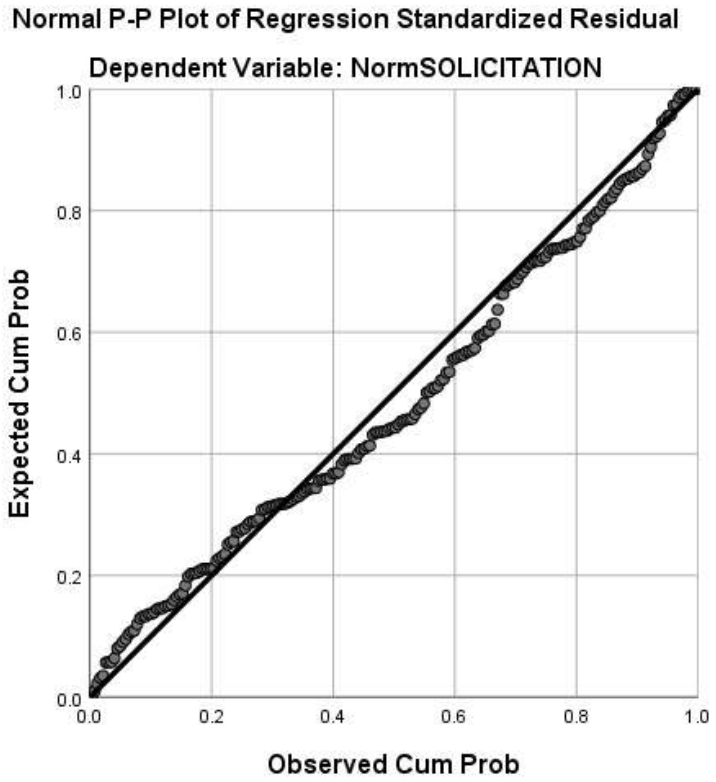

c) Scatterplot – Dependent variable

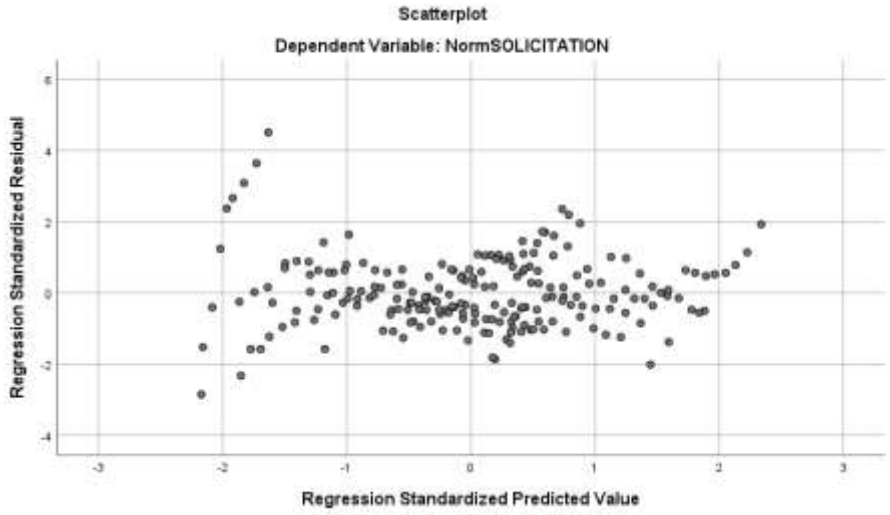

d) Partial Regression Plots

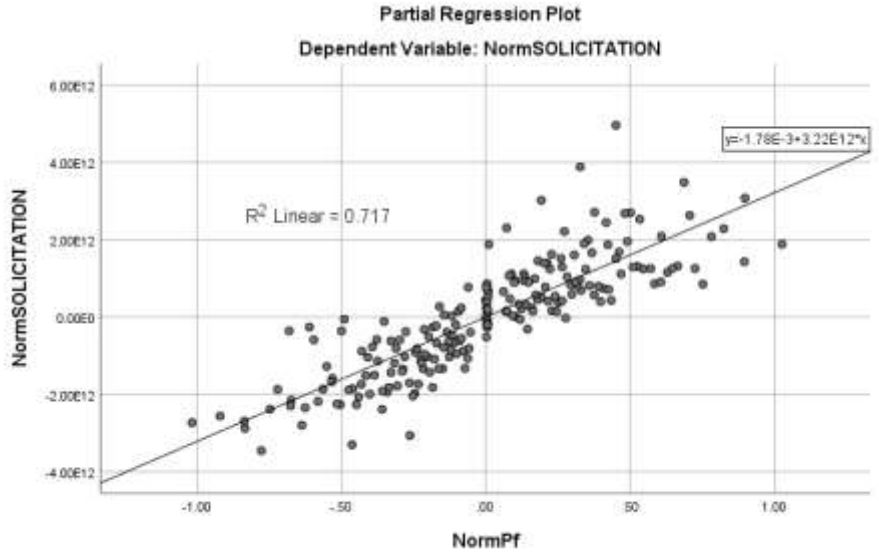

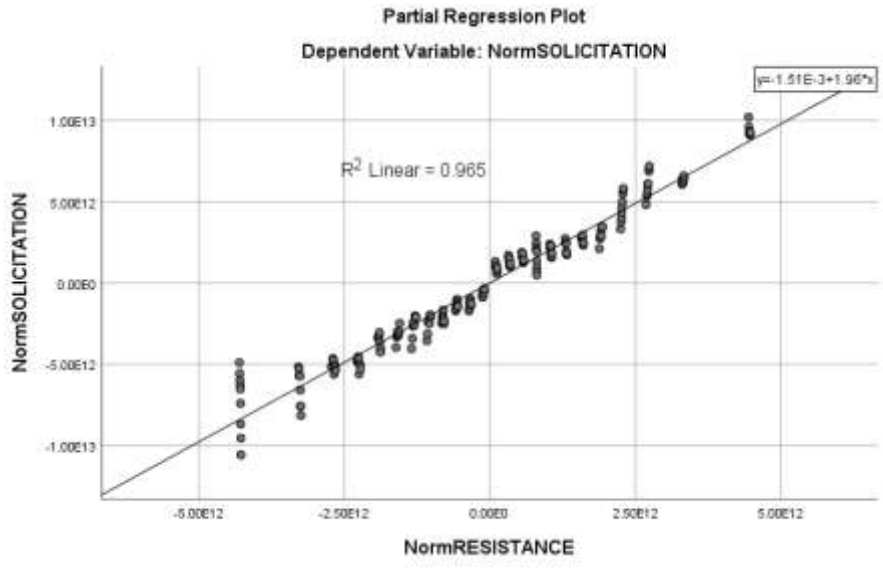

MODEL 4

a) Histogram -Standardized residual

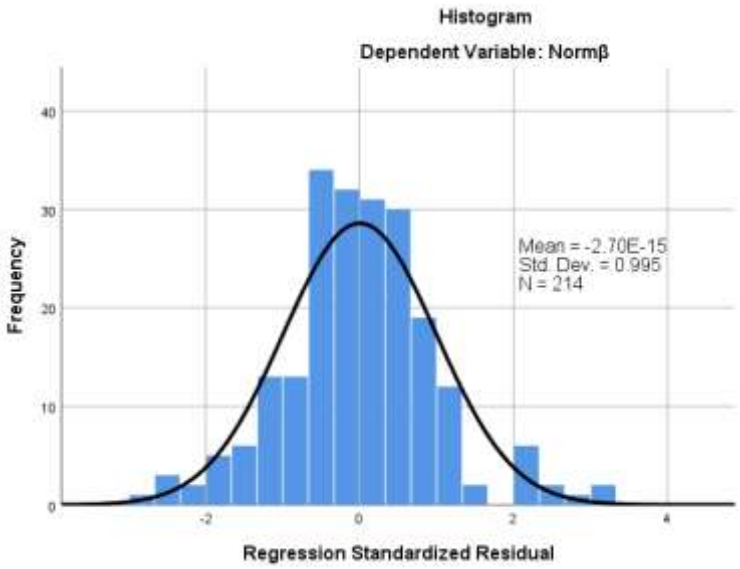

b) Normal P-P Plot of Regression Standardized residual

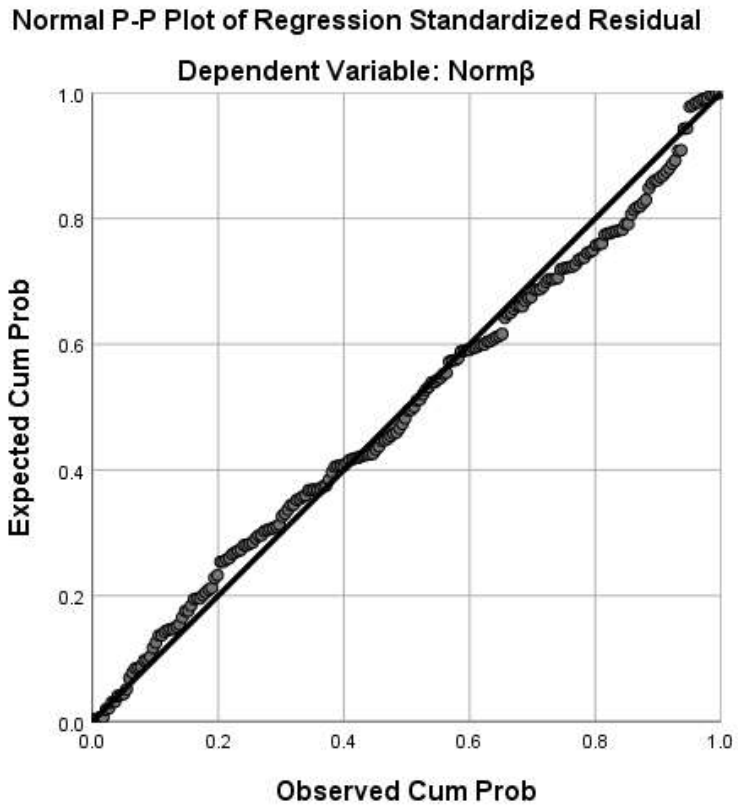

c) Scatterplot – Dependent variable

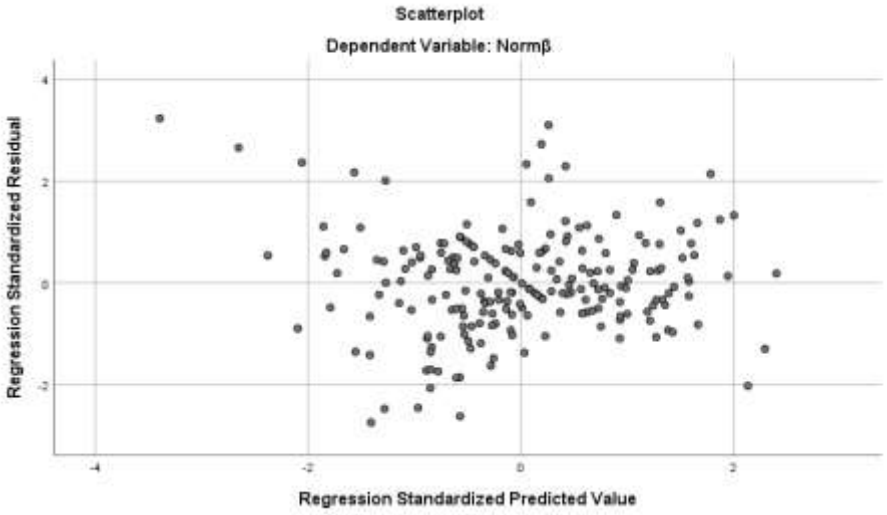

d) Partial Regression Plots